



School of Medicine
Molecular Biosciences Program

EVALUATION OF NKG2D CHIMERIC ANTIGEN RECEPTOR REDIRECTED CD45RA⁻ T CELLS AS TREATMENT FOR PEDIATRIC ACUTE LEUKEMIA

DOCTORAL THESIS

ADRIÁN FERNÁNDEZ MARTÍN

2022

Supervisor: Dr. Lucía Fernández Casanova

Co-supervisor: Dr. Antonio Pérez Martínez

H12O-CNIO Hematological Malignancies Group

Clinical Research Program

Spanish National Cancer Research Centre

“Nada en la vida es para ser temido, es sólo para ser comprendido. Ahora es el momento de entender más, de modo que podamos temer menos”

Marie Curie

A mis amigos.

A mi familia.

A mis padres, Arturo y Ana.

A mi mujer, Virginia.

AGRADECIMIENTOS

Después de quejarme tanto de los discursos eternos de agradecimiento de los Oscars o los Goya, voy a tener que romper una lanza a su favor. Porque este trabajo, aunque esté a mi nombre, ha podido realizarse gracias a la ayuda de muchas, pero que muchas personas, y no puedo sino dar las gracias a todas ellas.

En primer lugar, quiero agradecer a las fundaciones CRIS Contra el Cáncer y Uno Entre Cien Mil por la gran labor y esfuerzo que hacen para financiar proyectos de investigación en nuestro país, incluyendo este, ya que es algo imprescindible para acabar con esta enfermedad, el cáncer.

En segundo lugar, me gustaría destacar la disposición por ayudar que tenían todas y cada una de las personas que, de una manera u otra, han colaborado en este proyecto. ¿Que necesitamos unos *buffy coats*?, la doctora Aurora Viejo y los compañeros de la Unidad de Banco de Sangre del Hospital La Paz los conseguía en cuanto podía. ¿Que no llegamos a unos títulos virales decentes?, Raúl Torres nos da una clase magistral de producción lentiviral. ¿Que tenemos dudas con unos paneles citometría?, las chicas de la Unidad de Citometría del CNIO, Lola, Julia y Sara, enseguida nos echaban una mano (y alguna que otra regañina) con una sonrisa. Siempre que necesitábamos ayuda, un consejo, un reactivo, lo que sea, ahí estaban, a nuestra disposición. Agradecer por ello a Diego, Manu y todo el equipo de la Unidad de Microscopía Confocal del CNIO, así como a Manuel Izquierdo, de la UAM, por su ayuda, consejos y asesoramiento con las técnicas de imagen; a Orlando y el equipo de la Unidad de Genómica del CNIO por su ayuda con la secuenciación; a la Unidad de Histopatología del CNIO por su colaboración en las tinciones de tejidos.

Gracias también al grupo de investigación de Cáncer de Pulmón del CNIO, por acogerme al principio de los tiempos como un polizón y ayudarme a dar mis primeros pasos en el CNIO. Mención especial a Patricia Yagüe, por su amabilidad y enseñanzas (y por esa manita con las IV), y a Santi García, que además de estar siempre atento y disponible (y traer postres), se ha convertido en un gran amigo, a pesar de que me pinte la cara en las carreras y en el tenis.

Una parte muy importante de este trabajo se ha desarrollado en el animalario del CNIO, y cabe destacar el trabajo de toda la Unidad para su correcto funcionamiento. Concretamente, dar las gracias a Gema y Flor por enseñarme con tanto cariño a tratar a los animales, siempre desde el respeto y la ética.

Cuando empecé este proyecto, iniciamos una colaboración en el laboratorio de Mar Valés, del CNB, que se convirtió en mi segunda (aunque por momentos primera) casa. La acogida y el trato fueron inmejorables. Gran parte de este trabajo se realizó allí,

donde aprendí “a cascoporro” sobre ligandos NKG2D y compartí grandes momentos con la propia Mar, Hugh, Gloria, Mareen, Ane y por supuesto con Carmen Campos, que estuvo conmigo desde el primer día cargada de paciencia, cariño y ganas de enseñar.

Por supuesto, el grupo de investigación de Idipaz, junto con los compañeros de INGEMM y del propio Hospital La Paz, han sido un pilar para la consecución de esta tesis, siempre aportando su granito de arena en los *lab-meeting* y *Journal club* y compartiendo reactivos (“Alfonsoooo, ¿tenéis anti-MICA?”), protocolos (“Carmeeeee, ¿qué *settings* usas para pasar estas muestras?”), penas (“pero Isa, ¿cómo puede pedir esto la AEMPs?”) y risas (el *Queen’s* sabe...). Adela, Cristina, Alfonso, Carmen, Bea, Carla, Isabel, Laura, Karima, Carla, Víctor, Carlos ¡gracias por todo!

Gracias al Dr. Joaquín Martínez López por acogerme en su grupo de investigación.

Y qué voy a decir de mi grupo, Tumores Hematológicos del CNIO... ¡Que sois mi familia! No podría tener unos compañeros mejores. Un millón de gracias por vuestro apoyo en el día a día, por estar siempre ahí para cualquier cosa que necesitara, por dejar vuestras tareas para ayudarme con las mías, por el buen rollo y la confianza que trasmitís, por las risas... en fin, por ser como sois: Lucía, Pedro, Michel, María, Marta, Miguel, Alejandra, Alba, Michael, os admiro a todos y todas.

Especialmente quiero dar las gracias de corazón al doctor Antonio Pérez Martínez, jefe de Servicio de Hemato-Oncología Pediátrica del Hospital La Paz, por su labor como médico y por su acogida y confianza en mí para llevar a cabo este proyecto de investigación, con un trato impecable y mucho cariño.

Y por encima de todo... Lucía Fernández Casanova, has sido jefa, compañera, madre, amiga, psicóloga. Nunca podré agradecerte la confianza y la fe que tuviste en mí. Me diste una oportunidad que pocas veces dan y he disfrutado muchísimo en esta aventura. La mejor directora de tesis que podría tener, tanto por lo mucho que he aprendido de ti (eres una científica de la cabeza a los pies) como por el buen ambiente y la confianza que trasmites. Este trabajo es tanto tuyo como mío.

Finalmente, yo no sería nada sin mis padres, Arturo y Ana, un ejemplo a seguir que me han hecho ser quien soy (para bien o para mal), y se lo agradeceré siempre. Ahora, además, mejoro cada día gracias a mi flamante reciente mujer, Virginia. *No puedo vivir sin ti, no hay manera.*

TABLE OF CONTENTS

TABLE OF CONTENTS

ABBREVIATION INDEX	5
ABSTRACT	11
RESUMEN.....	15
1. INTRODUCTION	19
1.1. Pediatric acute leukemia.....	21
1.1.1. Precursor B-cell acute lymphoblastic leukemia (B-ALL).....	23
1.1.2. Precursor T-cell acute lymphoblastic leukemia (T-ALL).	26
1.1.3. Acute myeloblastic leukemia (AML).	28
1.1.4. Biphenotypic acute leukemia.	29
1.2. New therapeutic approaches for acute leukemia.	30
1.3. CAR T cells.....	32
1.4. Role of NKG2D-NKG2DL axis in cancer.	36
1.4.1. NKG2D receptor.	36
1.4.2. NKG2D ligands.....	37
1.4.3. NKG2D-CAR T cells for cancer treatment.....	39
1.5. Mechanisms of immunoescape.....	41
2. HYPOTHESIS	43
3. OBJECTIVES	47
4. MATERIALS AND METHODOLOGY	51
4.1. Materials.....	53
4.1.1. Cell lines.....	53
4.1.2. Antibodies and dyes.	53
4.2. Methodology: preclinical studies.	56
4.2.1. Primary cells.....	56
4.2.2. Flow cytometry.	57
4.2.3. Production of LV particles carrying NKG2D-CAR construct.	58
4.2.4. NKG2D-CART production.....	62
4.2.5. <i>In vitro</i> cytotoxicity of NKG2D-CART.	63

4.2.6.	<i>In vivo</i> efficacy and safety of NKG2D-CART.....	65
4.2.7.	Histopathology analysis by IHC.	67
4.2.8.	Analysis of sNKG2DL in leukemia samples.	68
4.2.9.	Effects of soluble NKG2D ligands on NKG2D-CART.	68
4.2.10.	Time lapse, epifluorescence and confocal microscopy.	70
4.2.11.	Effects of TGF- β and soluble factors on NKG2D-CART.....	71
4.2.12.	Impact of NKG2D-CART on leukemia-initiating cells.....	71
4.2.13.	Transcriptome analysis by RNA-seq.....	72
4.3.	Methodology: Translation to the clinic.	74
4.3.1.	Starting Material.	74
4.3.2.	Manufacturing of Clinical-Grade NKG2D-CART.....	74
4.3.3.	Analysis of viability and surface immunophenotype by FCM and Western Blot.....	75
4.3.4.	Effector function.....	76
4.3.5.	Analysis of non-cellular impurities.....	76
4.3.6.	Microbiological test.	76
4.3.7.	Genetic Tests, Genome Integrated Vector Copy Number, and determination of Replication Competent Lentivirus in the Supernatant.	76
4.3.8.	Effects of cryopreservation on NKG2D-CART.....	77
4.4.	Statistical analysis.	78
5.	RESULTS.....	79
5.1.	Preclinical studies.....	81
5.1.1.	Lipofectamine and second generation production achieved higher LV titers.....	81
5.1.2.	LV transduction of CD45RA ⁺ T cells achieved robust expression of NKG2D while not affecting cell viability.	82
5.1.3.	NKG2DL are expressed in leukemia cell lines.	84
5.1.4.	NKG2DL are expressed in primary leukemic blasts of pediatric patients independently of the stage of the disease.	85
5.1.5.	NKG2D-CART target leukemic blasts <i>in vitro</i>	86

5.1.6. NKG2D-CART reduce tumor progression and prolong survival in a murine model of T-ALL.	89
5.1.7. In treated mice, infused NKG2D-CART home to the bone marrow and respond against leukemia cells.	91
5.2. Immunoescape mechanisms.	93
5.2.1. Jurkat T-ALL cell line released sULBP2.	93
5.2.2. sNKG2DL were found in the serum of patients suffering from acute leukemia.	94
5.2.3. Supraphysiological levels of sNKG2DL downmodulated chimeric NKG2D receptor and promoted CD45RA ⁺ NKG2D-CAR T cell proliferation.	97
5.2.4. Cytotoxicity of NKG2D-CART remained unaltered upon exposure to sNKG2DL.	100
5.2.5. NKG2D-CART retained their capability to form productive immune synapses after treatment with high amounts of sMICA.	101
5.2.6. The levels of TGF- β secreted by leukemia cells do not affect NKG2D-CART cytotoxicity.	104
5.2.7. NKG2D-CART target leukemia-initiating cells compartment.	105
5.2.8. Upon exposure to NKG2D-CART, Jurkat cells upregulate genes related to proliferation, stemness and survival.	107
5.3. Translation to the clinic.	110
5.3.1. Manufacturing Process: activation, transduction, and expansion.	110
5.3.2. Purity of CD45RA ⁺ starting cells.	110
5.3.3. High Transduction efficiency was achieved by using low MOI.	111
5.3.4. Manufacturing of NKG2D-CART achieved sufficient numbers for clinical use.	112
5.3.5. Manufactured NKG2D-CART are enriched in CD4 ⁺ and mainly present an effector memory phenotype	113
5.3.6. Manufactured NKG2D-CART are highly cytotoxic against T-ALL and osteosarcoma cell lines.	114
5.3.7. NKG2D-CART comply with the regulatory specifications regarding safety and sterility	115

5.3.8. Cryopreserved NKG2D-CART maintain viability, expression of CAR and cytotoxicity.	116
6. DISCUSSION	117
6.1. NKG2D-NKG2DL axis represents a suitable strategy to target pediatric acute leukemia.....	120
6.2. Transduction efficiency and characteristics of NKG2D-CART.....	121
6.3. Evaluation of anti-leukemia efficacy of NKG2D-CART.....	122
6.4. NKG2D-CART effectively target leukemia cells <i>in vivo</i>	123
6.5. NKG2D-CART bypass the canonic tumor immunoescape mechanisms.	125
6.6. Manufacturing of clinical-grade large-scale NKG2D-CART is feasible and reproducible.	129
7. CONCLUSIONS	131
7.1. Preclinical studies.....	133
7.2. Translation to the clinic.	133
8. CONCLUSIONES	135
8.1. Estudios preclínicos.....	137
8.2. Investigación traslacional.....	138
9. REFERENCES	139
10. ANNEXES	165
10.1. Maps of plasmids used for LV particles production.....	167
10.2. Table showing characteristics of B-ALL pediatric patients.	170
10.3. Table showing characteristics of T-ALL pediatric patients.	173
10.4. Table showing characteristics of AML pediatric patients.....	174
Manuscripts.....	176

ABBREVIATION INDEX

ADAMs A disintegrin and metalloproteases	c-kit CD117
AEMPS Spanish Regulatory Agency of Medicines and Medical Devices	CMAC 7-amino-4-chloromethylcoumarin
ALL Acute lymphoblastic leukemia	CML Chronic myelogenous leukemia
AML Acute myeloblastic leukemia	CNIO Spanish National Cancer Research Centre
ANOVA Analysis of variance	CNS Central Nervous Systems
APC Antigen presenting cells	CR Complete remission
ATMPs Advanced therapy medicinal products	CRS Cytokine release syndrome
B-ALL B-cell Acute lymphoblastic leukemia	cTCR T cell receptor constant
BCK Background	DAP10 DNAX-activating protein of 10 kDa
BF Bright field	DCV Vybrant™ DyeCycle™ Violet Stain dye
BiTE Bispecific T-cell engager	DLBCL Diffuse large B-cell lymphoma
BM Bone marrow	DMEM Dulbecco's Modified Eagle's Medium
BMM Bone marrow microenvironment	DMSO Dimethyl sulfoxide
BMTCT Bone Marrow Transplant and Cell Therapy Unit	DNA Deoxyribonucleic acid
BSA Bovine serum albumin	<i>E. Coli</i> <i>Escherichia Coli</i>
CAFs Cancer-associated fibroblasts	E:T Effector to target
CAR Chimeric antigen receptor	ECM Extracellular matrix
CAR T Chimeric antigen receptor expressed on T cells	EDTA Ethylenediaminetetraacetic acid
CART19 CAR T cells targeting CD19	ELISA Enzyme linked immunosorbent assay
CGH Comparative genome hybridization	Eu Ph European Pharmacopeia
	Fab Fab antigen-binding fragment

FBS Fetal Bovine Serum	IHC Immunohistochemistry
FCM Flow cytometry	IL Interleukin
FDA Food and Drug Administration	IMDM Iscove's Modified Dulbecco's Medium
FMO Fluorescence minus one	INGEMM Institute of Medical and Molecular Genetics
FSC-A Forward scatter area	LB Luria Broth
FSC-W Forward scatter width	LICs Leukemia-initiating cells
GFP Green fluorescence protein	LTR Long terminal repeat
GM-CSF Granulocyte macrophage colony-stimulating factor	Luc Luciferase
GPI Glycosyl-phosphatidyl-inositol	MAX Maximum lysis
Grb2 Growth factor receptor-bound protein 2	MDSCs Myeloid-derived suppressor cells
GvHD Graft-versus-host-disease	MEM Minimum essential medium
GvL Graft-versus-leukemia	MFI Median fluorescence intensity
H/E Hematoxylin and eosin	MHC Major histocompatibility complex
HEPES 4-(2-hydroxyethyl)-1-piperazineethanesulfonic acid	MICA MHC Class I-related chain A
HLA Human leukocyte antigen	MICB MHC Class I-related chain B
HRP Horseradish peroxidase	miRNA Micro-RNA
HSCT Hematopoietic stem cell transplantation	MLL Mixed lineage leukemia
HSF1 Heat shock transcription factor 1	MMPs Matrix metalloproteinases
HULP La Paz University Hospital	MRD Minimal residual disease
ICANS Immune effector cell-associated neurotoxicity syndrome	mRNA Messenger ribonucleic acid
IDO Indoleamine 2,3-dioxygenase	MSCs Mesenchymal stem cells
IFN-γ Interferon gamma	MTOC Microtubule-organizing center
	NK Natural Killer cell

NKAES	Activated and expanded NK cells	RES	Reserpine
NKG2D	Natural Killer group 2 Member D	rh	Recombinant human proteins
NKG2DL	NKG2D ligands	RNA	Ribonucleic acid
NSG	NOD.Cg-Prkdc ^{scid} Il2rg ^{tm1Wjl} /SzJ mice	RNA-seq	Transcriptome sequencing
OS	Overall survival	RPMI	Roswell Park Memorial Institute medium
P/S	Penicillin-streptomycin	rRNA	Ribosomal ribonucleic acid
PB	Peripheral blood	RT	Room temperature
PBMCs	Peripheral blood mononuclear cells	scFv	Single-chain variable fragment domain
PBS	Phosphate buffered saline	SEM	Standard Error of Mean
PCR	Polymerase chain reaction	SFI	Specific fluorescence intensity
PD-1	Programmed cell death protein 1	SIN	Self-inactivating
PD-L1	Programmed cell death Ligand 1	sMICA	Soluble MICA
PEF	PBS + EDTA 3 mM + FBS 3%	sMICB	Soluble MICB
PEI	Polyethylenimine	sNKG2DL	Soluble NKG2D ligands
PFA	Paraformaldehyde	SP	Spontaneous lysis
PI	Propidium iodide	SSC-A	Side scatter area
PI3-K	Phosphoinositide 3-kinase	sULBP1	Soluble ULBP1
PVDF	Polyvinylidene fluoride	sULBP2	Soluble ULBP2
qPCR	quantitative PCR	sULBP3	Soluble ULBP3
r/r	Relapsed/refractory	sULBP4	Soluble ULBP4
RAET1	Retinoic acid early transcripts-1	TAA	Tumor-associated antigens
RCL	Replication Competent Lentivirus	T-ALL	T cell acute lymphoblastic leukemia
		TAMs	Tumor-associated macrophages

T_{CM} Central memory T cells

TCT T cell transduction

TdT Terminal deoxynucleotidyl transferase

T_{EFF} Effector T cells

T_{EM} Effector memory T cells

Tert Telomerase reverse transcriptase

TGF- β Tumor growth factor beta

TM Transmembrane domain

TME Tumor microenvironment

TNF- α Tumor necrosis factor alpha

T_{regs} Regulatory T cells

ULBP1-6 UL-16 binding proteins 1 to 6

UT Untransduced

VCN Vector Copy Number

vp/ml Viral particles per ml

WB Western Blot

WBC White blood cells

ABSTRACT

Acute leukemia is the most frequent cancer in children and teens, and the second leading cause of cancer-related death in pediatric patients. Although treatment with CD19 chimeric antigen receptor expressed on T cells (CAR T) has achieved remarkable clinical success for B-cell malignancies, an effective and safe CAR T cell therapy both for relapsed/refractory (r/r) non-B cell leukemia and for those B-cell malignancies that relapse after CAR T cells targeting CD19 (CART19) treatment is yet to be found. Interactions between Natural Killer Group 2 Member D (NKG2D) receptor, expressed in cytotoxic immune cells, and NKG2D ligands (NKG2DL) that are upregulated in leukemic blasts, are important for anti-leukemia immunosurveillance. However, leukemic blasts may develop different immunoescape strategies like TGF- β release, downregulation of NKG2DL or NKG2DL shedding, which may downregulate NKG2D receptor, hindering anti-leukemia effects.

In this study, we hypothesized that NKG2D-CAR T cells could overcome these limitations and become a novel therapeutic approach for pediatric acute leukemia. We found that NKG2D-CAR T cells *in vitro*, efficiently targeted pediatric acute leukemia cells, especially for acute myeloid leukemia (AML) and T cell acute lymphoblastic leukemia (T-ALL). Furthermore, when tested *in vivo*, NKG2D-CAR T cells decreased T-ALL progression and prolonged survival of the treated mice, but failed to completely eradicate the leukemia in our mice model. Additionally, it was observed that cytotoxicity of NKG2D-CAR T cells remained unaltered upon exposure soluble NKG2DL (sNKG2DL) and/or TGF- β . Interestingly, we found that after co-culture with NKG2D-CAR T cells, remaining leukemic blasts showed higher proliferation and stemness-related markers. This result could indicate that treatment with NKG2D-CAR T cells may only be effective against tumor cells with a more mature phenotype, while those with a rather stem phenotype and increased proliferation are able to circumvent the treatment.

In conclusion, our results show NKG2D-CAR T cells exert anti-leukemia effects and are resistant to canonic resistance mechanisms, and therefore, could be a novel therapeutic agent for pediatric patients. The modest efficacy observed *in vivo* suggests that the use of NKG2D-CAR T cells as single agent may not be sufficient to cure the patients, and combination with other therapeutic approaches, e.g. as an induction agent and bridge to HSCT or as adoptive cell therapy after HSCT, may be more advantageous.

RESUMEN

La leucemia aguda es el cáncer más frecuente en niños y adolescentes, y la segunda causa de muerte relacionada con el cáncer en pacientes pediátricos. Aunque la terapia de células T redirigidas con el receptor antigénico quimérico (T CAR) hacia la diana CD19 ha logrado un gran éxito clínico para las neoplasias malignas de células B, aún no se ha encontrado una terapia de células T CAR eficaz y segura para la leucemia linfoblástica de células T (LLA-T) o para la leucemia aguda mieloblástica (LMA). Tampoco en el caso de recaídas de leucemias linfoblásticas agudas de células B (LLA-B) tras tratamiento con la terapia T CAR dirigida contra CD19 (CART19). Las interacciones entre el receptor de grupo 2D de linfocitos *Natural Killer* (NKG2D), expresado en células inmunitarias citotóxicas, y sus ligandos (NKG2DL), que están sobreexpresados en los blastos leucémicos, son importantes para la inmunovigilancia contra la leucemia. Sin embargo, los blastos leucémicos pueden desarrollar diferentes estrategias de escape inmunológico, como la liberación de TGF- β , la regulación de la expresión de NKG2DL o la liberación de NKG2DL para disminuir la expresión del receptor NKG2D, lo que dificulta los efectos antileucémicos.

En este estudio, planteamos la hipótesis de que las células T CAR NKG2D podrían superar esta limitación y convertirse en una estrategia terapéutica novedosa para la leucemia aguda pediátrica. Nuestros resultados muestran que *in vitro*, las células T CAR NKG2D eliminan eficazmente células de leucemia aguda pediátrica, especialmente LMA y LLA-T. Además, *in vivo* son capaces de controlar la progresión de LLA-T y prolongaron la supervivencia de los ratones tratados, aunque no consiguieron erradicar el tumor por completo. También observamos que tras la exposición de las células T CAR NKG2D a ligandos de NKG2D solubles (sNKG2DL) y/o TGF- β , la capacidad citotóxica permaneció inalterada. Sin embargo, después del co-cultivo con células T NKG2D-CAR, los blastos leucémicos T restantes se enriquecieron en marcadores *stem* y relacionados con la proliferación. Este resultado podría indicar que las células T CAR NKG2D pueden seleccionar células tumorales con un fenotipo más inmaduro y con mayor capacidad de proliferación. En suma, estos resultados podrían explicar la incapacidad de la terapia T CAR NKG2D para erradicar la leucemia en nuestro modelo murino.

En conjunto, los resultados mostrados en esta tesis muestran el efecto contra la leucemia de las células T CAR NKG2D y su resistencia a los mecanismos canónicos de evasión inmune. De esta forma, podría convertirse en una nueva terapia para el tratamiento de pacientes pediátricos. La modesta eficacia observada en los estudios *in vivo*, sugiere que el uso de las células T CAR NKG2D como único agente puede no ser suficiente para curar a los pacientes, y por tanto la combinación con otras terapias como el trasplante de progenitores hematopoyéticos (TPH) podría ser más ventajoso.

1. INTRODUCTION

1.1. Pediatric acute leukemia.

Acute leukemia is a heterogeneous hematologic disease originating from hematopoietic stem and progenitor cells that lose their capacity for proper self-renewal, differentiation and apoptosis, causing uncontrolled proliferation of hematopoietic stem cells from myeloid or lymphoid lineages in the bone marrow (BM) (Davis, Viera, and Mead 2014; Milan et al. 2019). Depending on the cell lineage affected, leukemias can be classified in acute lymphoblastic leukemia (ALL) -when lymphoid progenitors are the origin of the disease-, or AML -when myeloid progenitors are altered-. The diagnosis of acute leukemia generally requires demonstration of $\geq 20\%$ BM blasts on hematopathology review of BM aspirate and biopsy materials (Brown et al. 2020).

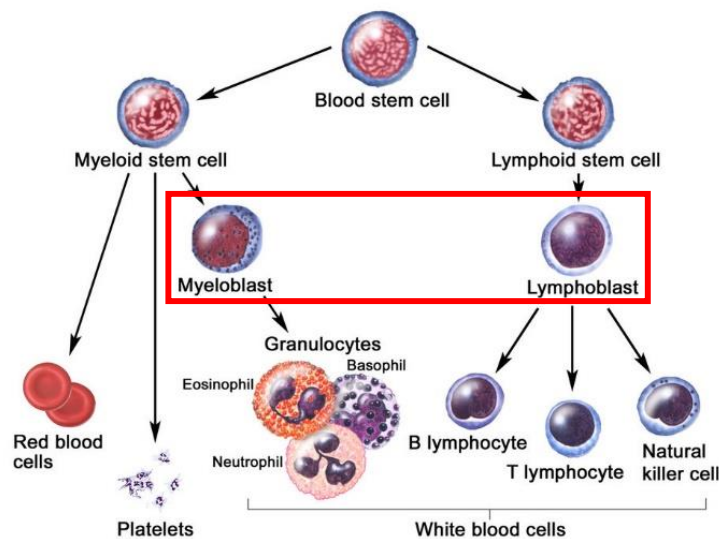


Figure 1. Diagram representing the hematopoiesis: evolution of blood cells differentiating from blood stem cells towards mature cells. Arrestment of the process at myeloblast and lymphoblast level contribute to leukemia development. Adapted from Terese Winslow, 2007.

Leukemia in children arise from naïve, pre-antigen stages, typically leading to primitive precursor blast cell leukemic populations. That is, the majority of childhood leukemia belongs to a pre-B cell or, to a lesser extent, pre-T cell phenotype. In contrast, adults typically develop hematopoietic cancers (lymphomas and leukemia) from post-antigen stimulated B and T-cells and the myeloid lineage (Whitehead et al. 2016). In addition, biphenotypic acute leukemia is characterized by blasts that express antigenic determinants of both myeloid and lymphoid lineages or of both B and T lineages (Legrand et al. 1998). Interestingly, biphenotypic acute leukemia incidence was higher in adults than in children (Matutes et al. 2011).

The only clear external cause of ALL is ionizing radiation. Although additional to this, several other risk factors have been proposed such as parental smoking, paint and household chemicals, pesticides, maternal diet, traffic fumes, electric fields and infections (Asenjo et al. 2021; Cárceles-Álvarez et al. 2017, 2019; Soldin et al. 2009; Wakeford 2008).

Over the last few decades, the leukemia incidence rate has increased reaching 36,2 and 8,7 cases per 1.000.000 in ALL and AML, respectively (Howlader et al. 2021). Acute leukemia is the most frequent cancer in children (28%), followed by brain cancers (26%) which represents 30% of total childhood cancer deaths while leukemia accounts for 25% (Coalition Against Childhood Cancer 2021). Nevertheless, in the last 40 years patient outcomes for childhood leukemia have significantly improved due to advancements in treatments (Mussai et al. 2015). However, cure rates in AML remain lower than in ALL, thus emphasizing that patient outcomes are highly dependent on the specific subgroup of leukemia involved (Bolouri et al. 2018). Therefore, understanding the biological and physiopathological characteristics of the different pediatric acute leukemia is essential to both improve the current treatments and to develop better new therapies, increasing the cure rates of the patients.

Leukemia survivors have an increased risk of subsequent cancers, likely due to the cellular damage caused by chemotherapy or radiation. The 30-year cumulative incidence of neoplasm after leukemia is 5,6%, and the median time to occurrence of the subsequent cancer is 9 years. The most common second neoplasms in childhood leukemia survivors are different subtypes of leukemia, or even lymphoma. Other second neoplasms can also include bone, soft tissue, or central nervous system (CNS) tumors. Moreover, treatment with certain chemotherapeutic agents or radiation can affect cardiac function, including ejection fraction and electrical conduction of the heart, leading to a congestive heart failure. Finally, endocrine abnormalities are also common after leukemia treatment, including metabolic syndrome, thyroid function abnormalities, and gonadal failure (Davis et al. 2014; Diller 2011; Friedman et al. 2010; Kadan-Lottick et al. 2008).

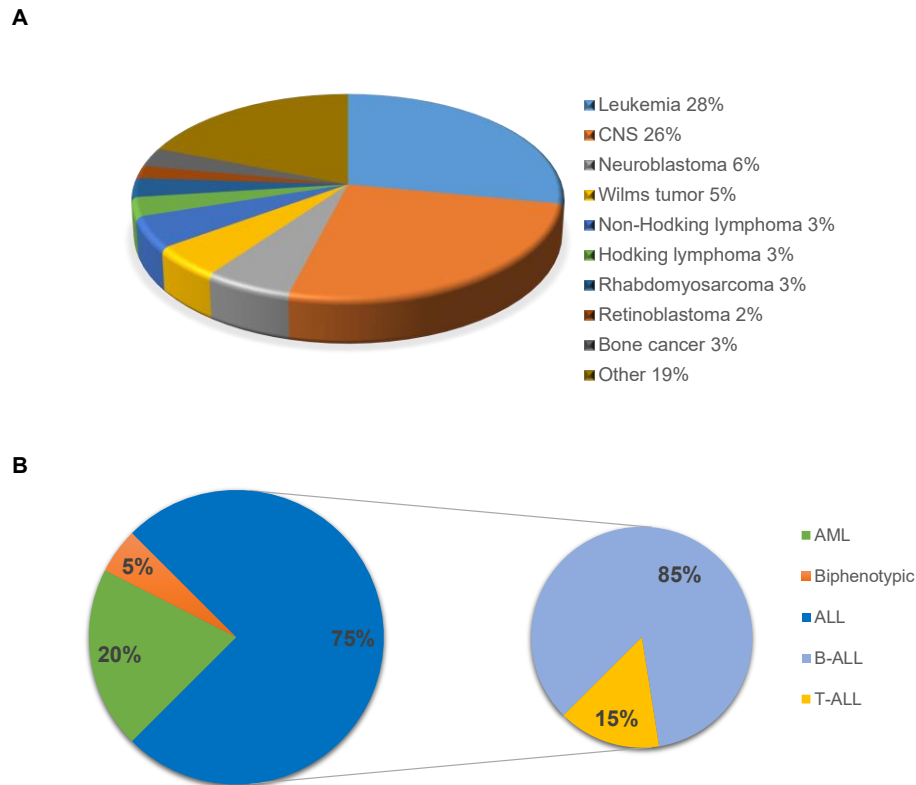


Figure 2. A) Incidence percentage of pediatric cancer (Coalition Against Childhood Cancer 2021). B) Percentage of different leukemia subtypes (Esparza and Sakamoto 2005; Hunger and Mullighan 2015; Young et al. 2016).

1.1.1. Precursor B-cell acute lymphoblastic leukemia (B-ALL).

ALL is the most common pediatric malignancy, representing 75%–80% of acute leukemia among children (Esparza and Sakamoto 2005). B-ALL is a heterogeneous hematologic disease characterized by the proliferation of immature lymphoid B cells in the BM, peripheral blood (PB) and other organs, and makes up 80-85% of ALL cases (Brown et al. 2020). It is morphologically characterized by a population of small to medium sized blasts with scant cytoplasm, moderately condensed to dispersed chromatin and inconspicuous nucleoli. The blood and BM are the principal sites of involvement (Brunning 2003).

Several genetic factors, like Down's syndrome, are associated with an increased risk of ALL, but most patients have no recognized inherited factors. Genome Wide association studies have identified polymorphic variants in several genes (including GATA3, ARID5B, IKZF1 and CEBPE) that are associated with an increased risk of ALL or specific ALL subtypes. Rare germline mutations in ETV6 and PAX5 are linked to familial ALL

(Hunger and Mullighan 2015). In addition, most childhood B-ALL cases harbor specific genetic abnormalities. These include hyperdiploidy (20-25%), hypodiploidy (1%) and recurring translocations, including t(12;21)(p13;q22), encoding ETV6-RUNX1 (TEL-AML1) (20-22%); mixed lineage leukemia (MLL) rearrangement involving 11q23 with a wide range of partner genes (6%); t(1;19)(q23;p13), encoding TCF3-PBX1 (E2A-PBX1) (4%); and t(9;22)(q34;q11), encoding BCR-ABL1 (2%). Notably, high hyperdiploidy and ETV6-RUNX1 are associated with favorable outcome, whereas low hypodiploidy and MLL rearrangement are associated with a dismal prognosis (Brown et al. 2020; Inaba, Greaves, and Mullighan 2013; Pui et al. 2012). Few environmental risk factors are associated with ALL in children, including exposure to radiation and certain chemicals, but these associations explain only a very small percentage of cases.

Precursor B lymphoblasts express human leukocyte antigen (HLA)-DR. Other frequent markers include surface CD19 and CD79a, and intracellular terminal deoxynucleotidyl transferase (TdT). In most cases, the blasts express CD10 and CD24. However, cases associated with t(4;11)(q21;q23) present lymphoblast that are normally CD10 and CD24 negative. While there is a variable membrane expression of CD20 and CD22, cytoplasmic CD22 is considered lineage specific. Also, CD13 and CD33 may be expressed in a minority of cases (Brunner RD, Matutes E, Borowitz MJ, Flandrin G, Head D 2001). Three stages of differentiation based on the immunophenotypic profile have generally been recognized: early pre B ALL in which the blasts express surface CD19, cytoplasmic CD79a and CD22 and nuclear TdT; intermediate stage -the so called common ALL- in which blasts express CD10 in addition to the markers of the early stage; and late or mature stage -“pre B” ALL-, in which blasts express cytoplasmic immunoglobulin μ chains (Brunner RD, Borowitz M, Matutes E 2001a).

Patients suffering from B-ALL develop symptoms related to the infiltration of blasts in the BM, lymphoid system, and extramedullary sites (Esparza and Sakamoto 2005). These symptoms may include anemia, thrombocytopenia and leucopenia, which promote fatigue or lethargy, fevers, night sweats, weight loss, dyspnea, dizziness, infections and easy bruising or bleeding. In some children, pain in the extremities or joints caused by the buildup of leukemia cells near the surface of the bone or inside the joint, may be the only reported symptom. The presence of lymphadenopathy, splenomegaly, and/or hepatomegaly on physical examination may be found in approximately 20% of patients (Brix and Rosthøj 2014; Brown et al. 2020; Faderl et al. 2010; Jabbour, Faderl, and Kantarjian 2005).

Advances in the understanding of the molecular genetics and pathogenesis of the disease, the incorporation of risk-adapted therapy, the advent of new targeted agents, and the use of allogeneic HSCT have largely contributed to the improvement of survival rates of pediatric patients with B-ALL (Ma, Sun, and Sun 2015). The 5-year survival rate has increased between 1975 and 2018 from 60% to approximately 89% (Howlader N, et al. 2021). However, for infants younger than the age of 1, survival rate has not improved over the past 30 years, with a 6-year overall survival (OS) rate of 58,2% (Pieters et al. 2019).

Treatment for acute leukemia may include chemotherapy, radiation, monoclonal antibodies or HSCT. The types of treatment chosen would depend on the leukemia subtype, cytogenetic and molecular findings, patient age, and comorbid conditions (Davis et al. 2014). There are 4 major components in the treatment of newly diagnosed ALL, reflecting a reliance on multidrug regimens to avoid development of resistance.

Remission induction is the first block of chemotherapy, lasting 4 to 6 weeks. The goal of this block of therapy is to induce a complete remission (CR) by its endpoint. The treatment eradicates the initial leukemia cell burden and restores normal hematopoiesis in 96-99% of children (Hunger et al. 2012). The agents used during induction include vincristine, corticosteroids (prednisone, dexamethasone), and asparaginase, with most regimens adding an anthracycline as well (usually doxorubicin or daunorubicin) (Inaba and Pui 2010).

This is followed by a consolidation therapy block, which aims to eradicate the submicroscopic residual disease that remains after the complete remission is achieved. This block varies in length (6 to 9 months) and intensity among different protocols, with those patients with higher-risk disease receiving longer and more intensive consolidation regimens. This phase of chemotherapy involves combinations of different chemotherapeutic agents to maximize synergy and minimize drug resistance, often including agents not used in the initial remission induction, such as mercaptopurine, thioguanine, methotrexate, cyclophosphamide, etoposide, and cytarabine.

Allogeneic HSCT is also considered for children with very high-risk ALL and/or persistent disease (Balduzzi et al. 2005). Contemporary HSCT protocols with high resolution HLA typing, case-based conditioning, and improved supportive care have reduced relapse-related mortality, regimen-related toxicity, and infection (Leung et al. 2011).

Finally, maintenance chemotherapy is the last and longest block of treatment in pediatric ALL, based on a much less intensive regimen than the prior chemotherapy. It has been demonstrated that a prolonged maintenance phase is related with a lower risk of relapse

once remission has been established. It usually lasts at least 2 years. Methotrexate and mercaptopurine are the typical compounds used in this treatment block. The fourth component of the treatment of ALL is therapy directed against the leukemic blasts remaining at the CNS. This approach includes both treatment of patients with clinical and subclinical CNS disease. Although BM remission could be achieved using systemic chemotherapy, most children eventually develop CNS relapse in the absence of specific therapy directed toward this sanctuary site (Cooper and Brown 2015; Inaba et al. 2013).

1.1.2. Precursor T-cell acute lymphoblastic leukemia (T-ALL).

T-ALL is a malignant disorder resulting from leukemic transformation of thymic T-cell precursors that promotes the proliferation of T lymphoblast with extensive blood and marrow involvement (Brunning 2003; Karrman and Johansson 2017). T-ALL arise from clones from various stages of the intrathymic development. The European Group for the Immunological Classification of Leukemia divides T-ALL according to developmental stage in pro-T, pre-T or immature, cortical-T and mature-T (Bene et al. 1995). The lymphoblasts in T ALL are TdT positive with variable expression of CD1a, CD2, CD3, CD4, CD5, CD7, and CD8. Only CD3 is considered lineage specific. Aberrant expression of CD10, CD79a, CD13, CD33, and CD117 (c-kit) may be observed (Brunning RD, Borowitz M, Matutes E 2001b). T-ALL present genetic and phenotypic heterogeneity and is often related to genetic alterations in transcription factors involved in hematopoietic stem and progenitor cell (HSPC) homeostasis and in master regulators of T-cell development (Weng et al. 2004).

Symptoms associated with T-ALL include leukocytosis, neurological abnormalities, respiratory difficulties, fever, recurrent infections, fatigue, paleness, skin/mucosal bleeding, bone pain and arthralgia, related to suppressed BM functions and deficiency of normal PB cells (Karrman and Johansson 2017).

T-ALL comprises 10-15% of all newly diagnosed leukemia cases in children, while the incidence in adults rises to 20-25% (Hunger and Mullighan 2015; Litzow and Ferrando 2015). Historically, patients with T-ALL have shown worse outcomes than patients with B-ALL. In addition, patients with T-ALL are generally older, thus contributing to the poorer outcomes reported. With more aggressive modern regimens, however, many patients with T-ALL have survival rates approaching those of B-ALL. Despite the increment in the survival rates of T-ALL patients by the use of intensive chemotherapy regimens, the OS remains lower than 70%, with r/r T-ALL having a particularly poor outcome (20%) (Sánchez-Martínez et al. 2019). Considering the poor survival after relapse, it is of vital

importance to identify patients at an early stage of treatment who are at increased risk of such an event. Thus, minimal residual disease (MRD) monitoring has proved important to evaluate the effect of the treatment given, thereby assessing the risk of relapse. MRD analysis may be performed by three different approaches: 1) real-time quantitative PCR (qPCR) analyses of monoclonal IG/TCR rearrangements; 2) flow cytometry (FCM) detection of aberrant leukemic immunophenotypes; and 3) qPCR analyses of leukemia-specific fusion genes and/or gene mutations (van Dongen et al. 2015).

Compared with B-ALL, T-ALL is more often cytogenetically normal with only a minority of all reported ALL cases presenting an aberrant karyotype. In fact, less than 650 cytogenetically abnormal T-ALLs in children and adolescents have been reported. Importantly, the subgroup with rare TCR rearrangements had a significantly worse outcome than all other cases (Karrman et al. 2009; Mitelman F, Johansson B 2009). On the other hand, T-ALL is more genetically diverse than B-ALL, and no genetic alterations have been identified that can predict outcome in a reproducible and independent manner. T-ALL can be discriminated according to the increased expression of various transcription factors, including TAL1, TLX1, TLX3, LMO1, LMO2, MEF2C, and HOXA. Notably, the most common abnormally activated pathway in T-ALL is the one mediated by Notch-1 (70–80% of patients). Although the majority of genetic lesions in B-ALL and T-ALL are mutually exclusive, some lesions can be found in both such as KMT2A (formerly known as MLL) rearrangement and BCR-ABL1. The most common gene fusion in pediatric T-ALL involves the STIL–TAL1 genes, leading to an overexpression of TAL1 (along with frequent overexpression of SLC17A9) which is not seen to the same extent in adult T-ALL (Chen et al. 2018). Somatic translocations involving MLL on 11q23 occur in 2–5% of childhood cases of ALL and approximately 75% of infant patients with ALL. In T-ALL, MLL rearrangement occurs in 5–10% of cases. Similar to B-cell ALL, prognosis varies based on fusion partners (Andersson et al. 2015; Girardi et al. 2017; Liu et al. 2017; Tasian and Hunger 2017; Teachey and Hunger 2013; Teachey and Pui 2019).

Treatment for T-ALL include the same stages described above for B-ALL: remission induction, consolidation and maintenance of chemotherapy. B-ALL and T-ALL blasts had different sensitivities to many conventional cytotoxic chemotherapeutics, including hydrocortisone, daunorubicin, asparaginase, cytarabine, and methotrexate. Despite some study groups use different treatment approaches for B-ALL and T-ALL, the same 12–15 cytotoxic drugs are typically used for both, and the primary differences account for the dosing and scheduling of the drugs (Teachey and Hunger 2013) (Pieters et al. 1993).

1.1.3. **Acute myeloblastic leukemia (AML).**

AML is a biologically, phenotypically and genetically heterogeneous clonal disorder caused by malignant transformation of a BM-derived, self-renewing stem cell or progenitors, leading to the accumulation of immature, nonfunctional, malignant myeloid cells. It is considered acute when the BM presents more than 20% immature leukemic blasts (Bonnet and Dick 1997). The expression of various proteins that are relatively lineage-specific for AML include CD33, CD13, CD14, CDw41, CD15, CD11B, CD36, and anti-glycophorin A. Lineage-associated B-lymphocytic antigens CD10, CD19, CD20, CD22, and CD24 may be present in 10% to 20% of AML cases, but monoclonal surface immunoglobulin and cytoplasmic immunoglobulin heavy chains are usually absent. Similarly, CD2, CD3, CD5, and CD7 lineage-associated T-lymphocytic antigens are present in 20% to 40% of AML cases (Kuerbitz et al. 1992; Smith et al. 1992).

Approximately 20% of childhood leukemia are of myeloid origin and they represent a spectrum of hematopoietic malignancies (Young et al. 2016). Based on morphology, immunophenotype, cytogenetic abnormalities, patients' outcome and clinical features, AML could be classified in several subtypes according to the World Health Organization (WHO): 1) AML with recurrent genetic abnormalities -such as t(8;21)(q22;q22) *RUNX1-RUNX1T1* comprising 5-12% of cases, t(16;16)(p13.1;q22) *CBFB-MYH11* making up 10-12% of AML, or (9;11)(p21.3;q23.3) *MLLT3-KMT2A* comprising 5-6% of cases of AML; 2) AML with myelodysplasia-related features, characterized by the presence of over 20% blasts in the blood or BM and dysplasia in two or more myeloid cell lines, generally including megakaryocytes; 3) therapy-related myeloid neoplasms, that arise secondary to cytotoxic chemotherapy and/or radiation therapy, and could be divided in alkylating agent-related AML and topoisomerase II inhibitor-related AML; 4) AML, Not otherwise specified (Arber et al. 2016; Brunning 2003; Caligiuri, Strout, and Gilliland 1997; Swerdlow SH, Campo E, Harris NL, Jaffe ES, Pileri SA, Stein H 2017).

Pediatric AML, in contrast to AML in adults, is a pathology with a prototypical occurrence of chromosomal alterations. Within the pediatric age range, certain gene fusions occur primarily in children younger than 5 years (*NUP98* gene fusions, *KMT2A* gene fusions, and *CBFA2T3-GLIS2*), while others occur primarily in children aged 5 years and older (*RUNX1-RUNX1T1*, *CBFB-MYH11*, and *NPM1-RARA*). However, pediatric patients with AML have one of the lowest mutation rates of all cancers, with less than one somatic change in a protein-coding region per megabase in most cases (Bolouri et al. 2018; Creutzig et al. 2012; Tarlock and Meshinchi 2015).

In AML, the 5-year survival rate increased between 1975 and 2010 from less than 20% to 68% for children younger than 15 years-old, and from less than 20% to 57% for adolescents aged from 15 to 19 years-old. Patients may present symptoms that include weakness, fever, infection, pallor and bleeding (Smith et al. 2014). Intensive chemotherapy combinations based on nucleoside analogs plus anthracyclines remain the standard front-line treatment of AML, followed by allogeneic HSCT, based on patients' eligibility, to consolidate CR and to prevent relapse (Baroni et al. 2020; Cornelissen and Blaise 2016; Robak 2003). There is, however, a wide range in the final outcome depending on the different biological subtypes of AML.

Treatment of pediatric AML includes an induction stage followed by a post-remission therapy. Induction phase protocols achieve an 85% to 90% CR rates. This stage promotes profound BM aplasia, which increases the morbidity by infections and treatment-related complications, where 2% to 3% of patients die during this process. The treatment at this phase includes chemotherapy -being cytarabine and anthracycline the two most effective drugs-; an immunotherapeutic approach to intensify inductions regimens by using a CD33 monoclonal antibody (gemtuzumab); or a targeted therapy to leukemia specific mutations, like the use of *FLT3* inhibitors. However, the induction failure occurs in 10% to 15% of children with AML, with similar outcomes to patients with an early relapse (Aplenc et al. 2008; Cooper et al. 2012; Creutzig et al. 2001; Gamis et al. 2014; Perl 2019). Post-remission therapy for AML aims to prolong the duration of the initial remission by the use of chemotherapy, HSCT and targeted therapy. Post-remission chemotherapy includes some of the drugs used in induction but includes non-cross-resistant drugs and, commonly, high-dose cytarabine as well. In addition, HSCT during the first remission of pediatric ALL patients achieves long term remission in 60-70% of cases (Creutzig et al. 2001; Horan et al. 2008).

1.1.4. *Biphenotypic acute leukemia.*

Biphenotypic acute leukemia, which comprises 2-5% of newly diagnosed acute leukemia (Maruffi et al. 2018), is characterized by blasts that express antigenic determinants of either both myeloid and lymphoid lineages or both B and T lineages (Legrand et al. 1998). There is considerable controversy in regards to terminology for these leukemia and a number of terms have been proposed including mixed lineage and mixed phenotype. The diagnosis of biphenotypic acute leukemia is based on the immunophenotypic detection of antigenic markers specific for two different lineages on the blast population. Biphenotypic acute leukemia is morphologically diverse, even though the majority of

cases show no differentiating features. However, some cases may be regarded as a myeloid subtype, while others have the morphologic features of acute lymphoblastic leukemia and rare cases present with dual populations of myeloid and lymphoid appearing blasts. Cytogenetic abnormalities are present in a high percentage of cases of biphenotypic acute leukemia. These include the Philadelphia chromosome - $t(4;11)(q21;q23)$ -, or other 11q23 abnormalities. In these cases, the lymphoid lineage component is B cell, being CD10⁺ in the Philadelphia chromosome cases and CD10⁻ in the $t(4;11)$ cases (Brunner 2003; Brunner RD, Matutes E, Borowitz MJ, Flandrin G, Head D 2001; Carbonell et al. 1996).

1.2. New therapeutic approaches for acute leukemia.

Despite great progress in the treatment of children with acute leukemia, a considerable number of patients continue to die from it and even in survivor patients, the short and long-term toxicities of standard therapy are substantial (Hase et al. 2013; Wayne, Reaman, and Helman 2008). Over the past 5 years, a shift has occurred in the treatment of patients with r/r B-ALL, and a number of targeted therapies and immunotherapies have shown to be remarkably efficient, leading to an improved OS for this disease. Unfortunately, neither targeted therapies nor immunotherapies have been successful in the treatment of T-ALL (Teachey and Pui 2019). Monoclonal antibodies against surface antigens such as CD19, CD20, CD22, and CD52 have been used either in an unconjugated form (rituximab and epratuzumab), conjugated to immunotoxins or chemotherapeutic agents (moxetumomab and inotuzumab ozogamicin), or as a bispecific antibody (blinatumomab) (Hoelzer 2011). Blinatumomab is a bispecific T-cell engager (BiTE) anti-CD19/CD3 molecule, which enhances natural cytotoxic killing of T cells by binding a protein expressed on the leukemic blast (CD19) and one expressed on autologous T cells (CD3). Indeed, Blinatumomab firstly showed promising clinical efficacy as a means of eradicating persistent MRD after upfront chemotherapy (Hoffman and Gore 2014; Topp et al. 2011). Another example is Inotuzumab ozogamicin, which is a calicheamicin-based antibody-drug conjugate targeting CD22. Pretreated children with r/r B-ALL who received inotuzumab achieved CR in 67% of all cases, with MRD-negative CR occurring in 71% of those patients (Bhojwani et al. 2019). In T-ALL, anti-CD38 monoclonal antibody daratumumab have shown promising efficacy (Bride et al. 2018).

One of the early treatments for patients with advanced acute leukemia included adoptive cell therapy to induce a graft-versus-leukemia (GvL) effect. In this regard, chimeric antigen receptor (CAR) based therapies, that redirect T cells specificity and function,

have emerged as a promising strategy that has demonstrated impressive antitumoral effects in patients with leukemia. There are several clinical trials using CAR T cells that differ in the receptor construct for patients with acute leukemia. Four CAR T cell products targeting CD19 are now approved for clinical use by the Food and Drug Administration (FDA): tisagenlecleucel (Kymriah™) (U.S. Food and Drug Administration 2017a) for pediatric B-ALL and adult diffuse large B-cell lymphoma subtypes (DLBCL), axicabtagene ciloleucel (Yescarta™) (U.S. Food and Drug Administration 2017b) for DLBCL, brexucabtagene autoleucel (Tecartus™) (Gilead 2020) for adults with mantle cell lymphoma, and isocabtagene maraleucel (Breyanzi™) (Bristol-Myers Squibb 2021) for adults with r/r large B-cell lymphoma (Brown et al. 2020; Brudno and Kochenderfer 2019). In addition, anti-CD22 and anti-CD20 CAR-transduced T cells hold therapeutic promise for children and adults with B-ALL (Haso et al. 2013; Jensen et al. 1998). Unfortunately, translating immunotherapies into a T-ALL setting has considerable problems, including the risk of severe immunodeficiency derived from the elimination of normal T lymphocytes -the so-called fratricide by T-cell-targeted clones. Despite these issues, preclinical studies of T-ALL have indicated efficacy with CAR T cells targeting a number of antigens, including CD1a, CD2, CD5, and CD7 (Gomes-Silva et al. 2017; Sánchez-Martínez et al. 2019; Teachey and Pui 2019). In spite of the increasing number of targeted therapeutic tactics to treat AML, patient outcomes have remained poor, probably because of the heterogeneous and extremely polyclonal character of AML. Several CARs have been developed in order to redirect T-cell against CD33, CD133 or CD123 antigens expressed in AML, with controversial results. Although clinical efficacy has been demonstrated, myeloablative toxicity has also been found (Baroni et al. 2020; Bueno et al. 2019; Fathi et al. 2020).

The increase of CR of patients treated with CAR T cells and the possibility to receive HSCT suggest that this promising immunotherapy could be used as a primary front-line treatment or may provide a bridge for allogenic HSCT (Brown et al. 2020; Davila et al. 2014). Currently, over 500 CAR T cell trials are being conducted worldwide and 5 CAR T cell products are already available on the market: the four explained above, targeting CD19 for different adult and pediatric hematological malignancies, plus Abecma™ (U.S. Food and Drug Administration 2021) for multiple myeloma expressing BCMA.

1.3. CAR T cells.

CARs are synthetic proteins firstly generated by Eshhar and colleagues in 1989, which are based on the T cell receptor constant (cTCR) domains fused to the variable domains of a monoclonal antibody (Gross, Waks, and Eshhar 1989). This combination results in chimeric genes endowing T lymphocytes with antibody-type specificity, potentially allowing cellular adoptive immunotherapy against types of tumors that could not otherwise be targeted by these cells. In order to optimize and extend the applicability of these so-called T-bodies, a single-chain approach was developed in 1993 by designing chimeric genes composed of a single-chain variable fragment domain (scFv) of an antibody linked to a CD3 ζ chain, the common signal transducing subunits of the immunoglobulin receptor and the TCR (Eshhar et al. 1993). These minimal structures, termed first generation CARs, effectively redirected T cell cytotoxicity by the recognition of native cell-surface antigens independently of antigen processing or MHC-restricted presentation. Therefore, CARs do not have to be matched to the patient's HLA and can recognize tumors that have downregulated HLA expression (Cheadle, Gilham, and Hawkins 2008; Sadelain, Brentjens, and Rivière 2009; Seliger, Ritz, and Soldano 2006). However, first generation CARs do not sustain T-cell response because the activation of effector cells without costimulation signaling results in a poor T cell proliferation, and/or in the induction of anergy or apoptosis (Harding et al. 1992; Krause et al. 1998).

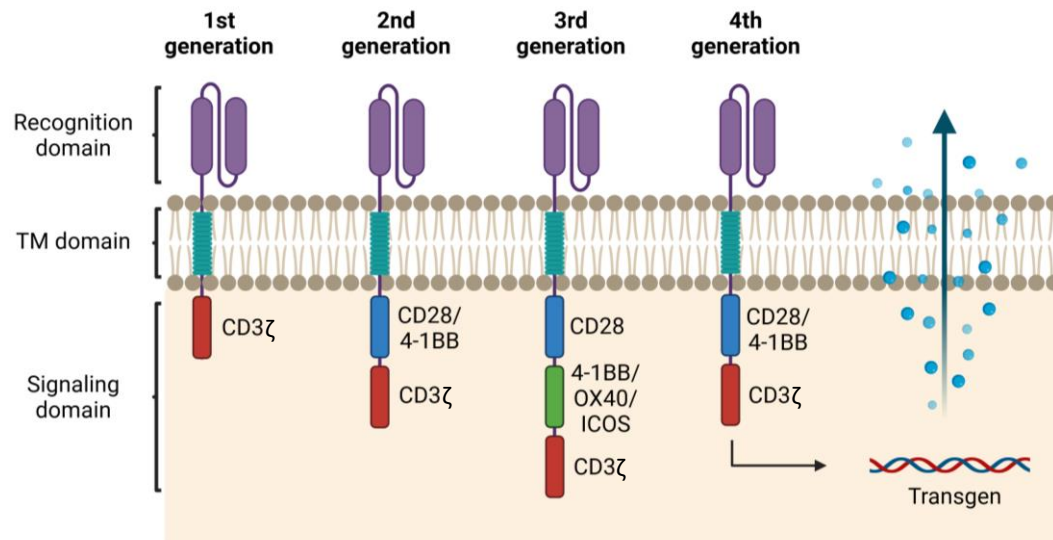
With the aim of overcoming this problem, the second generation CARs incorporated costimulatory domains (initially CD28) to the CD3 ζ signaling domains while keeping tumor-associated antigens (TAA) recognition and anti-tumor ability. In response to TAA, effector cells expressing second generation CARs showed increased interleukin (IL) 2 secretion, T cell proliferation and enhanced tumor rejection, in the absence of exogenous costimulation. (Maher et al. 2002). In the following years, a newer second generation CARs were developed using different costimulatory signaling domains, including 4-1BB, OX40, DAP10, CD80, CD86, CD70 and ICOS, each one of them conferring different characteristics to the CAR expressing effector cells (Brentjens et al. 2007; Finney, Akbar, and Lawson 2004; Guedan et al. 2014, 2018; Sadelain et al. 2009; Sadelain, Brentjens, and Rivière 2013; van der Stegen, Hamieh, and Sadelain 2015). CARs containing either CD28 or 4-1BB costimulatory domains have been the most used and studied to date, showing impressive responses in clinical trials, mainly against hematological malignancies (Brentjens et al. 2013; Kochenderfer et al. 2012; Maude et al. 2014; Porter et al. 2011). CD28 intracellular domain stimulates greater CAR T cell functionality, whereas the 4-1BB intracellular domain promotes greater CAR T cell persistence (Guedan et al. 2019). Several factors can influence the persistence of adoptively

transferred T cells, including patient preconditioning, *ex vivo* culture conditions, development of T cell exhaustion, host immune responses against the cellular infusion product, or the molecular design of CARs (Guedan et al. 2018).

Consequently, CAR designs must include 3 modules: an extracellular target binding module, a transmembrane domain (TM) and an intracellular signaling domain that transmits activation signals. The moieties used to bind to antigen are divided into 3 categories: 1) scFv derived from antibodies; 2) Fab antigen-binding fragment (Fab) selected from libraries; or 3) nature ligands that engage their cognate receptor (Sadelain et al. 2013). TM domains are primarily considered a structural requirement, anchoring the CAR in the cell membrane, and are usually derived from molecules regulating T cell function, such as CD8 and CD28. The intracellular module typically consists on the T cell receptor CD3 ζ chain and one or more costimulatory signaling domains (Guedan et al. 2018; Sadelain et al. 2013).

Despite the impressive results obtained with CAR T cells, the principal issue revealed in the initial trials has been the poor *in vivo* persistence. One approach to solve this caveat is to incorporate two costimulatory signaling domains in tandem into the signaling module. These so-called third generation CARs exhibit improved proliferation, cytokine secretion, resistance to apoptosis and *in vivo* persistence as compared to second-generation CARs (Carpenito et al. 2009; Hartmann et al. 2017; Zhong et al. 2010). CAR constructs combining the CD28 and 4-1BB intracellular domains are the most widely studied (Tamma et al. 2010; Till et al. 2012; Wang et al. 2007).

In addition, although adoptive CAR T cells therapy has shown efficacy against several malignancies, cancer cells may lose expression of the targeted antigen promoting misrecognition by CAR T cells. Fourth generation CARs, also termed TRUCKs or armored CARs, combine the expression of a second generation CAR with factors that enhance anti-tumor activity, such as cytokines, costimulatory ligands or enzymes that degrade the extracellular matrix of solid tumors (Chmielewski and Abken 2015; Hartmann et al. 2017). Another approach to improve CAR T cells efficacy against antigen loss include upfront treatment with dual-targeting agents, especially in leukemia, taking advantage of markers that are commonly expressed in B-ALL such as CD22, CD123 and CD20 (Ruella and Maus 2016; Zah et al. 2016).



transgenic protein, such as cytokines, costimulatory ligands, or enzymes. Created with BioRender.com.

CD19 has become the most investigated CAR target and a paradigm for CAR therapy because of its association with all B cell malignancies, its expression in most -if not all- tumor cells, its absence from vital tissues, and the proved effectiveness of different second generation CARs targeting CD19 (Sadelain 2015). CART19 induces complete remission, including molecular remission, in patients for whom chemotherapies, often utilizing multiple drug combinations, have led to drug resistance and tumor progression. Taken together, the preclinical and clinical studies on CD19 CARs have validated the development of second generation CARs, established the feasibility of implementing T cell engineering in the clinic, and demonstrated the effective potency of CAR therapy in a group of hematological malignancies with a common feature: the expression of CD19. In 2011, the first promising results showing complete remission from patients with chronic lymphocytic leukemia (CLL) were reported (Kalos et al. 2011). Shortly after, in 2013, CART19 was evaluated to treat patients with B-ALL (Brentjens et al. 2013). These results led to the FDA approval of CD19 CAR T cells for r/r ALL and for DLBCL in 2017. On the other hand, studies based on CART19 have revealed three potential toxicities of CAR therapy: B cell aplasia, severe cytokine release syndrome (CRS), and immune effector cell-associated neurotoxicity syndrome (ICANS), although these toxic effects are reverted when the target cell is eliminated or when CAR T cells engraftment is terminated

(June and Sadelain 2018). Furthermore, it is expected that the selective pressure imparted by CAR T cells will sometimes yield antigen escape variants by losing CD19 expression. The CD19 paradigm has showed the enormous potential and current limitations of CAR technology, providing insights into its application to solid tumors, which is one of the major challenges for the CAR field (Sadelain 2015).

Most clinical trials use autologous effector cells that are genetically modified to express the CAR of choice to later on CAR T cells being expanded and reinfused into the patient. However, autologous cell sources may have some disadvantages, such as a low T cell number or poor quality of the cells due to the previous treatments, which may lead to manufacture failure; T cells dysfunction mediated by immunosuppressive mechanism exerted by the tumor; manufacture failure; or the time required for the manufacturing production rendering this approach useless for patients with rapid disease progression. (Morgan et al. 2020). The use of allogeneic effector cells could provide more flexibility for treatment protocols by preparing and storing ready-to-use CAR T cells. However, allogeneic approaches are associated with two major inconvenients. First, allogeneic T cells may cause life-threatening graft-versus-host disease (GvHD). Second, these allogeneic T cells may be rapidly eliminated by the host immune system, limiting their antitumoral activity. Several approaches have been developed for administering allogeneic CAR T cells with reduced risk of GvHD: usage of donor-derived allogeneic T cells in stem cell transplant recipients, usage of virus-specific memory T cells, usage of non- $\alpha\beta$ T cells, and gene editing with TCR deletion in $\alpha\beta$ T cells. NK cells, invariant NKT cells and $\gamma\delta$ T cells have a reduced risk of producing GvHD and have also been used for CAR therapy (Depil et al. 2020). Another method of non-reactive allogeneic effector cells enrichment is using antigen-experienced memory T cells for CAR transduction. Memory T cells express CD45RO marker while lack CD45RA expression. CD45RA⁻ CD45RO⁺ memory T cells exert a memory response to prior pathogens or vaccines and can mediate graft-versus-tumor effects without inducing GvHD (Anderson et al. 2003; Zheng et al. 2008). Additionally, using allogeneic CAR T cells leads to an off-the-shelf production that allows the production of a ready-to-use therapy for patients with low or deficient T cells, as it usually happens in pediatric patients.

Although different targets for AML and T-ALL are currently being explored, a successful CAR T cell therapy for these diseases has not been found yet and requires further research to overcome different hurdles as T cell aplasia or myelosuppression.

1.4. Role of NKG2D-NKG2DL axis in cancer.

The NKG2D receptor plays an important role in protecting the host from infections and cancer. It modulates lymphocyte activation by recognizing ligands induced on infected, DNA-damaged, stressed or tumor cells, thus promoting immunity to eliminate ligand expressing cells. Because these ligands are not widely expressed on healthy tissues, NKG2DL may constitute a useful target for immunotherapeutic approaches in cancer (Spear, Wu, et al. 2013).

1.4.1. *NKG2D receptor.*

NKG2D, also known as Klrk1, is a C-type lectin-like receptor firstly described in 1993. In humans, it is constitutively expressed in $\gamma\delta$ T cells, CD8⁺ $\alpha\beta$ T cells and Natural Killer cells (NK), playing a role as an activating immune receptor (Bauer et al. 1999; Yabe et al. 1993). Under certain conditions, human CD4⁺ T cells can also express NKG2D, such as cytomegalovirus infection, Crohn's disease, rheumatoid arthritis and cancer (Allez et al. 2007; Groh et al. 2003; Sáez-Borderías et al. 2006). NKG2D is a type II transmembrane glycoprotein, which lacks signaling elements in the intracellular domain, therefore needing to associate with an adaptor molecule to initiate the activation cascade. In humans, this adaptor molecule is DNAX-activating protein of 10 kDa (DAP10) (Wu et al. 1999). Therefore, the NKG2D receptor consists of a homodimer of two disulfide-linked transmembrane proteins associated with four adaptor molecules to form a hexameric complex (Campos-Silva, Kramer, and Valés-Gómez 2018; Wensveen, Jelenčić, and Polić 2018). DAP10 contains a YXXM tyrosine-based motif, similar to that found in the co-stimulatory molecules CD28 and ICOS (Wu et al. 1999), which recruits and activates the p85 subunit of phosphoinositide 3-kinase (PI3-K) and growth factor receptor-bound protein 2 (Grb2) (Upshaw et al. 2006). Thus, DAP10 provides a costimulation signal to T cells rather than a primary activation signal (Sentman and Meehan 2014). In addition, ubiquitination of DAP10 mediates ligand-induced endocytosis of NKG2D. Moreover, NKG2D engagement, apart from promoting cell activation and the downregulation of NKG2D expression, also promotes degradation of the CD3 ζ signaling adaptor by inducing caspase-3/7 activation (Campos-Silva et al. 2018).

NKG2D expression and signaling can be regulated by cytokines and tumor-derived factors. On the one hand, cytokines such as IL-2, IL-7, IL-12, IL-15 increase cell surface expression of NKG2D. IL-15 signaling not only regulates NKG2D expression but also

increases the expression of DAP10 and phosphorylates the adaptor molecule to prime NKG2D signaling (Dhanji and Teh 2003; Horng, Bezbradica, and Medzhitov 2007; Zhang et al. 2008). On the other hand, interferon gamma (IFN- γ) and tumor growth factor beta (TGF- β) have been shown to decrease NKG2D expression. In addition, IL-21 has been shown to reduce expression of DAP10 and NKG2D in human CD8⁺ T cells and NK cells (Burgess et al. 2006, 2008).

1.4.2. NKG2D ligands.

NKG2DL mark cellular stress and they are expressed by many types of tumor cells, including pediatric acute leukemia, and virus-infected cells (Groh et al. 2001; Pende et al. 2002; Schlegel et al. 2015; Torelli et al. 2014). Human NKG2DL can be classified into two families: the major histocompatibility complex (MHC) Class I-related chains A (MICA) and B (MICB) and retinoic acid early transcripts-1 (RAET1), also known as UL-16 binding proteins 1 to 6 (ULBP1-6) (Zhang, Basher, and Wu 2015). MICA/B proteins generally contain transmembrane regions, while the ULBPs are mainly anchored to the membrane via glycosyl-phosphatidyl-inositol (GPI) moieties (Campos-Silva et al. 2018). The NKG2DL MICA and MICB have α 1, α 2, and α 3 extracellular domains and transmembrane domains, sharing structural homology with MHC-I. ULBP1-6 ligands, however, lack the α 3 domain (Zhang et al. 2015). NKG2DL are highly polymorphic proteins, specially MICA and MICB, which can affect the affinity of receptor-ligand interaction (Romphruk et al. 2009; Stephens 2001). For example, the MICA-129Met variant triggers stronger NKG2D signaling leading to an increased degranulation and IFN- γ production than the MICA-129Val variant, although MICA-129Met isoform triggers faster and stronger NKG2D downregulation (Isernhagen et al. 2015).

While NKG2DL expression is tightly restricted in healthy tissues, these ligands can get upregulated under many different types of stress situations (Eagle, Jafferji, and Barrow 2009). The expression of NKG2DL at the cell surface arises from multiple levels of regulation (figure 4) such transcription, messenger ribonucleic acid (mRNA) stability, translation, protein stabilization, and excretion/shedding of ligands from cells (Campos-Silva et al. 2018; Duan et al. 2019; Spear, Wu, et al. 2013; Zingoni et al. 2018).

Firstly, NKG2DL can be regulated at transcriptional level by multiple molecular pathways, such as different stress signals, including proliferative signals, malignant transformation, infection, or oxidative stress activate deoxyribonucleic acid (DNA) damage responses. In this context, NKG2DL can be upregulated by the sensor kinases ATM/ATR signaling,

heat-shock response and proliferative signals that enhance E2F activity (Fionda et al. 2009; Gasser et al. 2005; Jung et al. 2012). Different mechanisms of transcriptional repression have also been described, like STAT3 transcription factors interacting with the promotor of MICA and repressing its expression, or several promotor polymorphisms associated with a decreased expression (Bedel et al. 2011; Rodríguez-Rodero et al. 2007).

Secondly, although mRNA coding for several NKG2DL can be found in healthy cells, these molecules are rarely expressed at the cell surface in the absence of pathology, which imply post-transcriptional and post-translational regulation (Raulet et al. 2013). In this regard, micro-RNAs (miRNA) have been shown to interact with NKG2DL mRNA affecting their expression. One example occurs during human cytomegalovirus (HCMV) infection, when miRNA miRUL112 downregulates MICB and ULBP1 expression, promoting the immune evasion of virus-infected cells (Stern-Ginossar et al. 2008). This also happens in cancer cells, as miR-519a-3p inhibits NK cells cytotoxicity of breast cancer by downregulation of ULBP2 and MICA expression (Breunig et al. 2017).

Finally, the surface expression levels of NKG2DL can be controlled by mechanisms implicated in the regulation of its release as soluble form by various processes, including protease-mediated cleavage, exosome secretion, and alternative splicing (Salih, Rammensee, and Steinle 2002; Zingoni et al. 2018). NKG2DL can be proteolytically shed from the cell surface by matrix metalloproteinases (MMPs) and a disintegrin and metalloproteases (ADAMs), or liberated from the membrane by phospholipase C in the case of glycosylphosphatidylinositol (GPI)-anchored molecules. Moreover, NKG2DL can be secreted in extracellular microvesicles (exosomes) together with other tumor-derived molecules (Chitadze et al. 2013). Specific NKG2DL are preferentially, although not exclusively, released by one of these two mechanisms and the biochemical basis for this difference resides mainly on the nature of the membrane attachment of the protein (Campos-Silva et al. 2018). The allelic variant MICA*008, GPI-anchored, is resistant to proteolytic cleavage and is mostly released from cells in association with exosomes (Ashiru et al. 2010). In addition, ULBP1 and ULBP3 that are anchored to the membrane by GPI, are more resistant to cleavage and preferentially secreted like exosome vesicles. However, the type of membrane anchoring is not the only factor that determines NKG2DL release. In the case of ULBP2 and ULBP3, both proteins are GPI-anchored to the membrane but only ULBP2 is usually released as a soluble form because of an increased susceptibility to metalloprotease-mediated cleavage (Fernández-Messina et al. 2010).

In addition to shedding and exosome secretion, alternative splicing and ubiquitination represents another way of generating soluble forms of some ligands (Cao et al. 2008; Fernández-Messina, Reyburn, and Valés-Gómez 2016).

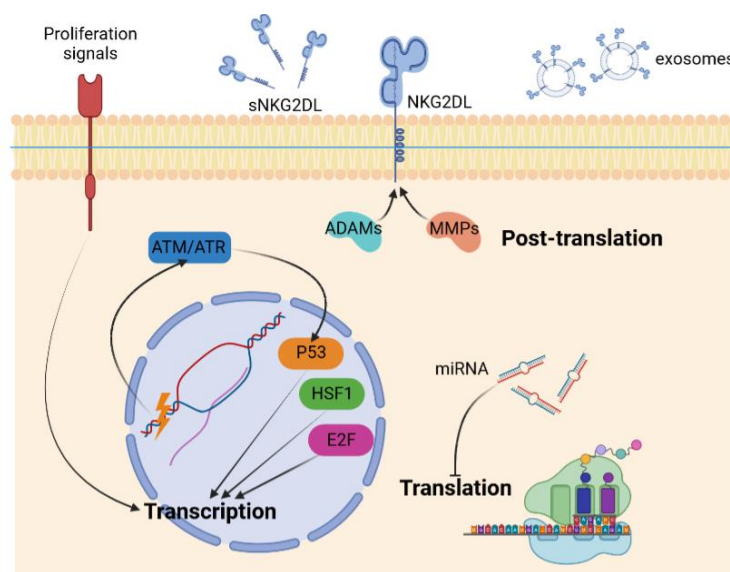


Figure 4. Levels of regulation of NKG2DL expression. Transcriptional level: Transcription factors like P53, E2F or heat shock transcription factor 1 (HSF1) promote the transcription of NKG2DL genes; proliferative signals can also upregulate NKG2DL expression through ATM/ATR pathway. Translational level: miRNAs interact with NKG2DL mRNA affecting their expression. Post-translational level: ADAMs and MMPs produce NKG2DL shedding as soluble forms or exosomes. Adapted from Duan et al. 2019. Created with BioRender.com.

1.4.3. NKG2D-CAR T cells for cancer treatment.

Due to the fact that the NKG2D receptor-ligand axis provides a specific system for immune cells to recognize tumor cells, NKG2D-based CAR T cells have recently emerged as a potential strategy to redirect T cells against different tumors. This novel therapeutic approach has important advantages: 1) it is based on the natural occurring NKG2D-NKG2DL tumor immunosurveillance pathway; 2) NKG2D-CAR construct is fully human, avoiding immunogenicity produced by CARs based on mouse-derived antibodies; 3) NKG2D-CAR T cells recognize 8 different NKG2DL, avoiding tumor immunoescape by antigen loss; and 4) NKG2D-CAR T cells target the tumor microenvironment (TME) (Spear, Wu, et al. 2013).

The first NKG2D-based CAR therapy was reported in 2005 (Zhang, Lemoi, and Sentman 2005). These results established the first proof of concept for the use of NKG2D-CAR T cells in human cancer. After this first publication, many authors have demonstrated the efficacy of NKG2D-CAR T cells against different human tumor types including multiple myeloma, ovarian carcinoma, lymphoma, Ewing's sarcoma and osteosarcoma both *in*

vitro and *in vivo* (Barber et al. 2008; Fernández et al. 2017; Lehner et al. 2012; Spear, Barber, et al. 2013). In addition, NKG2D CAR can recognize NKG2DL expressed on immunosuppressive cells, such as myeloid-derived suppressor cells (MDSC), regulatory T cells, and tumor vasculature cells within the TME support tumor survival and progression (Barber, Rynda, and Sentman 2009; Zhang and Sentman 2013).

Regarding the constructs, different designs for NKG2D CARs have been proposed. On the one hand, constructs based on the full-length NKG2D receptor fused with the CD3 ζ have been developed. The full length NKG2D associates with the adaptor molecule DAP10, which is necessary for surface expression and signaling, allowing those first generation-like structures to function as a second generation CAR (Lonez et al. 2018; Raulet 2003; Zhang et al. 2005). Similarly, another NKG2D-DAP10-CD3 ζ construct was designed by Campana *et al.* to engineer NK cells (Chang et al. 2013). On the other hand, several groups have been using second generation CARs combining the extracellular domain of NKG2D for ligand recognition fused with costimulatory domains CD28/4-1BB and the cytotoxic domain CD3 ζ . (Fernández et al. 2017; Lehner et al. 2012; Song et al. 2013). Effector cells that express DAP10-associating CARs produce IFN- γ , granulocyte macrophage colony-stimulating factor (GM-CSF) and tumor necrosis factor α (TNF- α) while second generations NKG2D CARs produce IL-2, IL-5, IFN- γ and TNF- α (Sentman and Meehan 2014). Moreover, NKG2D-CAR T cells carrying CD28/4-1BB costimulatory domains show a great expansion *in vivo* (Porter et al. 2011), while NKG2D CARs that associate with DAP10 do not persist long *in vivo* in animal studies (Barber, Meehan, and Sentman 2011).

The expression of endogenous NKG2D receptor may be downregulated in the presence of immune regulatory cytokines, sNKG2DL or TGF- β . Consequently, the anti-tumor immunosurveillance of effector cells that relies in NKG2D-NKG2DL interactions would decrease. However, the activity of NKG2D-CAR T cell remains unimpaired after exposure to sNKG2DL (Groh et al. 2002; Zhang, Barber, and Sentman 2006). Importantly, these CARs designs include a full human receptor in contrast to usual scFv-based CARs derived from mouse, thus reducing the immunogenicity of the chimeric receptor (Sentman and Meehan 2014).

1.5. Mechanisms of immunoescape.

Despite the proven efficacy of CAR T cells for the treatment of cancer, specifically hematological malignancies, there are some patients that barely respond to CAR T cell therapy. Some limitations for CAR T cells application include the lack of tumor-specific target antigens, tumor heterogeneity and plasticity which can lead to tumor escape due to loss of antigen expression, T cell dysfunction driven by CAR-mediated tonic signaling or chronic antigen exposure, and inactivation of CAR T cells by the immunosuppressive TME (Rodriguez-Garcia et al. 2020).

A common mechanism of resistance to CAR T cells is the onset of tumors with loss or downregulation of the target antigen. The CD19-loss is a specific tumor immunoescape mechanism linked to poor prognosis leukemia and observed in the treatment of hematological malignancies by CD19-directed immunotherapies. This is related with the cancer heterogeneity and its capability to evolve over time adapting to the environment (Ruella and Maus 2016). CD19-negative leukemia resulting after CD19-directed therapy show mutations in the CD19 gene and CD19 splicing variants. In particular, exon 2 of CD19 is frequently spliced out, lacking the CAR-recognized epitope (Sotillo et al. 2015). Furthermore, the induction of a long-term myeloid switch CD19 negative and the selection of a preexisting CD19-negative myeloid clone by CART19 treatment have also been proposed as mechanisms of escape (Gardner et al. 2016; Jacoby et al. 2016). In addition, tumors may develop mechanisms to evade NKG2D-mediated immunosurveillance as release of NKG2DL from the cell surface (Salih et al. 2002). This strategy has two different effects: on one hand the release of NKG2DL as soluble forms reduce their cell surface expression, avoiding tumor cell recognition by NKG2D-redirected therapies; on the other hand, the presence of sNKG2DL causes downmodulation of the NKG2D receptor and impairs tumor clearance by immune cells. Although these effects on wild type NKG2D have been established, it has been shown that the anti-tumor potential of NKG2D-CAR bearing T cells remained unimpaired after exposure to a high concentrations of soluble MICA (Zhang et al. 2006). Moreover, CARs can provoke reversible antigen loss through trogocytosis, an active process in which the target antigen is transferred to T cells, thereby decreasing target density on tumor cells and abating T cell activity by promoting fratricide T cell killing and T cell exhaustion (Hamieh et al. 2019). Furthermore, it has been demonstrated that in chemotherapy-resistant leukemic stem cells from AML patients, the expression of NKG2DL is lost thus enabling their immune evasion (Paczulla et al. 2019).

The bone marrow microenvironment (BMM) has been shown to participate in resistance of acute leukemia to chemotherapy and immunosuppression (Ayala et al. 2009; Zanetti et al. 2020). The BMM is a well-established site of sanctuary for hematological malignancies. In leukemia, the BMM serves as the site of initiation and progression of the disease (Moses et al. 2016). Two non-mutually exclusive contributions for hematopoietic niches to leukemogenesis have been proposed: the acquisition of mutations or functional alterations by niche cells that predispose for malignancy development, and niche remodeling by transformed hematopoietic cells that facilitates disease manifestation and/or progression (Méndez-Ferrer et al. 2020). The BM is also the primary site where residual leukemic cells survive during standard chemotherapy and is the most frequent location of leukemia relapse (Zanetti et al. 2020).

The leukemia microenvironment contains several cell types which can dampen T cell responses. These include leukemia blasts, myeloid-derived suppressor cells (MDSCs), regulatory T cells (T_{regs}), tumor-associated macrophages (TAMs), and dendritic cells. Additionally, structural elements also compound the BMM, including hematopoietic, endothelial, osteoblastic, and stromal components. Mesenchymal stem cells (MSCs) are stromal cells that highly express indoleamine 2,3-dioxygenase (IDO), which correlates with expansion T_{regs} and could inhibit CAR T cell effector function. Furthermore, T_{regs} secrete immunosuppressive cytokines such as IL-10 or TGF- β and mediate suppression of antigen presenting cells (APC) by CTLA-4, which in turn suppresses antigen-specific CD8⁺ T cell cytotoxicity (Liyanage et al. 2002; Togashi, Shitara, and Nishikawa 2019). TGF- β itself reduces the surface expression of NKG2D in NK and T cells (Lazarova and Steinle 2019). Moreover, TAMs contribute to suppression of effective adaptive immunity by producing IL-10 and TGF- β , immunosuppressive prostaglandins and IDO, resulting in metabolic starvation of T cells. (Mantovani et al. 2017; Zhang et al. 2012). Myeloid-derived suppressor cells (MDSCs) also accumulate in the tumor niche, supporting leukemia progression, and are associated with poor prognosis (Zhang et al. 2016). Similar to TAMs, MDSCs have also been seen to be implicated in limiting the effects of CAR T cell therapy by elimination of nutrients needed for T cell proliferation such as arginine, cysteine, or tryptophan, production of IL-10 and TGF- β , and induction of T_{regs} (Gabrilovich and Nagaraj 2009).

Finally, many suppressive effects of the leukemia microenvironment are mediated through soluble environmental factors, including secreted anti-inflammatory cytokines (IL-10 and TGF- β) and alteration of chemokine-mediated trafficking (CCL4, CXCL10). In addition, metabolic changes could drive the BMM to support leukemic cell growth and survival while limiting immune responses (Epperly, Gottschalk, and Velasquez 2020).

2. HYPOTHESIS

Based on the importance of NKG2D/NKG2DL axis in the anti-tumor immunosurveillance, we hypothesize that leukemic blasts from pediatric patients could overexpress NKG2DL and would thus represent an interesting target for NKG2D CAR T cells.

In this regard, engineering CD45RA⁺ T cells with a second generation NKG2D-41BB-CD3 ζ CAR cells could efficiently eliminate leukemic blasts and become a novel therapeutic approach for pediatric acute leukemia.

Additionally, we hypothesize that GMP-like manufacturing of clinical-grade allogenic CD45RA⁺ NKG2D-CAR T cells (hereinafter NKG2D-CART, unless otherwise specified) could be feasible and reproducible allowing translation of this therapy to the clinical setting.

3. OBJECTIVES

The main objectives of this research project were to:

- Explore the suitability and the efficacy of using NKG2D CAR T cells as therapeutic approach for pediatric acute leukemia.
- Optimize a GMP-compliant manufacturing protocol to produce NKG2D-CAR T cells for clinical use.

Additionally, the secondary objectives of this project were to:

- Determine the expression of NKG2DL in pediatric acute leukemia samples and cell lines.
- Optimize the production of NKG2D CAR encoding lentiviral particles.
- Analyze the cytotoxicity of NKG2D-CART against pediatric acute leukemia primary samples and cell lines.
- Explore the anti-tumor ability of NKG2D-CART in a murine model of human T-ALL.
- Study the effects of different immunoescape mechanisms such as sNKG2DL, TGF- β and leukemia-initiating cells (LICs) in NKG2D-CART.
- Analyze NKG2D-CAR T cell products to comply with the specifications derived from the quality and complementary controls carried out in accordance with the instructions of the Spanish Regulatory Agency of Medicines and Medical Devices (AEMPS) for the manufacture of investigational advanced therapy medicinal products (ATMPs).

4. MATERIALS AND METHODOLOGY

4.1. Materials

4.1.1. *Cell lines.*

All human cell lines used in this project are summarized in Table 1. Jurkat cells expressing green fluorescent protein (GFP) and luciferase (Luc) were kindly provided by Dr. Pablo Menéndez, from Josep Carreras Leukemia Research Institute (Barcelona, Spain). Dulbecco's Modified Eagle's Medium with GlutaMAX™ (DMEM; Gibco, NY, USA, 61965-026), Iscove's Modified Dulbecco's Medium (IMDM; Gibco, 12440-046) and Roswell Park Memorial Institute medium-1640, (RPMI; Sigma-Aldrich, MO, USA, R8758) were employed as cell culture media, supplemented with Fetal Bovine Serum (FBS; Cytiva, WA, USA, 16SV30160.03). The specific cell culture medium and percentage of FBS used for each cell line are specified in Table 1.

4.1.2. *Antibodies and dyes.*

All antibodies and dyes used in this project are compiled in Table 2.

Cell line	Disease/tissue	Culture method	Reference
B-ALL			
NALM-6	Acute lymphoblastic leukemia	RPMI, 10% FBS	ATCC, VA, USA, CRL-3273
REH	Acute lymphocytic leukemia (non-T; non-B)	RPMI, 10% FBS	ATCC, CRL-8286
RS4;11	Acute lymphoblastic leukemia	RPMI, 10% FBS	ATCC, CRL-1873
TOM-1	Acute lymphoblastic leukemia	RPMI, 10% FBS	DSMZ, Germany, ACC 578
T-ALL			
CEM	Acute lymphoblastic leukemia T	RPMI, 10% FBS	ATCC, CRL-2265
JURKAT	Acute T cell leukemia	RPMI, 10% FBS	ATCC, TIB-152
MOLT-3	Acute lymphoblastic leukemia T	RPMI, 10% FBS	ATCC, CRL-1552
MYELOID			
KASUMI-1	Acute myeloblastic leukemia	RPMI, 20% FBS	ATCC, CRL-2724
K562	Chronic myelogenous leukemia (CML)	IMDM, 10% FBS	ATCC, CCL-243
ME-1	Acute myeloid leukemia	RPMI, 20% FBS	DSMZ, ACC 537
BIPHENOTYPIC			
MV4;11	Biphenotypic B myelomonocytic leukemia	IMDM, 10% FBS	ATCC, CRL-9591
SEM	Acute lymphoblastic leukemia	IMDM, 10% FBS	DSMZ, ACC 546
OTHERS			
HEK293T	Human embryonic kidney	DMEM, 10% FBS	ATCC, CRL-11268

Table 1. Summary of cell lines according to disease/tissue subtypes and culture method.

Reactivity	Antigen/ dye	Clone	Fluorochrome	Reference
Human	MICA	159227	PE	R&D systems, MN, USA, FAB1300P
Human	MICB	236511	APC	R&D systems, FAB1599A
Human	ULBP-1	170818	PE	R&D systems, FAB1380P
Human	ULBP-2,5,6	165903	APC	R&D systems, FAB1298A
Human	ULBP-3	166510	PE	R&D systems, FAB1517P
Human	ULBP-4	709116	APC	R&D systems, FAB6285A
Human	CD45RA	HI100	APC	Biolegend, CA, USA, 304111
Human	NKG2D	1D11	PE	Biolegend, 320806
Mouse	CD45	30F11	APC	Biolegend, 103112
Human	CD45	2D1	PerCP-Cy5.5	Biolegend, 368504
Human	CD3	HIT3a	PE-Cy7	Biolegend, 300316
Human	CD8	SK1	FITC	Biolegend, 344703
Human	CD4	OKT4	APC-Cy7	Biolgend, 317418
Human	CD4	OKT4	PerCP	Biolgend, 31743125
Human	PD-1	EH12.2H7	APC	Biolegend, 329907
Human	TIM-3	F38-2E2	APC-Cy7	Biolegend, 345025
Human	CD25	BC96	APC	Biolegend, 302610
Human	CD127	A019D5	PE-Cy7	Biolegend, 351320
Human	CCR7	3D12	PE	BD Biosciences, NJ, USA, 552176
Human	CD45	HI30	FITC	BD Biosciences, 555482
Human	CD3	OKT3	FITC	Biolegend, 317306
Human	CD4	OKT4	PerCP-Cy5.5	Biolegend, 317428
Human	CD8	SK1	PE-Cy7	Biolegend, 344712
-	DAPI	-	-	Sigma-Aldrich, D8417
-	7AAD	-	-	BD Bisciences, 559925
-	CellTrace Violet™	-	-	Thermo Fischer, MA, USA C34557

Table 2. Characteristics of Fluorochrome-conjugated antibodies and dyes in FCM experiments. PE, phycoerythrin; APC, allophycocyanin; PerCP, peridinin chlorophyll protein; Cy5.5; cyanine 5.5; Cy7, cyanine 7; FITC, fluorescein Isothiocyanate; DAPI, 4',6-Diamidino-2-phenylindole dihydrochloride; 7-AAD, 7-Aminoactinomycin D.

4.2. Methodology: preclinical studies.

4.2.1. Primary cells.

Primary cells were obtained from La Paz University Hospital (Madrid, Spain). All donors (or their guardians) gave their written informed consent in accordance with the Declaration of Helsinki protocol, and the study was performed according to the guidelines of the local ethics committee (code PI-3374). All donors complied with the requirements regarding quality and safety for donation, obtaining, storage, distribution, and preservation of human cells and tissues under the Spanish specific regulation. Peripheral blood mononuclear cells (PBMCs) were isolated from buffy coats from healthy volunteers by using Ficoll-Paque Plus (Cytiva, 17-1440-02) through gradient centrifugation (as described in Figure 5). Samples were diluted 1:1 with phosphate buffered saline (PBS) and added 3:1 over Ficoll-Paque Plus. After centrifugation at 300x g for 30 minutes without brake, PBMC layer was collected for subsequent procedures. PBMCs were cultured in RPMI 10% FBS. Buffy coats were obtained from the Transfusions Centre of the Comunidad de Madrid upon institutional review board approval.

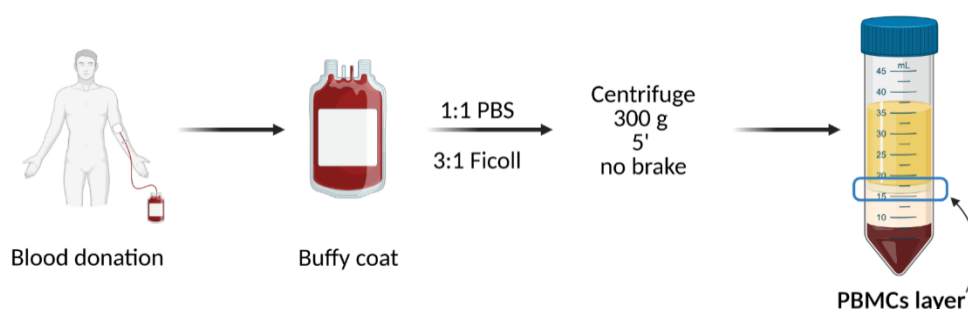


Figure 5. Procedure to obtain PBMCs from buffy coat by Ficoll centrifugation. Created with BioRender.com.

BM or PB samples from pediatric leukemia patients were obtained at the time of diagnosis prior to therapy, at follow up and/or in complete remission (CR), as indicated. PBMCs were obtained after gradient centrifugation as described above. For cryopreservation, cells were resuspended in freezing medium comprising FBS with 10% dimethyl sulfoxide (DMSO; Sigma-Aldrich, D2650). Vials were then placed in a Nalgene Cryo 1°C Freezing Container (Bio-Rad, CA, USA, 5100-0001) and stored at -80°C. After 24-48 h at -80°C, vials were kept in a liquid nitrogen tank for long term storage.

All cell lines were routinely tested for mycoplasma. A DNA-binding dye-based qPCR system was employed for the detection of mycoplasma DNA in cell cultures. The assay

was developed by the Genomics Unit in collaboration with the Monoclonal Antibodies Unit, both from the Spanish National Cancer Research Centre (CNIO), to detect 16s ribosomal RNA (rRNA) gene sequences from up to 70 *Mollicutes* species.

4.2.2. Flow cytometry.

- FCM analysis:

The different cell populations were determined in a FACSCanto II flow cytometer (BD Biosciences) or Gallios flow cytometer (Beckman Coulter, CA, USA) using the fluorochrome-conjugated antibodies and viability exclusion dyes summarized in Table 2. Discrimination of single cells from aggregates or doublets is typically performed at the beginning of the gating strategy using a Forward Side Channel-Area (FSC-A) versus Forward Side Channel-Height (FSC-H) bivariate plot. In single cells, these two measurements increase proportionally, whereas aggregates will show a clear deviation from the linearity. Once single cells were selected, alive cells were identified as DAPI/7AAD negative. To exclude debris from cell analysis, a plot showing side scatter area (SSC-A) versus FSC-A was used. Finally, multicolor FCM was performed to characterize cellular population of interest (Figure 6). To ensure a high quality analysis, at least 10.000 to 20.000 events of the population of interest were acquired.

Between $2 \cdot 10^5$ - $5 \cdot 10^5$ cells were resuspended in 100-200 μ l of staining/FCM buffer (PBS, 2% FBS) and stained with the appropriate amount of the specific antibody, as previously determined by titration test. Samples were then incubated at 4°C in the darkness for 30 minutes. After incubation, stained cells were washed using 2 ml of FCM buffer and centrifuged at 300x g for 5 minutes. Lastly, supernatants were discarded and remaining cells were resuspended in 150-300 μ l of FCM buffer and 0,5 μ l of viability dye DAPI at 200 μ g/ml were added per sample prior to being analyzed in the cytometer.

- FCM controls:

One consideration when performing multicolor fluorescence studies is the possibility of spectral overlap between fluorophores. Because the fluorophores used in flow cytometry emit photons of multiple energies and wavelengths, a mathematical method called compensation is needed to address the measurement of the photons of one fluorophore in multiple detectors. The definition of a compensation control is simple: for each fluorophore used in the experiment, a single-stained cell or bead sample must also be prepared. In order to compensate overlapping between fluorochromes and set the laser voltage, UltraComp eBeads (Invitrogen, MA, USA, 1-2222-42) were used. One drop of

beads was stained with an appropriate amount of individual antibodies and incubated at 4°C in the darkness for 15 minutes. Stained beads were washed using 2 ml of PBS and centrifuged at 3100x g for 5 minutes, supernatants were discarded and stained beads were resuspended in 200 µl of PBS for data acquisition.

Unstained samples were used to determine the level of background fluorescence or autofluorescence and set the laser voltages as well as to identify the negative population. Fluorescence minus one (FMO) controls were used to determine accurate gates and avoid spillover induced background. FMO controls are the experimental cells stained with all the fluorophores minus one fluorophore.

Data analysis was performed using Kaluza 2.1.1 (Beckman Coulter), FlowJo 10 (BD Biosciences) or FCS Express 7 (De Novo Software, CA, USA) software.

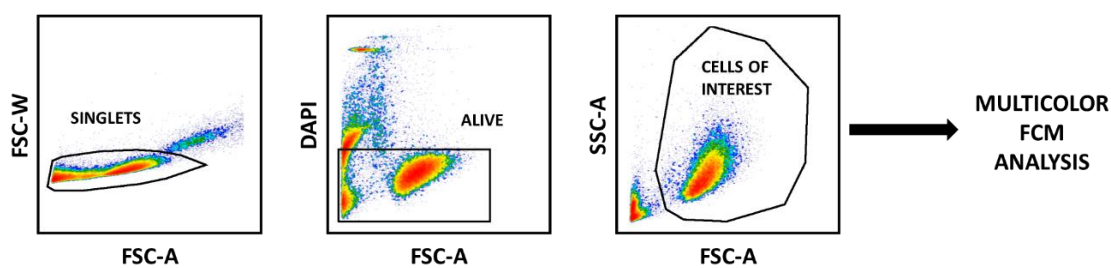


Figure 6. Gating strategy to identify cells of interest in FCM analysis.

4.2.3. Production of LV particles carrying NKG2D-CAR construct.

Viral vectors encoding for NKG2D-41BB-CD3ζ CAR construct (Figure 7) were manufactured following second or third generation-like CAR production and using different transfection reagents such as Polyethylenimine (PEI; Polysciences, PA, USA, 23966-2) or Lipofectamine-2000 (Invitrogen, 11668027) as previously described (Martinez-Lage et al. 2020), in order to optimize the protocol. On the one hand, second generation lentiviral production is based on a three-plasmid system in which two helper plasmids, coding for *gag*, *pol*, *rev* and the envelope, and the transfer vector are required. This production system is easier to produce and usually leads to higher vector titer than the third generation systems. On the other hand, third generation production is a four-plasmid system, consisting of three helper plasmids and the transfer vector plasmid (Merten, Hebben, and Bovolenta 2016). The third generation lentiviral vectors are considered to be replication incompetent and self-inactivating vectors. These third

generation lentivector systems have a number of additional safety features over the second generation: the viral *tat* gene, which is essential for replication, has been deleted; vector packaging functions have been separated onto three separate plasmids instead of two, in order to reduce the risk of recombination during plasmid amplification and viral vector manufacture; an altered 3' long terminal repeat (LTR) renders the vector self-inactivating (SIN) in order to prevent integrated genes from being repackaged (Gándara, Affleck, and Stoll 2018).

For second generation production, the following plasmids were used: envelope plasmid CAG-VSVG (VSVG pseudotyping), packaging plasmid psPAX2 (*rev/gag/pol*; Addgene, MA, USA, 12260) and transfer plasmid HL20i-4r-MND-NKG2D-CAR (CAR transgene). In the case of third generation protocol, the previous packaging plasmid was split into two different plasmids: CAG4-RTR2 (*tat/rev*) and CAG-kGP1-1R (*gag/pol*). Although this system still contained the *tat* gene, SIN sequences and functions separation into three plasmids allowed 3rd generation-like production. Maps of the plasmids can be found at the Annex section. Plasmids were kindly provided by Dr. Jean-Yves Metais (St. Jude Children's Research Hospital, TN, USA). All plasmids were amplified by transforming One Shot Stbl3 competent *Escherichia Coli* (*E. Coli*; Invitrogen, C737303), spreading 50-100 µl of bacteria on Ampicillin selective plates (Condalab, Spain, 0997) and incubating overnight at 37°C. Bacteria colonies were picked and precultured in 2,5 ml of Luria Broth (LB) with 2,5 µl of carbenicillin disodium salt antibiotic 100 mg/ml (Sigma-Aldrich, C3416) for 6h at 37°C in the shaker. After that, preculture was inoculated in 250 ml of LB with 250 µl of carbenicillin 100 mg/ml and culture was incubated overnight at 37°C in the shaker. The following day, the culture was centrifuged at 6000g for 30 minutes at 4°C and plasmid DNA was extracted from cell pellet using a Maxiprep Kit (Qiagen, Germany, 12662) and DNA quantity and quality was measured using a Nanodrop ND-1000 Spectrophotometer (Thermo Fischer).

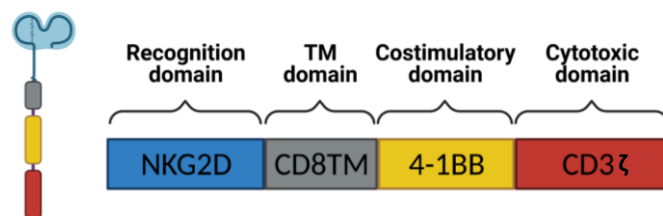


Figure 7. Sc
domain; CD3
BioRender.c

tion
with

PLASMID	2 nd generation/ μ g	3 rd generation/ μ g
CAG-VSVG	3,2	1
psPAX2	5,9	-
HL20i4r-MND-NKG2D-CAR	9	6
CAG4-RTR2	-	1
CAG-kGP1-1R	-	3

Table 3. Amount of plasmid required for LV production.

For both LV production strategies, HEK293T cell line was used as packaging cells. A density of $4 \cdot 10^6$ cells were seeded in 10 ml of DMEM 10% FBS on P100 plates, using 5 plates for each production. The following day, transfection mixings were prepared individually for each plate, when reached 70% cell confluency. Specifically, 25 μ l of Lipofectamine or 22 μ l of PEI were added to 600 μ l of serum-free DMEM and incubated for 5 minutes at room temperature (RT). Meanwhile, 600 μ l of DMEM serum-free media were mixed with plasmid DNA, as indicated in Table 3. Lipofectamine/PEI was added over DNA mixing drop by drop and making bubbles to produce smaller DNA complexes. Preparations were incubated for 25 minutes at RT. Cell culture medium of those cells plated the day before was changed for 4,5 ml serum-free DMEM. After incubation, DNA complexes were added over packaging cells drop by drop and homogeneously. Plates were incubated for 4h at 37°C, 5% CO₂, when complexes can be observed at microscope as small dots along the plates (Figure 8). Medium was changed for 7 ml of DMEM 10% FBS and cells were incubated at 37°C, 5% CO₂ for 48h.

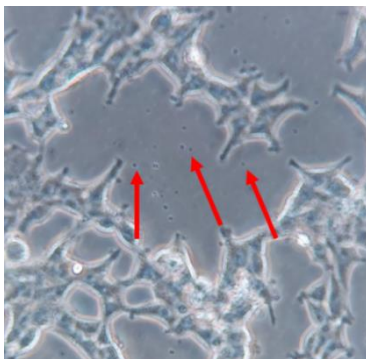


Figure 8. Microscope image of HEK293T cells after transfection. Arrows point DNA-complexes formed during the transfection process, identified as small dots.

At 48h, supernatants were collected and centrifuged at 300x g for 5 minutes to discard cell debris, filtered using 0,45 μ m sterile filters and concentrated by ultracentrifugation at 89.500x g, 4°C for 2h (Optima XPN-100 Ultracentrifuge, Beckman Coulter). After that, supernatants were discarded and pellets were resuspended in 1 ml of infection medium, either X-VIVO (Lonza, Belgium BE02-060F). LV particles were finally aliquoted in 100 μ l and stored at -80°C in 100 μ l aliquots for later use.

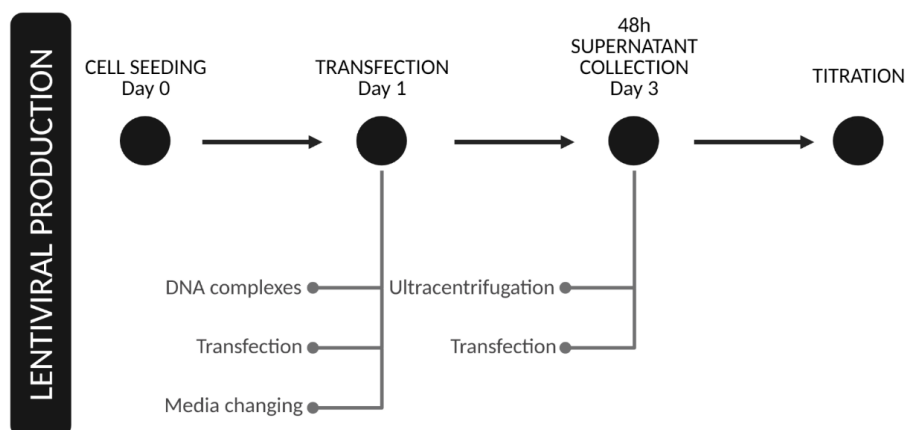


Figure 9. Scheme of workflow of lentiviral particles production.

Once LV particles were produced, titration was required to evaluate the concentration, measure as viral particles per ml (vp/ml). At day 0, $2 \cdot 10^5$ HEK293T cells/well were seeded into 6-well plate in 2 ml of DMEM 10% FBS. At day 1, cells were infected with concentrated LV particles using serial dilutions:

- 1 X: 2 μ l of stock + 8 μ l of medium \leftrightarrow 1 μ l virus.
- 1/10 X: 1 μ l of 1x + 9 μ l of medium \leftrightarrow 0,1 μ l virus.
- 1/100 X: 1 μ l of 1/10x + 9 μ l of medium \leftrightarrow 0,01 μ l virus.
- 1/1.000 X: 1 μ l of 1/100x + 9 μ l medium \leftrightarrow 0,001 μ l virus.
- No virus.

5 μ l of each dilution were added in different wells of pre-plated cells and incubated at 37°C, 5% CO₂. One well was left uninfected and cells counted for titer calculation. 24h after viral infection, medium was replaced for fresh DMEM 10% FBS. At day 3, 48h after viral infection, cells were collected after trypsinization with TrypLE Express (Gibco, 12604-013), followed by quenching with 2 ml of DMEM 10% FBS and washed with 2ml of FCM buffer by centrifugation at 300x g for 5 minutes. Cells were then stained with PE anti-human NKG2D antibody and analyzed in a FACSCantoII flow cytometer (Figure 9). FCSEXPRESS 7 software was used to analyze NKG2D expression. For titer calculation, we applied the following mathematical formula:

$$\text{Viral titer} \left(\frac{\text{vp}}{\text{ml}} \right) = \frac{\left[(\text{Number of cells infected}) \cdot \left(\frac{\% \text{ FCM positive cells}}{100} \right) \right]}{\mu\text{l of virus used}} \cdot 1000 \frac{\mu\text{l}}{\text{ml}}$$

Infection efficiency between 2-20% was used for calculation in order to maintain titration linearity and ensure that at most one viral particle infect each cell, avoiding titer underestimations.

4.2.4. NKG2D-CART production.

- Isolation of CD45RA⁻ negative cells:

NKG2D-CART were produced by LV transduction of CD45RA⁻ cells. To isolate CD45RA⁻ T cells, PBMCs were pelleted and resuspended in 80 µl of buffer PBS 0,5% bovine serum albumin (BSA; Sigma-Aldrich, A7906) per 10⁷ total cells. Then, PBMCs were labeled with 20 µl of CD45RA MicroBeads (Miltenyi Biotec, 130-045-901) per 10⁷ total cells and incubated at 4°C for 15 minutes. After that, cells were washed with 1-2 ml of buffer PBS 0,5% BSA per 10⁷ total cells, centrifuged at 300x g for 5 minutes and resuspended in 500 µl of buffer PBS 0,5% BSA per 10⁸ total cells. Non-labeled cells, corresponding to CD45RA⁻ fraction, were collected using AutoMACS separator (Miltenyi Biotec) and selecting “Depletes” program in the device settings (Figure 9). Isolated CD45RA⁻ cells were then washed to eliminate depletion buffer, counted and plated at a 2x10⁶ cells/ml in 12-well plates.

- Activation and transduction of CD45RA⁻ T cells.

T cells have to be activated before genetic engineering because resting T lymphocytes are not susceptible to transduction with VSV-LVs (Amirache et al. 2014). For activation, cells were cultured in X-VIVO 15 media (Lonza, BE02-060Q) supplemented with 5% of human AB serum (Sigma-Aldrich, H4522), 250 IU/ml of IL-2 premium grade (Miltenyi Biotec, 130-097-748) and 10 ng/ml CD3 (OKT3) (Biolegend, 317325)/CD28 (Biolegend, 302933). Cells were seeded at density of 2·10⁶ cells/ml in 12-well plates (SPL Life Sciences, Korea 30012), using 1ml/well, and incubated for 24h at 37°C, 5% CO₂. Following activation, cells were washed and media was changed to eliminate human AB serum from supplemented X-VIVO 15 medium. CD45RA⁻ T cells were transduced with LV particles encoding for NKG2D CAR using a multiplicity of infection (MOI) ranging from 2 to 5 LV particles per cell. Then, 500 µl of cells were seeded in 12-well plates at a density of 4·10⁶ cells/ml and incubated at 37°C, 5% CO₂ for 4-6h. Afterwards, 500 µl of supplemented X-VIVO 15 with 5% human AB serum were added to transduced cells to achieve a cell density of 2·10⁶ cells/ml. NKG2D-CART were expanded for 10-14 days *in vitro* until they were used for further experiments (Figure 10). CAR transduction was checked by FCM at day 4-6 using PE anti-human NKG2D, FITC anti-human CD8, APC-

Cy7 anti-human CD4, PE-Cy7 anti-human CD3 and APC anti-human CD45RA antibodies, FACSCantoll flow cytometer and FCSExpress 7 software.

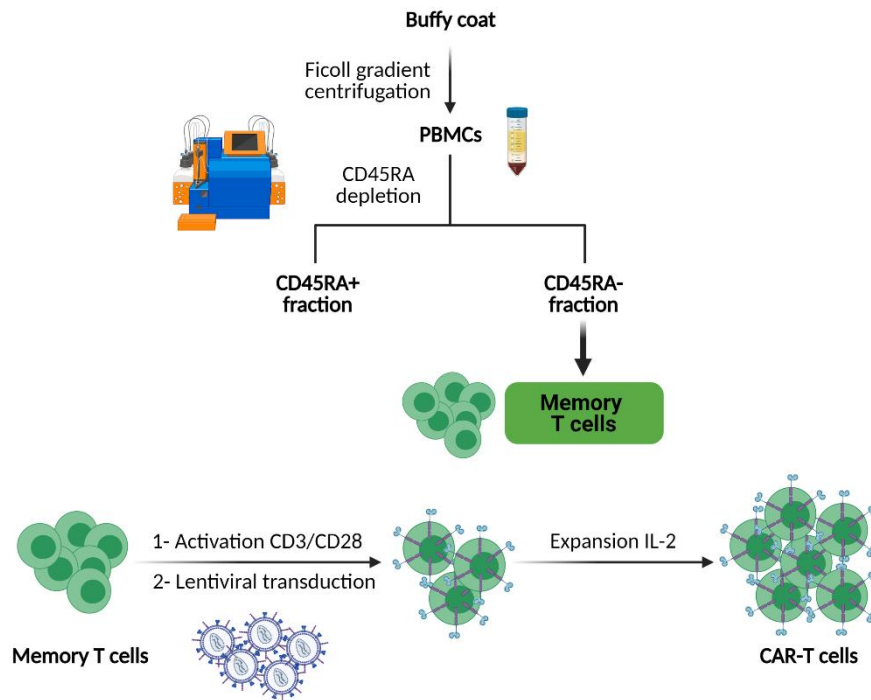


Figure 10. Workflow of CD45RA⁻ T cells isolation and NKG2D-CAR transduction. Created with BioRender.com.

4.2.5. *In vitro* cytotoxicity of NKG2D-CART.

Cytotoxicity of NKG2D-CART against leukemia cell lines and primary leukemia blasts was evaluated *in vitro* by performing conventional 4 h Europium-TDA assays at 20:1, 10:1, 5:1 and 2,5:1 effector to target (E:T) ratios. In these experiments, $2 \cdot 10^6$ target cells (either leukemia cell lines or primary blasts), were labeled with 3,5 μ l DELFIA BATDA labeling reagent (Perkin Elmer, MA, USA, C136-100) at 37°C for 30 minutes. Labeled cells were then washed twice with cell culture medium by centrifugation at 300x g for 5 minutes. Pellet was resuspended and viable cells were manually counted by using Trypan blue staining 0,4% (Gibco, 15250-061) and an improved Neubauer cell counting chamber. Cell dilution was adjusted to a concentration of $5 \cdot 10^4$ cells/ml in X-VIVO 15 medium. This dilution was used to set up the experiment and the different experimental controls, including: 1) background (BCK) of labeling process, which was established by centrifugation of $25 \cdot 10^4$ cells at 300x g for 5 minutes and keeping the supernatant; 2) spontaneous lysis (SP) of target cells, obtained by seeding target cells without effector

cells; 3) maximum lysis (MAX) of target cells, established by adding 100 µl of Triton X-100 1X (VWR Life Sciences, OH, USA, 0694) to 700 µl of target cells and pipetting up and down vigorously for one minute followed by vortexing for another minute to ensure cell lysis. Dilutions of effector cells (NKG2D-CART) associated to different E:T ratios were prepared starting from a concentration of $1 \cdot 10^6$ cells/ml, corresponding to the 20:1 ratio. Subsequent ratios were established by serial 1/2 dilutions. Total volume was 200 µl/well. For the experimental controls, 100 µl of each control condition plus 100 µl of X-VIVO 15 medium were seeded per well. For the different E:T ratios, 100 µl/well of the appropriate effector cells dilution were co-cultured along with $5 \cdot 10^3$ of target cells. Experimental and control conditions were plated in triplicates in a U bottom 96 well plate (Corning, 3598) (Figure 11). Plates were then incubated for 4 h at 37°C and 5% CO₂. After 4 h incubation, plates were centrifuged at 300x g for 5 minutes, and 20 µl of supernatant from each well were transferred to its corresponding well of a 96 well DELFIA yellow reading plate containing 200 µl/well of Europium solution. Reading plates were incubated for 5-10 minutes in the darkness and time-resolved fluorescence was measured in a 1420 Victor Plate Reader (Perkin Elmer) using the excitation and emission filters D340 and D615, respectively. Reproducibility of the assay was calculated using the following formula:

$$\% \text{ Reproducibility} = \frac{SP - BCK}{MAX - BCK} \cdot 100$$

To consider the assay as reproducible, the result from this formula must be less than 50%.

Specific lysis was calculated using the formula:

$$\% \text{ Specific lysis} = \frac{\text{Experimental lysis} - SP}{MAX - SP} \cdot 100$$

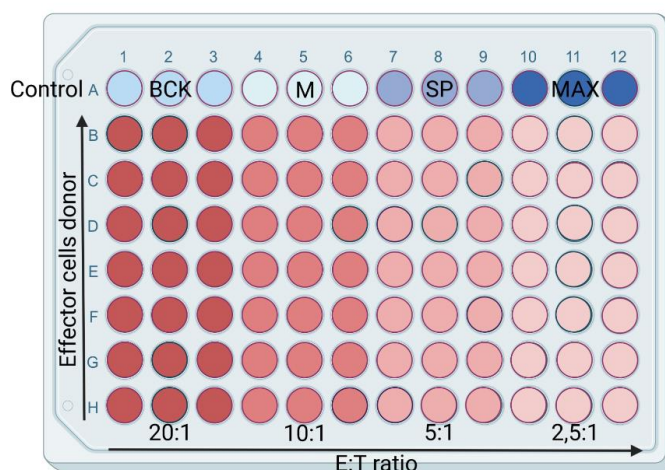


Figure 11. Scheme of *in vitro* Europium-TDA cytotoxicity assays using different E:T ratios. Controls: Background (BCK); culture media (M); spontaneous lysis (SP); maximum lysis (MAX). Created with BioRender.com.

4.2.6. *In vivo* efficacy and safety of NKG2D-CART.

- Experimental design:

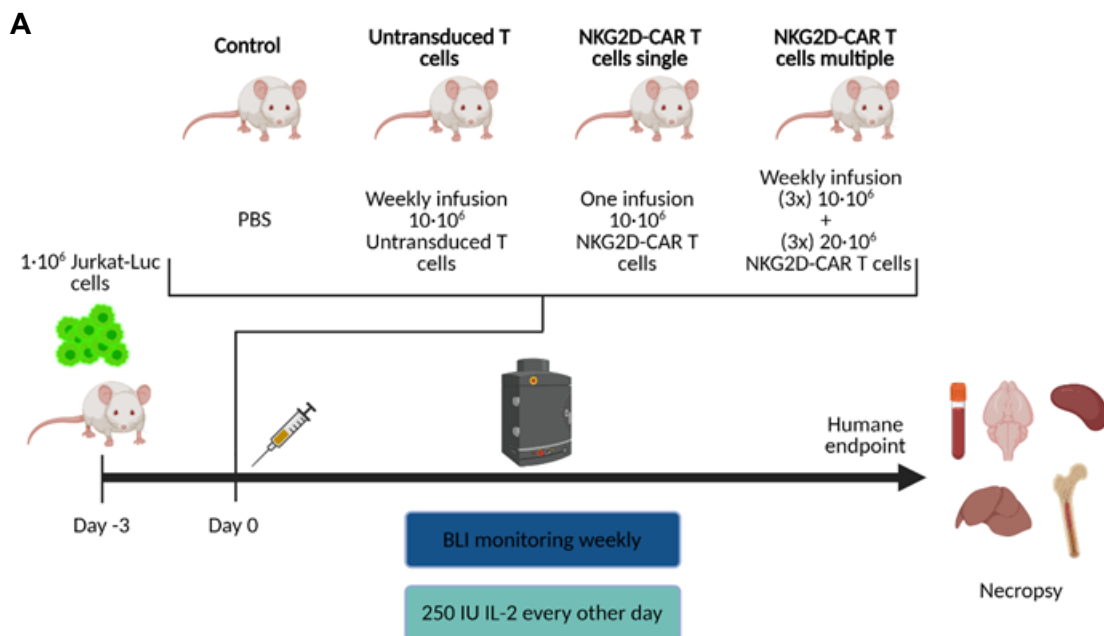
All the procedures were approved by the CNIO Animal Care and Use Committee, by the ethics committee of the Instituto de Salud Carlos III (ISCIII) and the Comunidad de Madrid (CAM) (approved under the PROEX173/17) and according to the EU Directive 2010/63/EU and the spanish Royal Decree RD53/2013. Immunodeficient NOD.Cg-Prkdc^{scid} Il2rg^{tm1Wjl} / SzJ (NSG) mice were bred at the Animal Facility Unit of CNIO. Initially, 5-to-8 week old mice were engrafted with $1 \cdot 10^6$ of Jurkat-GFP-Luc cells by intravenous (IV) injection through the tail vein at day -3. At day 0, mice were randomized in 4 groups: untreated control group receiving IV infusions of PBS (n = 4), mice receiving multiple infusions of untransduced (UT) CD45RA⁻ T cells (n = 4), mice receiving a single infusion of $1 \cdot 10^7$ NKG2D-CART/mouse (n = 5), mice receiving weekly infusions of NKG2D-CART, up to 3 infusions of $1 \cdot 10^7$ cells/mouse and 3 infusions of $2 \cdot 10^7$ cells/mouse (n = 5). Cell therapy was infused IV at day 0 and stimulated with subcutaneous (SC) administration of IL-2 (250 IU/mice) every other day for 3 weeks. Multiple-dose mice were treated once a week with $1 \cdot 10^7$ cells for 3 weeks followed by IV infusions of $2 \cdot 10^7$ cells for 3 more weeks (Figure 12A).

In a second experiment, a total of 10 mice were engrafted with $1 \cdot 10^6$ Jurkat-GFP-Luc cells. Mice were then divided into two groups, one receiving PBS injections (untreated control group; n = 5) and the other one receiving three weekly infusions of $1 \cdot 10^7$ NKG2D-CART (Figure 12B). Mice receiving CAR T cells infusions also received IL-2 and were

monitored as previously described in the experiment 1. At humane end point, mice were sacrificed by CO₂ asphyxiation. PB, BM and spinal cord samples were collected.

- Monitoring of tumor progression:

Tumor burden was monitored weekly by bioluminescence of Luc-expressing cells using Xenogen IVIS 200 Imaging System (Perkin Elmer) 10 minutes after intraperitoneal administration of 200 μ l D-luciferin at 15 mg/ml concentration (Perkin Elmer). Bioluminescence images were analyzed using the Living Image 3.0 software (Perkin Elmer). Mice were euthanized in a CO₂ chamber when displayed clinical symptoms of leukemia progression including leg paralysis. Necropsy was performed to collect mice samples, including PB, BM, spleen, brain and cerebrospinal fluid (CSF). The persistence of CAR T cells (CD45human⁺, GFP⁻, NKG2D⁺) and leukemia burden (CD45human⁺, GFP⁺) were analyzed by FCM in BM, spleen and PB using GFP fluorescence and APC anti-mouse CD45, PerCP-Cy5.5 anti-human CD45 and PE anti-human NKG2D antibodies. FACSCantoll flow cytometer and FCSExpress software were employed for FCM analysis. In addition, liver, brain and BM tissues were collected to evaluate CAR T cell infiltration and possible signs of treatment related toxicity by histopathology analysis through immunohistochemistry (IHC). Transcriptome sequencing (RNA-seq) and enzyme linked immunosorbent assay (ELISA) were performed to evaluate possible mechanism of immune escape.



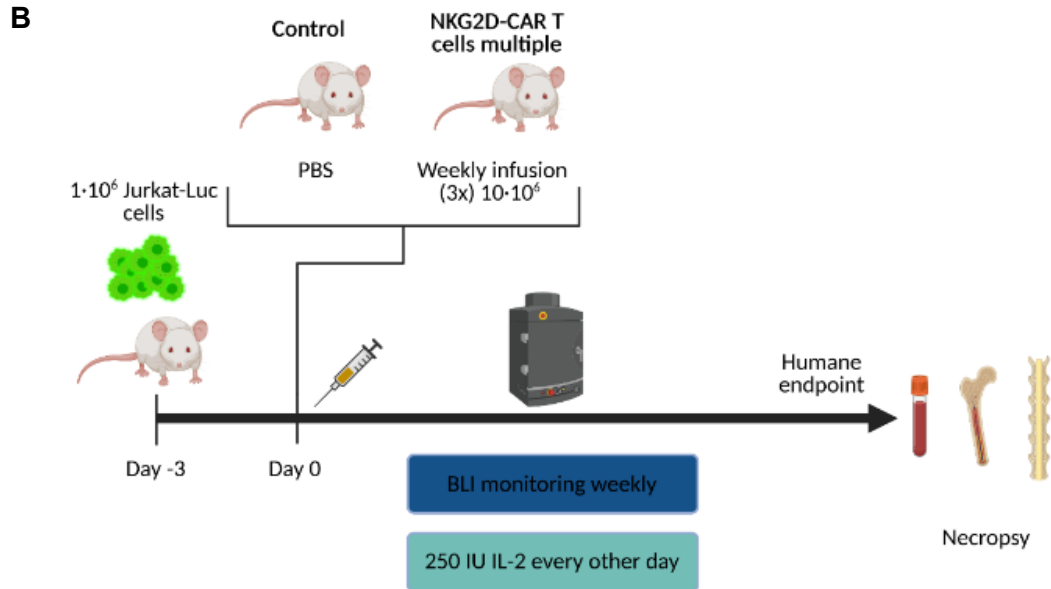


Figure 12. Scheme of the first (A) and second (B) *in vivo* experiments. Created with BioRender.com

4.2.7. Histopathology analysis by IHC.

Tissue samples were fixed in 10% neutral buffered formalin (4% formaldehyde in solution), then paraffin-embedded and cut at 3 μ m thickness, mounted in superfrost™ plus slides and dried overnight. Slides were then deparaffinized in xylene and re-hydrated through a series of graded ethanol until water. Consecutive sections were stained with hematoxylin and eosin (H/E) and used for immunohistochemistry (IHC). IHC reactions were performed in an automated immunostaining platform (AutostainerLink 48, Agilent, CA, USA). Antigen retrieval was first performed with the appropriate pH buffer, (High pH buffer, Agilent) and endogenous peroxidase was blocked (peroxide hydrogen at 3%). Then, slides were incubated with the primary antibody mouse monoclonal anti-granzyme B (GrB-7; 1/10. Agilent, M7235). After incubation, secondary antibody was added (host y tag anti-mouse, Abcam, ab133469) and a visualization systems (Novolink Polymer Linker, Leica, Germany) conjugated with horseradish peroxidase immunohistochemical reaction was developed using 3, 30-diaminobenzidine tetrahydrochloride (DAB) and nuclei were counterstained with Carazzi's hematoxylin. Finally, the slides were dehydrated, cleared and mounted with a permanent mounting medium for microscopic evaluation. Control sections known to be primary antibody were included for each staining run. Whole slides were acquired with a slide scanner (AxioScan Z1, Zeiss, Germany), and images captured with the Zen Blue Software (V3.1 Zeiss).

4.2.8. Analysis of sNKG2DL in leukemia samples.

The concentration sNKG2DL was measured in the supernatant of leukemia cell lines and in the serum of leukemia patients by ELISA. Confluent cultures of leukemia cells lines were centrifuged at 300x g for 5 minutes and supernatants were collected and stored at -80°C. PB samples from *in vivo* experiments were collected in non-ethylenediaminetetraacetic acid (EDTA) tubes, incubated at RT for 1 h and centrifuged at 13400x g, 10 minutes, 4°C. to isolate the serum, which was kept at -80°C for further analysis. PB samples from leukemia patients were obtained by venipuncture, centrifuged twice at 2.000 rpm for 10 minutes and serums kept at -80°C.

Flat-bottom 96-well plates were coated overnight at 4°C with 100 µl of 5 mg/ml of MICA (MAB1300), MICB (AF1599), ULBP1 (AF1380), ULBP2 (AF1298), ULBP3 (AF1517), or ULBP4 (MAB6285) antibodies (all from R&D Systems). Plates were then washed twice with 0,05% PBS-Tween and blocked with 2% PBS-BSA for 2-3 h at 37°C. Samples were centrifuged at 13400x g and 4°C for 5 min and diluted 1/2 with 2% PBS-BSA. We prepared calibration curves by serial dilution of the following recombinant human (rh) proteins: rhMICA (1300-MA), rhMICB (1599-MB), rhULBP1 (1380-UL), rhULBP2 (1298-UL), rhULBP3 (1517-UL), and rhULBP4 (6285-UL) (all from R&D Systems). Thus, 100 µl of sample/calibration curve preparations were added to each well and incubated overnight at 4 C. Plates were washed twice with 0,05% PBS-Tween and incubated for 1 h at 37°C with the following secondary antibodies (100 µl, 0,4 mg/ml): biotin-conjugated MICA (BAF1300), MICB (BAF1599), ULBP-1 (BAF1380), ULBP-2 (BAF1298), ULBP-3 (BAF1517); or goat-anti-ULBP-4 (AF6285) (all from R&D Systems). Plates were washed again three times with 0,05% PBS-Tween and then incubated with 100 µl of either horseradish peroxidase (HRP)-streptavidin (Biolegend, 405210; dil 1:2000) or donkey HRP anti-goat (Invitrogen, A16005; 1:5000) 1 h at room temperature. Lastly, protein detection was performed after washing the plates 4 times by adding 100 µl of 1-step Ultra TMB (Thermo Fischer, 34028) and reading the plates on a SUNRISE microplate reader (Tecan, Switzerland) at 405-492 nm.

4.2.9. Effects of soluble NKG2D ligands on NKG2D-CART.

- Effects of sNKG2DL on surface expression of NKG2D-CART:

The downregulation of NKG2D CAR by sNKG2DL was assessed by culturing $5 \cdot 10^4$ NKG2D-CART without or with 20 or 500 ng/ml of rhMICA, rhMICB, rhULBP1, rhULBP2, rhULBP3 and rhULBP4 proteins as sNKG2DL. To test the effects of IL-2 on NKG2D CAR

expression and proliferation in the presence of sNKG2DL, either 0, 20 or 100 IU/ml of IL-2 were added to the cultures. Using 96 well U-bottom plates, cells were seeded with the different amounts of sNKG2DL and IL-2 in a final volume of 200 µl using X-VIVO 15 and cultured for 1 week. Plates were then centrifuged at 300x g, 5 minutes and cells were collected in FCM tubes, washed with PBA buffer (PBS, 1% BSA, 0,05% sodium azide) through centrifugation at 300x g for 5 minutes and stained with FITC anti-human CD3, PE anti-human NKG2D, PerCP-Cy5.5 anti-human CD4 and PE-Cy7 anti-human CD8 antibodies (see Table 2) for 30 minutes at 4°C in the dark. Stained cells were washed again with PBA, resuspended in 200 µl of buffer and analyzed in a Gallios flow cytometer. Data analysis was performed using Kaluza 2.1.1 software.

- Effects of sNKG2DL on NKG2D-CART proliferation:

CD45RA⁻ NKG2D-CAR or UT T cells were firstly labeled with CellTrace Violet™ 1 µM for 20 minutes at RT in darkness. Cells were then washed with RPMI 10% by centrifugation at 300x g for 5 minutes and resuspended in RPMI 10%. Labeled NKG2D-CART were incubated at 37°C, 5% CO₂ for 1 week in the same conditions described above for NKG2D downregulation experiments. Plates were then centrifuged at 300x g, 5 minutes and supernatants were collected, centrifuged at 13400x g for 5 minutes and stored at -80°C for cytokines analysis. Cells were collected in FCM tubes and washed with PBA buffer (PBS, 1% BSA, 0,05% sodium azide) by centrifugation at 300x g for 5 minutes. Labeled cells were resuspended in 200 µl of the buffer and analyzed in a Gallios flow cytometer. Data analysis was performed using Kaluza 2.1.1 software.

- Effects of sNKG2DL on NKG2D-CART anti-tumor activity:

To evaluate the effects of sNKG2DL on NKG2D-CART cytotoxicity, two different types of experiments were carried out. First, $1 \cdot 10^6$ cells/ml of UT or NKG2D-CAR transduced CD45RA⁻ cells were treated with sMICA and soluble ULBP2 (sULBP2) for 72 h at different concentrations (0 ng/ml, 20 ng/ml and 500 ng/ml). Following this, the cytotoxicity of treated T cells was tested by Europium-TDA assays using Jurkat or K562 cells at a 10:1 E:T ratio. The effects of sNKG2DL on NKG2D CAR expression was analyzed in the 72h treated cells by FCM, using PE anti-human NKG2D, FITC anti-human CD8, APC-Cy7 anti-human CD4, PE-Cy7 anti-human CD3 and APC anti-human CD45RA antibodies. FACSCantoll flow cytometer and FCSEXPRESS 7 software were used for this analysis. In different experiment, the sNKG2DL were added at the time of the Europium-

TDA experiment to explore if this ligand could have an instant impact on the anti-tumor ability of NKG2D-CART. Specific lysis of treated or non-treated cells were compared to determine the downmodulation effect of sNKG2DL.

4.2.10. Time lapse, epifluorescence and confocal microscopy.

The effects of sNKG2DL in the immunological synapse formed between effector cells (NKG2D-CART) and target cells (Jurkat cells) were evaluated by time lapse and epifluorescence microscopy, as previously described (Bello-Gamboa et al. 2019). First, NKG2D-CART were incubated with 500 ng/ml of sMICA for 72 h while untreated NKG2D-CART were used as a control. After that, an 8-microwell chamber slide (Ibidi, Germany, 80826) was coated with 150 μ l/well of 0,1 μ g/ml fibronectin (Sigma, ECM001) and incubated at 37°C for 1 h. Fibronectin was aspirated and wells were washed twice with PBS 1X. In the meantime, Jurkat cells were labelled with 10 μ M 7-amino-4-chloromethylcoumarin (CMAC; Thermofisher, C2110) and 100.000 cells were seeded in 200 μ l/well in the chamber slide to be incubated at 37°C, 5% CO₂ for 1 h. Then, medium was aspirated and CMAC-labelled Jurkat cells were challenged with 100.000 of treated or untreated NKG2D-CART (E:T ratio 1:1) in a total volume of 200 μ l to form synaptic conjugates. Immediately, time lapse acquisition was performed during 4 h by using wide-field, time-lapse microscopy with a stage incubator (Oko-lab, Italy) to maintain cell culture ambient (5% CO₂, 37°C, 100% humidity) on an Eclipse TiE microscope (Nikon, Japan) equipped with a DS-Qi1MC digital camera and a Plan Fluor ELWD 40x/0,6NA air objective (Nikon). For time-lapse imaging, simultaneous acquisition of both transmittance and UV (CMAC) channels was performed at 1 frame each 5 min, in at least 7 different microscopic fields, by using NIS-AR software (Nikon).

In parallel, some microwells were fixed with 4% paraformaldehyde (PFA; Sigma, P6148) after 30 minutes in order to perform an end-point immunofluorescence. Quenching solution (PBS 1X, 50 mM NH₄CL) was added to the microwells after fixation and blocking was performed by adding PBS 1X, 5% BSA, 0,1% saponin for 1 h at RT. Samples were then washed three times with PB buffer (PBS 1X, 15mM glycine, 0,5% BSA, 0,1% saponin, 10 mM HEPES) and stained with the following primary antibodies for 1h at RT: mouse monoclonal anti-NKG2D-PE (Biolegend, 320806; dilution 1/200); rabbit polyclonal anti-pericentrin (Abcam, UK, ab4448; dilution 1/2000) to label microtubule-organizing center (MTOC), at 1/2000 dilution; and Phalloidin AF647 (Thermo Fisher, A22287; dilution 1/100) to localize F-actin, at 1/100 dilution. After incubation with the primary antibodies, we washed samples three times with PB buffer and incubated with

the secondary antibodies: goat-anti-rabbit IgG AF488 (Thermo Fisher, A-11034; dilution 1/200) and goat-anti-mouse IgG AF546 (Thermo Fisher, A-11030; dilution 1/200). Finally, samples were washed again three times with PB, once with PBS and lastly water, before being mounted using Prolong Gold (Thermofisher, P10144). Epifluorescence imaging of fixed synapses was performed using a Nikon Eclipse TiE microscope equipped with a Prime BSI digital camera (Photometrics, CA, USA) and a PlanApo VC 60x/1.4NA OIL objective (Nikon). Images were mounted using FIJI ImageJ software (National Institutes of Health, MD, USA). Confocal imaging was performed using a Leica SP5 confocal microscope (Leica) at 40 × magnification. The images were exported as 8-bit.tif files for analysis using the software FIJI ImageJ.

4.2.11. Effects of TGF- β and soluble factors on NKG2D-CART.

To evaluate the effects of TGF- β on NKG2D-CART, we first measured the levels of secreted protein by leukemia cells in ELISA assays, following the manufacturer's instructions (Elabscience, TX, USA, E-EL-0162). The effects of TGF- β in NKG2D-CART cytotoxicity was tested by Europium-TDA cytotoxic assays using 20:1, 10:1, 5:1 and 2,5.1 E:T ratios, as previously described. Prior to the co-culture, we treated effector cells with 2,5 ng/ml or 8 ng/ml of TGF- β (Abcam, AB50036-2UG) in X-VIVO 15 medium for 24h. CAR T cells in X-VIVO without TGF- β were used as control. As Jurkat cells may secrete other soluble factors different to sNKG2DL and TGF- β that could impair NKG2D-CART function, we cultured CAR T cells in Jurkat conditioned medium for 24h and analyzed NKG2D CAR expression and cytotoxicity. NKG2D-CART cultured in RPMI 10% FBS were used as controls.

4.2.12. Impact of NKG2D-CART on leukemia-initiating cells.

One functional characteristic of LICs is their clonogenicity, evidenced by their ability to grow as colonies. Additionally, LICs can be identified by FCM as a side population that effluxes Vybrant™ DyeCycle™ Violet Stain dye (DCV; Thermo Fisher, V35003). Based on these two characteristics, we evaluated the anti-tumoral potential of NKG2D-CART against the LIC compartment of Jurkat cells by performing two different types of experiments. Firstly, the effect of NKG2D-CART in the colony forming unit (CFU) capacity of LICs was quantified by co-culturing UT and NKG2D-CART (effector cells) with Jurkat-GFP-Luc (target) at 20:1, 10:1 and 5:1 E:T ratios. In 96 well U-bottom plates,

2.000 Jurkat-Luc cells (4X) were seeded in 100 µl along with 100 µl of the different ratios of effector cells (4X) or RPMI as CFU control condition. Cells were incubated at 37°C, 5% CO₂ for 4 h. After incubation, co-cultures were mixed with 3,8 ml of methylcellulose MethoCult (Stemcell Technologies, Canada, 4230) by vortexing. Mixtures were let stand to remove bubbles and 1 ml was seeded in triplicates in P35 plates using a syringe. Calculations were made to seed approximately 500 target cells in the controls. Plates were incubated in a humidity chamber at 37°C, 5% CO₂ for 1 week and colonies counted under the microscope.

Secondly, the cytotoxic capability of NKG2D-CART against side population cells, which are enriched in tumor initiating cells, was assessed. In these experiments, NKG2D-CART were co-cultured with Jurkat GFP-luc cells at a 1:5 E:T ratio for 16h at 37°C and 5% CO₂. After the incubation, cells were collected, counted and $5 \cdot 10^6$ cells were centrifuged at 300x g for 5 minutes and resuspended in RPMI 2%, maintaining them at 4°C. Samples were prewarmed at 37°C and an aliquote was used as an inhibition control. This control consisted on the incubation with 50 µM ABC transporter inhibitor reserpine (RES; Sigma-Aldrich, R0875-1G) for 20 minutes at 37°C prior to DCV addition, in order to leave the cells and loose fluorescence. Prewarmed samples were stained with 5 µM DCV and incubated at 37°C for 90 minutes. After incubation, samples were centrifuged at 400x g, 4°C for 7 minutes. Supernatants were discarded and cells were resuspended in PBS + EDTA 3 mM + FBS 3% supplemented with 2mM 4-(2-hydroxyethyl)-1-piperazineethanesulfonic acid (HEPES; Thermo Fisher, 15630080). Side population of GFP positive cells, associated to Jurkar-GFP-Luc cells, was detected after addition of viability marker 5 µg/ml propidium iodide (PI; Sigma-Aldrich, P4864) by FCM analysis in a FACSCanto II flow cytometer using FCSExpress 7 software. Furthermore, GFP positive cells were sorted using (FACSAria™ Fusion flow cytometer, BD Biosciences) and resuspended in 600 µl of lysis buffer RLT (Qiagen, 79216) with 6 µl of β-mercaptoethanol (Sigma-Aldrich, M625) and stored at -80°C for later RNA extraction and analysis.

4.2.13. Transcriptome analysis by RNA-seq.

Sorted Jurkat-GFP-Luc cells remaining after an overnight exposition to NKG2D-CART were washed in PBS and pelleted in RLT lysis buffer supplemented with 1:1000 β-mercaptoethanol. Total RNA was isolated using the RNeasy Mini kit (Qiagen, 74106) according to the manufacturer's instructions. To remove residual genomic DNA, the RNA samples were digested with DNase I. The RNA concentration was assessed by

fluorescence quantitation using Qubit 2.0 and the High Sensitivity RNA assay kit (Thermo Fisher, Q32852), the RNA purity by spectrophotometry using Nanodrop 2000 (Thermo Fisher) and the RNA integrity by electrophoresis using TapeStation 4200 RNA ScreenTape (Agilent).

Reads from RNA-seq were analyzed to quantify genes through the RSEM (Li and Dewey 2011) with hg19 as reference for annotation. The differential expression was carried out with edgeR (Robinson, McCarthy, and Smyth 2010) and the statistical cut-off point was set as $FDR < 0,05$ and $\log FC > 2$. Genes were filtered based on a minimum expression of one Counts Per Million (CPM) in more than one sample. Normalization was performed by the TMM method (trimmed mean of M-values) (Robinson and Oshlack 2010). Functional enrichment of differentially expressed genes was carried out in PFAM (Mistry et al. 2021), GOTERM_BP_DIRECT (Ashburner et al. 2000) and KEGG REACTOME (Kanehisa, Sato, and Kawashima 2022)

4.3. Methodology: Translation to the clinic.

4.3.1. *Starting Material.*

Non-mobilized apheresis were obtained from healthy donors at the Bone Marrow Transplant and Cell Therapy Unit (BMTCT) of La Paz University Hospital (HULP) using the CliniMACS Plus device (Miltenyi Biotec). All donors gave their written informed consent in accordance with the Declaration of Helsinki protocol, and the study was performed according to the guidelines of the local ethics committee (code PI-3374). All donors complied with the requirements regarding quality and safety for donation, obtaining, storage, distribution, and preservation of human cells and tissues under the European EU Directive 2004/23/EC and Spanish Royal Decree 1716/2011. CD45RA⁺ cells were depleted by immunomagnetic separation using CliniMACS CD45RA Reagent (Miltenyi Biotec, 701-46) and CliniMACS Plus system, following manufacturer's instructions. CD45RA⁻ cells were either processed immediately or stored at 2–8°C for subsequent processing but no later than 24 h after depletion. The viability and purity of CD45RA⁻ fraction were analyzed by FCM, as described above, before activation, transduction, and expansion.

4.3.2. *Manufacturing of Clinical-Grade NKG2D-CART.*

Activation, transduction, and expansion of CD45RA⁻ cells were performed on the CliniMACS Prodigy™ (Miltenyi Biotec) using Tubing set TS520 (Miltenyi Biotec; 170-076-600) and T cell transduction (TCT) process. Specifically, at day 0, cultivation was initiated with 10⁸ CD45RA⁻ cells in a total volume of 70 ml of TexMACs GMP medium (Miltenyi Biotec, 170-076-306) with 100 IU/ml of MACS GMP human recombinant IL-2 (Miltenyi Biotec, 170-076-147). MACS GMP TransAct CD3/CD28 Kit (Miltenyi Biotec, 170-076-156) was used for a 24 h activation at a final dilution of 1:17,5, as recommended by the manufacturer. The following day, cells were transduced with NKG2D-4-1BB-CD3ζ LV particles at MOI = 2. The vector was diluted in 10 ml of medium in a 150 ml transfer bag, which was attached to the CliniMACS Prodigy™ by sterile welding. The vector was automatically transferred in the culture chamber, and the vector bag was further rinsed with 20 ml of medium to bring the total culture volume to 100 ml. Residual TransAct was removed by an automated culture wash on day 4. Cells were then expanded for 10-13 days before being harvested. Sampling was performed at days +6 and +8 for in-process controls including cell counts, cytotoxicity, and FCM. At the end of the expansion, cells

were automatically collected in 0,9% sodium chloride solution supplemented with 0,5% human serum albumin (Albutein 20%, Grifols, Spain, 670612) and transferred into a sterile bag. Release quality controls were performed at the end of the process.

4.3.3. Analysis of viability and surface immunophenotype by FCM and Western Blot.

At day +6 and between days +8 and +10, in the case of in-process controls, and at harvest, in the case of release controls, CD45RA⁺ NKG2D-CAR T cell products were counted in a CELL-DYN Emerald hematology analyzer (Abbott, IL, USA) and their viability, immunophenotype, NKG2D-CAR expression, and activation status analyzed by FCM. The viability was tested using DAPI or 7AAD as dead cell exclusion markers. Cells were analyzed using FACS CANTO II and FlowJo 10 software. As NKG2D FCM antibody recognizes both endogenous NKG2D receptor and NKG2D CAR, we ensured NKG2D CAR expression on the transduced cells by performing Western Blot (WB) to detect CD3 ζ , as the size band differs in TCR and NKG2D CAR. Total PBMCs, activated and expanded NK cells (NKA-E), UT CD45RA⁺, and NKG2D-CAR T were pelleted and frozen at -80°C. Cell lysates were obtained by incubating cell pellets with RIPA buffer (Millipore, 20188) supplemented with phosphatase inhibitors (PhosSTOP; Roche, Switzerland, 4906845001) and protease inhibitors (cOmplete Mini; Roche, 11836153001). Proteins were quantified using Bradford reagent (Bio-Rad, 500-0205) and measuring absorbance at 595 nm in a Victor Plate Reader. Cell lysates were then mixed with the Laemmli sample buffer (Bio-Rad, 161-0747), and equal amounts of protein (20 μ g) were loaded on 4-15% Mini-PROTEAN TGX Gels (Bio-Rad, 456-1086). Gels were transferred to Immun-Blot™ polyvinylidene fluoride (PVDF, Bio-Rad, 1620177) membranes and blocked to mask unspecific binding by 5% BSA/TBS. Blots were incubated with the mouse anti-human CD3 ζ (BD Biosciences, 551033) or rabbit anti-human β -actin (Cell Signaling Technology, MA, USA, 4967S) primary antibodies at 4°C overnight. HRP-conjugated anti-mouse (Agilent, P0447) and anti-rabbit (Agilent, P0448) were used as secondary antibodies. The membranes were developed by enhanced chemiluminescence with ClarityWestern ECL substrate (Bio-Rad, 170-5060) and acquire with a MACHINE. The immunoblotting images were analyzed using the Image Lab software 6.0.1 (Bio-Rad).

4.3.4. Effector function.

To test the cytotoxicity of manufactured NKG2D-CART, 4 h Europium-TDA assays were performed as described above using a 20:1 E:T ratio. The NKG2DL-expressing cell lines Jurkat and 531MII were used as targets. Cytotoxicity assays were performed on days +6 and +8 as well as at the end of the process. The 531MII primary osteosarcoma cell line was kindly provided by Dr. Patiño-García (Pediatrics Laboratory, Universidad de Navarra, Pamplona, Spain) and was cultured in minimum essential medium (MEM; Gibco, 22571-020) supplemented with 10% FBS and penicillin-streptomycin (P/S; Gibco, 15140-122).

4.3.5. Analysis of non-cellular impurities.

The detection of non-cellular impurities was carried out in accordance with the methodology recommendations of Chapter 2.6.21 and 2.6.7 of the European Pharmacopeia (Eu Ph) for *Mycoplasma sp* and Chapter 2.6.14 for endotoxins. A DNA-binding dye-based qPCR system was employed for the detection of *Mycoplasma sp* DNA in cell cultures, as previously described. The Clinical Microbiology and Parasitology Service of HULP carried out the endotoxin test Endosafe-PTS (Charles River, MA, USA) to quantify endotoxin levels at day +8 and in final products.

4.3.6. Microbiological test.

At day +6 and between days +8 and +10 as in-process controls and at the end of manufacturing protocol, CD45RA⁺ NKG2D-CAR T cell products were tested for sterility according to Eu Ph 2.6.1. The microbiological tests were developed by the Clinical Microbiology and Parasitology Service of HULP by conventional microbiology techniques. In summary, sample tests were inoculated into separate culture media, and the growth of viable microorganisms was tested after several days.

4.3.7. Genetic Tests, Genome Integrated Vector Copy Number, and determination of Replication Competent Lentivirus in the Supernatant.

Genetic tests and determination of vector copy number (VCN) and replication competent lentivirus (RCL) in the supernatant were carried out at day +6 and between days +8 and

+10 as quality controls during process validation, and at the end of the manufacturing process between days 10 and 13. To rule out chromosomal aberrations caused by LV transduction, comparative genome hybridization (CGH) analysis was performed as previously described (Fernández et al. 2017). Genome integrated LV copy number and viral particles in supernatant were measured by qPCR according to Christodoulou and colleagues. (Christodoulou et al. 2016) using TaqMan Universal PCR Master Mix (Thermo Fisher, 4304437) and LightCycler 480 (Roche) after viral RNA extraction with RNeasy (Qiagen, 74104) and cDNA retrotranscription with Superscript II (Thermo Fisher, 18064014). The lack of oncogenic effects of the NKG2D.CAR T cell products was verified using reverse transcriptase polymerase chain reaction (PCR) to detect *c-myc* and telomerase reverse transcriptase (*tert*) expression. Total RNA was isolated from the PBMCs using the RNeasy kit (Qiagen, 74104), followed by reverse transcription using SuperScript™ IV First- Strand Synthesis System (Thermo Fisher, 18091050). The resulting cDNA was amplified with the following specific TaqMan probes: Hs00972650_m1 (*tert*), Hs00153408_m1 (*myc*), and Hs02800695_m1 (HPRT1, housekeeping) from Life Technologies and the LightCycler 480 System (Roche). Finally, the data were analyzed by the comparative Ct methods as previously described (Schmittgen and Livak 2008). The genetic tests were performed at the Institute of Medical and Molecular Genetics of HULP (INGEMM).

4.3.8. Effects of cryopreservation on NKG2D-CART.

As infusion of freshly manufactured CAR T cells is not always possible, the effects of cryopreservation on viability, NKG2D CAR expression, and cytotoxicity of NKG2D-CART were assessed. To this aim, harvested CAR T cells were frozen at a concentration of $2.5 \cdot 10^5$ cells/ μ L either by using HypoThermosol (Sigma-Aldrich, H4416), M199 media (PAN-Biotech, Germany, P04-07500) supplemented with 10% human serum albumin and 5% DMSO, or in autologous plasma supplemented with 5% DMSO. One year after cryopreservation, NKG2D-CART were thawed and evaluated for viability, NKG2D expression, and CD45RA⁺ purity by FCM and for cytotoxicity by Europium-TDA as described above.

4.4. Statistical analysis.

All statistical analyses were performed using GraphPad Prism 8 software (GraphPad Software, CA, USA). D'Agostino/Saphiro column statistics analysis was performed to evaluate the normality of the data before conducting any further statistical test. Data are presented as mean \pm Standard Error of Mean (SEM), except in Box and Whiskers graphs where median, minimum and maximum and quartile 1 and 3 are represented or otherwise stated in the figure legend. Further details of the statistical analysis performed are given in each figure legend. When comparing two parametric groups, paired or unpaired two-tailed Student t-tests were applied. In case of nonparametric data, Wilcoxon or Mann-Whitney two-tailed t-tests were performed for paired or unpaired values, respectively. When more than two groups were compared, one-way analysis of variance (ANOVA) following Dunn's post-hoc test was carried out to these groups with only one variable. Friedman or Kruskal-Wallis test was applied for paired or unpaired nonparametric data, respectively. When analyzing more than two groups that had two different variables, a two-way ANOVA analysis was performed following Sidak's or Tukey's multiple comparison post-hoc test when two or more families were involved, respectively. To correlate two variables, Pearson correlation test was performed. Finally, the survival curves from the first *in vivo* experiments were analyzed by applying the Kaplan-Meier method. Statistical significance was considered when p values obtained in the different analysis remained lower than 0,05. The following significance levels were taken into account: $p < 0.05$ (*), $p < 0,01$ (**), $p < 0,001$ (***)

5. RESULTS

5.1. Preclinical studies

5.1.1. Lipofectamine and second generation production achieved higher LV titers.

Manufacture of LV particles encoding for NKG2D CAR was optimized in an attempt to obtain a reproducible and reliable transduction process.

Firstly, transfection reagent efficiency was tested using PEI or Lipofectamine-2000 following third generation production. PEI-based production achieved viral titers close to 10^6 vp/ml (Figure 13). However, LV production with Lipofectamine-2000 reached viral titer 10 times higher, close to 10^7 vp/ml (Figures 14, 15). Although Lipofectamine-2000-based in combination with third generation procedure showed a tendency to increase the viral titer compared to PEI transfection, it remained too low to carry out the transduction of high amounts of CAR T cells.

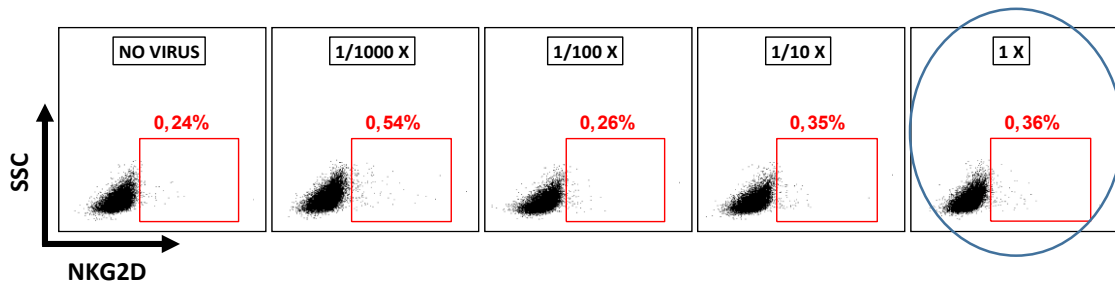


Figure 13. Percentages of NKG2D-positive HEK293T packaging cells by FCM. Cells were infected using PEI-based manufactured LV particles and third generation method production.

$$\frac{vp}{ml} = \frac{\left(365.000 \text{ cells} \cdot \frac{0,35\%}{100}\right)}{1 \mu l} \cdot 1000 \frac{\mu l}{ml} = 1,31 \cdot 10^6 \frac{vp}{ml}$$

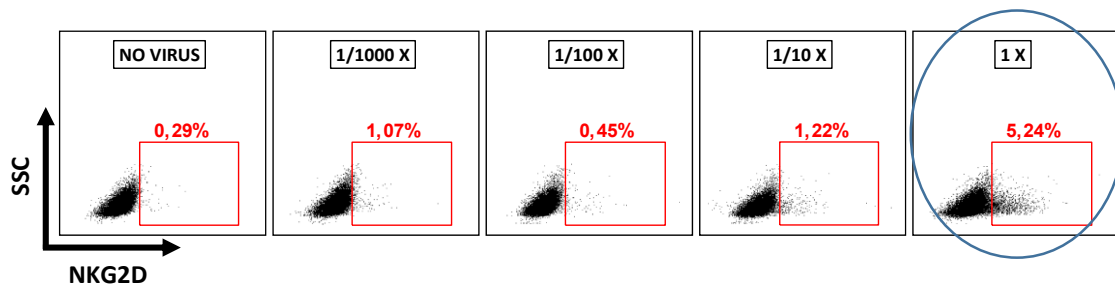


Figure 14. Percentages of NKG2D-positive HEK293T packaging cells by FCM. Cells were infected using Lipofectamine-2000-based manufactured LV particles and third generation method production.

$$\frac{vp}{ml} = \frac{\left(365.000 \text{ cells} \cdot \frac{5,24\%}{100}\right)}{1 \mu l} \cdot 1000 \frac{\mu l}{ml} = 1,91 \cdot 10^7 \frac{vp}{ml}$$

Secondly, to improve LV production, second generation protocol was performed using the Lipofectamine-2000, as it previously gave better transfection results. Viral titer increased up to 10^8 vp/ml (Figure 15) compared to 10^7 vp/, which allowed us to obtain high quality batches of LV productions.

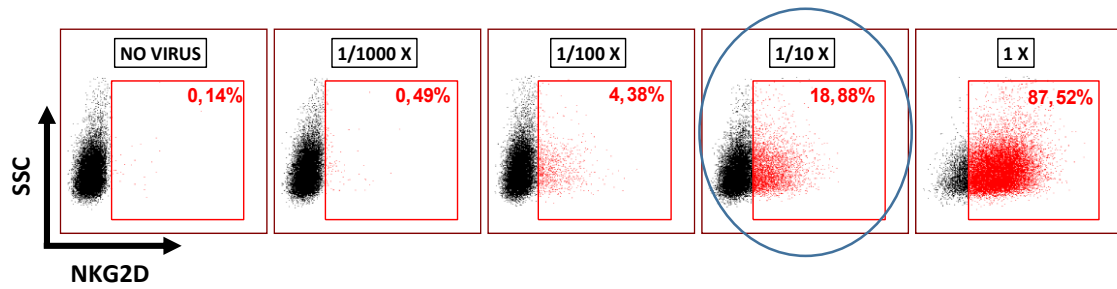
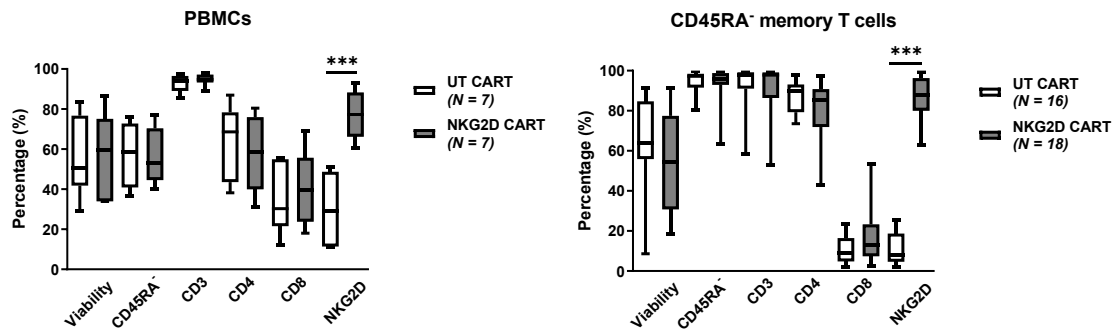


Figure 15. Percentages of NKG2D-positive HEK293T packaging cells by FCM. Cells were infected using Lipofectamine-based manufactured LV particles and second generation method production.

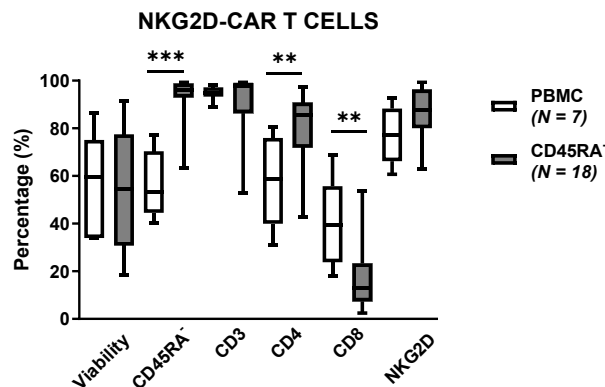
$$\frac{vp}{ml} = \frac{\left(380.000 \text{ cells} \cdot \frac{18,88\%}{100}\right)}{0,1 \mu l} \cdot 1000 \frac{\mu l}{ml} = 7,17 \cdot 10^8 \frac{vp}{ml}$$

5.1.2. LV transduction of CD45RA⁻ T cells achieved robust expression of NKG2D while not affecting cell viability.

After CD45RA depletion and transduction, immunophenotyping of total PBMCs and CD45RA⁻ cells, both transduced and untransduced with NKG2D CAR, was performed by FCM. Cells were analyzed for viability, using DAPI staining, and CD45RA, CD3, NKG2D, CD4 and CD8 expression. In both PBMCs and CD45RA⁻ T cells, the transduction process using a MOI = 2 did not affect viability or the subpopulations analyzed, but it significantly increased the expression of NKG2D ($p = 0,0006$ for PBMCs; $p < 0,0001$ for CD45RA⁻), as shown in Figure 16. Based on this result we decided to stablish the MOI = 2 for all the NKG2D-CAR T productions we performed.



Viability ranged from 33,90 to 86,30% ($56,73 \pm 7,81\%$) in NKG2D-CAR PBMCs and from 18,50 to 91,51% ($54,83 \pm 5,42\%$) for NKG2D-CAR CD45RA⁻ T cells. No significant differences were observed when comparing the viability between both populations. However, CD45RA depletion achieved a CD45RA⁻ purity of $93,81 \pm 1,98\%$, significantly higher than the values for PBMCs, $57,89 \pm 5,40\%$ ($p = 0,0003$). Furthermore, regarding the CD4:CD8 ratio, we also observed significant differences between transduced PBMC and CD45RA⁻ T cells. The expression of CD4 in PBMCs and CD45RA⁻ T cells was $57,12 \pm 7,39\%$ and $79,80 \pm 3,76\%$, respectively ($p = 0,0085$), while CD8 expression was $40,55 \pm 6,98\%$ in NKG2D-CAR PBMCs and $17,20 \pm 3,3\%$ NKG2D-CAR CD45RA⁻ T cells ($p = 0,0049$). In addition, efficacy of NKG2D transduction remained similar in both populations with values always higher than 60% ($77,14 \pm 4,33\%$ expression of NKG2D for PBMCs and $86,61 \pm 2,63\%$ for CD45RA⁻ T cells) (Figure 17).



5.1.3. *NKG2DL are expressed in leukemia cell lines.*

The expression of NKG2DL was evaluated in representative acute leukemia cell lines as well as in primary leukemic blasts by FCM. Specific fluorescence intensity (SFI) of each ligand was obtained dividing median fluorescence intensity (MFI) of stained samples by the unstained ones. We considered a positive expression of a determined NKG2DL when SFI values were ≥ 2 . We observed that NKG2DL were heterogeneously expressed in the different leukemia cells lines, as shown in Figure 18 and Table 4.

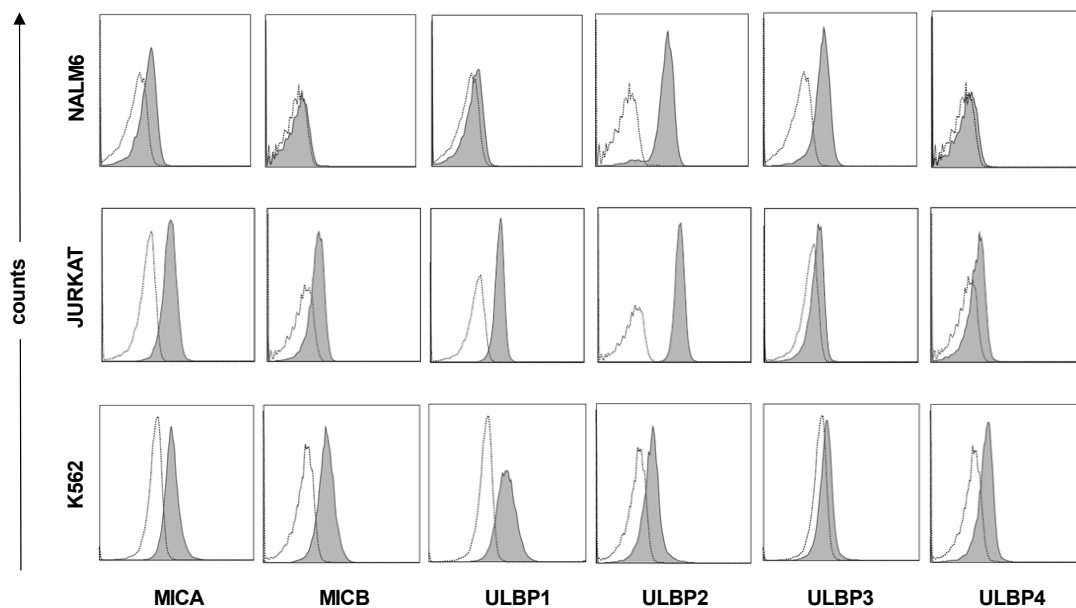


Figure 18. Representative histograms showing NKG2DL expression of different leukemia cell lines by FCM. Filled histograms represent stained samples while blank histograms are related to unstained cells.

Overall, all the leukemia cell lines showed upregulation of at least two different NKG2DL, and thus becoming a potential target for NKG2D-CART. ULBP2, MICA and ULBP1 were the NKG2DL most consistently expressed. More precisely, ULBP2 was expressed in all cell lines with SFI values ranging from 2,73 to 49,98. Except for TOM-1 cells, which showed an SFI = 1,82, MICA was upregulated in all cell lines as well. ULBP1 showed overexpression in all the analyzed leukemia cell lines but NALM-6 (1,78), RS4-11 (1,71) and SEM (1,91). ULBP3 was the less expressed NKG2DL, being upregulated in only 3 out of the 12 leukemia cell lines (NALM-6, REH and MV4-11). Jurkat cells showed high values of ULBP2 ($49,48 \pm 4,52$), ULBP1 ($11,82 \pm 3,06$) and MICA ($4,48 \pm 0,53$).

		MFI					
		MICA	MICB	ULBP1	ULBP2	ULBP3	ULBP4
B-ALL	NALM-6	2,57	1,4	1,78	27,95	5,84	1,8
	REH	3,74	1,89	2,85	5,82	5,28	2,45
	RS4;11	2,31	1,86	1,71	2,74	1,46	2,14
	TOM-1	1,82	1,21	6,93	2,73	1,48	1,69
T-ALL	MOLT-3	2,84	2,61	3,95	13	1,73	3,8
	CEM	2,31	1,72	2,55	4,8	1,36	2,12
	JURKAT	4,48	3,62	11,82	49,48	1,53	2,51
AML	K562	2,52	4,43	2,8	2,29	1,36	2,63
	ME-1	4,26	2,64	2,19	2,16	1,47	2,12
	KASUMI	2,76	7,77	3,09	2,16	1,28	2,26
Biphenotypic	MV4;11	1,77	1,4	3,71	3,15	4,6	2,02
	SEM	2,08	1,99	1,91	2,48	1,32	2,05

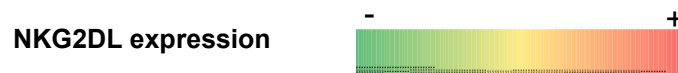


Table 4. SFI values of NKG2DL expression by FCM of different leukemia cell lines ($N = 3$). Color gradient represent SFI values from lower (green) to higher (red).

5.1.4. *NKG2DL are expressed in primary leukemic blasts of pediatric patients independently of the stage of the disease.*

As leukemia cell lines may differ significantly from primary leukemic blasts, we therefore used FCM to analyze the expression of NKG2DL in B-ALL, T-ALL and AML blasts from pediatric patients. As downregulation and release of NKG2DL by leukemic blasts is a well-known immunoescape mechanism, we ought to determine if the levels of NKG2DL expressed on cell surface correlated with disease progression. To this aim, we explored the expression of NKG2DL at diagnosis (Dx), relapse (R) or follow-up status. Overall, when we compared NKG2DL expression at diagnosis and relapse we found no significant differences. Moreover, the different leukemia entities showed similar NKG2DL expression patterns, with no significant differences among them (Figure 19). We next analyzed the expression of the different NKG2DL at Dx in B-ALL, T-ALL and AML. In B-ALL, we found MICA showed higher expression than the rest of the NKG2DL, and this difference was statistically significant when compared with all the others NKG2DL, except for ULBP4. We observed no differences in NKG2DL expression at Dx in AML and T-ALL, as shown in Figure 20. Further clinical details of pediatric patients studied are compiled in the Annex section.

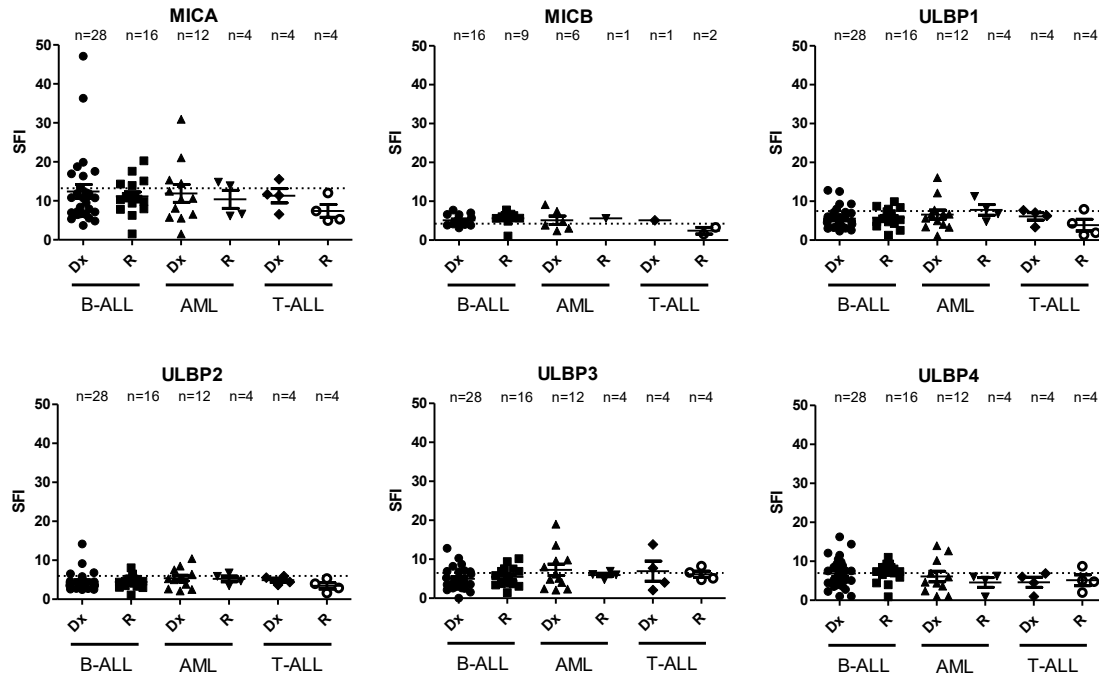


Figure 19. Expression of NKG2DL by FCM of B-ALL, T-ALL and AML pediatric patients blasts at diagnosis and relapse. Dotted line represents the expression of NKG2DL at follow-up status. Nonparametric Mann-Whitney test was used to compare 2 groups. * $p < 0,05$; ** $p < 0,01$; *** $p < 0,001$.

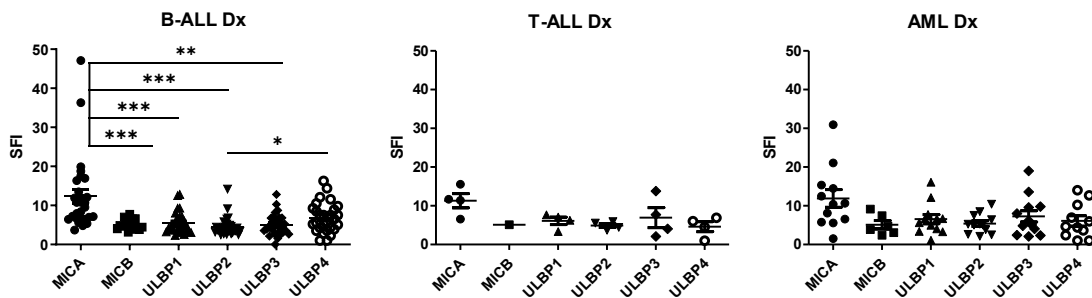


Figure 20. Expression of NKG2DL by FCM of B-ALL ($N = 28$; except for MICB, $N = 16$), T-ALL ($N = 4$; except for MICB, $N = 1$) and AML ($N = 12$; except for MICB, $N = 6$) pediatric patients blasts at diagnosis. Kruskal-Wallis one-way ANOVA following Dunn's post-hoc test was performed. * $p < 0,05$; ** $p < 0,01$; *** $p < 0,001$.

5.1.5. NKG2D-CART target leukemic blasts in vitro.

To evaluate the cytotoxic activity of effector cells, we first compared the specific lysis produced by NKG2D-CAR transduced CD45RA⁺ T cells versus UT T cells against B-ALL, T-ALL, AML and biphenotypic leukemia cell lines (Figure 21). As expected, NKG2D-CART produced higher lysis than UT T cells in all tested leukemia cells lines. While CARTs achieved lysis values between 15,65 and 75,34%, UT T cells only produced a cytotoxic effect below 20% (6,02 – 14,26%), which was considered unspecific. Significant differences were found when R4;11 ($p = 0,042$), Jurkat ($p = 0,011$), MOLT-3 ($p = 0,033$),

Kasumi ($p = 0,009$), K562 ($p = 0,041$), ME-1 ($p = 0,006$), MV4;11 ($p = 0,002$) and SEM ($p = 0,016$) were used as target cells. We also reported that specific lysis was very heterogeneous depending on the donor used to produce the NKG2D-CART and the experimental conditions, as shown in Figure 22A. As expected, the highest E:T ratio achieved the highest cytotoxic.

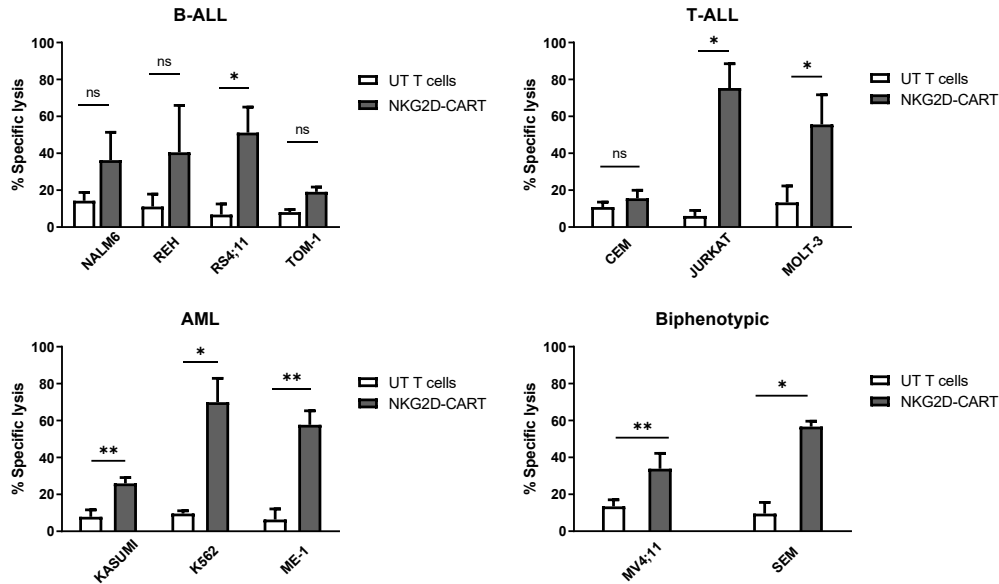
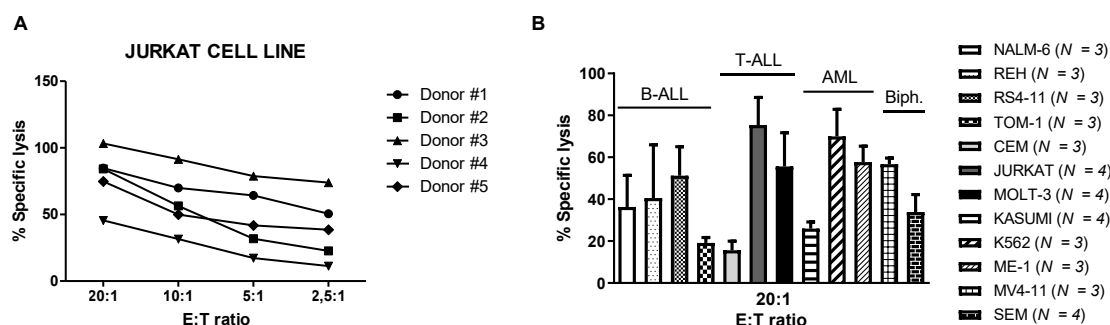


Figure 21. Specific lysis by EU-TDA assays of NKG2D-CART and UT T cells against leukemia cell lines at 20:1 E:T ratio. Student's t test was used to compare 2 groups. Paired t test was applied in NALM6 ($N = 3$), REH ($N = 3$), CEM ($N = 3$) and MOLT-3 ($N = 4$) cell lines. Unpaired t test was applied in RS4;11 ($N = 3$), ME-1 ($N = 3$) and MV4;11 ($N = 3$) cell lines. Mann-Whitney test was applied in TOM-1 ($N = 3$), Kasumi ($N = 4$) and SEM ($N = 4$) cell lines. Welch's t test was applied in Jurkat ($N = 4$) and K562 ($N = 3$) cell lines. * $p < 0,05$; ** $p < 0,01$; *** $p < 0,001$; ns, not significant.

When comparing the specific lysis against the different cell lines grouped by disease, we found that T-ALL and AML cell lines, reaching values around 70% of specific lysis, trended to be more sensitive to NKG2D-CAR T cytotoxicity than B-ALL cell lines, despite differences were not significant. On average, the percentage of specific lysis was: 48,9% for AML, 51,2% for T-ALL, 45,3% for bi-phenotypic and 37% for B-ALL at a 20:1 E:T ratio. (Figure 22B). Indeed, Jurkat cell line (T-ALL) resulted the more susceptible target to CART-mediated lysis, with $75,34\% \pm 13,24\%$ specific lysis.



Since we observed important differences in the cytotoxicity of NKG2D-CART against the multiple leukemia cell lines studied, we wondered if this could be associated with the heterogeneity of NKG2DL expression. We thus compared the expression of NKG2DL of leukemia cell lines versus the specific lysis produced by CAR T cells. However, we did not find a significant correlation between the percentage of lysis and the surface expression of any ligand (Figure 23).

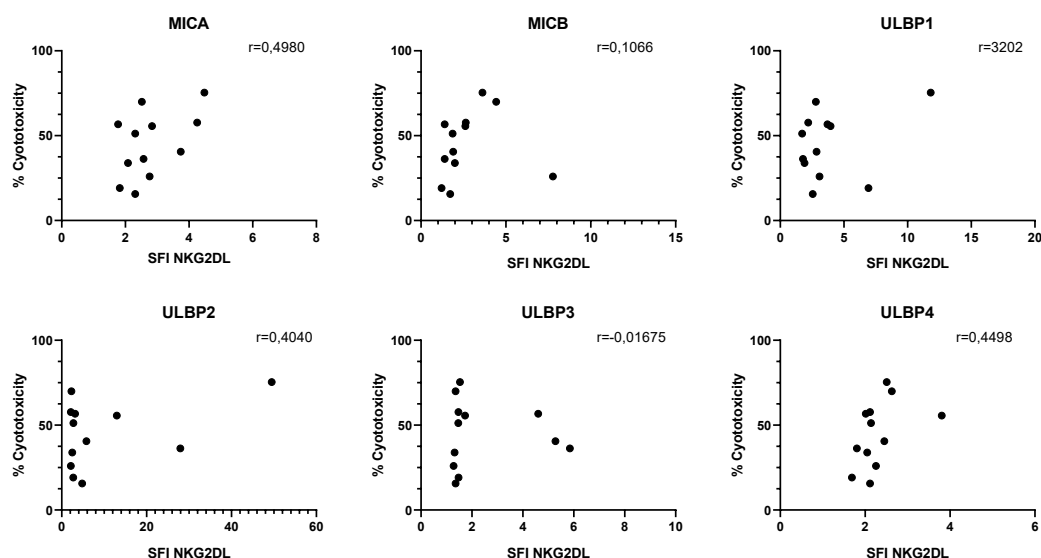


Figure 23. Correlation analysis between NKG2DL expression of leukemia cell lines and their susceptibility to NKG2D-CART cytotoxicity. Parametric Pearson correlation analysis was applied between X and Y values.

When primary blasts were used as targets, AML showed the highest sensitivity (50,3% of specific lysis on average), followed by T-ALL (31%) and B-ALL (19,5%) at a 20:1 E:T ratio. These values, with the exemption of AML, remained lower than those achieved when leukemia cell lines were used as a target. Furthermore, the lytic capacity of

NKG2D-CART against both the different cell lines and primary blasts from patients was tremendously heterogeneous, as illustrated in Figures 22A and 24, respectively. The intrinsic differences between the healthy donors from which CAR T cells were produced and between patients, contributed to the observed heterogeneity.

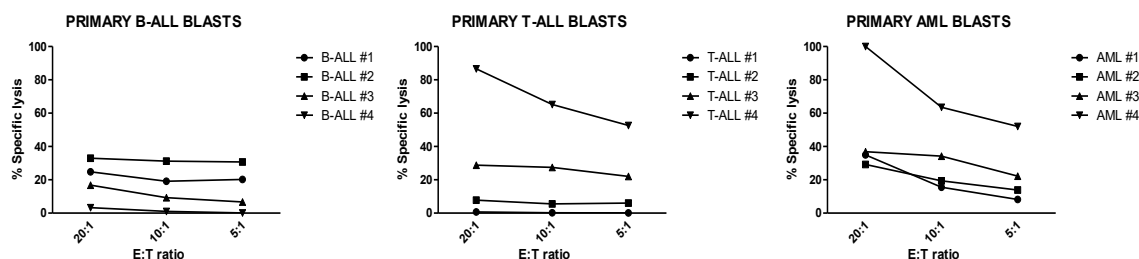
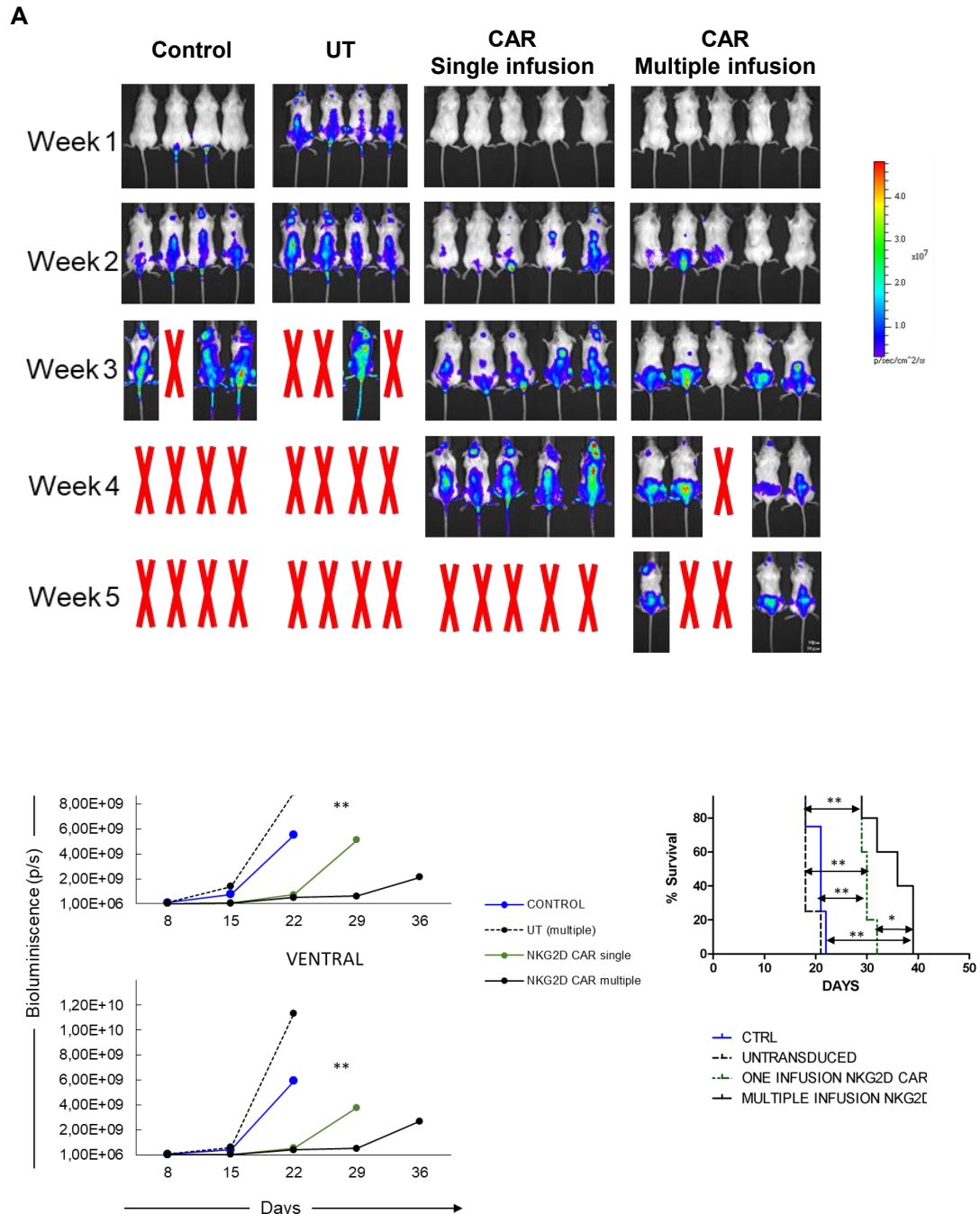


Figure 24. Specific lysis by Eu-TDA assays of NKG2D-CART against primary blasts of pediatric patients suffering from B-ALL, TALL or AML at different E:T ratios.

5.1.6. NKG2D-CART reduce tumor progression and prolong survival in a murine model of T-ALL.

Having shown the ability of NKG2D-CART to target leukemia cell lines *in vitro*, we then moved a step forward and tested the efficacy of NKG2D-CART in a murine model of T-ALL using Jurkat GFP-Luc as targets. In this experiment, a total of 18 T-ALL bearing mice were divided into 4 different groups: group A (control group) was left untreated, group B received multiple infusions of untransduced CD45RA⁺ T cells, group C received a sole infusion of NKG2D-CART, and group D received multiple infusions of NKG2D-CART. A scheme with the specific times and doses is shown in the Materials and Methods section (Figure 11). Leukemia progression was monitored weekly by bioluminescence. Mice that were left untreated or those receiving infusions of UT CD45RA⁺ T cells showed more leukemia burden than the treated mice, as seen with significantly higher average dorsal and ventral bioluminescent signals 22 days after leukemia infusion (Figure 25A, B). Based on BLI, both control groups had a similar pattern of leukemia progression and showed no statistical differences in survival ($p = 0,18$). Between days +18 and +22 post-infusion, mice from the control and UT groups showed massive tumor burden by BLI and leukemia clinical symptoms, and under ethical consideration they were euthanized by humane endpoint. On the contrary, those mice treated with either single or multiple doses of NKG2D-CART, showed a leukemia progression controlled until day +22 (Figure 25A, B). However, at day +29, mice treated with an only infusion of NKG2D-CART, showed an increased BLI. In the group receiving multiple infusions, leukemia progression remained controlled still at day +29. However, by day +36, an increment in BLI was measured, indicating leukemia progression. Kaplan-

Meier estimation demonstrated significant differences between treated and control groups (Figure 25C). These data indicate NKG2D-CART could control leukemia progression and prolong survival of the treated mice, but failed to completely eradicate the tumor and cure the animals.



infusions of $1 \cdot 10^7$, followed by three weekly infusions of $2 \cdot 10^7$ NKG2D-CART (A). B) Tumor burden monitoring of mice receiving the different treatments of dorsal or ventral acquisition. Control mice (blue line), UT (dashed line), CAR single (green line) and CAR multiple (bold black line). C) Kaplan–Meier survival curves for control mice (blue line), UT (dashed line), CAR single (dotted line) and CAR multiple (bold black line). * $p < 0,05$; ** $p < 0,01$; *** $p < 0,001$.

5.1.7. In treated mice, infused NKG2D-CART home to the bone marrow and respond against leukemia cells.

As previously shown, we found that the control of leukemia progression was NKG2D-CART dose dependent, as mice treated with several infusions performed better than those receiving a single infusion. FCM analysis of tumor burden (identified as humanCD45⁺ GFP⁺ cells) in PB, BM and spleen confirmed the BLI data. We also analyzed NKG2D-CAR T cell persistence (identified as humanCD45⁺ GFP⁻) in all hematopoietic tissues by FCM. In those mice which had received an only infusion of NKG2D-CART 32 days prior to sample collection, we observed no remaining NKG2D-CART in BM, PB and spleen. However, mice receiving multiple infusions and whose samples were collected 4 days after the last infusion, showed presence of NKG2D-CART in PB, BM and spleen (Figure 26).

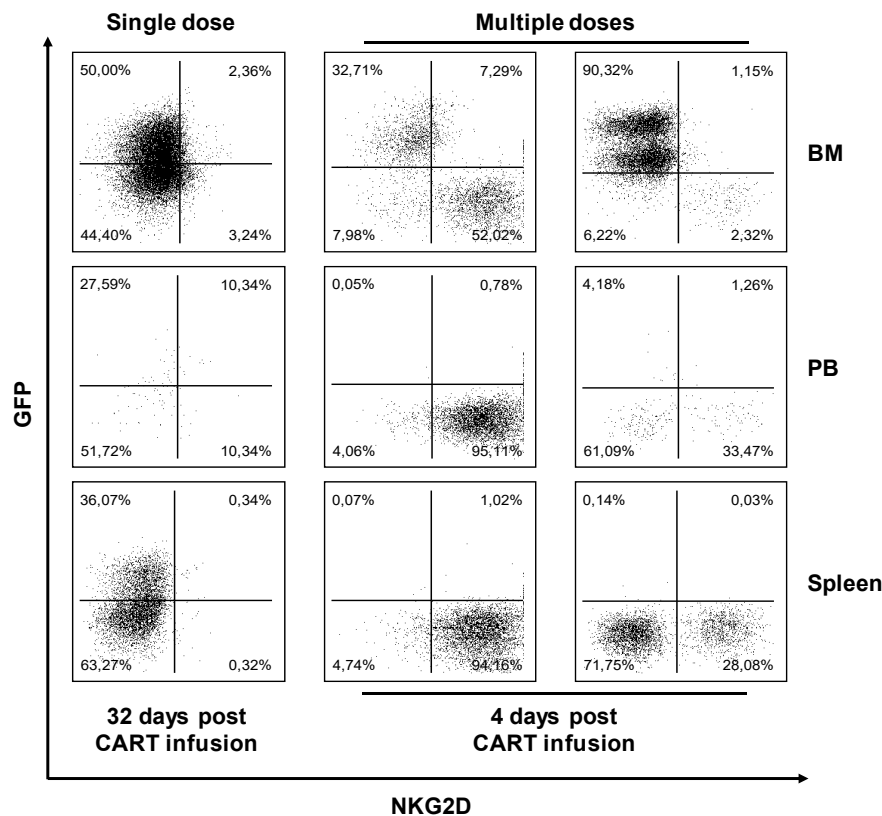


Figure 26. Dot plots obtained by FCM analysis of BM, PB and spleen samples from mice engrafted with Jurkat-GFP-Luc cells and treated with single or multiple doses of NKG2D-CART. Leukemia cells were identified as GFP positive cells while CART cells were detected as NKG2D positive population.

FCM analysis revealed NKG2D-CART were homing to the BM when multiple doses were used. As the results from our *in vivo* experimentation were not as successful as we had

expected taking into account the *in vitro* results obtained, we then wanted to explore if those NKG2D-CART infiltrating the BM kept their anti-tumor cytotoxic ability. To this aim, femur samples of treated mice were paraffin embedded, immunostained for granzyme B and H/E counterstained. IHC analysis revealed the presence of granzyme B positive human T cells (in brown) surrounding leukemia cells (small and disordered purple cells) in samples of treated groups, indicating NKG2D-CART were homing to the BM and secreting lytic granules in response to leukemic blasts (Figure 27). Furthermore, multiple infusion of NKG2D-CART promoted higher infiltration of effector cells in the BM, as the density of granzyme B positive cells was higher in this treatment group. Additionally, IHC confirmed the leukemia burden we had observed by FCM and BLI (Figure 27).

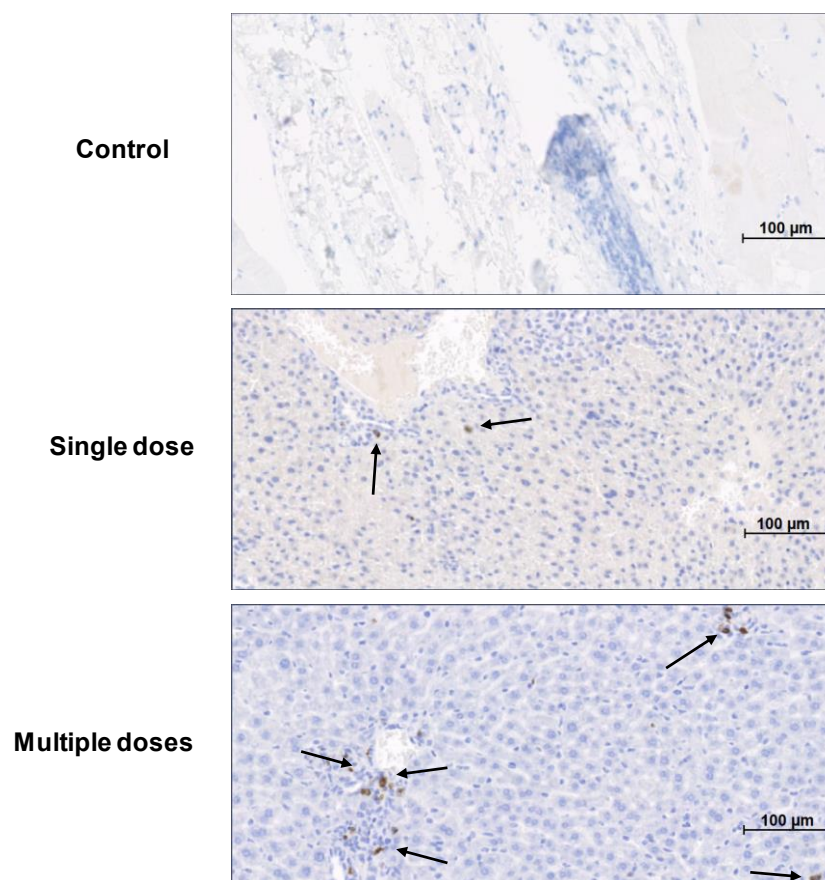


Figure 27. IHC staining of a BM sections of mice remained untreated (control), treated with single dose of NKG2D-CART (sample collected 32 days post CAR T cells infusion) or with multiple doses of NKG2D-CART (sample collected 4 days post CART cells infusion). Brown color correspond to granzyme B staining (arrows), which associates with the presence of degranulating NKG2D-CART in the sample.

5.2. Immunoescape mechanisms.

5.2.1. *Jurkat T-ALL cell line released sULBP2.*

Our previous data proved that NKG2D-CART were able to reach the BM and exert an anti-tumor response against leukemic blasts. However, they were still not able to completely eradicate the tumor and cure the animals. Release of sNKG2DL by tumor cells has been demonstrated to be an immune escape mechanism that can reduce surface expression of NKG2DL in the tumor cells thus inducing downregulation of NKG2D receptor on NK cells, blocking the immunosurveillance axis NKG2D/NKG2DL. Based on this, we next explored if this mechanism could be hindering the anti-tumor ability of NKG2D-CART in the murine model. To this aim, we measured the levels of sNKG2DL secreted by leukemia cell lines, *in vivo* samples or serum from patients suffering from acute leukemia by ELISA. While sNKG2DL levels were barely detected in the supernatant of leukemia cell lines, low levels of sULBP2 ligand were detected in the supernatant of NALM-6 and Kasumi cell lines (0,66 ng/ml and 0,02 ng/ml, respectively). However, in the supernatant of Jurkat-GFP-Luc cells, 3,11 ng/ml of sULBP2 and low levels of sULBP1 (0,60 ng/ml) were detected (Figure 28).

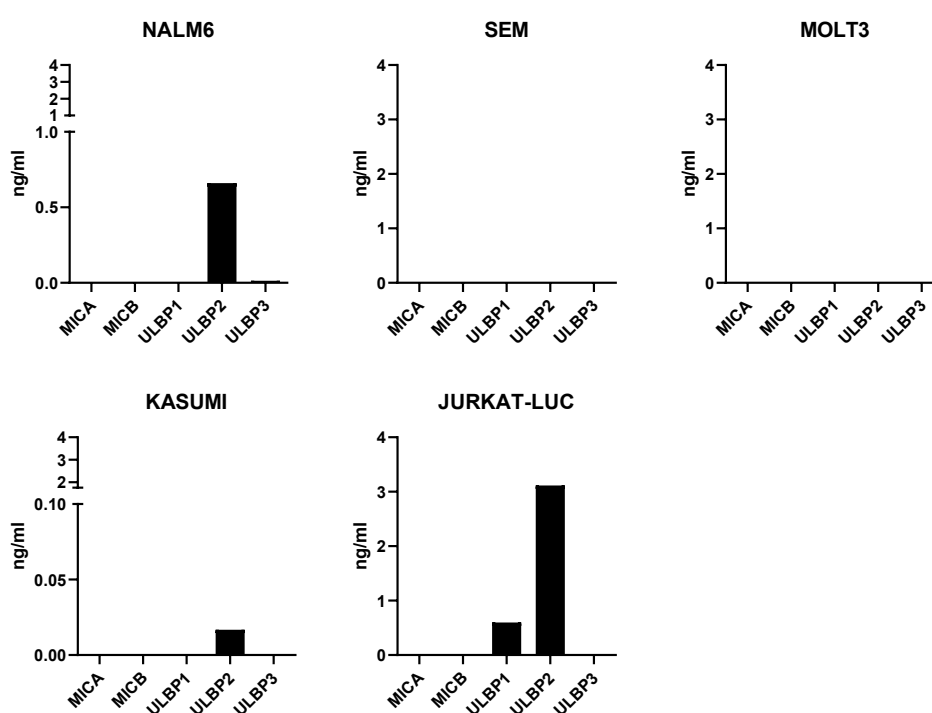
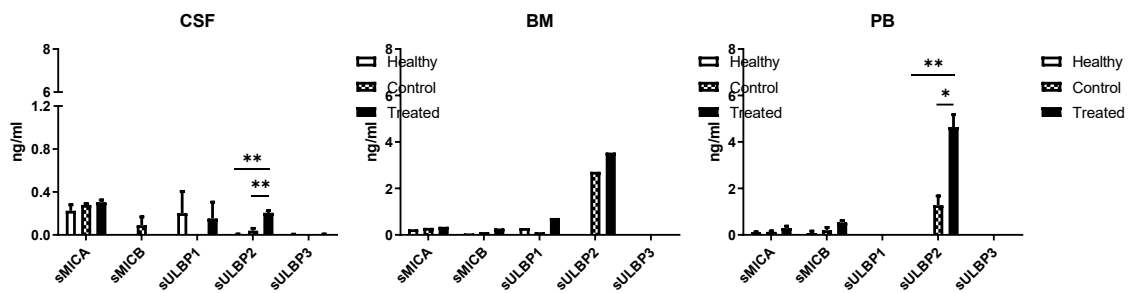


Figure 28. Expression of sNKG2DL in supernatants of representative leukemia cells lines by ELISA.

To further confirm the possible mechanisms behind the inability of NKG2D-CART to eradicate the tumor in the *in vivo* model, we measured the levels of sNKG2DL in T-ALL bearing mice, either left untreated or treated with multiple infusions of NKG2D-CART. As human and murine NKG2DL present NKG2D-binding domains with maintained structural homology, healthy NSG mice were used as controls for basal detection of sNKG2DL.

When analyzing the expression of sNKG2DL in samples from NKG2D-CART treated or untreated mice and comparing them with the expression of the engrafting Jurkat-GFP-Luc cell line, we found that those mice bearing leukemia cells showed a significantly increased amount of sULBP2 compared to those measured in control NSG mice, indicating that T-ALL cells released NKG2DL in their soluble form. Additionally, sULBP2 ligand was overexpressed in CSF samples of mice receiving CART treatment compared to those mice remained untreated (Figure 29), which could be an escape mechanism of leukemia against the treatment pressure. In BM samples, sULBP2 also seemed to be overexpressed in treated mice compared to untreated and healthy control mice, but due to the low number of samples, statistics could not be applied.



< 0,05; ** p < 0,01; *** p < 0,001.

5.2.2. sNKG2DL were found in the serum of patients suffering from acute leukemia.

To explore if sNKG2DL could impact the efficacy of NKG2D-CART in the clinical setting, we analyzed the presence of sNKG2DL in the serum of B-ALL, T-ALL and AML pediatric patients. First, we explored across the different leukemia subtypes if the levels of sNKG2DL changed with the disease status. The levels of sNKG2DL measured in the serum of healthy donors were used as basal control. In B-ALL, we found that the expression of sMICA ($p = 0,003$), sMICB ($p = 0,022$) and sULBP2 ($p = 0,004$) were significantly higher at diagnosis compared with controls, while sULBP3 was upregulated

at diagnosis compared to follow-up samples ($p = 0,047$) (Figure 30A). Overall, the levels of sNKG2DL showed a tendency to be higher at diagnosis than at relapse, which could be attributed to the higher number of blasts at the moment of diagnosis. However, no statistically differences were observed. At the moment of diagnosis, sULBP2 and sMICB were the most expressed ligands for pediatric B-ALL (0,89 ng/ml and 1,49 ng/ml, respectively), as showed in Figure 30B.

In the case of pediatric AML, sMICA ($p = 0,035$) and sMICB ($p = 0,009$) were overexpressed at diagnosis compared to the other disease stages (Figure 31A). Unfortunately, the levels of sNKG2DL at relapse and follow-up could not be statistically compared because of the lack of samples. At diagnosis, sMICB and sULBP2 resulted the more expressed sNKG2DL (1,11 ng/ml and 0,70 ng/ml, respectively) (Figure 31B).

We also analyzed the expression pattern of sNKG2DL in pediatric T-ALL. However due to the low number of samples collected, we could not establish comparisons amongst the different disease stages nor the individual ligands (Figure 32A, B).

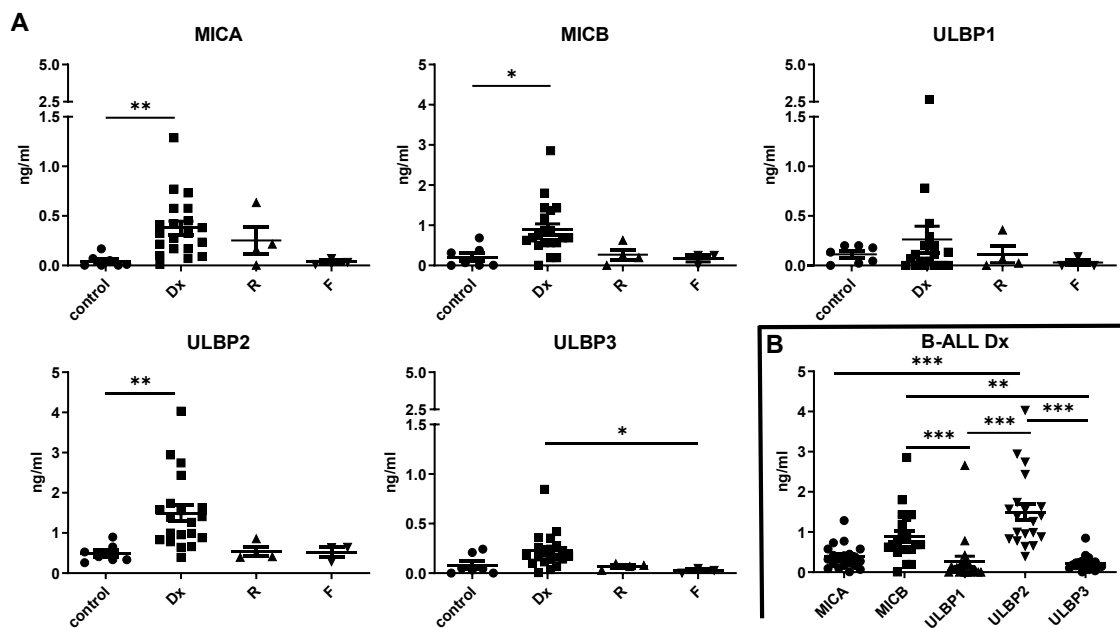


Figure 30. A) Expression of sNKG2DL measured by ELISA in the serum of pediatric B-ALL patients at diagnosis (Dx; $N = 20$), relapse (R; $N = 4$) and follow-up (F; $N = 3$) compared to healthy donors (control; $N = 7$). Control samples were collected from healthy donors. B) Comparison of different sNKG2DL expression at diagnosis for B-ALL samples. Kruskal-Wallis one-way ANOVA following Dunn's post-hoc test was performed. * $p < 0,05$; ** $p < 0,01$; *** $p < 0,001$.

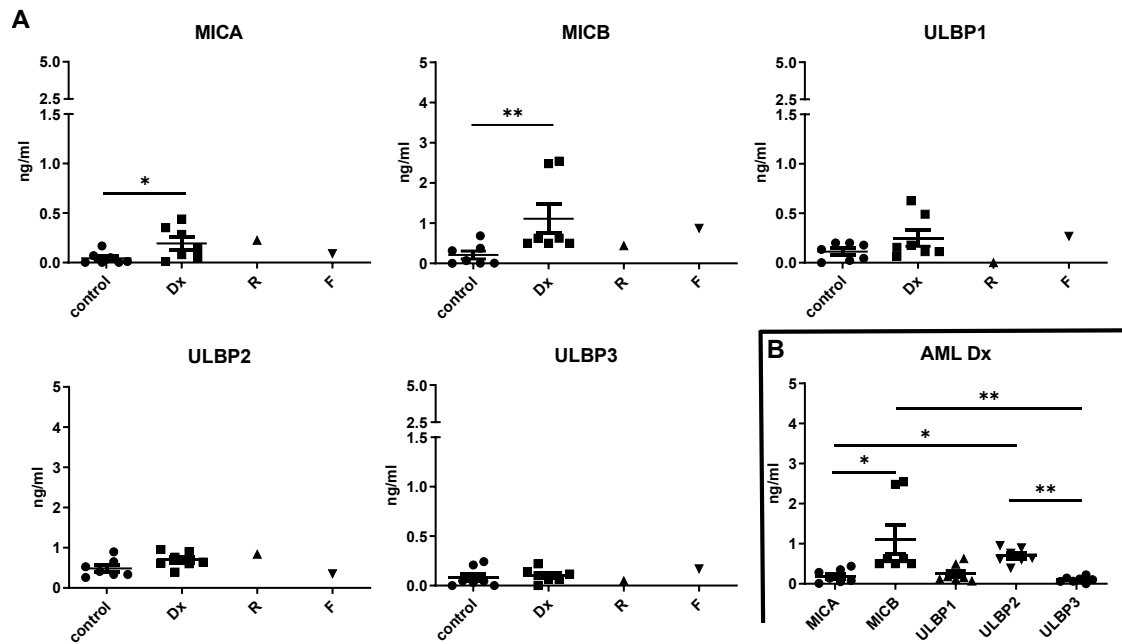


Figure 31. A) Expression of sNKG2DL measured by ELISA in the serum of pediatric AML patients at diagnosis (Dx; $N = 7$), relapse (R; $N = 1$) and follow-up (F; $N = 1$) compared to healthy donors (control; $N = 7$). Control samples were collected from healthy donors. B) Comparison of different sNKG2DL expression at diagnosis for AML samples. Mann-Whitney test was applied to compare controls and diagnosis samples; Kruskal-Wallis one-way ANOVA following Dunn's post-hoc test was performed. * $p < 0,05$; ** $p < 0,01$; *** $p < 0,001$.

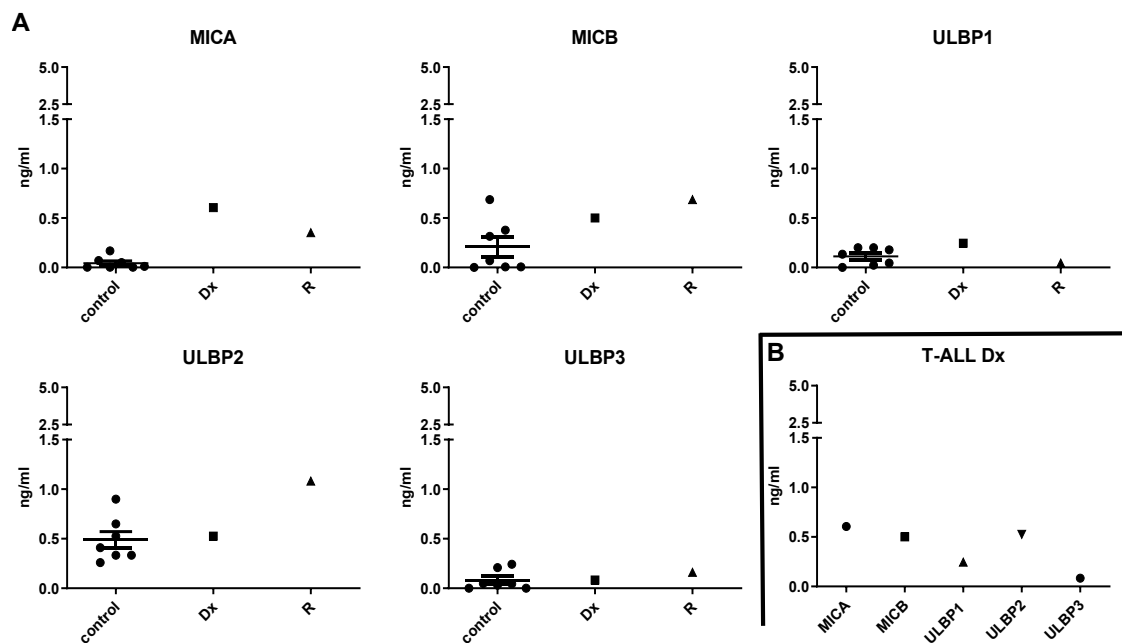


Figure 32. A) Expression of sNKG2DL measured by ELISA in the serum of pediatric T-ALL patients at diagnosis (Dx; $N = 1$), relapse (R; $N = 1$) and follow-up (F; $N = 0$) compared to healthy donors (control; $N = 7$). Control samples were collected from healthy donors. B) Comparison of different sNKG2DL expression at diagnosis for T-ALL samples.

Finally, as the highest levels of sNKG2DL were measured at diagnosis, we next compared the expression of the sNKG2DL at this stage in the different leukemia entities. In general, B-ALL showed higher levels of sNKG2DL than AML and T-ALL, but these differences were only significant for sULBP2 ($p = 0,003$) and sULBP3 ($p = 0,032$). When looking at T-ALL cases, we could not establish statistical comparisons due to the scarcity of samples (Figure 33).

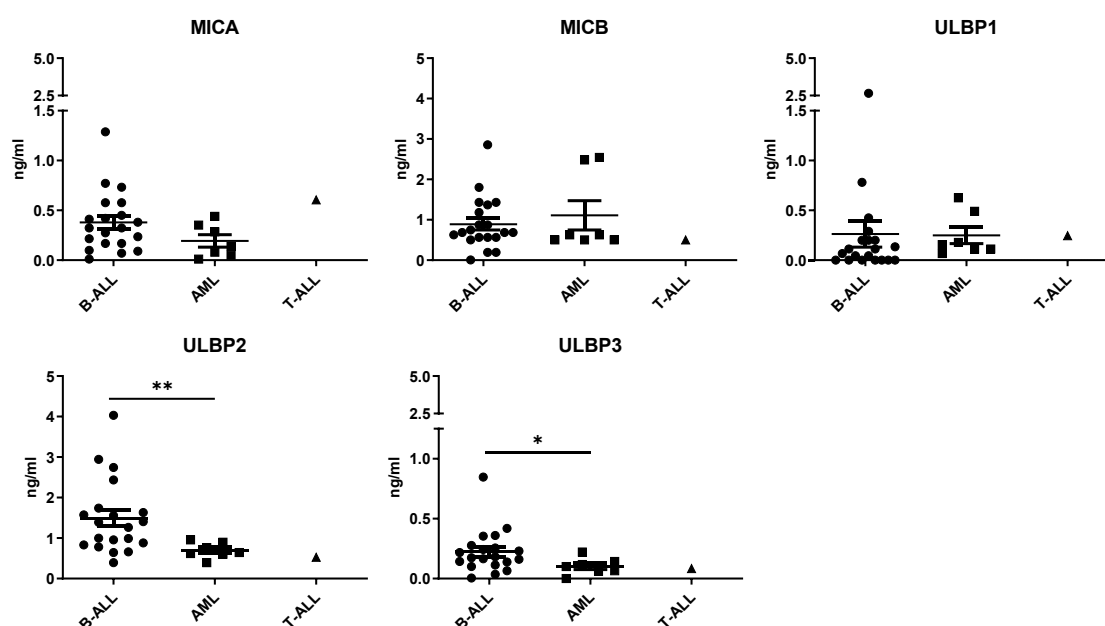
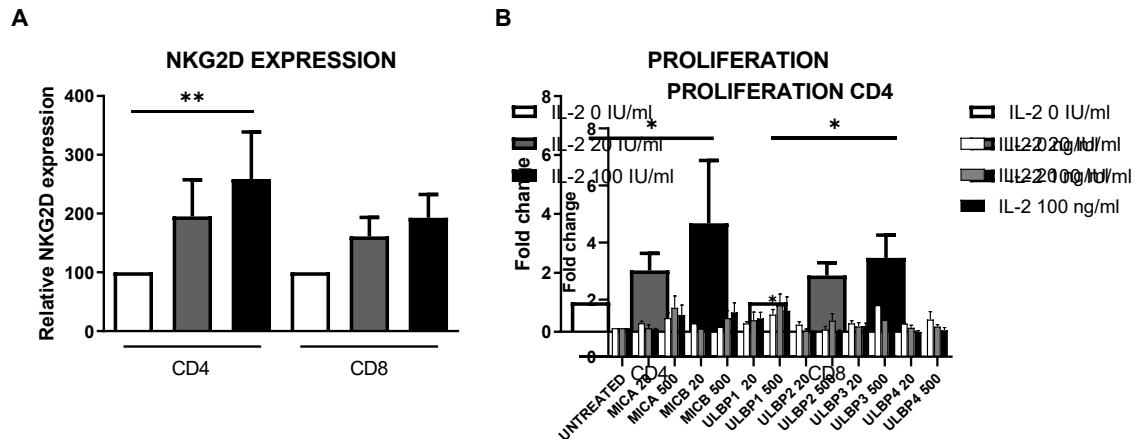


Figure 33. Expression of sNKG2DL measured by ELISA in the serum of pediatric patients of B-ALL ($N = 20$), AML ($N = 7$) and T-ALL ($N = 1$) at diagnosis. Mann-Whitney test was applied to compare B-ALL and AML samples. * $p < 0,05$; ** $p < 0,01$; *** $p < 0,001$.

5.2.3. Supraphysiological levels of sNKG2DL downmodulated chimeric NKG2D receptor and promoted CD45RA⁺ NKG2D-CAR T cell proliferation.

The negative impact of sNKG2DL in the endogenous NKG2D receptor is well established (Hilpert et al. 2012; Salih et al. 2003, 2002). However, the effects on NKG2D CARs have been studied at a lesser extent. In an attempt to explore how sNKG2DL could affect the efficacy of NKG2D-CART, we cultured NKG2D-CART with different concentrations of sNKG2DL for 7 days and analyzed NKG2D expression, proliferation and anti-tumor potential of NKG2D-CART. We also aimed to explore whether IL-2 added to the culture to explore if this cytokine could quench the effects of sNKG2DL on NKG2D-CART. Thus, we first evaluated the effects of IL-2 in NKG2D expression and cell proliferation. We found IL-2 enhanced NKG2D expression and promoted proliferation of NKG2D-CART in both CD4 and CD8 subsets in a dose-dependent manner. However, the differences

observed in NKG2D were only significant in the CD4 subset and when 100 IU/ml of IL-2 were used, where NKG2D expression was more than doubled in comparison with those cells cultured without IL-2 (Figure 34A). In addition, CAR T cells proliferation was significantly increased in both CD4 and CD8 subsets when 100 IU/ml of IL-2 were added to the culture (Figure 34B).



* $p < 0,05$; ** $p < 0,01$; *** $p < 0,001$.

Then, we analyzed the effects of sNKG2DL in the expression of NKG2D and cell proliferation of NKG2D-CART. As shown in Figure 35, The effects of sNKG2DL varied with each studied ligand. Additionally, inter-donor variability was also observed. High concentrations of sNKG2DL (500 ng/ml) decreased the expression of NKG2D receptor in both CD4 and CD8 populations compared to the untreated condition (Figure 35A). When treating the cells with physiological concentrations (20 ng/ml) we did not observe NKG2D downregulation but on the contrary, the expression levels of the receptor increased and this effect was enhanced by the addition of IL-2. However, we only obtained significant differences in downregulation with supraphysiological concentrations of sMICA and sMICB (500 ng/ml) for CD4 subset. For CD8 CAR T cells, downregulation of NKG2D was only observed when 500 ng/ml of sMICA were added to the culture. Regarding the proliferative stimulation by sNKG2DL, only high amounts of sULBP1 had a significant effect on CD4 cells compared to the untreated condition. Nevertheless, the treatment with supraphysiological concentrations of sMICA, sMICB and sULBP1 did increase the proliferation of CD8 CD45RA⁺ CAR T cells, as represented in Figure 35B.

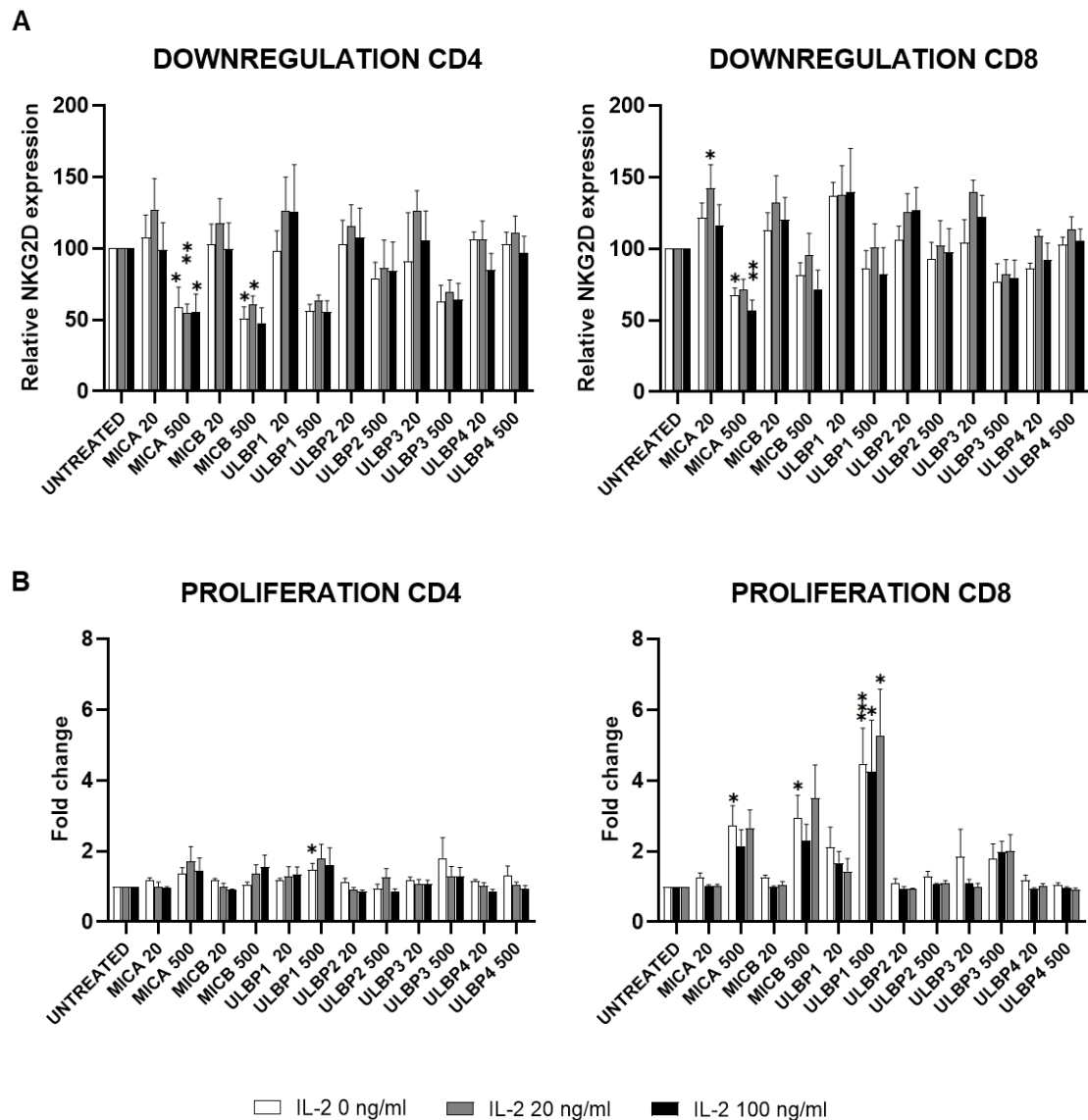


Figure 35. Effect of sNKG2DL on NKG2D-CART measured by FCM. Cells were cultured with different amounts of IL-2 and treated with sNKG2DL at physiological (20 ng/ml; 20; $N = 3$) or supraphysiological (500 ng/ml; 500; $N = 6$) concentrations. Relative expression of NKG2D receptor (A) and fold change proliferation (B) in CD4 and CD8 subsets. Friedman one-way ANOVA following Dunn's post-hoc test was performed. * $p < 0,05$; ** $p < 0,01$; *** $p < 0,001$.

5.2.4. Cytotoxicity of NKG2D-CART remained unaltered upon exposure to sNKG2DL.

As some sNKG2DL decreased the expression of NKG2D-CAR in our effector cells, we next investigated if sNKG2DL-mediated CAR downregulation could affect the cytotoxic capability of NKG2D-CART. In these experiments, sMICA and sULBP2 were used. We used sMICA, as it caused NKG2D downregulation in both CD4 and CD8 subsets. sULBP2 was used because it is the most secreted sNKG2DL by Jurkat cells, and thus, could be affecting NKG2D-CART cytotoxicity in our murine model. We observed that after incubating the NKG2D-CART with sNKG2DL for 72h, their cytotoxicity against Jurkat cells remained unaffected. Furthermore, when the K562 cell line was used as a target in the same conditions, we observed that only 500 ng/ml of sMICA significantly decreased the specific lysis of NKG2D-CART. Then, in order to try to mimic a hypothetical clinical situation, when a patient suffering from leukemia and with a certain amount of sNKG2DL in the plasma, is treated with NKG2D-CART, this time the different sNKG2DL were added to the co-cultures at the same moment of the cytotoxicity assay, in which. In this case, no effects on anti-tumor activity were observed regardless of the sNKG2DL and the concentrations used (Figure 36).

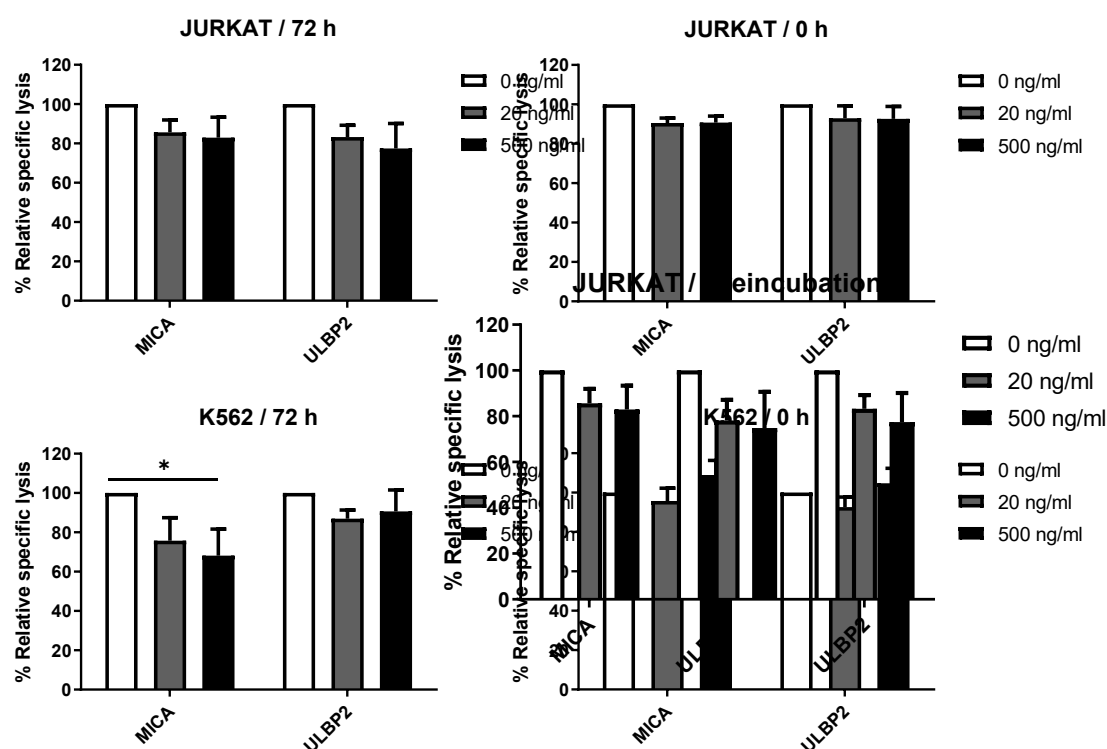
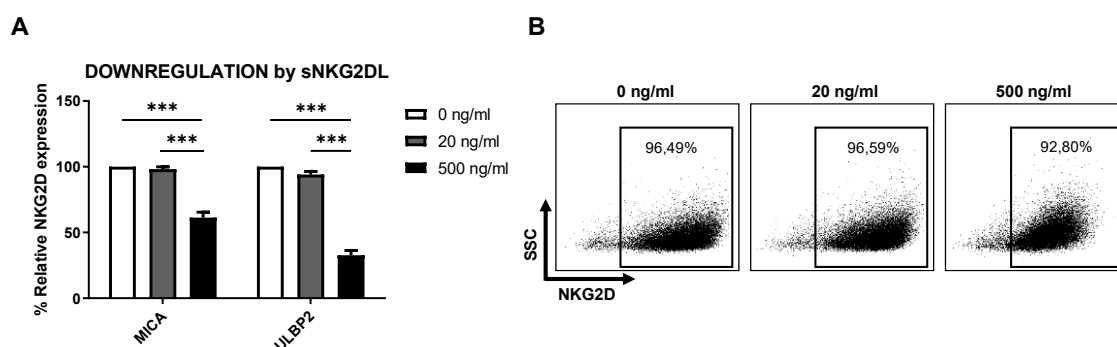


Figure 36. sNKG2DL-mediated downmodulation of NKG2D-CART cytotoxicity mediated by performing Eu-TDA assays. Jurkat and K562 cell lines were used as a target. Effector cells were treated with sNKG2DL for 72 h or they were added in the moment of the assay (t = 0) at physiological (20 ng/ml) or supraphysiological (500 ng/ml) concentrations (N = 5). Two-way ANOVA following Tukey's post-hoc test was performed. *p < 0,05; **p < 0,01; ***p < 0,001.

The effector cells used for these experiments were analyzed by FCM to correlate the downregulation and downmodulation effect produced by sNKG2DL treatment. We found that supraphysiological concentrations of the used ligands, sMICA, and sULBP2, produced a significant decrease in NKG2D expression on CAR T cells. We observed a decrease in NKG2D expression below 50% after sULBP2 treatment (Figure 37A). In spite of the decrease on NKG2D MFI, which is associated with the receptor density, the percentage of NKG2D positive cells barely changed (Figure 37B) which could explain the unaltered cytotoxic ability of NKG2D-CART.

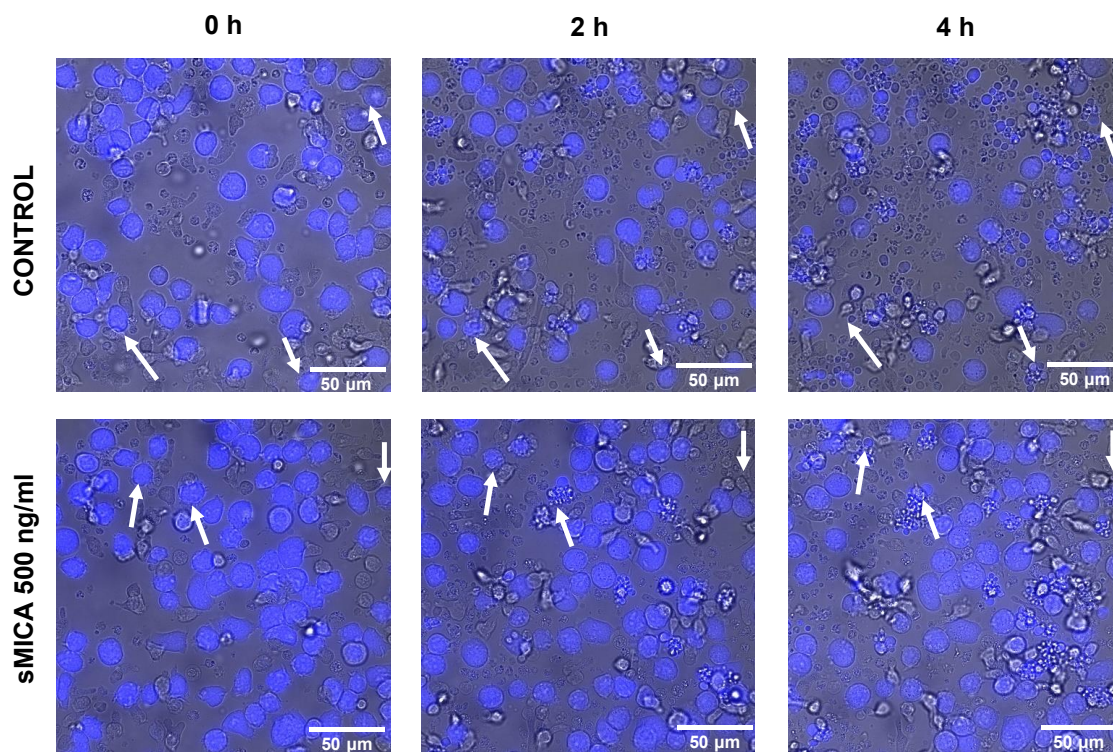


5.2.5. NKG2D-CART retained their capability to form productive immune synapses after treatment with high amounts of sMICA.

Once we had shown that NKG2D-CART were resistant to sNKG2DL regulation, we aimed to study in more detail the immune synapsis between effector and target cells in the presence or absence of sMICA by epifluorescence and confocal microscopy techniques. For that, NKG2D-CART were treated with or without 500 ng/ml sMICA for 72 h and co-cultured with CMAC labelled-Jurkat cells as target cells. As observed in a 4 h-time lapse microscopy, both treated and untreated NKG2D-CART eliminated Jurkat target cells similarly, with no alteration of the killing capability produced by sMICA treatment (Figure 38).

In another set of experiments, effector-target co-cultures were fixed and immunostained at end point upon synaptic conjugate formation (4h) to visualize F-actin (phalloidin), MTOC (anti-pericentrin) and NKG2D by performing epifluorescence and confocal

microscopy. As shown in Figure 39, sMICA-treated NKG2D-CART formed productive immune synapses, characterized by F-actin reorganization at the synapse, that finally led to the elimination of target cells, to the same extension that untreated cells. For both conditions, we observed different synapsis stages: 1) emerging synapses, when F-actin (red) was very intense in the interface between Jurkat cells (CMAC⁺, blue) and NKG2D-CART (gray) and MTOC (green) was not yet polarized, located far away from the synapse; 2) polarized synapses, when MTOC was located close by to the synapse; 3) ending synapses, when F-actin intensity at the synapse decreased and MTOC was not polarized (Figure 39A, C). These observations were confirmed by confocal microscopy showing immune synapses imaging with more resolution (Figure 39 B, D).



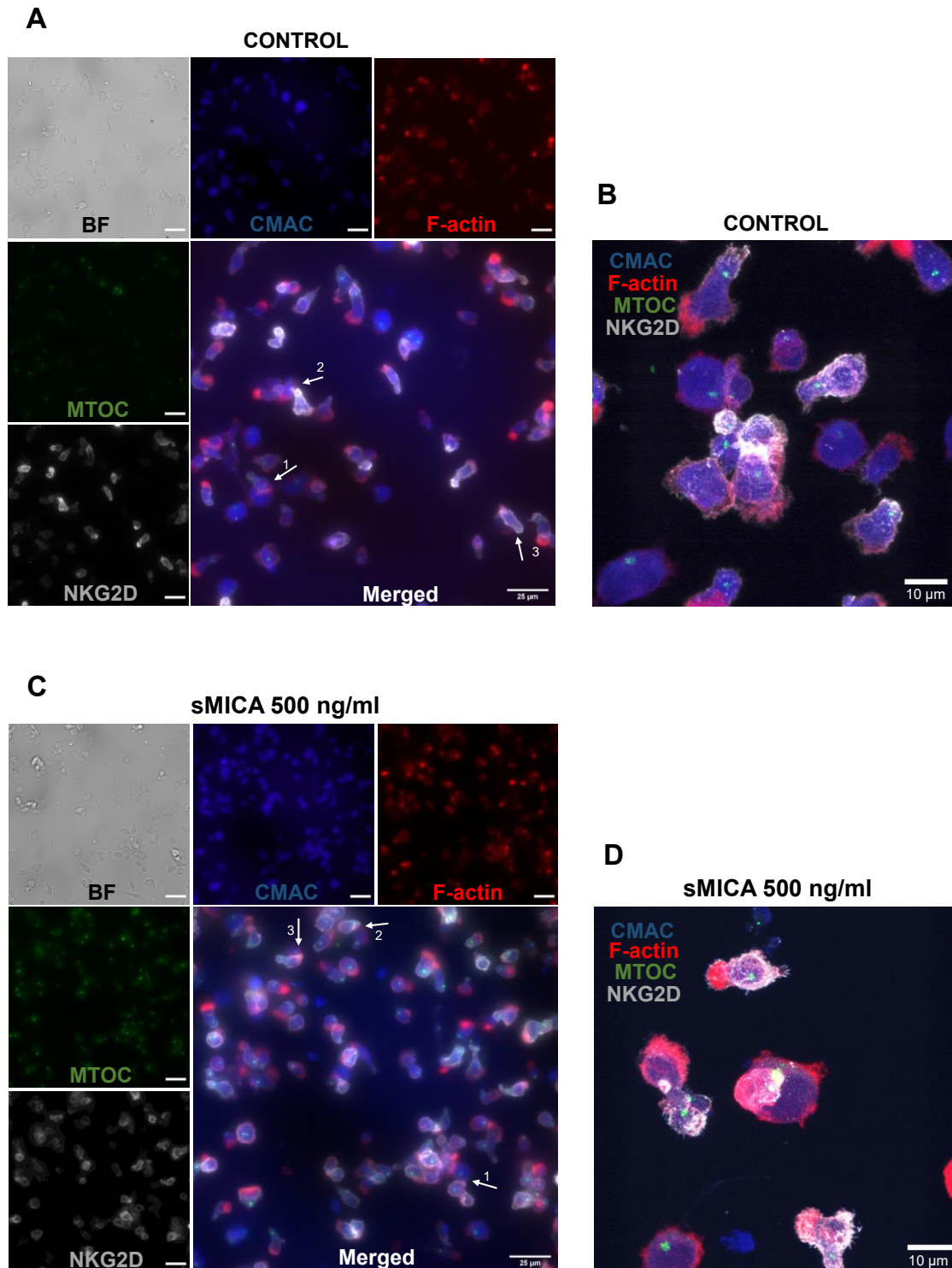
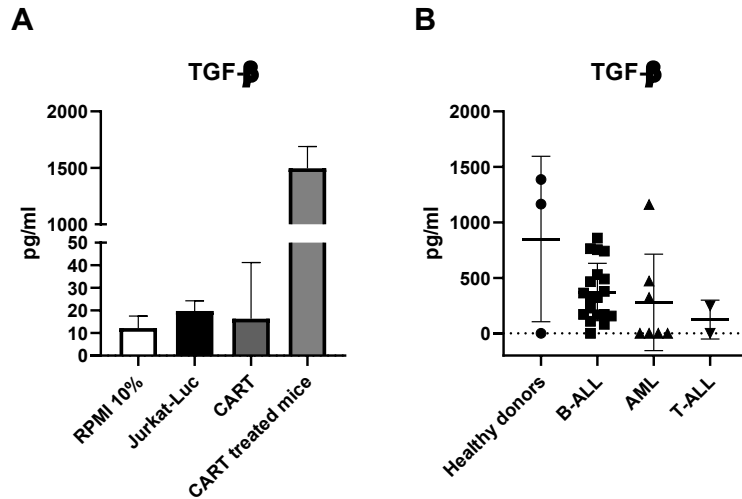


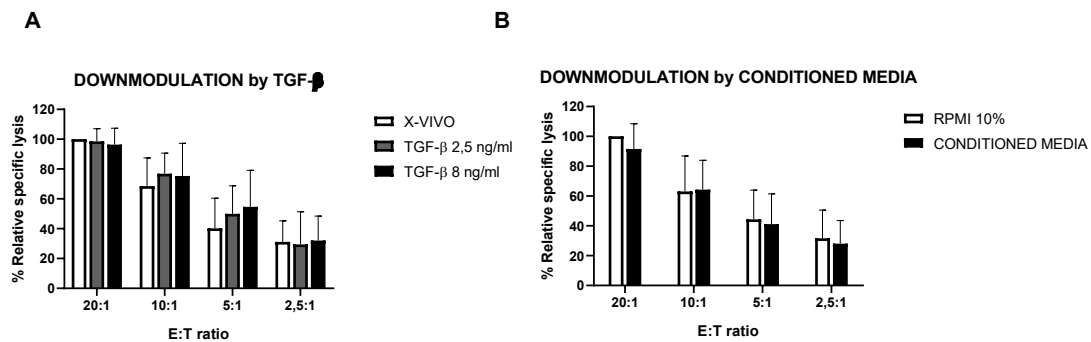
Figure 38. Epifluorescence (A, C) and confocal (B, D) microscopy images of immune synapses when CMAC-labelled Jurkat cells (blue) were challenged with NKG2D-CART at 1:1 E:T ratio for 30 minutes. NKG2D-CART remained untreated (control; A, B) or were treated with sMICA at 500 ng/ml for 72 h (C, D). Phalloidin were used to localize actin (red); anti pericentrin antibody were used to label MTOC (green); anti NKG2D antibody were used to localize NKG2D receptor (gray) of NKG2D-CART. BF, bright field. 1, emerging synapses; 2, polarized synapses; 3, ending synapses.

5.2.6. The levels of TGF- β secreted by leukemia cells do not affect NKG2D-CART cytotoxicity.

In our previous experiments using sNKG2DL, we could not find a robust explanation for the treatment failure in the murine model. It has been demonstrated that TGF- β released by tumor cells has an inactivating effect on NKG2D-NKG2DL immunosurveillance. For this reason, we next explored the impact of TGF- β on NKG2D-CART cytotoxicity. First, the concentration of TGF- β secreted by Jurkat-GFP-Luc cells cultured *in vitro* and in the plasma samples of CART-treated mice from the *in vivo* experiment was measured. To rule out TGF- β could also be released by effector cells, levels of TGF- β in the supernatant of NKG2D-CART was measured as well. Neither cultured T-ALL cells nor CARTs secreted significant amounts of the cytokine compared to basal levels found on supplemented RPMI culture media, with all measured values below 20 pg/ml. On the contrary, we found higher amounts of TGF- β in the serum of treated mice, reaching up to $1,496 \pm 111$ pg/ml levels (Figure 40A). Additionally, when we analyzed the expression of TGF- β in the serum of pediatric acute leukemia patients, we found a wide heterogeneity between samples, with values ranging from 0 to 1,385 pg/ml. Moreover, no significant differences were observed when comparing different leukemia entities. Strikingly, the levels of TGF- β measured in healthy donors were comparable to those from patients (Figure 40B). Furthermore, median values of healthy donor remained higher than those from leukemia patients. To further explore the effects of TGF- β , we treated NKG2D-CART with different concentrations of the cytokine for 24 h and evaluated their cytotoxicity against Jurkat-GFP-Luc cells. As shown in Figure 41A, specific lysis of NKG2D-CART remained unaltered after TGF- β treatment. Additionally, as leukemia cells may secrete soluble factors other than sNKG2DL and TGF- β that could be playing an inactivating role on NKG2D-CART, we evaluated the cytotoxic capability of NKG2D-CART after treatment with conditioned medium derived from Jurkat-GFP-Luc cultured for 24 h. Similarly, no changes on NKG2D-CART anti-tumor activity were observed (Figure 41A, B).



was performed.



5.2.7. NKG2D-CART target leukemia-initiating cells compartment.

It has been shown that LICs have self-renewal ability and are more resistant to treatment than other leukemia cells. Additionally, downregulation of NKG2DL in AML LICs and a consequent failure of NKG2DL directed therapy has been reported (Paczulla et al. 2019). To elucidate if NKG2D-CART could target this specific compartment in T-ALL, we performed colony forming assays and side population experiments using Jurkat GFP-

Luc cells. To do so, we co-cultured effector and targets cells at different E:T ratios for 4 h. Cells were then seeded in methylcellulose for 1 week, and CFU counted. As shown in Figure 42A, NKG2D-CART significantly decreased the number of CFU in a dose-dependent manner. Furthermore, Jurkat-GFP-Luc cells were co-cultured overnight with NKG2D-CART at 1:5 E:T ratio to analyze the percentage of survivor Jurkat-GFP-Luc cells within the side population. Jurkat-GFP-Luc cells cultured alone were used as controls. Compared to unexposed Jurkat-GFP-Luc cells, we observed a slight decrease in the side-population of those Jurkat-GFP-Luc cells that remained alive after co-culture with NKG2D-CART, however, these differences were not statistically significant (Figure 42B).

In addition, the expression of NKG2DL, c-kit and PD-L1 were explored in Jurkat-GFP-Luc cells cultured in suspension, as colonies and after exposure to NKG2D-CART. As illustrated in Figure 42C, the expression of c-kit and PD-L1 were comparable in the three conditions. Likewise, NKG2DL expression remained stable in the different samples analyzed (Figure 42D).

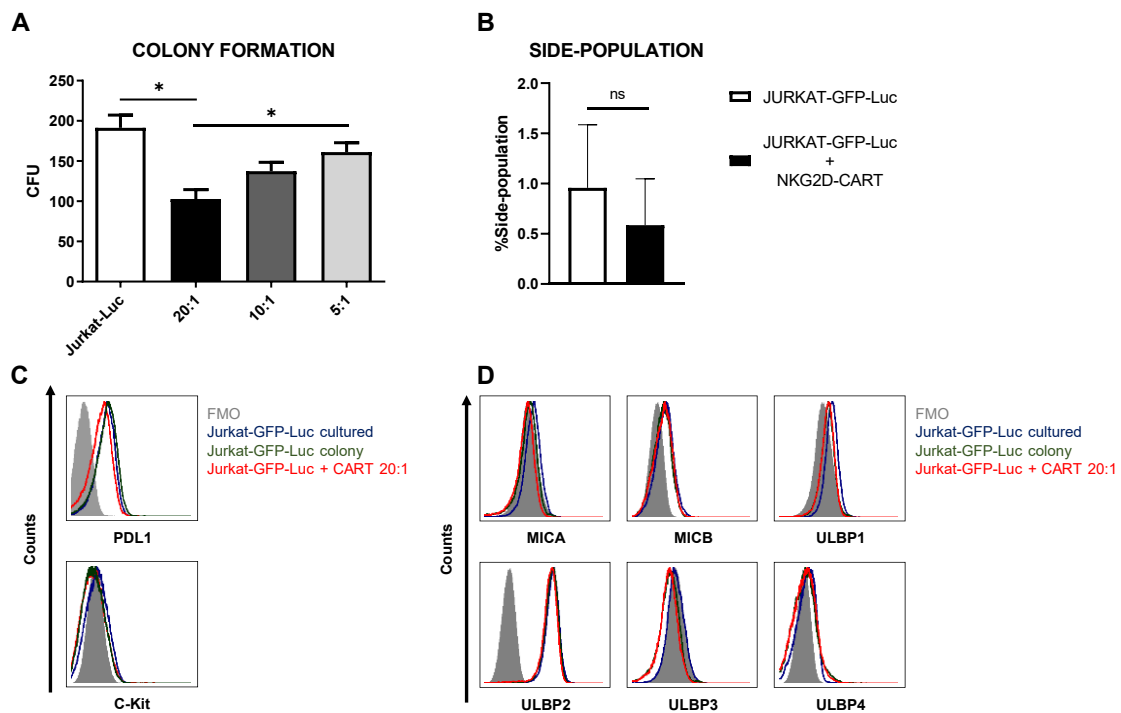
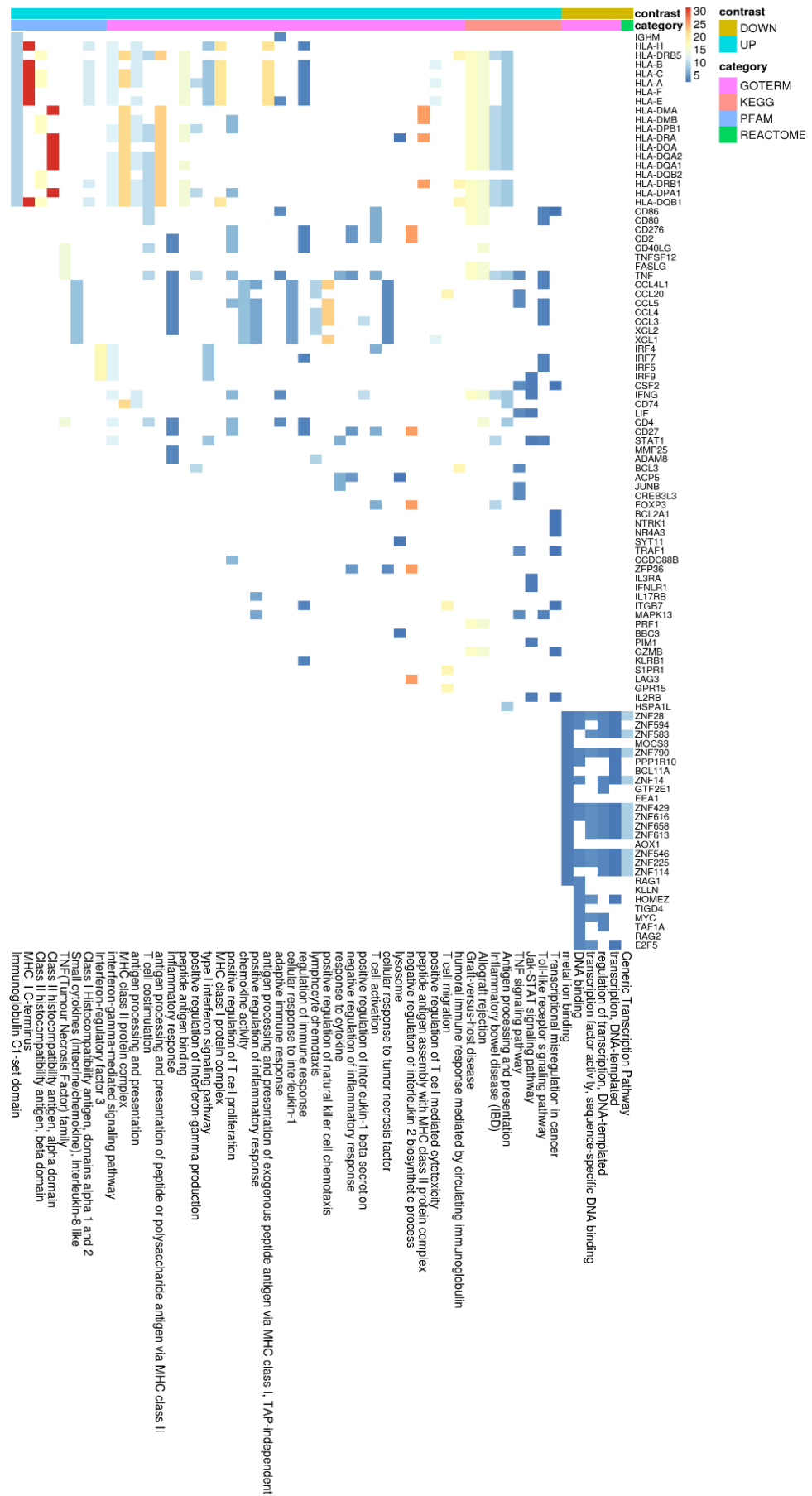


Figure 42. Jurkat-GFP-Luc cells were co-cultured with NKG2D-CART at different E:T ratios for 4 h. Remaining cells were used to evaluate CFU by colony formation assays ($N = 3$) (A) and the percentage of side population by FCM at E:T ratio = 1:5 ($N = 6$) (B). Expression of stemness markers, c-kit and PDL1 (C), and NKG2DL (D) in Jurkat-GFP-Luc in culture (blue histogram), Jurkat-GFP-Luc from a colony (green histogram) and Jurkat-GFP-Luc co-cultured with NKG2D-CAR T cells at 20:1 E:T ratio (red histogram). Kruskal-Wallis one-way ANOVA following Dunn's post-hoc test was performed for multiple comparisons. Unpaired t-test was applied for two columns comparison * $p < 0,05$; ** $p < 0,01$; *** $p < 0,001$.

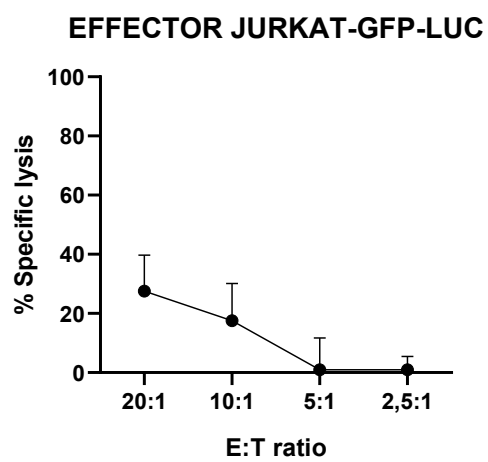
5.2.8. Upon exposure to NKG2D-CART, Jurkat cells upregulate genes related to proliferation, stemness and survival.

Because none of the previous studied factors seemed to affect NKG2D-CART cytotoxic activity in a way that could explain the moderate effect in the *in vivo* experiment, we decided to explore the transcriptome profile of Jurkat-GFP-Luc after being in contact with effector cells and compare it to normal cultured cells. To this aim, we co-cultured Jurkat cells with NKG2D-CART for 16h and RNA of sorted Jurkat cells was used to perform transcriptome analysis by RNAseq. We found out that, upon co-culture with NKG2D-CART, Jurkat cells upregulated stemness, proliferation and survival genes like STAT1 (proliferation), SMAD and LIF (promote self-renewal of hematopoietic cells) or L1CAM, a cancer stem cell marker. Furthermore, different gene clusters involved in immune response were upregulated in these cells, like IFN- γ mediated signaling pathways, MHC class II complex, antigen processing and presenting, T cell costimulation, or GvHD, where CD86 and HLA family genes are implied (Figure 43A). Based on this findings, and taking into account that Jurkat is a T-ALL cell line, we wondered if Jurkat cells could be striking back to NKG2D-CART by exerting a cytotoxic response against them. To elucidate this hypothesis, we performed cytotoxicity assays using Jurkat as effector cells and NKG2D-CART as a target. As represented in Figure 43B, specific lysis remained under 30% at E:T ratio 20:1, similarly than the basal value obtained when UT CD45RA⁺ T cells were used as effector cells.

A



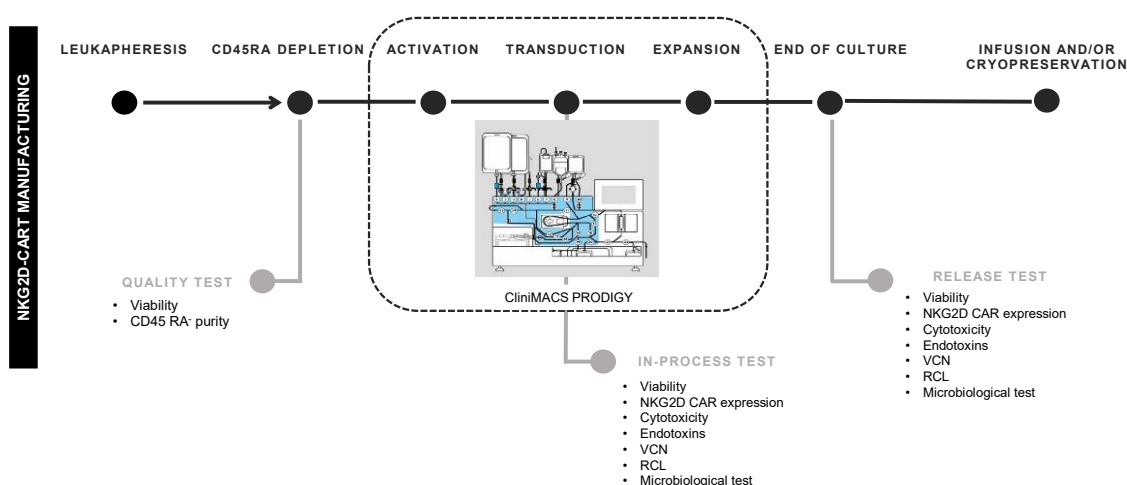
B



5.3. Translation to the clinic.

5.3.1. Manufacturing Process: activation, transduction, and expansion.

CD45RA⁻ cells from four different donors were activated, transduced, and expanded in CliniMACS Prodigy™ in four different experiments. In-process tests were carried out at days +6 and +8. At the end of culture, between days +10 and +13, cells were harvested, and quality/release assays performed. A schema of the different steps for NKG2D-CART manufacturing and the quality tests conducted along the process is shown in Figure 44.



Prodigy™ is Copyrighted © 2015 by Miltenyi Biotec GmbH, used with permission.

5.3.2. Purity of CD45RA⁻ starting cells.

CD45RA⁻ cells were obtained after depletion of CD45RA⁺ subset from non-mobilized apheresis from four different healthy donors at CliniMACS Plus. Median of purity of CD45RA⁻ population was 99,8 (range 99,7–99,9), and median of viability was 97,9 (range 97,7–99,9). Data from each experiment are summarize in Table 5.

Validation	% Viability	% CD45RA ⁻
#1	98,1	99,8
#2	99,9	99,9
#3	97,7	99,9
#4	97,7	99,7

Table 5. Viability and purity of CD45RA⁻ starting cells. Percentages were obtained by FCM after staining with 7AAD for viability and anti-CD45RA antibody to discern CD45RA⁻ subset.

5.3.3. *High Transduction efficiency was achieved by using low MOI.*

We transduced CD45RA⁺ cells 1 day after cell activation. A LV construct encoding for NKG2D CAR was used at MOI = 2. As CD45RA⁺ cells only have basal levels of NKG2D receptor expression, we considered that the expression of NKG2D observed by FCM in NKG2D-CAR T cell products corresponded to NKG2D CAR. Our target goal was to achieve ≥50% transduction of total cells. This goal was achieved for all four final products. Data from NKG2D CAR expression along the process are shown in Table 6. Representative dot plots of NKG2D staining at the different times are shown in Figure 45A. The anti-NKG2D antibody that we use for FCM does not discriminate between the NKG2D endogenous receptor and the NKG2D CAR. In order to analyze the expression of NKG2D CAR in the transduced cells, we performed a western blot using an anti-CD3ζ antibody to detect the CAR protein. NKG2D CAR protein is 40 kDa, whereas endogenous CD3ζ is 16 kDa. As shown in Figure 45B, bands corresponding to the NKG2D CAR were only observed in those cell lysates from transduced CD45RA⁺ cells, whereas they were absent in the different negative controls, including activated and expanded NK cells (NKAES), PBMC, and CD45RA⁺ UT cells.

Validation	%NKG2D CAR expression			Viability		
	Day +6	Day +8	Final	Day +6	Day +8	Final
#1	73	60,5	60,6	85	82,5	86,3
#2	41	43	55	73	77	65
#3	24	82	87,4	70	82	81,4
#4	62	75	91	80	84	82

Table 6. Transduction efficiency and viability of NKG2D-CART during the manufacturing process. Data were collected at in-process controls (day +6, day +8) and at the end of process. Percentages were obtained by FCM after staining with anti-NKG2D antibody to identify NKG2D CAR and DAPI for viability.

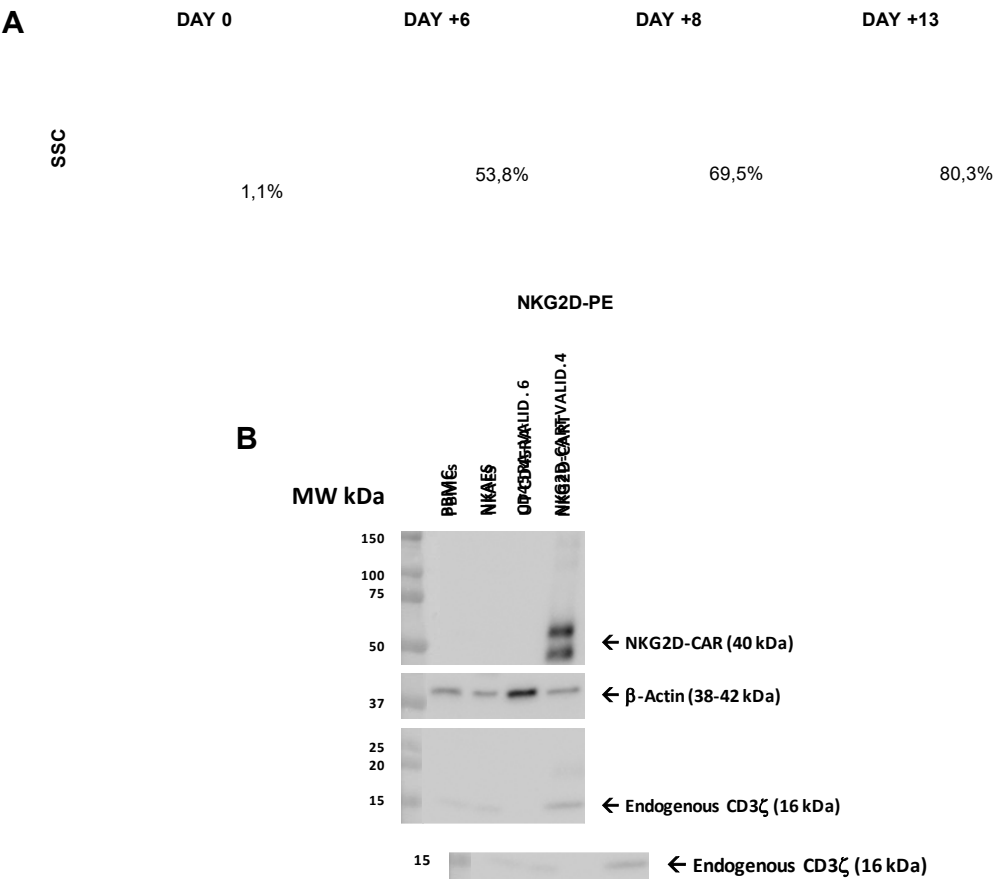


Figure 45. NKG2D CAR expression in CD45RA⁻ cells after transduction. A) Representative FCM plots showing an increase in NKG2D-CAR expression along the manufacturing process. B) Analysis of NKG2D CAR expression in transduced cells and controls (PBMCs, NKAES and UT CD45RA⁻ cells) by western blot detecting CD3 ζ .

5.3.4. Manufacturing of NKG2D-CART achieved sufficient numbers for clinical use.

After CD45RA⁺ depletion, 10^8 of CD45RA⁻ cells were transferred into a sterile bag and connected to CliniMACS Prodigy™ for further processing. The number of cells recovered after CD45RA depletion exceeded this limit for all experiments. For the final products, the fold expansion ranged from 13,4 to 38,6; thus, in all cases, the total number of cells obtained was enough to perform a clinical treatment in a multiple-dose regimen. Data of cell expansion from each experiment are shown in Figure 46.

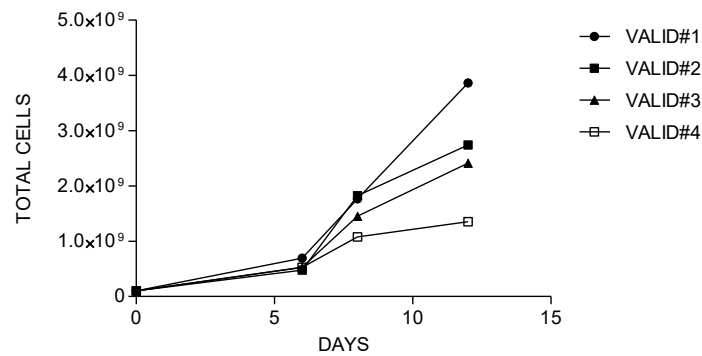


Figure 46. Fold expansion of NKG2D-CART along the manufacturing process of each validation.

5.3.5. *Manufactured NKG2D-CART are enriched in CD4⁺ and mainly present an effector memory phenotype*

Starting and final CAR T cell products were analyzed for viability and CD3, CD4, and CD8 contents. Naïve and memory populations were also identified by using CD45RA and CCR7 markers. The activation/exhaustion status of starting and final cells was analyzed by CD25, PD-1, and TIM-3 markers. The presence of CD4⁺CD25⁺CD127^{low/neg} (T_{regs}) was also analyzed in the starting and final products. Both starting CD45RA⁻ cells and final NKG2D-CAR T cell products were CD3⁺ and showed an enrichment in CD4⁺ vs. CD8⁺ T cells. Both before and after the manufacturing process, T cells were negative for CD45RA and CCR7, indicating an effector memory (T_{EM}) phenotype. TIM-3 and CD25 activation/exhaustion markers were upregulated in final NKG2D-CAR T cell products compared to starting CD45RA⁻ cells; however, PD-1 expression was downregulated at the end of the process (Figure 47).

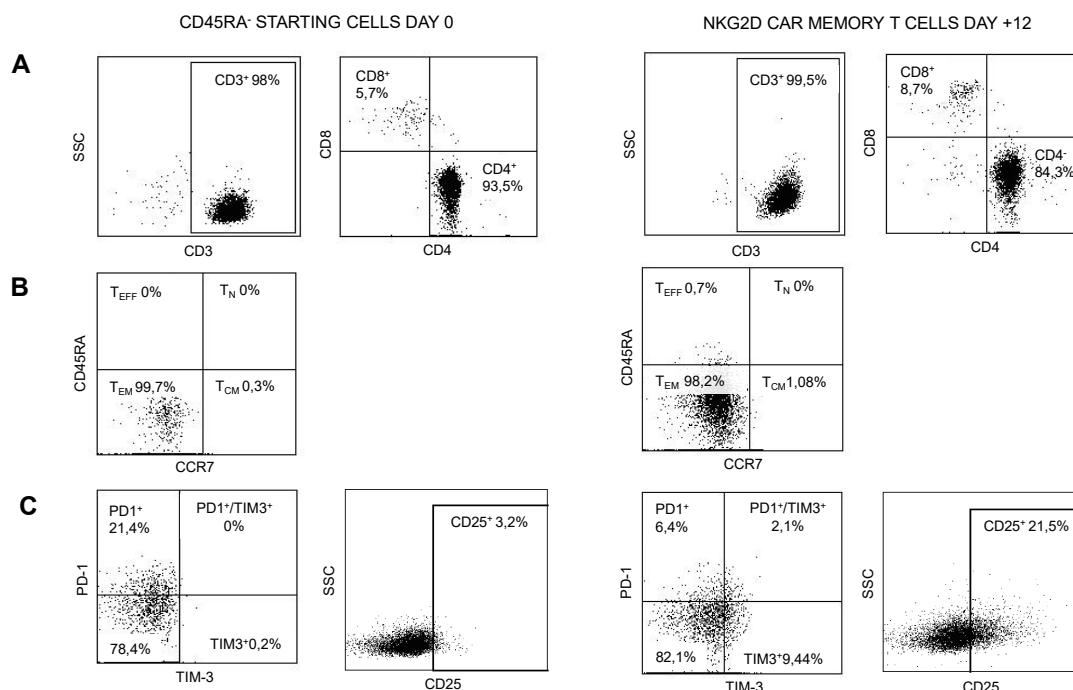


Figure 47. Representative FCM data of CD45RA⁻ starting cells at day 0 and NKG2D-CAR at the end of the manufacturing process (day 12). Plots represent CD3, CD4 and CD8 subsets (A); naïve and memory phenotype(B); expression of activation/exhaustion markers (C). T_{EFF}, effector T cells; T_{CM}, central memory T cells; T_{EM}, effector memory T cells.

5.3.6. Manufactured NKG2D-CART are highly cytotoxic against T-ALL and osteosarcoma cell lines

Lysis ability of NKG2D-CART was tested against the NKG2DL-expressing cell lines Jurkat (T-ALL) and 531MII (metastatic osteosarcoma) by performing conventional 4h Europium-TDA assays. Although donor variability was observed, all final NKG2D-CAR T cell products analyzed were able to target Jurkat and 531MII cells with a percentage of cytotoxicity $\geq 20\%$, therefore meeting the established requirements. For validation #1, owing to technical issues, cytotoxicity against Jurkat cells was only tested using cryopreserved NKG2D-CART. Cytotoxicity of final NKG2D-CART against Jurkat was higher (median 80%, range 28,2–100%) than against 531MII cells (median 42,3%, range 20–74,6%) for all analyzed products, although this difference was not statistically significant. Data of cytotoxicity levels from each experiment are shown in Table 7.

Validation	% Cytotoxicity vs. Jurkat	% Cytotoxicity vs. 531MII
#1	NR	74,6
#2	100	19,5
#3	79,8	42,3
#4	28,2	NR

Table 7. Cytotoxicity of NKG2D-CART at the end of the process by Europium-TDA assays at E:T ratio 20:1. Jurkat and 531MII cells were used as a target.

5.3.7. NKG2D-CART comply with the regulatory specifications regarding safety and sterility

To meet regulatory specifications (acceptable thresholds in parentheses), samples were taken at days +6, and between days +8 and +10 as in-process controls and at the end of process as release controls, and they were evaluated for VCN (≤ 5 copies/cell), free LV particles in the supernatant (LVPS) ($\leq 0,05\%$), oncogenic gene expression (no overexpression), and genetic stability (normal CGH). A Gram stain (no organisms seen) as a quick method and microbiological tests (0 CFU) ensured no bacterial contamination. Other release controls performed included those relating to the purity of the final product: measurement of endotoxin levels, whose limits for administration depend on the product and the parenteral administration route, where the pyrogenic threshold dose of endotoxin per kilogram of body mass in a single hour in the case of transduced cells is 5 IU/kg/h. All final products analyzed fulfilled the specifications except for validation #3, which showed VCN of 12 instead of ≤ 5 copies/cell, and for validation #4, which showed overexpression of *myc*. Complete data regarding genetic tests are shown in Table 8. All samples showed no microbiological contamination. Endotoxin levels were below 5 IU/kg/h, and the presence of mycoplasma was undetectable (Table 9).

Validation	VCN	RCL	CGH	<i>Tert</i> expression	<i>Myc</i> expression
#1	NA	Undetectable	Normal	No overexpression	No overexpression
#2	3,6	Undetectable	Normal	No overexpression	No overexpression
#3	12,3	Undetectable	Normal	No overexpression	No overexpression
#4	2,4	Undetectable	Normal	No overexpression	<i>Myc</i> overexpression

Table 8. Results related to safety and genetic stability of NKG2D-CART at the end of the manufacturing process.

Validation	Gram staining	Mycoplasma	Endotoxins EU/ml
#1	Negative	Negative	NA
#2	Negative	Negative	0,019
#3	Negative	Negative	0,0035
#4	Negative	Negative	0,01

Table 9. Results obtained from sterility test of NKG2D-CART at the end of manufacturing process.

5.3.8. Cryopreserved NKG2D-CART maintain viability, expression of CAR and cytotoxicity.

CliniMACS Prodigy™ allows the production of sufficient number of CAR T cells to be administered in multiple doses. Although the first dose could be administered right after harvesting, spare cells need to be cryopreserved for future infusions. To explore if cryopreservation could have a negative impact on manufactured CAR T cells, we tested three different freezing media and evaluated cell counts, viability CD45RA⁺ purity, NKG2D expression, and cytotoxicity of cryopreserved NKG2D-CART 1 year after freezing. We observed that those NKG2D-CART cryopreserved in autologous plasma +5% DMSO showed the highest viability and cytotoxicity indicating that, whenever possible, this should be the freezing media of preference, followed by M199 + 10% albumin and 5% DMSO (Table 10).

Freezing medium	Viability %	NKG2D %	CD45RA ⁺ %	Cytotoxicity vs. Jurkat %	Cytotoxicity vs. 531MII %
M199 + ALB + DMSO v4	47,9	61,5	99,2	55,2	17,3
Hypothermosol v4	14,1	61,5	99,2	NA	NA
Auto plasma + DMSO v5	74,6	69,9	97,1	78,6	60,3

Table 10. Stability of NKG2D-CART, produced in the manufacturing process, after cryopreservation. Percentage of viability, NKG2D expression and CD45RA⁺ were obtained by FCM. Cytotoxicity of effector cells was measured by performing Europium-TDA assays.

6. DISCUSSION

Acute leukemia is the second leading cause of cancer-related death in children in developed countries. Despite the great progress in the traditional treatments and new approaches, where targeted therapies and immunotherapies have increased the OS, considerable numbers of patients continue dying of this disease (Wayne et al. 2008). Unfortunately, the clinical success of CAR T cell therapy for CD19-positive hematological malignancies, has not been replicated in T-ALL, AML or those B-ALL which relapse with undetectable CD19. For these leukemia entities, the development of CAR T cell options is particularly challenging for three main reasons: first, CARTs recognizing pan T-cell antigens can induce fratricide, impeding CAR T cell manufacturing; second, CARTs targeting pan T-cell/myeloid antigens will induce T-cell aplasia or myelosuppression, leading to a life-threatening immunodeficiency; third, the difficulty of finding a TAA widely expressed in relapsed leukemia.

For some patients the use of “off- the-shelf” allogeneic CAR T cells could ensure the access to this therapy. However, life-threatening GvHD and rapid elimination of CAR T cells by the host immune system must be avoided. CAR redirected CD45RA- T cells have demonstrated less alloreactivity while keeping potent anti-tumor effects (Chan et al. 2014, Fernández et al. 2017) representing an attractive source for allogeneic CART generation. Based on these previous findings, we explored if NKG2D CD45RA- cells could be a novel therapeutic approach to treat r/r pediatric acute leukemia.

The main objectives of this thesis are 1) to explore suitability and the efficacy of NKG2D CAR T cells as a therapeutic approach for pediatric acute leukemia, with focus on T-ALL and AML, and 2) to optimize a GMP-compliant manufacturing protocol to produce NKG2D-CAR T cells for clinical use.

Subsequently, this thesis is divided into two sections: to the first one developing preclinical evidence for the suitability of using NKG2D-CAR T cells to treat pediatric acute leukemia; and the second one validating the large scale production of NKG2D-CART for its use in patients.

6.1. NKG2D-NKG2DL axis represents a suitable strategy to target pediatric acute leukemia.

It has been demonstrated that NKG2DL are expressed in different types of tumors, including leukemia (Salih et al. 2003). Indeed, the interactions between NKG2D receptor and NKG2DL have been shown to be essential for NK cell tumor immunosurveillance (Bauer et al. 1999; Raulet 2003). Many studies show the potent anti-tumor effects of NK cells both *in vitro* and in preclinical models. However, in the clinical setting NK cells present limitations such as the need to infuse a large number of cells due to, dispersion of therapy, absence of memory, and limited *in vivo* expansion (Bodduluru et al. 2015; Klingemann 2015; Pérez-Martínez et al. 2015).

In an attempt to circumvent these hurdles, different groups -including ours, have taken advantage of this natural-occurring anti-tumor mechanism to design CARs with NKG2D specificity. Promisingly, their ability to target different hematological and solid tumors including multiple myeloma, osteosarcoma, ovarian and acute leukemia, among other, has been proven in preclinical studies, (Barber et al. 2008; Driouk et al. 2020; Fernández et al. 2017; Song et al. 2013). Supporting the hypothesis that T cells can be redirected against leukemia cells through NKG2D axis, we have explored the surface expression of NKG2DL in leukemia cell lines and primary leukemic blasts from pediatric patients. We found that all the evaluated cell lines and primary blasts showed upregulation of at least one ligand ($SFI \geq 2$) (Salih et al. 2003), supporting the rationale for the use of NKG2D CAR based therapies to treat pediatric acute leukemia. That expression threshold was exceeded by not only most leukemia samples analyzed, but by healthy PBMCs as well, that even surpassed the level expression of each ligand. This is contrary to the established concept that NKG2DL are poorly expressed on normal cells so the safety of NKG2D-CAR T therapy could be in doubt (Zingoni et al. 2018). However, there are preclinical data supporting the use and safety of NKG2D CAR redirected CD45RA⁺ T cells (Fernández et al. 2017). Most importantly, *in vitro*, NKG2D CAR redirected effector cells are innocuous against different healthy tissues, which may have a basal expression of NKG2DL such as CD34⁺ progenitor cells, PBMC or gut epithelial cells. According to previous reports, we observed a considerable heterogeneous NKG2DL expression among the different cell lines and individuals. Interestingly, MICA is significantly higher expressed than the rest of the ligands in B-ALL blasts although NKG2DL expression patterns did not correlate with particular leukemic subtype (Driouk et al. 2020; Salih et al. 2003). In general, expression levels of NKG2DL that we found in acute leukemia samples were higher than those previously reported for this disease (Hilpert et al. 2012). Notably, Hilpert et al. studied adult leukemia while our group is focus

on pediatric cancer, therefore such differences could be attributed to this fact. Regarding leukemia cell lines, we found that B-ALL and T-ALL expressed higher levels of ligands than AML. However, we did not observe major differences between leukemia subtypes when analyzing patient blasts. Despite the lack of differences, ligands trended to be more expressed at diagnosis than at relapse, particularly MICA, both in B-ALL, AML and T-ALL, which could be due to ligands being released as a tumor mechanism to evade NKG2D-mediated immunosurveillance (Hilpert et al. 2012; Salih et al. 2002). Due to the low prevalence of AML and T-ALL compared to B-ALL, we encounter difficulties to access these samples, thus making statistical analysis unfeasible (Esparza and Sakamoto 2005).

In addition, multiple infusion of NKG2D-CAR T cells achieved long term CR without CRS or neurotoxic effects in a patient suffering from r/r AML (Sallman et al. 2018), supporting our hypothesis of NKG2D-CAR T cells as therapy to treat pediatric leukemia. In contrast with other NKG2D CAR approaches, where NKG2DL expression on NKG2D CAR T cells leads to fratricide (CAR T-self antigen targeting) and hampers CAR T cell manufacturing (Bremann et al. 2018; Song et al. 2013), generation of CAR T cells from CD45RA⁻ subset avoids fratricide, since this T cell compartment have no surface expression of NKG2DL (Fernández et al. 2019).

6.2. Transduction efficiency and characteristics of NKG2D-CART.

Once we had proven that leukemic blasts upregulate NKG2DL and thus confirmed the suitability of using NKG2D CAR T cells to target pediatric acute leukemia, we next produced NKG2D-CART by LV transduction of effector cells derived from healthy donors' PBMCs. Both γ -retroviral and LV vectors can be used to effectively produce stable transduction of T lymphocytes. However, despite both vectors integrate semi-randomly in the human genome, LV are less genotoxic, making them more attractive for gene therapy (Montini et al. 2009; Rivière and Sadelain 2017). The highest viral titer was achieved using Lipofectamine-2000 instead of PEI as a transfection reagent, along with second-generation LV vectors. Although third-generation vectors are required for clinical application due to their additional safety features, second-generation systems are preferentially used in a preclinical development in order to enhance viral titer (Gándara et al. 2018). In contrast with other studies using values close to 10, (Castella et al. 2019; Sánchez-Martínez et al. 2019) we transduced CD45RA⁻ cells with a MOI as low as 2, which was enough to achieve an excellent transduction efficacy without affecting viability nor proliferation, as compared to untransduced CD45RA⁻ cells.

Commonly, efficacy of adoptive cell therapy has been attributed to CD8 T cells subset while CD4 T cells are related to CD8 enhancing and helper function (Zhang, Zhao, and Huang 2020). Most CAR T cells products are derived from PBMCs or selected T cells, which comprise random composition of CD4:CD8 T cells (Castella et al. 2019; Sánchez-Martínez et al. 2019). Others have reported a 1:1 ratio of CD4:CD8 CAR T cells, which allowed the identification of correlative factors production optimization and improved antitumor response due to a synergistic effect of both subsets (Sommermeyer et al. 2016; Turtle et al. 2016). However, CD4 CAR T cells have demonstrated equivalent cytotoxic effect against tumor cells with less exhaustion both *in vitro* and *in vivo* (Agarwal et al. 2020; Yang et al. 2017). According to this, after CD45RA depletion our memory NKG2D CAR T cells were defined by a 4:1 ratio of CD4:CD8 and showed a high ability to recognize and eliminate leukemia cells comparable to PBMCs-derived CAR T cells.

6.3. Evaluation of anti-leukemia efficacy of NKG2D-CART.

Once we proved the upregulation of NKG2DL in acute leukemia, supporting the use of redirected NKG2D-CART-based therapy, we moved to investigate the *in vitro* ability of those effector cells. NKG2D-CART effectively lysed target leukemia cell lines, specially AML and T-ALL compared to B-ALL. For most CAR T cell therapies, a higher expression of TAA correlates with higher tumor-cell lysis. Contrary to this, we found no correlation between NKG2DL expression and NKG2D-CAR mediated cytotoxicity, and similar results have been reported for adult AML (Driouk et al. 2020) and osteosarcoma (Chang et al. 2013; Fernández et al. 2017). This suggests that other signals on the tumor cells besides NKG2DL expression, may be needed for triggering NKG2D-CAR T cells cytolytic activity. Additionally, this result points out that if a specific threshold of NKG2DL expression exists to predict the efficacy of NKG2D-CAR T cells, it is yet to be determined. Unfortunately, it was not possible for us to measure the levels of NKG2DL expressed by the primary blast used in our cytotoxic assays, so we could not establish a correlation between CART cytotoxicity and NKG2DL in acute leukemia patients. In this regard, the future establishment of routinely analysis of ligand expression along to susceptibility of primary blasts to NKG2D-CAR T lysis should be considered in order to predict the outcome of CART-treated patients and their chance to be enrolled in clinical trials. In addition, as it seems that no specific ligand itself enhanced CART-mediated lysis but that it is rather the expression of at least one ligand or the combination of some of them, we are interested in evaluating the expression of NKG2DL targeting all at once by using a NKG2D-Fc chimera antibody (Chang et al. 2013). In this way, we will characterize

samples by the expression of any ligand as a whole like a mark of susceptibility by NKG2D-CART.

Importantly, CAR-transduced T cells clearly produced higher specific lysis than those T cells that remained untransduced. In addition, NKG2D-CART demonstrated to kill primary blasts derived from pediatric leukemia patients, although killing potential was lower against primary leukemia compared to cell lines, according to previous findings (Ruella et al. 2016; Sánchez-Martínez et al. 2019). We found that, when targeting leukemia cell lines, B-ALL blasts were less sensitive to NKG2D-CAR T lysis than those derived from AML and T-ALL patients. Altogether, our data point out that NKG2D-CART could be preferentially used to treat non-B cell malignancies.

Importantly, due to the toxicity that BATDA reagent causes on target cells when used for times longer than 4h, we wonder if co-culturing NKG2D CART with leukemic blasts for longer periods could enhance the cytotoxic effects. To explore this possibility, and based on previous reports (Castella et al. 2019; Sánchez-Martínez et al. 2019) we are implementing other cytotoxicity assays that enable longer co-culture periods, including LDH release or FCM-based assays. Based on this, we are planning to set up a new protocol that will allow us to increase the time of cytotoxicity assays for future projects, so we will be able to further investigate more parameters regarding the activity of NKG2D-CART, such as similar E:T ratios, CART persistence, T cell exhaustion and escape mechanism..

6.4. NKG2D-CART effectively target leukemia cells *in vivo*.

To further explore the anti-leukemia ability of NKG2D-CART, we developed a murine model of human T-ALL using Jurkat-GFP-Luc cells as targets. According to previous reports using CD45RA⁺ CAR T cells, none of the treated mice displayed treatment-related toxicity nor GvHD signs (Chan et al. 2014; Fernández et al. 2017). Supporting our hypothesis, mice receiving NKG2D-CART treatment exhibited delayed disease progression and prolonged survival compared to control mice. Importantly, the therapy was more effective when weekly doses of NKG2D CART were administered, indicating that in a future clinical use, multiple infusions of CAR T cells may be needed to observe a clinical response. However, even in this case, NKG2D CART did not completely eradicate the tumor, and the mice finally died from leukemia progression. These results were somehow striking, as in the *in vitro* assays CAR T cells had shown great efficiency targeting Jurkat cells in just 4h. Several factors could explain the differences observed

in the *in vitro* and the *in vivo* experiments. The most obvious one is related to the experiment setting, as in the *in vitro* experiments, cells are co-cultured in U bottom P96 plates, so CAR T cells can easily contact the target cells and exert their cytotoxic effect. However, *in vivo*, effector cells have to circulate through the circulatory system of mice where they can find different obstacles that may hinder their function. For this reason, we first analyzed the ability of CAR T cells to infiltrate the BM and contact the tumor cells. FCM data confirmed persistence of CAR T cells in hematopoietic tissues. CAR T cells were found in BM, spleen and PB at least up to 4 days after they were infused but not at day 32 post-infusion. Considering that exploring more time points would have been more appropriate, this finding suggests that a single infusion of NKG2D-CART do not achieve long-term persistence so multiple infusions should be established as a treatment protocol in order to assure the presence of effector cells in the tumor site. In addition, IHC analysis of Granzyme B revealed NKG2D-CART were able to infiltrate the BM and exert degranulation in response to leukemia cells. Thus, an impaired ability to contact the target cells or the inactivation of CAR T cells in BM TME/niche could be discarded as the main reason to the treatment failure.

Another explanation for the limited efficacy of the *in vivo* treatment could be related to the use of CD45RA⁻ T cells as effector cells, despite their proven efficacy in preclinical setting (Chan et al. 2014; Fernández et al. 2017). As previously described, CD1a-specific CAR T cells exhibit robust cytotoxicity against T-ALL in the same murine model of T-ALL, although they used total PBMCs as effector cells instead of CD45RA⁻ (Sánchez-Martínez et al. 2019). To rule out that CD45RA⁻ CAR T cells exerted less cytotoxic capability, we compared the cytotoxicity of NKG2D CAR T cells derived from CD45RA⁻ T cells, PBMCs or CD45RA⁺ T cells against leukemia (data not shown) and osteosarcoma cells (Fernández et al. 2017). In this regard, we did not observe any difference between effector cells cytotoxicity *in vitro*, even though the limitation of co-cultured time on assays could hinder it. Therefore, due to their different composition in T naïve, T_{EM} and T_{CM}, different *in vivo* behavior cannot be ruled out. Longer *in vitro* assays and developing an *in vivo* model treating mice with PBMCs-based NKG2D CAR T cells could give us more information about the role of CD45RA⁻ cells in the failure of the therapy.

Another important limitation is derived from the use of NSG immunodeficient mice for testing immunotherapies, since they lack a functional immune system and many cell components from the bone marrow niche like MDSC, regulatory T cells or NK cells, are missing. Therefore, they do not recapitulate the clinical scenario with human cancers and immunotherapy (Byrne et al. 2017; Epperly et al. 2020). In an attempt to better

simulate human conditions, we are planning to develop humanized mice models in which immunodeficient mice are reconstituted with human hematopoietic and immune systems. This humanized mouse models would permit the evaluation of antitumor responses in immunocompetent hosts, to test the efficacy of NKG2D-CART in different malignancies, and to study underlying mechanisms of resistance and toxicity.

6.5. NKG2D-CART bypass the canonic tumor immunoescape mechanisms.

Since we only observed a moderate response to NKG2D CAR T cells in the murine model, we ought to unravel the mechanisms behind this observation. It is well established that tumor cells can release ligands in their soluble form, reducing NKG2DL surface expression and causing downregulation and/or internalization of the NKG2D receptor. This mechanism has been widely reported for NKG2D endogenous receptor (Hilpert et al. 2012; Salih et al. 2003, 2002) however, the negative impact of sNKG2DL on NKG2D CAR is less studied. In this regard, moderate levels of ULBP2 were found in the supernatant of Jurkat cells, and this ligand was the most widely expressed in the surface of this cell line. According to this, ULBP2 was the most abundant sNKG2DL measured in the serum of the T-ALL bearing mice, suggesting an intrinsic characteristic of Jurkat cells. In addition, we found increased sNKG2DL in those mice engrafted with T-ALL, compared to healthy control mice, indicating release of sNKG2DL from Jurkat cells. Furthermore, higher levels of sNKG2DL were measured in the treated mice, suggesting that leukemia increased the release of ligands as a defense mechanism against CART pressure. Moreover, pediatric acute leukemia patients released more sNKG2DL than healthy volunteers, which emphasize the potential relevance of this mechanism of escape. We also found that levels of sNKG2DL at diagnosis were higher than at relapse, although significant differences were not found. Importantly, this expression differences could be explained by the different percentage of blasts at diagnosis and relapse, having the diagnosis samples, may be enriched in ligands-releasing cells. Overall, the concentration of sNKG2DL that we obtained was in the range previously reported (Salih et al. 2003).

Different mechanism could explain the fact that sNKG2DL levels were higher in treated than in untreated mice: 1) NKG2D CART may release sNKG2DL and thus increase their concentration measured in CART treated mice. In our experience, NKG2D-CART have no surface expression of NKG2DL (Fernández et al. 2019) and thus, the shedding of sNKG2DL from NKG2D-CART seems unlikely. However, the expression and release of NKG2DL are subjected to many post-transcriptional and post-translational regulation

steps (Campos-Silva et al. 2018; Spear, Wu, et al. 2013), and we did not measure the levels of sNKG2DL secreted by NKG2D-CART cultured alone, therefore, this possibility cannot be completely ruled out. 2) Tumor lysis caused by NKG2D CART could release sNKG2DL to the serum, boosting the detection of sNKG2DL. 3) A defense mechanism of the Jurkat cells in response to the attack of NKG2D CART could intensify the release of sNKG2DL in order to avoid CAR T cells recognition, thus explaining the increased levels of sNKG2DL in the treated mice. Unfortunately, since none of these hypotheses were proved they cannot be completely discarded.

Once we had shown that sNKG2DL can be found in the supernatant of Jurkat cells, in the serum of T-ALL bearing mice and in the serum of pediatric patients suffering from leukemia, we ought to evaluate the effects of sNKG2DL on NKG2D CAR expression, proliferation and cytotoxicity, since the suppressive role of sNKG2DL in the endogenous NKG2D receptor has been widely reported (Groh et al. 2002; Matusali et al. 2013; Salih et al. 2003). Supraphysiological concentrations of sNKG2DL stimulated CART proliferation. Interestingly, CD4⁺ subset showed more susceptibility to NKG2D downregulation while CD8⁺ cells proliferation was more affected, suggesting that CD45RA⁻ NKG2D-CAR T cell, more enriched in CD4 subpopulation, could be more affected by sNKG2DL regulation. However, when exploring the effect of sNKG2DL in the NKG2D-CART's cytotoxicity ability, we found that CARTs retained their capability to lyse Jurkat cells, even after treating with supraphysiological concentrations of sNKG2DL. Interestingly, although sNKG2DL decreased the density of NKG2D receptor expression (measured as SFI) on CAR T cells, the percentage of NKG2D positive cells remained unchanged, and the cytotoxic ability of NKG2D CARTs was also intact. Moreover, upon exposure to sMICA, the formation of functional immunological synapses between NKG2D CART and Jurkat cells, leading to the elimination of target cells, was also unaltered. These data taken together suggest that NKG2D CAR is more resistant to the immunosuppressive impact of sNKG2DL than endogenous NKG2D receptor, and similar observations had been previously reported by Zhang and colleagues (Zhang et al. 2006). Taking into account that the highest concentration of sNKG2DL measured in the sera of mice remained quite lower than the supraphysiological amounts used in the assays, it does not seem very likely that sNKG2DL are a major cause of treatment failure in the *in vivo* model. However, since the levels of sNKG2DL at local tumor areas (BM niche) could be higher than in the serum, and we did not measure sNKG2DL in the BM, we cannot completely rule out some immunosuppressive effect. Further experiments to measure sNKG2DL at specific tumor sites could help us to decipher this possibility. Additionally,

it is well known that NKG2DL can also be released in tumor-derived exosomes (Campos-Silva et al. 2018). Measuring the amounts of NKG2DL-exosomes secreted by leukemia cells and evaluate the effect in NKG2D CART may contribute to discern their implication as immunosuppressive mechanism of pediatric acute leukemia.

TGF- β is another well-known soluble factor that can affect NKG2D expression and anti-tumor immunity (Lazarova and Steinle 2019). Very low levels of TGF- β were found in the supernatant of Jurkat-Luc cells and in the serum of T-ALL-engrafted mice that had been treated with NKG2D-CART. We also determined the levels of TGF- β in the serum of patients suffering from pediatric acute leukemia and in healthy donors. When different leukemia subtypes were compared, no significant differences were found. Strikingly, TGF- β levels resulted higher in healthy donors than in patients. TGF- β is not only involved in tumor surveillance and immune evasion, but also in several physiological pathways, like cell proliferation, gene expression, cell differentiation and wound healing (Morikawa, Derynck, and Miyazono 2016), therefore an activation of some of these processes could account for the differences observed. Nevertheless, a higher number of samples from healthy donors are needed to obtain a more robust conclusion. Importantly, *in vitro*, we observed that even levels of TGF- β far above than those measured in mice and patients were enough to decrease the cytotoxicity of NKG2D-CARTs against leukemia cells, and this result contrasts with previous reports showing immunosuppression of immune cells. (Dahmani and Delisle 2018; Thomas and Massagué 2005). Overall, with our results, inactivation of NKG2D-CAR T cells by TGF- β can be discarded as a main mechanism for treatment failure in the *in vivo* model. Additionally, treatment of NKG2D-CAR T cells retained specific lysis after incubation with conditioned medium of Jurkat cells, thus discarding that other soluble factors than NKG2DL or TGF- β) secreted by Jurkat cells, could be accounting for inactivation of CAR T.

In AML, LICs show reduced expression of NKG2DL, and this confers resistance to NK cell mediated killing (Paczulla et al. 2019). We then explored if Jurkat cells also contained a LIC subset with enhanced resistance to NKG2D-CART. A functional characteristic of LICs is their clonogenicity or the ability of a single cell to grow into a colony, as well as the capability of releasing Hoechst dye through ABC transporters forming a side population that can be identified by FCM (Zhou et al. 2001). Upon incubation with NKG2D-CART, Jurkat cells showed impaired ability to grow of as colonies, and this observation was further confirmed by FCM analysis of the side population contained in Jurkat cells before and after co-culture with NKG2D CAR T cells. It is important to note that, in our experiments, NKG2D-CAR T cells reduced the LIC subset, but they were not

capable of totally eliminating this compartment since some colonies still achieved to grow and a small percentage of cells within the side population remained after exposition to NKG2D-CART. Additionally, no differences in NKG2DL expression were observed in Jurkat cells either cultured in suspension (bulk) or forming colonies (LICs), suggesting that those remaining LICs are still targetable by NKG2D CAR T cells regardless of the previous incubation or not with CAR T cells. Therefore, an immunoescape mechanism of LICs from NKG2D-CART mediated by reduced expression of NKG2DL could be ruled out, as LICs remained targetable by NKG2D-CART. We then further explored if upon co-culture with NKG2D-CART, the remaining Jurkat cells had different expression patterns compared to unexposed Jurkat cells. At transcriptional level, we found that after being in contact with NKG2D-CART, Jurkat cells upregulated the expression of genes involved in proliferation, survival, migration and stemness. These results could indicate that despite the results obtained from the colony formation assays and the unchanged expression of NKG2DLs in the LICs, the culture of Jurkat cells with NKG2D CAR may select tumor cells with a more immature and stem phenotype and an increased ability to proliferate, and these results could explain, at least partially, the inability of the therapy to completely eradicate the leukemia in the murine model.

In summary, we provide preclinical evidence of the efficacy evidence of the anti-tumor activity of CD45RA⁺ NKG2D-CAR T cells against pediatric acute leukemia and enhanced resistance to well established tumor immunoescape mechanisms affecting NKG2D. Based on our results, the use of NKG2D-CAR T cells as single agent may not be sufficient to cure the patients. Instead, we propose using NKG2D-CAR T cells in combination with other therapeutic approaches, e.g. as an induction agent and bridge to HSCT or as adoptive cell therapy after HSCT. In particular, there are early signs that subsequent transplantation of patients who have achieved remission with CAR-T may be a potentially viable and successful strategy (Appelbaum and Milano 2018; Ghosh, Politikos, and Perales 2017). However, further studies are needed in order guarantee the safety and efficacy of this approach.

6.6. Manufacturing of clinical-grade large-scale NKG2D-CART is feasible and reproducible.

Based on clinical success of CAR T cells we have validated and provided detailed description of a GMP-like manufacturing protocol and the characteristics of NKG2D-CART. A total of four manufacturing processes were completed, and the CAR T cell products obtained were analyzed to discern if CD45RA⁺ NKG2D-CAR T cell products met release criteria.

The cell expansion data we achieved were in line with other manufacturing protocols using CliniMACS Prodigy™ (Mock et al. 2016; Zhang et al. 2018). Additionally, according to the number of CAR T cells that have been infused in other clinical trials (Baumeister et al. 2019; Geyer and Brentjens 2016), the number of NKG2D-CART we achieved would have been enough to treat patients in a multiple-dose regimen. During the process, a decrement in viability was observed on day +6. This temporary drop on cell viability is attributed to LV transduction and has been already reported by other groups (Lock et al. 2017; Tumaini et al. 2013). Some authors have reported that NKG2D-CART may induce fratricide, hindering the expansion and the viability of cultured cells (Bremann et al. 2018). The fold NKG2D-CAR T cell expansion observed in this study, along with the viability of the final cell products, suggests that no NKG2D-CAR T cell-mediated fratricide is occurring during the manufacturing protocol. To further explore if fratricide could be taking place in our experiments, the expression of NKG2DL on NKG2D-CART expanded at small scale was analyzed by FCM. No upregulation of NKG2DL was observed in these cells (data not shown). Nevertheless, we only analyzed the expression of NKG2DL at day +8 post-activation, and it has been described that activated T cells upregulate NKG2DL in a temporal manner, specially between days 2 and 5 upon activation (Bremann et al. 2018). Thus, with our data, we cannot totally rule out an upregulation of NKG2DL and, consequently, a fratricide phenomenon in other moments of the culture. A more detailed study of NKG2DL expression kinetics on NKG2D-CART along the manufacturing procedure would provide more information on this regard.

Activated CD45RA⁺ cells were transduced with LV particles at MOI = 2 according to preclinical data using the same vector, which achieved transduction efficiencies higher than 95% (Fernández et al. 2017). This MOI is lower compared to other research works where MOIs up to 10 are reported (Castella et al. 2019; Zhang et al. 2018). Interestingly, the lower expression values we obtained are comparable with those reported in other publications (Castella et al. 2019; Lock et al. 2017) and were enough to efficiently eliminate Jurkat and primary osteosarcoma cells (531MII) at a 20:1 effector to target

ratio. Due to technical issues, some cytotoxicity assays were non-reproducible, and thus, potency of NKG2D-CART could not be evaluated at some time points either during manufacturing procedure or at the end of culture. Nevertheless, those cytotoxicity assays that were reproducible also fulfilled the specification for potency, indicating manufactured NKG2D-CART were cytotoxic against the target cells.

At the end of the expansion protocol, different quality tests were need to be performed in order to ensure safety and purity of manufactured CAR T cells prior to the administration in patients. Three out of four validations showed lower than 5 genome integrated vector copies, fulfilling the specifications required. However, in validation #3, up to 12,3 genome integrated vector copies were detected. These data are striking, as a MOI of 2 was used in all experiments and does not match the hypothesis that one viral particle is able to infect one cell. Despite that higher-than-expected VCN was found in these cells, the percentage of NKG2D CAR positive cells in this validation was 87%, indicating transduction efficiency was not above the usual levels. Additionally, CGH and expression of *myc* and *tert* oncogenes were normal in this batch, suggesting that even though more than five copies were integrated, they caused no genetic alterations. Finally, to rule out a potential oncogenic effect of NKG2D-CART, the expression of *myc* and *tert* oncogenes was analyzed. All validations showed no overexpression of these genes except for validation #4, which presented overexpression of *myc*, and consequently did not fulfill the specifications required. Although *myc* overexpression in NK cell products has been previously demonstrated to be safe and to induce no complications nor secondary neoplasia in patients (Leivas et al. 2016), it is important to be aware of this and to increase the monitoring of these cell products to ensure safety before being administered to patients. The percentage of RCL in the supernatants remained under the specification limit, indicating that there is no potential risk of virus infection after infusion. It is important to note that specifications of the final products were set up by the manufacturer to assure a safety and high-quality products, but there is not a mandatory regulation that must be fulfilled. In this regard, specific results that did not meet the release criteria did not mean that the manufactured cells were unsafe or unusable.

In summary, we demonstrated the feasibility and reproducibility of a manufacturing protocol to obtain clinical-grade large-scale NKG2D-CART in CliniMACS Prodigy™ system. Most importantly, the manufacturing process described here shows flexibility and admits further improvements for future NKG2D-CAR T cell trials.

7. CONCLUSIONS

7.1. Preclinical studies.

1. NKG2D-CART target leukemic blasts and leukemia cell lines *in vitro*.
2. NKG2D-CART reduce tumor progression and prolong survival in a murine model of human T-ALL. However, they are not sufficient to cure the animals
3. NKG2DL are expressed by leukemia cell lines and primary leukemic blasts of pediatric patients at different stages of the disease, and are suitable targets for NKG2D CAR therapy.
4. LV production by lipofectamine and second generation production achieve higher LV titers.
5. LV transduction of CD45RA⁺ T cells achieve robust expression of NKG2D while did not affect cell viability.
6. NKG2D-CART are resistant to the immunosuppressive effects exerted by sNKG2DL. Downregulation of NKG2D expression in NKG2D CAR T cells upon exposure to sNKG2DL is insufficient to impair NKG2D CAR T cells cytotoxicity.
7. NKG2D CAR T cells are resistant to the immunosuppressive effects exerted by TGF- β .
8. Jurkat LICs maintain NKG2DL expression and are targeted by NKG2D CAR T cells.
9. Jurkat cells upregulate genes involved in immune response, survival, proliferation and stemness, upon exposure to NKG2D-CART.

7.2. Translation to the clinic.

1. Manufacturing of clinical-grade large-scale NKG2D-CART by CliniMACS Prodigy™ system is feasible and reproducible.
2. NKG2D-CART met the release criteria for expansion, NKG2D CAR expression, cytotoxicity, and sterility.

8. CONCLUSIONES

8.1. Estudios preclínicos.

1. Las células T CAR NKG2D eliminan líneas celulares de leucemia y blastos primarios *in vitro*.
2. Las células T CAR NKG2D NKG2D-CART reducen la progresión tumoral y alargan la supervivencia en un modelo murino de LLA-T aunque no consiguieron erradicar completamente el tumor.
3. Las líneas celulares de leucemia, así como los blastos de pacientes pediátricos de leucemia aguda expresan NKG2DL en los distintos estadios de la enfermedad, siendo una diana adecuada para las células T CAR NKG2D
4. La producción de partículas lentivirales con Lipofectamina y métodos de segunda generación consigue elevados títulos lentivirus.
5. La transducción de células T CD45RA⁺ T con partículas lentivirales produce una elevada expresión de NKG2D sin afectar a la viabilidad celular.
6. Las células T CAR NKG2D NKG2D-CART son resistentes al efecto inmunosupresor mediado por sNKG2DL. La modulación de la expresión del receptor NKG2D tras la exposición a sNKG2DL es insuficiente para impedir el efecto citotóxico de las células T CAR NKG2D.
7. Las células T CAR NKG2D son resistentes a la inmunosupresión por TGF- β .
8. Las células *stem* iniciadoras de leukemia de las células Jurkat mantienen la expresión de NKG2DL y son reconocidas y eliminadas por las células T CAR NKG2D.
9. Las células Jurkat sobreexpresan genes implicados en la respuesta inmune, supervivencia y proliferación tras ser expuestas a células T CAR NKG2D.

8.2. Investigación traslacional.

1. La producción en grado clínico a gran escala de células T CAR NKG2D mediante el sistema CliniMACS Prodigy™ es factible y reproducible.
2. Las células T CAR NKG2D producidas a escala clínica cumplieron los criterios de aprobación para la expresión del CAR NKG2D, citotoxicidad y esterilidad.

9. REFERENCES

- Agarwal, Shiwani, Julia D. S. Hanauer, Annika M. Frank, Vanessa Riechert, Frederic B. Thalheimer, and Christian J. Buchholz. 2020. "In Vivo Generation of CAR T Cells Selectively in Human CD4+ Lymphocytes." *Molecular Therapy* 28(8):1783–94. doi: 10.1016/j.ymthe.2020.05.005.
- Allez, Matthieu, Vannary Tieng, Atsushi Nakazawa, Xavier Treton, Vincent Pacault, Nicolas Dulphy, Sophie Caillat-Zucman, Pascale Paul, Jean–Marc Gornet, Corinne Douay, Sophie Ravet, Ryad Tamouza, Dominique Charron, Marc Lémann, Lloyd Mayer, and Antoine Toubert. 2007. "CD4+NKG2D+ T Cells in Crohn's Disease Mediate Inflammatory and Cytotoxic Responses Through MICA Interactions." *Gastroenterology* 132(7):2346–58. doi: 10.1053/j.gastro.2007.03.025.
- Amirache, Fouzia, Camille Lévy, Caroline Costa, Philippe-Emmanuel Mangeot, Bruce E. Torbett, Cathy X. Wang, Didier Nègre, François-Loïc Cosset, and Els Verhoeyen. 2014. "Mystery Solved: VSV-G-LVs Do Not Allow Efficient Gene Transfer into Unstimulated T Cells, B Cells, and HSCs Because They Lack the LDL Receptor." *Blood* 123(9):1422–24. doi: 10.1182/blood-2013-11-540641.
- Anderson, Britt E., Jennifer McNiff, Jun Yan, Hester Doyle, Mark Mamula, Mark J. Shlomchik, and Warren D. Shlomchik. 2003. "Memory CD4+ T Cells Do Not Induce Graft-versus-Host Disease." *Journal of Clinical Investigation* 112(1):101–8. doi: 10.1172/JCI200317601.
- Andersson, Anna K., Jing Ma, Jianmin Wang, Xiang Chen, Amanda Larson Gedman, Jinjun Dang, Joy Nakitandwe, Linda Holmfeldt, Matthew Parker, John Easton, Robert Huether, Richard Kriwacki, Michael Rusch, Gang Wu, Yongjin Li, Heather Mulder, Susana Raimondi, Stanley Pounds, Guolian Kang, Lei Shi, Jared Becksfort, Pankaj Gupta, Debbie Payne-Turner, Bhavin Vadodaria, Kristy Boggs, Donald Yergeau, Jayanthi Manne, Guangchun Song, Michael Edmonson, Panduka Nagahawatte, Lei Wei, Cheng Cheng, Deqing Pei, Rosemary Sutton, Nicola C. Venn, Albert Chetcuti, Amanda Rush, Daniel Catchpoole, Jesper Heldrup, Thoas Fioretos, Charles Lu, Li Ding, Ching-Hon Pui, Sheila Shurtleff, Charles G. Mullighan, Elaine R. Mardis, Richard K. Wilson, Tanja A. Gruber, Jinghui Zhang, and James R. Downing. 2015. "The Landscape of Somatic Mutations in Infant MLL-Rearranged Acute Lymphoblastic Leukemias." *Nature Genetics* 47(4):330–37. doi: 10.1038/ng.3230.
- Aplenc, Richard, Todd A. Alonzo, Robert B. Gerbing, Beverly J. Lange, Craig A. Hurwitz, Robert J. Wells, Irwin Bernstein, Patrick Buckley, Kathleen Krimmel, Franklin O. Smith, Eric L. Sievers, and Robert J. Arceci. 2008. "Safety and Efficacy of Gemtuzumab Ozogamicin in Combination With Chemotherapy for Pediatric Acute Myeloid Leukemia: A Report From The Children's Oncology Group." *Journal of Clinical Oncology* 26(14):2390–95. doi: 10.1200/JCO.2007.13.0096.
- Appelbaum, Jacob S., and Filippo Milano. 2018. "Hematopoietic Stem Cell Transplantation in the Era of Engineered Cell Therapy." *Current Hematologic Malignancy Reports* 13(6):484–93. doi: 10.1007/s11899-018-0476-4.
- Arber, Daniel A., Attilio Orazi, Robert Hasserjian, Jürgen Thiele, Michael J. Borowitz, Michelle M. Le Beau, Clara D. Bloomfield, Mario Cazzola, and James W. Vardiman. 2016. "The 2016 Revision to the World Health Organization Classification of Myeloid Neoplasms and Acute Leukemia." *Blood* 127(20):2391–2405. doi: 10.1182/blood-2016-03-643544.
- Asenjo, Santiago, Olivier Nuñez, Jordi Segú-Tell, Elena Pardo Romaguera, Adela Cañete Nieto, Iván Martín-Méndez, Alejandro Bel-lan, Javier García-Pérez,

- Alberto Cárceles-Álvarez, Juan Antonio Ortega-García, and Rebeca Ramis. 2021. "Cadmium (Cd) and Lead (Pb) Topsoil Levels and Incidence of Childhood Leukemias." *Environmental Geochemistry and Health*. doi: 10.1007/s10653-021-01030-w.
- Ashburner, Michael, Catherine A. Ball, Judith A. Blake, David Botstein, Heather Butler, J. Michael Cherry, Allan P. Davis, Kara Dolinski, Selina S. Dwight, Janan T. Eppig, Midori A. Harris, David P. Hill, Laurie Issel-Tarver, Andrew Kasarskis, Suzanna Lewis, John C. Matese, Joel E. Richardson, Martin Ringwald, Gerald M. Rubin, and Gavin Sherlock. 2000. "Gene Ontology: Tool for the Unification of Biology." *Nature Genetics* 25(1):25–29. doi: 10.1038/75556.
- Ashiru, Omodele, Philippe Boutet, Lola Fernández-Messina, Sonia Agüera-González, Jeremy N. Skepper, Mar Valés-Gómez, and Hugh T. Reyburn. 2010. "Natural Killer Cell Cytotoxicity Is Suppressed by Exposure to the Human NKG2D Ligand MICA*008 That Is Shed by Tumor Cells in Exosomes." *Cancer Research* 70(2):481–89. doi: 10.1158/0008-5472.CAN-09-1688.
- Ayala, F., R. Dewar, M. Kieran, and R. Kalluri. 2009. "Contribution of Bone Microenvironment to Leukemogenesis and Leukemia Progression." *Leukemia* 23(12):2233–41. doi: 10.1038/leu.2009.175.
- Balduzzi, Adriana, Maria Grazia Valsecchi, Cornelio Uderzo, Paola De Lorenzo, Thomas Klingebiel, Christina Peters, Jan Stary, Maria S. Felice, Edina Magyarosy, Valentino Conter, Alfred Reiter, Chiara Messina, Helmut Gadner, and Martin Schrappe. 2005. "Chemotherapy versus Allogeneic Transplantation for Very-High-Risk Childhood Acute Lymphoblastic Leukaemia in First Complete Remission: Comparison by Genetic Randomisation in an International Prospective Study." *The Lancet* 366(9486):635–42. doi: 10.1016/S0140-6736(05)66998-X.
- Barber, A., K. R. Meehan, and C. L. Sentman. 2011. "Treatment of Multiple Myeloma with Adoptively Transferred Chimeric NKG2D Receptor-Expressing T Cells." *Gene Therapy* 18(5):509–16. doi: 10.1038/gt.2010.174.
- Barber, Amorette, Agnieszka Rynda, and Charles L. Sentman. 2009. "Chimeric NKG2D Expressing T Cells Eliminate Immunosuppression and Activate Immunity within the Ovarian Tumor Microenvironment." *The Journal of Immunology* 183(11):6939–47. doi: 10.4049/jimmunol.0902000.
- Barber, Amorette, Tong Zhang, Christina J. Megli, Jillian Wu, Kenneth R. Meehan, and Charles L. Sentman. 2008. "Chimeric NKG2D Receptor-Expressing T Cells as an Immunotherapy for Multiple Myeloma." *Experimental Hematology* 36(10):1318–28. doi: 10.1016/j.exphem.2008.04.010.
- Baroni, Matteo Libero, Diego Sanchez Martinez, Francisco Gutierrez Aguera, Heleia Roca Ho, Maria Castella, Samanta Zanetti, Talia Velasco Hernandez, Rafael Diaz de la Guardia, Julio Castaño, Eduardo Anguita, Susana Vives, Josep Nomdedeu, Helene Lapillone, Anne E. Bras, Vincent H. J. van der Velden, Jordi Junca, Pedro Marin, Alex Bataller, Jordi Esteve, Binje Vick, Irmela Jeremias, Angel Lopez, Marc Sorigue, Clara Bueno, and Pablo Menendez. 2020. "41BB-Based and CD28-Based CD123-Redirected T-Cells Ablate Human Normal Hematopoiesis in Vivo." *Journal for ImmunoTherapy of Cancer* 8(1):e000845. doi: 10.1136/jitc-2020-000845.
- Bauer, Stefan, Veronika Groh, Jun Wu, Alexander Steinle, Joseph H. Phillips, Lewis L. Lanier, and Thomas Spies. 1999. "Activation of NK Cells and T Cells by NKG2D, a Receptor for Stress-Inducible MICA." *Science* 285(5428):727–29. doi: 10.1126/science.285.5428.727.

- Baumeister, Susanne H., Joana Murad, Lillian Werner, Heather Daley, Helene Trebeden-Negre, Joanina K. Gicobi, Adam Schmucker, Jake Reder, Charles L. Sentman, David E. Gilham, Frédéric F. Lehmann, Ilene Galinsky, Heidi DiPietro, Kristen Cummings, Nikhil C. Munshi, Richard M. Stone, Donna S. Neuberg, Robert Soiffer, Glenn Dranoff, Jerome Ritz, and Sarah Nikiforow. 2019. "Phase I Trial of Autologous CAR T Cells Targeting NKG2D Ligands in Patients with AML/MDS and Multiple Myeloma." *Cancer Immunology Research* 7(1):100–112. doi: 10.1158/2326-6066.CIR-18-0307.
- Bedel, Romain, Antoine Thiery-Vuillemin, Camille Grandclement, Jeremy Balland, Jean-Paul Remy-Martin, Bernadette Kantelip, Jean-René Pallandre, Xavier Pivot, Christophe Ferrand, Pierre Tiberghien, and Christophe Borg. 2011. "Novel Role for STAT3 in Transcriptional Regulation of NK Immune Cell Targeting Receptor MICA on Cancer Cells." *Cancer Research* 71(5):1615–26. doi: 10.1158/0008-5472.CAN-09-4540.
- Bello-Gamboa, Ana, Juan Manuel Izquierdo, Marta Velasco, Solange Moreno, Alejandro Garrido, Laura Meyers, Juan Carlos Palomino, Víctor Calvo, and Manuel Izquierdo. 2019. "Imaging the Human Immunological Synapse." *Journal of Visualized Experiments* (154). doi: 10.3791/60312.
- Bene, M. C., G. Castoldi, W. Knapp, W. D. Ludwig, E. Matutes, A. Orfao, and M. B. van't Veer. 1995. "Proposals for the Immunological Classification of Acute Leukemias. European Group for the Immunological Characterization of Leukemias (EGIL)." *Leukemia* 9(10):1783–86.
- Bhojwani, Deepa, Richard Sposto, Nirali N. Shah, Vilmarie Rodriguez, Constance Yuan, Maryalice Stetler-Stevenson, Maureen M. O'Brien, Jennifer L. McNeer, Amrana Quereshi, Aurelie Cabannes, Paul Schlegel, Claudia Rossig, Luciano Dalla-Pozza, Keith August, Sarah Alexander, Jean-Pierre Bourquin, Michel Zwaan, Elizabeth A. Raetz, Mignon L. Loh, and Susan R. Rheingold. 2019. "Inotuzumab Ozogamicin in Pediatric Patients with Relapsed/Refractory Acute Lymphoblastic Leukemia." *Leukemia* 33(4):884–92. doi: 10.1038/s41375-018-0265-z.
- Bodduluru, Lakshmi Narendra, Eshvendar Reddy Kasala, Rajaram Mohan Rao Madhana, and Chandra Shaker Sriram. 2015. "Natural Killer Cells: The Journey from Puzzles in Biology to Treatment of Cancer." *Cancer Letters* 357(2):454–67. doi: 10.1016/j.canlet.2014.12.020.
- Bolouri, Hamid, Jason E. Farrar, Timothy Triche, Rhonda E. Ries, Emilia L. Lim, Todd A. Alonzo, Yussanne Ma, Richard Moore, Andrew J. Mungall, Marco A. Marra, Jinghui Zhang, Xiaotu Ma, Yu Liu, Yanling Liu, Jaime M. Guidry Auvil, Tanja M. Davidsen, Patee Gesuwan, Leandro C. Hermida, Bodour Salhia, Stephen Capone, Giridharan Ramsingh, Christian Michel Zwaan, Sanne Noort, Stephen R. Piccolo, E. Anders Kolb, Alan S. Gamis, Malcolm A. Smith, Daniela S. Gerhard, and Soheil Meshinchi. 2018. "The Molecular Landscape of Pediatric Acute Myeloid Leukemia Reveals Recurrent Structural Alterations and Age-Specific Mutational Interactions." *Nature Medicine* 24(1):103–12. doi: 10.1038/nm.4439.
- Bonnet, Dominique, and John E. Dick. 1997. "Human Acute Myeloid Leukemia Is Organized as a Hierarchy That Originates from a Primitive Hematopoietic Cell." *Nature Medicine* 3(7):730–37. doi: 10.1038/nm0797-730.
- Breman, Eytan, Benjamin Demoulin, Sophie Agaugué, Sebastien Mauën, Alexandre Michaux, Lorraine Springuel, Julien Houssa, Fanny Huberty, Céline Jacques-Hespel, Céline Marchand, Jérôme Marijsse, Thuy Nguyen, Nancy Ramelot, Benjamin Violle, Dorothée Daro, Peter De Waele, David E. Gilham, and Valérie

- Steenwinckel. 2018. "Overcoming Target Driven Fratricide for T Cell Therapy." *Frontiers in Immunology* 9. doi: 10.3389/fimmu.2018.02940.
- Brentjens, Renier J., Marco L. Davila, Isabelle Riviere, Jae Park, Xiuyan Wang, Lindsay G. Cowell, Shirley Bartido, Jolanta Stefanski, Clare Taylor, Malgorzata Olszewska, Oriana Borquez-Ojeda, Jinrong Qu, Teresa Wasielewska, Qing He, Yvette Bernal, Ivelise V. Rijo, Cyrus Hedvat, Rachel Kobos, Kevin Curran, Peter Steiner, Joseph Jurcic, Todd Rosenblatt, Peter Maslak, Mark Frattini, and Michel Sadelain. 2013. "CD19-Targeted T Cells Rapidly Induce Molecular Remissions in Adults with Chemotherapy-Refractory Acute Lymphoblastic Leukemia." *Science Translational Medicine* 5(177). doi: 10.1126/scitranslmed.3005930.
- Brentjens, Renier J., Elmer Santos, Yan Nikhamin, Raymond Yeh, Maiko Matsushita, Krista La Perle, Alfonso Quintás-Cardama, Steven M. Larson, and Michel Sadelain. 2007. "Genetically Targeted T Cells Eradicate Systemic Acute Lymphoblastic Leukemia Xenografts." *Clinical Cancer Research* 13(18):5426–35. doi: 10.1158/1078-0432.CCR-07-0674.
- Breunig, Christian, Jens Pahl, Moritz Küblbeck, Matthias Miller, Daniela Antonelli, Nese Erdem, Cornelia Wirth, Rainer Will, Alexander Bott, Adelheid Cerwenka, and Stefan Wiemann. 2017. "MicroRNA-519a-3p Mediates Apoptosis Resistance in Breast Cancer Cells and Their Escape from Recognition by Natural Killer Cells." *Cell Death & Disease* 8(8):e2973–e2973. doi: 10.1038/cddis.2017.364.
- Bride, Karen L., Tiffaney L. Vincent, Soo-Yeon Im, Richard Aplenc, David M. Barrett, William L. Carroll, Robin Carson, Yunfeng Dai, Meenakshi Devidas, Kimberly P. Dunsmore, Tori Fuller, Tina Glisovic-Aplenc, Terzah M. Horton, Stephen P. Hunger, Mignon L. Loh, Shannon L. Maude, Elizabeth A. Raetz, Stuart S. Winter, Stephan A. Grupp, Michelle L. Hermiston, Brent L. Wood, and David T. Teachey. 2018. "Preclinical Efficacy of Daratumumab in T-Cell Acute Lymphoblastic Leukemia." *Blood* 131(9):995–99. doi: 10.1182/blood-2017-07-794214.
- Bristol-Myers Squibb. 2021. "U.S. Food and Drug Administration Approves Bristol Myers Squibb's Breyanzi (Lisocabtagene Maraleucel), a New CAR T Cell Therapy for Adults with Relapsed or Refractory Large B-Cell Lymphoma." *Corporate/Financial News*. Retrieved January 11, 2022 (<https://news.bms.com/news/details/2021/U.S.-Food-and-Drug-Administration-Approves-Bristol-Myers-Squibbs-Breyanzi-lisocabtagene-maraleucel-a-New-CAR-T-Cell-Therapy-for-Adults-with-Relapsed-or-Refractory-Large-B-cell-Lymphoma/default.aspx>).
- Brix, Ninna, and Steen Rosthøj. 2014. "Bone Marrow Involvement Is Not Manifest in the Early Stages of Childhood Acute Lymphoblastic Leukaemia." *Danish Medical Journal* 61(8):A4883.
- Brown, Patrick, Hiroto Inaba, Colleen Annesley, Jill Beck, Susan Colace, Mari Dallas, Kenneth DeSantes, Kara Kelly, Carrie Kitko, Norman Lacayo, Nicole Larrier, Luke Maese, Kris Mahadeo, Ronica Nanda, Valentina Nardi, Vilmarie Rodriguez, Jenna Rossoff, Laura Schuettepelz, Lewis Silverman, Jessica Sun, Weili Sun, David Teachey, Victor Wong, Gregory Yanik, Alyse Johnson-Chilla, and Ndiya Ogba. 2020. "Pediatric Acute Lymphoblastic Leukemia, Version 2.2020, NCCN Clinical Practice Guidelines in Oncology." *Journal of the National Comprehensive Cancer Network* 18(1):81–112. doi: 10.6004/jnccn.2020.0001.
- Brudno, Jennifer N., and James N. Kochenderfer. 2019. "Recent Advances in CAR T-Cell Toxicity: Mechanisms, Manifestations and Management." *Blood Reviews* 34:45–55. doi: 10.1016/j.blre.2018.11.002.

- Brunning RD, Borowitz M, Matutes E, et al. 2001a. "Precursor B Lymphoblastic Leukaemia/Lymphoblastic Lymphoma Precursor B-Cell Acute Lymphoblastic Leukaemia) in Jaffe ES, Harris NL, Stein H, et Al (Eds): World Health Organization Classification of Tumours. Pathology and Genetics of Tumours of the Hematopo." *IARC Press, Lyon* 111–14.
- Brunning RD, Borowitz M, Matutes E, et al. 2001b. "Precursor T Lymphoblastic Leukaemia/Lymphoblastic Lymphoma (Precursor T-Cell Acute Lymphoblastic Leukaemia) in Jaffe ES, Harris NL, Stein H, et Al (Eds): World Health Organization Classification of Tumours. Pathology and Genetics of Tumours of the Hematopo." *IARC Press, Lyon* 115–17.
- Brunning RD, Matutes E, Borowitz MJ, Flandrin G, Head D, et al. 2001. "Acute Leukaemias of Ambiguous Lineage, in Jaffe ES, Harris NL, Stein H, et Al (Eds): World Health Organization Classification of Tumours. Pathology and Genetics of Tumours of the Hematopoietic and Lymphoid Tissues." *IARC Press, Lyon* 106–7.
- Brunning, Richard D. 2003. "Classification of Acute Leukemias." *Seminars in Diagnostic Pathology* 20(3):142–53. doi: 10.1016/S0740-2570(03)00031-5.
- Bueno, Clara, Talia Velasco-Hernandez, Francisco Gutiérrez-Agüera, Samanta Romina Zanetti, Matteo L. Baroni, Diego Sánchez-Martínez, Oscar Molina, Adria Closa, Antonio Agraz-Doblás, Pedro Marín, Eduardo Eyra, Ignacio Varela, and Pablo Menéndez. 2019. "CD133-Directed CAR T-Cells for MLL Leukemia: On-Target, off-Tumor Myeloablative Toxicity." *Leukemia* 33(8):2090–2125. doi: 10.1038/s41375-019-0418-8.
- Burgess, Steven J., Kerima Maasho, Madhan Masilamani, Sriram Narayanan, Francisco Borrego, and John E. Coligan. 2008. "The NKG2D Receptor: Immunobiology and Clinical Implications." *Immunologic Research* 40(1):18–34. doi: 10.1007/s12026-007-0060-9.
- Burgess, Steven J., Alina I. Marusina, Ishani Pathmanathan, Francisco Borrego, and John E. Coligan. 2006. "IL-21 Down-Regulates NKG2D/DAP10 Expression on Human NK and CD8⁺ T Cells." *The Journal of Immunology* 176(3):1490–97. doi: 10.4049/jimmunol.176.3.1490.
- Byrne, Annette T., Denis G. Alférez, Frédéric Amant, Daniela Annibali, Joaquín Arribas, Andrew V. Biankin, Alejandra Bruna, Eva Budinská, Carlos Caldas, David K. Chang, Robert B. Clarke, Hans Clevers, George Coukos, Virginie Dangles-Marie, S. Gail Eckhardt, Eva Gonzalez-Suarez, Els Hermans, Manuel Hidalgo, Monika A. Jarzabek, Steven de Jong, Jos Jonkers, Kristel Kemper, Luisa Lanfrancone, Gunhild Mari Mælandsmo, Elisabetta Marangoni, Jean-Christophe Marine, Enzo Medico, Jens Henrik Norum, Héctor G. Palmer, Daniel S. Peeper, Pier Giuseppe Pelicci, Alejandro Piris-Gimenez, Sergio Roman-Roman, Oscar M. Rueda, Joan Seoane, Violeta Serra, Laura Soucek, Dominique Vanhecke, Alberto Villanueva, Emilie Vinolo, Andrea Bertotti, and Livio Trusolino. 2017. "Erratum: Interrogating Open Issues in Cancer Medicine with Patient-Derived Xenografts." *Nature Reviews Cancer* 17(10):632–632. doi: 10.1038/nrc.2017.85.
- Caligiuri, M. A., M. P. Strout, and D. G. Gilliland. 1997. "Molecular Biology of Acute Myeloid Leukemia." *Seminars in Oncology* 24(1):32–44.
- Campos-Silva, C., M. K. Kramer, and M. Valés-Gómez. 2018. "NKG2D-Ligands: Putting Everything under the Same Umbrella Can Be Misleading." *HLA* 91(6):489–500. doi: 10.1111/tan.13246.
- Cao, Wei, Xueyan Xi, Zhun Wang, Liling Dong, Zhiyong Hao, Lianxian Cui, Chi Ma, and Wei He. 2008. "Four Novel ULBP Splice Variants Are Ligands for Human

- NKG2D." *International Immunology* 20(8):981–91. doi: 10.1093/intimm/dxn057.
- Carbonell, F., J. Swansbury, T. Min, E. Matutes, N. Farahat, V. Buccheri, R. Morilla, L. Secker-Walker, and D. Catovsky. 1996. "Cytogenetic Findings in Acute Biphentotypic Leukaemia." *Leukemia* 10(8):1283–87.
- Cárceles-Álvarez, Alberto, Juan A. Ortega-García, Fernando A. López-Hernández, José L. Fuster-Soler, Rebeca Ramis, Nicole Kloosterman, Luis Castillo, Manuel Sánchez-Solís, Luz Claudio, and Josep Ferris-Tortajada. 2019. "Secondhand Smoke: A New and Modifiable Prognostic Factor in Childhood Acute Lymphoblastic Leukemias." *Environmental Research* 178:108689. doi: 10.1016/j.envres.2019.108689.
- Cárceles-Álvarez, Alberto, Juan A. Ortega-García, Fernando A. López-Hernández, Mayra Orozco-Llamas, Blanca Espinosa-López, Esther Tobarra-Sánchez, and Lizbeth Alvarez. 2017. "Spatial Clustering of Childhood Leukaemia with the Integration of the Paediatric Environmental History." *Environmental Research* 156:605–12. doi: 10.1016/j.envres.2017.04.019.
- Carpenito, C., M. C. Milone, R. Hassan, J. C. Simonet, M. Lakhal, M. M. Suhoski, A. Varela-Rohena, K. M. Haines, D. F. Heitjan, S. M. Albelda, R. G. Carroll, J. L. Riley, I. Pastan, and C. H. June. 2009. "Control of Large, Established Tumor Xenografts with Genetically Retargeted Human T Cells Containing CD28 and CD137 Domains." *Proceedings of the National Academy of Sciences* 106(9):3360–65. doi: 10.1073/pnas.0813101106.
- Castella, Maria, Anna Boronat, Raquel Martín-Ibáñez, Vanina Rodríguez, Guillermo Suñé, Miguel Caballero, Berta Marzal, Lorena Pérez-Amill, Beatriz Martín-Antonio, Julio Castaño, Clara Bueno, Olga Balagué, Europa Azucena González-Navarro, Carles Serra-Pages, Pablo Engel, Ramon Vilella, Daniel Benitez-Ribas, Valentín Ortiz-Maldonado, Joan Cid, Jaime Tabera, Josep M. Canals, Miquel Lozano, Tycho Baumann, Anna Vilarrodona, Esteve Trias, Elías Campo, Pablo Menendez, Álvaro Urbano-Ispizua, Jordi Yagüe, Patricia Pérez-Galán, Susana Rives, Julio Delgado, and Manel Juan. 2019. "Development of a Novel Anti-CD19 Chimeric Antigen Receptor: A Paradigm for an Affordable CAR T Cell Production at Academic Institutions." *Molecular Therapy - Methods & Clinical Development* 12:134–44. doi: 10.1016/j.omtm.2018.11.010.
- Chan, W. K., D. Suwannasaen, R. E. Throm, Y. Li, P. W. Eldridge, J. Houston, J. T. Gray, C-h Pui, and W. Leung. 2014. "Chimeric Antigen Receptor-Redirected CD45RA-Negative T Cells Have Potent Antileukemia and Pathogen Memory Response without Graft-versus-Host Activity." *Leukemia* (April):1–9. doi: 10.1038/leu.2014.174.
- Chang, Yu-Hsiang, John Connolly, Noriko Shimasaki, Kousaku Mimura, Koji Kono, and Dario Campana. 2013. "A Chimeric Receptor with NKG2D Specificity Enhances Natural Killer Cell Activation and Killing of Tumor Cells." *Cancer Research* 73(6):1777–86. doi: 10.1158/0008-5472.CAN-12-3558.
- Cheadle, Eleanor J., David E. Gilham, and Robert E. Hawkins. 2008. "The Combination of Cyclophosphamide and Human T Cells Genetically Engineered to Target CD19 Can Eradicate Established B-Cell Lymphoma." *British Journal of Haematology* 142(1):65–68. doi: 10.1111/j.1365-2141.2008.07145.x.
- Chen, Bing, Lu Jiang, Meng-Ling Zhong, Jian-Feng Li, Ben-Shang Li, Li-Jun Peng, Yu-Ting Dai, Bo-Wen Cui, Tian-Qi Yan, Wei-Na Zhang, Xiang-Qin Weng, Yin-Yin Xie, Jing Lu, Rui-Bao Ren, Su-Ning Chen, Jian-Da Hu, De-Pei Wu, Zhu Chen, Jing-Yan Tang, Jin-Yan Huang, Jian-Qing Mi, and Sai-Juan Chen. 2018. "Identification

- of Fusion Genes and Characterization of Transcriptome Features in T-Cell Acute Lymphoblastic Leukemia." *Proceedings of the National Academy of Sciences* 115(2):373–78. doi: 10.1073/pnas.1717125115.
- Chitadze, G., J. Bhat, M. Lettau, O. Janssen, and D. Kabelitz. 2013. "Generation of Soluble NKG2D Ligands: Proteolytic Cleavage, Exosome Secretion and Functional Implications." *Scandinavian Journal of Immunology* 78(2):120–29. doi: 10.1111/sji.12072.
- Chmielewski, Markus, and Hinrich Abken. 2015. "TRUCKs: The Fourth Generation of CARs." *Expert Opinion on Biological Therapy* 15(8):1145–54. doi: 10.1517/14712598.2015.1046430.
- Christodoulou, I., P. Patsali, C. Stephanou, M. Antoniou, M. Kleanthous, and C. W. Lederer. 2016. "Measurement of Lentiviral Vector Titre and Copy Number by Cross-Species Duplex Quantitative PCR." *Gene Therapy* 23(1):113–18. doi: 10.1038/gt.2015.60.
- Coalition Against Childhood Cancer. 2021. "Childhood Cancer Fact Library." Retrieved January 24, 2022 (<https://cac2.org/interest-groups/awareness/childhood-cancer-fact-library/>).
- Cooper, Stacy L., and Patrick A. Brown. 2015. "Treatment of Pediatric Acute Lymphoblastic Leukemia." *Pediatric Clinics of North America* 62(1):61–73. doi: 10.1016/j.pcl.2014.09.006.
- Cooper, Todd M., Janet Franklin, Robert B. Gerbing, Todd A. Alonzo, Craig Hurwitz, Susana C. Raimondi, Betsy Hirsch, Franklin O. Smith, Prasad Mathew, Robert J. Arceci, James Feusner, Robert Iannone, Robert S. Lavey, Soheil Meshinchi, and Alan Gamis. 2012. "AAML03P1, a Pilot Study of the Safety of Gemtuzumab Ozogamicin in Combination with Chemotherapy for Newly Diagnosed Childhood Acute Myeloid Leukemia." *Cancer* 118(3):761–69. doi: 10.1002/cncr.26190.
- Cornelissen, Jan J., and Didier Blaise. 2016. "Hematopoietic Stem Cell Transplantation for Patients with AML in First Complete Remission." *Blood* 127(1):62–70. doi: 10.1182/blood-2015-07-604546.
- Creutzig, U., J. Ritter, M. Zimmermann, D. Reinhardt, J. Hermann, F. Berthold, G. Henze, H. Jürgens, H. Kabisch, W. Havers, A. Reiter, U. Kluba, F. Niggli, and H. Gadner. 2001. "Improved Treatment Results in High-Risk Pediatric Acute Myeloid Leukemia Patients After Intensification With High-Dose Cytarabine and Mitoxantrone: Results of Study Acute Myeloid Leukemia–Berlin–Frankfurt–Münster 93." *Journal of Clinical Oncology* 19(10):2705–13. doi: 10.1200/JCO.2001.19.10.2705.
- Creutzig, Ursula, Marry M. van den Heuvel-Eibrink, Brenda Gibson, Michael N. Dworzak, Souichi Adachi, Eveline de Bont, Jochen Harbott, Henrik Hasle, Donna Johnston, Akitoshi Kinoshita, Thomas Lehrnbecher, Guy Leverger, Ester Mejstrikova, Soheil Meshinchi, Andrea Pession, Susana C. Raimondi, Lillian Sung, Jan Stary, Christian M. Zwaan, Gertjan J. L. Kaspers, and Dirk Reinhardt. 2012. "Diagnosis and Management of Acute Myeloid Leukemia in Children and Adolescents: Recommendations from an International Expert Panel." *Blood* 120(16):3187–3205. doi: 10.1182/blood-2012-03-362608.
- Dahmani, Amina, and Jean Sébastien Delisle. 2018. "TGF- β in T Cell Biology: Implications for Cancer Immunotherapy." *Cancers* 10(6):1–21. doi: 10.3390/cancers10060194.
- Davila, Marco L., Isabelle Riviere, Xiuyan Wang, Shirley Bartido, Jae Park, Kevin

- Curran, Stephen S. Chung, Jolanta Stefanski, Oriana Borquez-Ojeda, Malgorzata Olszewska, Jinrong Qu, Teresa Wasielewska, Qing He, Mitsu Fink, Himaly Shinglot, Maher Youssif, Mark Satter, Yongzeng Wang, James Hosey, Hilda Quintanilla, Elizabeth Halton, Yvette Bernal, Diana C. G. Bouhassira, Maria E. Arcila, Mithat Gonen, Gail J. Roboz, Peter Maslak, Dan Douer, Mark G. Frattini, Sergio Giralt, Michel Sadelain, and Renier Brentjens. 2014. "Efficacy and Toxicity Management of 19-28z CAR T Cell Therapy in B Cell Acute Lymphoblastic Leukemia." *Science Translational Medicine* 6(224). doi: 10.1126/scitranslmed.3008226.
- Davis, Amanda S., Anthony J. Viera, and Monica D. Mead. 2014. "Leukemia: An Overview for Primary Care." *American Family Physician* 89(9):731–38.
- Depil, S., P. Duchateau, S. A. Grupp, G. Mufti, and L. Poirot. 2020. "'Off-the-Shelf' Allogeneic CAR T Cells: Development and Challenges." *Nature Reviews Drug Discovery* 19(3):185–99. doi: 10.1038/s41573-019-0051-2.
- Dhanji, Salim, and Hung-Sia Teh. 2003. "IL-2-Activated CD8⁺ CD44^{High} Cells Express Both Adaptive and Innate Immune System Receptors and Demonstrate Specificity for Syngeneic Tumor Cells." *The Journal of Immunology* 171(7):3442–50. doi: 10.4049/jimmunol.171.7.3442.
- Diller, Lisa. 2011. "Adult Primary Care after Childhood Acute Lymphoblastic Leukemia." *New England Journal of Medicine* 365(15):1417–24. doi: 10.1056/NEJMcp1103645.
- van Dongen, Jacques J. M., Vincent H. J. van der Velden, Monika Brüggemann, and Alberto Orfao. 2015. "Minimal Residual Disease Diagnostics in Acute Lymphoblastic Leukemia: Need for Sensitive, Fast, and Standardized Technologies." *Blood* 125(26):3996–4009. doi: 10.1182/blood-2015-03-580027.
- Driouk, Lina, Joanina K. Gicobi, Yusuke Kamihara, Kayleigh Rutherford, Glenn Dranoff, Jerome Ritz, and Susanne H. C. Baumeister. 2020. "Chimeric Antigen Receptor T Cells Targeting NKG2D-Ligands Show Robust Efficacy Against Acute Myeloid Leukemia and T-Cell Acute Lymphoblastic Leukemia." *Frontiers in Immunology* 11(December):1–17. doi: 10.3389/fimmu.2020.580328.
- Duan, Shixin, Weihua Guo, Zuxing Xu, Yunbo He, Chuting Liang, Yongzhen Mo, Yian Wang, Fang Xiong, Can Guo, Yong Li, Xiaoling Li, Guiyuan Li, Zhaoyang Zeng, Wei Xiong, and Fuyan Wang. 2019. "Natural Killer Group 2D Receptor and Its Ligands in Cancer Immune Escape." *Molecular Cancer* 18(1):29. doi: 10.1186/s12943-019-0956-8.
- Eagle, Robert, Insiya Jafferji, and Alexander Barrow. 2009. "Beyond Stressed Self: Evidence for NKG2D Ligand Expression on Healthy Cells." *Current Immunology Reviews* 5(1):22–34. doi: 10.2174/157339509787314369.
- Epperly, Rebecca, Stephen Gottschalk, and M. Paulina Velasquez. 2020. "A Bump in the Road: How the Hostile AML Microenvironment Affects CAR T Cell Therapy." *Frontiers in Oncology* 10. doi: 10.3389/fonc.2020.00262.
- Eshhar, Z., T. Waks, G. Gross, and D. G. Schindler. 1993. "Specific Activation and Targeting of Cytotoxic Lymphocytes through Chimeric Single Chains Consisting of Antibody-Binding Domains and the Gamma or Zeta Subunits of the Immunoglobulin and T-Cell Receptors." *Proceedings of the National Academy of Sciences* 90(2):720–24. doi: 10.1073/pnas.90.2.720.
- Esparza, Samuel D., and Kathleen M. Sakamoto. 2005. "Topics in Pediatric Leukemia--Acute Lymphoblastic Leukemia." *MedGenMed : Medscape General Medicine*

- Faderl, Stefan, Susan O'Brien, Ching-Hon Pui, Wendy Stock, Meir Wetzler, Dieter Hoelzer, and Hagop M. Kantarjian. 2010. "Adult Acute Lymphoblastic Leukemia." *Cancer* 116(5):1165–76. doi: 10.1002/cncr.24862.
- Fathi, Ezzatollah, Raheleh Farahzadi, Roghayeh Sheervalilou, Zohreh Sanaat, and Ilja Vietor. 2020. "A General View of CD33⁺ Leukemic Stem Cells and CAR-T Cells as Interesting Targets in Acute Myeloblastic Leukemia Therapy." *BLOOD RESEARCH* 55(1):10–16. doi: 10.5045/br.2020.55.1.10.
- Fernández-Messina, Lola, Omodele Ashiru, Philippe Boutet, Sonia Agüera-González, Jeremy N. Skepper, Hugh T. Reyburn, and Mar Valés-Gómez. 2010. "Differential Mechanisms of Shedding of the Glycosylphosphatidylinositol (GPI)-Anchored NKG2D Ligands." *Journal of Biological Chemistry* 285(12):8543–51. doi: 10.1074/jbc.M109.045906.
- Fernández-Messina, Lola, Hugh T. Reyburn, and Mar Valés-Gómez. 2016. "A Short Half-life of ULBP1 at the Cell Surface Due to Internalization and Proteosomal Degradation." *Immunology & Cell Biology* 94(5):479–85. doi: 10.1038/icb.2016.2.
- Fernández, Lucía, Adrián Fernández, Isabel Mirones, Adela Escudero, Leila Cardoso, María Vela, Diego Lanzarot, Raquel de Paz, Alejandra Leivas, Miguel Gallardo, Antonio Marcos, Ana Belén Romero, Joaquín Martínez-López, and Antonio Pérez-Martínez. 2019. "GMP-Compliant Manufacturing of NKG2D CAR Memory T Cells Using CliniMACS Prodigy." *Frontiers in Immunology* 10(October):1–12. doi: 10.3389/fimmu.2019.02361.
- Fernández, Lucía, Jean-Yves Metais, Adela Escudero, María Vela, Jaime Valentín, Isabel Vallcorba, Alejandra Leivas, Juan Torres, Antonio Valeri, Ana Patiño-García, Joaquín Martínez, Wing Leung, and Antonio Pérez-Martínez. 2017. "Memory T Cells Expressing an NKG2D-CAR Efficiently Target Osteosarcoma Cells." *Clinical Cancer Research* 23(19):5824–35. doi: 10.1158/1078-0432.CCR-17-0075.
- Finney, Helene M., Arne N. Akbar, and Alastair D. G. Lawson. 2004. "Activation of Resting Human Primary T Cells with Chimeric Receptors: Costimulation from CD28, Inducible Costimulator, CD134, and CD137 in Series with Signals from the TCR ζ Chain." *The Journal of Immunology* 172(1):104–13. doi: 10.4049/jimmunol.172.1.104.
- Fionda, Cinzia, Alessandra Soriani, Giulia Malgarini, Maria Luisa Iannitto, Angela Santoni, and Marco Cippitelli. 2009. "Heat Shock Protein-90 Inhibitors Increase MHC Class I-Related Chain A and B Ligand Expression on Multiple Myeloma Cells and Their Ability to Trigger NK Cell Degranulation." *The Journal of Immunology* 183(7):4385–94. doi: 10.4049/jimmunol.0901797.
- Friedman, Debra L., John Whitton, Wendy Leisenring, Ann C. Mertens, Sue Hammond, Marilyn Stovall, Sarah S. Donaldson, Anna T. Meadows, Leslie L. Robison, and Joseph P. Neglia. 2010. "Subsequent Neoplasms in 5-Year Survivors of Childhood Cancer: The Childhood Cancer Survivor Study." *JNCI: Journal of the National Cancer Institute* 102(14):1083–95. doi: 10.1093/jnci/djq238.
- Gabrilovich, Dmitry I., and Srinivas Nagaraj. 2009. "Myeloid-Derived Suppressor Cells as Regulators of the Immune System." *Nature Reviews Immunology* 9(3):162–74. doi: 10.1038/nri2506.
- Gamis, Alan S., Todd A. Alonzo, Soheil Meshinchi, Lillian Sung, Robert B. Gerbing, Susana C. Raimondi, Betsy A. Hirsch, Samir B. Kahwash, Amy Heerema-

- McKenney, Laura Winter, Kathleen Glick, Stella M. Davies, Patti Byron, Franklin O. Smith, and Richard Aplenc. 2014. "Gemtuzumab Ozogamicin in Children and Adolescents With De Novo Acute Myeloid Leukemia Improves Event-Free Survival by Reducing Relapse Risk: Results From the Randomized Phase III Children's Oncology Group Trial AAML0531." *Journal of Clinical Oncology* 32(27):3021–32. doi: 10.1200/JCO.2014.55.3628.
- Gándara, Carolina, Valerie Affleck, and Elizabeth Ann Stoll. 2018. "Manufacture of Third-Generation Lentivirus for Preclinical Use, with Process Development Considerations for Translation to Good Manufacturing Practice." *Human Gene Therapy Methods* 29(1):1–15. doi: 10.1089/hgtb.2017.098.
- Gardner, Rebecca, David Wu, Sindhu Cherian, Min Fang, Laïla-Aïcha Hanafi, Olivia Finney, Hannah Smithers, Michael C. Jensen, Stanley R. Riddell, David G. Maloney, and Cameron J. Turtle. 2016. "Acquisition of a CD19-Negative Myeloid Phenotype Allows Immune Escape of MLL-Rearranged B-ALL from CD19 CAR-T-Cell Therapy." *Blood* 127(20):2406–10. doi: 10.1182/blood-2015-08-665547.
- Gasser, Stephan, Sandra Orsulic, Eric J. Brown, and David H. Raulet. 2005. "The DNA Damage Pathway Regulates Innate Immune System Ligands of the NKG2D Receptor." *Nature* 436(7054):1186–90. doi: 10.1038/nature03884.
- Geyer, Mark B., and Renier J. Brentjens. 2016. "Review: Current Clinical Applications of Chimeric Antigen Receptor (CAR) Modified T Cells." *Cytotherapy* 18(11):1393–1409. doi: 10.1016/j.jcyt.2016.07.003.
- Ghosh, Arnab, Ioannis Politikos, and Miguel-Angel Perales. 2017. "Stop and Go: Hematopoietic Cell Transplantation in the Era of Chimeric Antigen Receptor T Cells and Checkpoint Inhibitors." *Current Opinion in Oncology* 29(6):474–83. doi: 10.1097/CCO.0000000000000408.
- Gilead. 2020. "U.S. FDA Approves Kite's Tecartus™, the First and Only CAR T Treatment for Relapsed or Refractory Mantle Cell Lymphoma." *Press Releases*. Retrieved January 11, 2022 (<https://www.gilead.com/news-and-press/press-room/press-releases/2020/7/us-fda-approves-kites-tecartus-the-first-and-only-car-t-treatment-for-relapsed-or-refractory-mantle-cell-lymphoma>).
- Girardi, Tiziana, Carmen Vicente, Jan Cools, and Kim De Keersmaecker. 2017. "The Genetics and Molecular Biology of T-ALL." *Blood* 129(9):1113–23. doi: 10.1182/blood-2016-10-706465.
- Gomes-Silva, Diogo, Madhuwanti Srinivasan, Sandhya Sharma, Ciaran M. Lee, Dimitrios L. Wagner, Timothy H. Davis, Rayne H. Rouce, Gang Bao, Malcolm K. Brenner, and Maksim Mamonkin. 2017. "CD7-Edited T Cells Expressing a CD7-Specific CAR for the Therapy of T-Cell Malignancies." *Blood* 130(3):285–96. doi: 10.1182/blood-2017-01-761320.
- Groh, V., A. Bruhl, H. El-Gabalawy, J. L. Nelson, and T. Spies. 2003. "Stimulation of T Cell Autoreactivity by Anomalous Expression of NKG2D and Its MIC Ligands in Rheumatoid Arthritis." *Proceedings of the National Academy of Sciences* 100(16):9452–57. doi: 10.1073/pnas.1632807100.
- Groh, Veronika, Rebecca Rhinehart, Julie Randolph-Habecker, Max S. Topp, Stanley R. Riddell, and Thomas Spies. 2001. "Costimulation of CD8αβ T Cells by NKG2D via Engagement by MIC Induced on Virus-Infected Cells." *Nature Immunology* 2(3):255–60. doi: 10.1038/85321.
- Groh, Veronika, Jennifer Wu, Cassian Yee, and Thomas Spies. 2002. "Tumour-Derived Soluble MIC Ligands Impair Expression of NKG2D and T-Cell Activation." *Nature*

- 419(6908):734–38. doi: 10.1038/nature01112.
- Gross, G., T. Waks, and Z. Eshhar. 1989. “Expression of Immunoglobulin-T-Cell Receptor Chimeric Molecules as Functional Receptors with Antibody-Type Specificity.” *Proceedings of the National Academy of Sciences* 86(24):10024–28. doi: 10.1073/pnas.86.24.10024.
- Guedan, Sonia, Hugo Calderon, Avery D. Posey, and Marcela V. Maus. 2019. “Engineering and Design of Chimeric Antigen Receptors.” *Molecular Therapy - Methods & Clinical Development* 12:145–56. doi: 10.1016/j.omtm.2018.12.009.
- Guedan, Sonia, Xi Chen, Aviv Madar, Carmine Carpenito, Shannon E. McGettigan, Matthew J. Frigault, Jihyun Lee, Avery D. Posey, John Scholler, Nathalie Scholler, Richard Bonneau, and Carl H. June. 2014. “ICOS-Based Chimeric Antigen Receptors Program Bipolar TH17/TH1 Cells.” *Blood* 124(7):1070–80. doi: 10.1182/blood-2013-10-535245.
- Guedan, Sonia, Avery D. Posey, Carolyn Shaw, Anna Wing, Tong Da, Prachi R. Patel, Shannon E. McGettigan, Victoria Casado-Medrano, Omkar U. Kawalekar, Mireia Uribe-Herranz, Decheng Song, J. Joseph Melenhorst, Simon F. Lacey, John Scholler, Brian Keith, Regina M. Young, and Carl H. June. 2018. “Enhancing CAR T Cell Persistence through ICOS and 4-1BB Costimulation.” *JCI Insight* 3(1). doi: 10.1172/jci.insight.96976.
- Hamieh, Mohamad, Anton Dobrin, Annalisa Cabriolu, Sjoukje J. C. van der Stegen, Theodoros Giavridis, Jorge Mansilla-Soto, Justin Eyquem, Zeguo Zhao, Benjamin M. Whitlock, Matthew M. Miele, Zhuoning Li, Kristen M. Cunanan, Morgan Huse, Ronald C. Hendrickson, Xiuyan Wang, Isabelle Rivière, and Michel Sadelain. 2019. “CAR T Cell Trogocytosis and Cooperative Killing Regulate Tumour Antigen Escape.” *Nature* 568(7750):112–16. doi: 10.1038/s41586-019-1054-1.
- Harding, Fiona A., James G. McArthur, Jane A. Gross, David H. Raulet, and James P. Allison. 1992. “CD28-Mediated Signalling Co-Stimulates Murine T Cells and Prevents Induction of Anergy in T-Cell Clones.” *Nature* 356(6370):607–9. doi: 10.1038/356607a0.
- Hartmann, Jessica, Martina Schüßler-Lenz, Attilio Bondanza, and Christian J. Buchholz. 2017. “Clinical Development of CAR T Cells—Challenges and Opportunities in Translating Innovative Treatment Concepts.” *EMBO Molecular Medicine* 9(9):1183–97. doi: 10.15252/emmm.201607485.
- Haso, Waleed, Daniel W. Lee, Nirali N. Shah, Maryalice Stetler-Stevenson, Constance M. Yuan, Ira H. Pastan, Dimitar S. Dimitrov, Richard A. Morgan, David J. Fitzgerald, David M. Barrett, Alan S. Wayne, Crystal L. Mackall, and Rimas J. Orentas. 2013. “Anti-CD22–Chimeric Antigen Receptors Targeting B-Cell Precursor Acute Lymphoblastic Leukemia.” *Blood* 121(7):1165–74. doi: 10.1182/blood-2012-06-438002.
- Hilpert, Julia, Ludger Grosse-Hovest, Frank Grünebach, Corina Buechele, Tina Nuebling, Tobias Raum, Alexander Steinle, and Helmut Rainer Salih. 2012. “Comprehensive Analysis of NKG2D Ligand Expression and Release in Leukemia: Implications for NKG2D-Mediated NK Cell Responses.” *The Journal of Immunology* 189(3):1360–71. doi: 10.4049/jimmunol.1200796.
- Hoelzer, Dieter. 2011. “Novel Antibody-Based Therapies For Acute Lymphoblastic Leukemia.” *Hematology* 2011(1):243–49. doi: 10.1182/asheducation-2011.1.243.
- Hoffman, Lindsey M., and Lia Gore. 2014. “Blinatumomab, a Bi-Specific Anti-CD19/CD3 BiTE® Antibody for the Treatment of Acute Lymphoblastic Leukemia:

- Perspectives and Current Pediatric Applications.” *Frontiers in Oncology* 4. doi: 10.3389/fonc.2014.00063.
- Horan, John T., Todd A. Alonzo, Gary H. Lyman, Robert B. Gerbing, Beverly J. Lange, Yaddanapudi Ravindranath, David Becton, Franklin O. Smith, and William G. Woods. 2008. “Impact of Disease Risk on Efficacy of Matched Related Bone Marrow Transplantation for Pediatric Acute Myeloid Leukemia: The Children’s Oncology Group.” *Journal of Clinical Oncology* 26(35):5797–5801. doi: 10.1200/JCO.2007.13.5244.
- Hornig, Tiffany, Jelena S. Bezbradica, and Ruslan Medzhitov. 2007. “NKG2D Signaling Is Coupled to the Interleukin 15 Receptor Signaling Pathway.” *Nature Immunology* 8(12):1345–52. doi: 10.1038/ni1524.
- Howlader N, Noone AM, Krapcho M, Miller D, Bishop K, Altekruse SF, Kosary CL, Yu M, Ruhl J, Tatalovich Z, Mariotto A, Lewis DR, Chen HS, Feuer EJ, Cronin KA (eds). 2021. “SEER Cancer Statistics Review 1975-2018 National Cancer Institute.” *SEER Cancer Statistics Review, 1975-2018, National Cancer Institute. Bethesda, MD, http://seer.cancer.gov/csr/1975_2018/, Based on November 2020 SEER Data Submission, Posted to the SEER Web Site, April 2021.*
- Hunger, Stephen P., Xiaomin Lu, Meenakshi Devidas, Bruce M. Camitta, Paul S. Gaynon, Naomi J. Winick, Gregory H. Reaman, and William L. Carroll. 2012. “Improved Survival for Children and Adolescents With Acute Lymphoblastic Leukemia Between 1990 and 2005: A Report From the Children’s Oncology Group.” *Journal of Clinical Oncology* 30(14):1663–69. doi: 10.1200/JCO.2011.37.8018.
- Hunger, Stephen P., and Charles G. Mullighan. 2015. “Acute Lymphoblastic Leukemia in Children.” *New England Journal of Medicine* 373(16):1541–52. doi: 10.1056/NEJMra1400972.
- Inaba, Hiroto, Mel Greaves, and Charles G. Mullighan. 2013. “Acute Lymphoblastic Leukaemia.” *The Lancet* 381(9881):1943–55. doi: 10.1016/S0140-6736(12)62187-4.
- Inaba, Hiroto, and Ching-Hon Pui. 2010. “Glucocorticoid Use in Acute Lymphoblastic Leukaemia.” *The Lancet Oncology* 11(11):1096–1106. doi: 10.1016/S1470-2045(10)70114-5.
- Isernhagen, Antje, Dörthe Malzahn, Elena Viktorova, Leslie Elsner, Sebastian Monecke, Frederike Bonin, Markus Kilisch, Janne Marieke Wermuth, Neele Walther, Yesilda Balavarca, Christiane Stahl-Hennig, Michael Engelke, Lutz Walter, Heike Bickeböller, Dieter Kube, Gerald Wulf, and Ralf Dressel. 2015. “The MICA-129 Dimorphism Affects NKG2D Signaling and Outcome of Hematopoietic Stem Cell Transplantation.” *EMBO Molecular Medicine* 7(11):1480–1502. doi: 10.15252/emmm.201505246.
- Jabbour, Elias J., Stefan Faderl, and Hagop M. Kantarjian. 2005. “Adult Acute Lymphoblastic Leukemia.” *Mayo Clinic Proceedings* 80(11):1517–27. doi: 10.4065/80.11.1517.
- Jacoby, Elad, Sang M. Nguyen, Thomas J. Fountaine, Kathryn Welp, Berkley Gryder, Haiying Qin, Yinmeng Yang, Christopher D. Chien, Alix E. Seif, Haiyan Lei, Young K. Song, Javed Khan, Daniel W. Lee, Crystal L. Mackall, Rebecca A. Gardner, Michael C. Jensen, Jack F. Shern, and Terry J. Fry. 2016. “CD19 CAR Immune Pressure Induces B-Precursor Acute Lymphoblastic Leukaemia Lineage Switch Exposing Inherent Leukaemic Plasticity.” *Nature Communications* 7(1):12320. doi:

10.1038/ncomms12320.

- Jensen, Michael, Giselle Tan, Stephen Forman, Anna M. Wu, and Andrew Raubitschek. 1998. "CD20 Is a Molecular Target for ScFvFc:Zeta Receptor Redirected T Cells: Implications for Cellular Immunotherapy of CD20+ Malignancy." *Biology of Blood and Marrow Transplantation* 4(2):75–83. doi: 10.1053/bbmt.1998.v4.pm9763110.
- June, Carl H., and Michel Sadelain. 2018. "Chimeric Antigen Receptor Therapy." *New England Journal of Medicine* 379(1):64–73. doi: 10.1056/NEJMr1706169.
- Jung, Heiyoun, Benjamin Hsiung, Kathleen Pestal, Emily Procyk, and David H. Raulet. 2012. "RAE-1 Ligands for the NKG2D Receptor Are Regulated by E2F Transcription Factors, Which Control Cell Cycle Entry." *Journal of Experimental Medicine* 209(13):2409–22. doi: 10.1084/jem.20120565.
- Kadan-Lottick, Nina S., Irina Dinu, Karen Wasilewski-Masker, Sue Kaste, Lillian R. Meacham, Anita Mahajan, Marilyn Stovall, Yutaka Yasui, Leslie L. Robison, and Charles A. Sklar. 2008. "Osteonecrosis in Adult Survivors of Childhood Cancer: A Report From the Childhood Cancer Survivor Study." *Journal of Clinical Oncology* 26(18):3038–45. doi: 10.1200/JCO.2007.14.9088.
- Kalos, Michael, Bruce L. Levine, David L. Porter, Sharyn Katz, Stephan A. Grupp, Adam Bagg, and Carl H. June. 2011. "T Cells with Chimeric Antigen Receptors Have Potent Antitumor Effects and Can Establish Memory in Patients with Advanced Leukemia." *Science Translational Medicine* 3(95). doi: 10.1126/scitranslmed.3002842.
- Kanehisa, Minoru, Yoko Sato, and Masayuki Kawashima. 2022. "<scp>KEGG</Scp> Mapping Tools for Uncovering Hidden Features in Biological Data." *Protein Science* 31(1):47–53. doi: 10.1002/pro.4172.
- Karrman, Kristina, Erik Forestier, Mats Heyman, Mette K. Andersen, Kirsi Autio, Elisabeth Blennow, Georg Borgström, Hans Ehrencrona, Irina Golovleva, Sverre Heim, Kristiina Heinonen, Randi Hovland, Johann H. Johannsson, Gitte Kerndrup, Ann Nordgren, Lars Palmqvist, and Bertil Johansson. 2009. "Clinical and Cytogenetic Features of a Population-Based Consecutive Series of 285 Pediatric T-Cell Acute Lymphoblastic Leukemias: Rare T-Cell Receptor Gene Rearrangements Are Associated with Poor Outcome." *Genes, Chromosomes and Cancer* 48(9):795–805. doi: 10.1002/gcc.20684.
- Karrman, Kristina, and Bertil Johansson. 2017. "Pediatric T-Cell Acute Lymphoblastic Leukemia." *Genes, Chromosomes and Cancer* 56(2):89–116. doi: 10.1002/gcc.22416.
- Klingemann, Hans. 2015. "Challenges of Cancer Therapy with Natural Killer Cells." *Cytotherapy* 17(3):245–49. doi: 10.1016/j.jcyt.2014.09.007.
- Kochenderfer, James N., Mark E. Dudley, Steven A. Feldman, Wyndham H. Wilson, David E. Spaner, Irina Maric, Maryalice Stetler-Stevenson, Gao Q. Phan, Marybeth S. Hughes, Richard M. Sherry, James C. Yang, Udai S. Kammula, Laura Devillier, Robert Carpenter, Debbie-Ann N. Nathan, Richard A. Morgan, Carolyn Laurencot, and Steven A. Rosenberg. 2012. "B-Cell Depletion and Remissions of Malignancy along with Cytokine-Associated Toxicity in a Clinical Trial of Anti-CD19 Chimeric-Antigen-Receptor–Transduced T Cells." *Blood* 119(12):2709–20. doi: 10.1182/blood-2011-10-384388.
- Krause, Anja, Hong-Fen Guo, Jean-Baptiste Latouche, Cuiwen Tan, Nai-Kong V. Cheung, and Michel Sadelain. 1998. "Antigen-Dependent CD28 Signaling

- Selectively Enhances Survival and Proliferation in Genetically Modified Activated Human Primary T Lymphocytes." *Journal of Experimental Medicine* 188(4):619–26. doi: 10.1084/jem.188.4.619.
- Kuerbitz, S. J., C. I. Civin, J. P. Krischer, Y. Ravindranath, C. P. Steuber, H. J. Weinstein, N. Winick, A. H. Ragab, M. V Gresik, and W. M. Crist. 1992. "Expression of Myeloid-Associated and Lymphoid-Associated Cell-Surface Antigens in Acute Myeloid Leukemia of Childhood: A Pediatric Oncology Group Study." *Journal of Clinical Oncology* 10(9):1419–29. doi: 10.1200/JCO.1992.10.9.1419.
- Lazarova, Mariya, and Alexander Steinle. 2019. "Impairment of NKG2D-Mediated Tumor Immunity by TGF- β ." *Frontiers in Immunology* 10(November):10–13. doi: 10.3389/fimmu.2019.02689.
- Legrand, Ollivier, Jean-Yves Perrot, Ghislaine Simonin, Marion Baudard, Monique Cadiou, Claude Blanc, Sylvie Ramond, Franck Vigui , Jean-Pierre Marie, and Robert Zittoun. 1998. "Adult Biphenotypic Acute Leukaemia: An Entity with Poor Prognosis Which Is Related to Unfavourable Cytogenetics and P-glycoprotein Over-expression." *British Journal of Haematology* 100(1):147–55. doi: 10.1046/j.1365-2141.1998.00523.x.
- Lehner, Manfred, Gabriel G tz, Julia Proff, Niels Schaft, Jan D rrie, Florian Full, Armin Ensser, Yves A. Muller, Adelheid Cerwenka, Hinrich Abken, Ornella Parolini, Peter F. Ambros, Heinrich Kovar, and Wolfgang Holter. 2012. "Redirecting T Cells to Ewing's Sarcoma Family of Tumors by a Chimeric NKG2D Receptor Expressed by Lentiviral Transduction or mRNA Transfection." *PLoS ONE* 7(2):e31210. doi: 10.1371/journal.pone.0031210.
- Leivas, Alejandra, Antonio Perez-Martinez, Mar a Jes s Blanchard, Estela Mart n-Clavero, Luc a Fern ndez, Juan Jos  Lahuerta, and Joaqu n Martinez-Lopez. 2016. "Novel Treatment Strategy with Autologous Activated and Expanded Natural Killer Cells plus Anti-Myeloma Drugs for Multiple Myeloma." *Oncotarget* 5(12):e1250051. doi: 10.1080/2162402X.2016.1250051.
- Leung, Wing, Dario Campana, Jie Yang, Deqing Pei, Elaine Coustan-Smith, Kwan Gan, Jeffrey E. Rubnitz, John T. Sandlund, Raul C. Ribeiro, Ashok Srinivasan, Christine Hartford, Brandon M. Triplett, Mari Dallas, Asha Pillai, Rupert Handgretinger, Joseph H. Laver, and Ching-Hon Pui. 2011. "High Success Rate of Hematopoietic Cell Transplantation Regardless of Donor Source in Children with Very High-Risk Leukemia." *Blood* 118(2):223–30. doi: 10.1182/blood-2011-01-333070.
- Li, Bo, and Colin N. Dewey. 2011. "RSEM: Accurate Transcript Quantification from RNA-Seq Data with or without a Reference Genome." *BMC Bioinformatics* 12(1):323. doi: 10.1186/1471-2105-12-323.
- Litzow, Mark R., and Adolfo A. Ferrando. 2015. "How I Treat T-Cell Acute Lymphoblastic Leukemia in Adults." *Blood* 126(7):833–41. doi: 10.1182/blood-2014-10-551895.
- Liu, Yu, John Easton, Ying Shao, Jamie Maciaszek, Zhaoming Wang, Mark R. Wilkinson, Kelly McCastlain, Michael Edmonson, Stanley B. Pounds, Lei Shi, Xin Zhou, Xiaotu Ma, Edgar Sioson, Yongjin Li, Michael Rusch, Pankaj Gupta, Deqing Pei, Cheng Cheng, Malcolm A. Smith, Jaime Guidry Auvil, Daniela S. Gerhard, Mary V Relling, Naomi J. Winick, Andrew J. Carroll, Nyla A. Heerema, Elizabeth Raetz, Meenakshi Devidas, Cheryl L. Willman, Richard C. Harvey, William L. Carroll, Kimberly P. Dunsmore, Stuart S. Winter, Brent L. Wood, Brian P.

- Sorrentino, James R. Downing, Mignon L. Loh, Stephen P. Hunger, Jinghui Zhang, and Charles G. Mullighan. 2017. "The Genomic Landscape of Pediatric and Young Adult T-Lineage Acute Lymphoblastic Leukemia." *Nature Genetics* 49(8):1211–18. doi: 10.1038/ng.3909.
- Liyanage, Udaya K., Todd T. Moore, Hong-Gu Joo, Yoshiyuki Tanaka, Virginia Herrmann, Gerard Doherty, Jeffrey A. Drebin, Steven M. Strasberg, Timothy J. Eberlein, Peter S. Goedegebuure, and David C. Linehan. 2002. "Prevalence of Regulatory T Cells Is Increased in Peripheral Blood and Tumor Microenvironment of Patients with Pancreas or Breast Adenocarcinoma." *The Journal of Immunology* 169(5):2756–61. doi: 10.4049/jimmunol.169.5.2756.
- Lock, Dominik, Nadine Mockel-Tenbrinck, Katharina Drechsel, Carola Barth, Daniela Mauer, Thomas Schaser, Carolin Kolbe, Wael Al Rawashdeh, Janina Brauner, Olaf Hardt, Natali Pflug, Udo Holtick, Peter Borchmann, Mario Assenmacher, and Andrew Kaiser. 2017. "Automated Manufacturing of Potent CD20-Directed Chimeric Antigen Receptor T Cells for Clinical Use." *Human Gene Therapy* 28(10):914–25. doi: 10.1089/hum.2017.111.
- Lonez, Caroline, Alain Hendlisz, Leila Shaza, Philippe Aftimos, Michaël Vouche, Vincent Donckier, Jean-Pascal H. Machiels, Marc Van Den Eynde, Jean-Luc Canon, Javier Carrasco, Kunle Odunsi, Solmaz Sahebjam, Sylvie Rottey, Nathalie Braun, Bikash Verma, David E. Gilham, and Frédéric F. Lehmann. 2018. "Celyad's Novel CAR T-Cell Therapy for Solid Malignancies." *Current Research in Translational Medicine* 66(2):53–56. doi: 10.1016/j.retram.2018.03.001.
- Ma, Haiqing, Huanhuan Sun, and Xiaoping Sun. 2015. "Survival Improvement by Decade of Patients Aged 0–14 Years with Acute Lymphoblastic Leukemia: A SEER Analysis." *Scientific Reports* 4(1):4227. doi: 10.1038/srep04227.
- Maher, John, Renier J. Brentjens, Gertrude Gunset, Isabelle Rivière, and Michel Sadelain. 2002. "Human T-Lymphocyte Cytotoxicity and Proliferation Directed by a Single Chimeric TCR ζ /CD28 Receptor." *Nature Biotechnology* 20(1):70–75. doi: 10.1038/nbt0102-70.
- Mantovani, Alberto, Federica Marchesi, Alberto Malesci, Luigi Laghi, and Paola Allavena. 2017. "Tumour-Associated Macrophages as Treatment Targets in Oncology." *Nature Reviews Clinical Oncology* 14(7):399–416. doi: 10.1038/nrclinonc.2016.217.
- Martinez-Lage, M., R. Torres-Ruiz, P. Puig-Serra, P. Moreno-Gaona, M. C. Martin, F. J. Moya, O. Quintana-Bustamante, S. Garcia-Silva, A. M. Carcaboso, P. Petazzi, C. Bueno, J. Mora, H. Peinado, J. C. Segovia, P. Menendez, and S. Rodriguez-Perales. 2020. "In Vivo CRISPR/Cas9 Targeting of Fusion Oncogenes for Selective Elimination of Cancer Cells." *Nature Communications* 11(1):5060. doi: 10.1038/s41467-020-18875-x.
- Maruffi, Maria, Richard Sposto, Matthew J. Oberley, Lynn Kysh, and Etan Orgel. 2018. "Therapy for Children and Adults with Mixed Phenotype Acute Leukemia: A Systematic Review and Meta-Analysis." *Leukemia* 32(7):1515–28. doi: 10.1038/s41375-018-0058-4.
- Matusali, Giulia, Hyppolite Kuekou Tchidjou, Giuseppe Pontrelli, Stefania Bernardi, Gabriella D'Ettorre, Vincenzo Vullo, Anna Rita Buonomini, Massimo Andreoni, Angela Santoni, Cristina Cerboni, and Margherita Doria. 2013. "Soluble Ligands for the NKG2D Receptor Are Released during HIV-1 Infection and Impair NKG2D Expression and Cytotoxicity of NK Cells." *FASEB Journal* 27(6):2440–50. doi: 10.1096/fj.12-223057.

- Matutes, Estella, Winfried F. Pickl, Mars van't Veer, Ricardo Morilla, John Swansbury, Herbert Strobl, Andishe Attarbaschi, Georg Hopfinger, Sue Ashley, Marie Christine Bene, Anna Porwit, Alberto Orfao, Petr Lemez, Richard Schabath, and Wolf-Dieter Ludwig. 2011. "Mixed-Phenotype Acute Leukemia: Clinical and Laboratory Features and Outcome in 100 Patients Defined According to the WHO 2008 Classification." *Blood* 117(11):3163–71. doi: 10.1182/blood-2010-10-314682.
- Maude, Shannon L., Noelle Frey, Pamela A. Shaw, Richard Aplenc, David M. Barrett, Nancy J. Bunin, Anne Chew, Vanessa E. Gonzalez, Zhaohui Zheng, Simon F. Lacey, Yolanda D. Mahnke, Jan J. Melenhorst, Susan R. Rheingold, Angela Shen, David T. Teachey, Bruce L. Levine, Carl H. June, David L. Porter, and Stephan A. Grupp. 2014. "Chimeric Antigen Receptor T Cells for Sustained Remissions in Leukemia." *New England Journal of Medicine* 371(16):1507–17. doi: 10.1056/NEJMoa1407222.
- Méndez-Ferrer, Simón, Dominique Bonnet, David P. Steensma, Robert P. Hasserjian, Irene M. Ghobrial, John G. Gribben, Michael Andreeff, and Daniela S. Krause. 2020. "Bone Marrow Niches in Haematological Malignancies." *Nature Reviews Cancer* 20(5):285–98. doi: 10.1038/s41568-020-0245-2.
- Merten, Otto-Wilhelm, Matthias Hebben, and Chiara Bovolenta. 2016. "Production of Lentiviral Vectors." *Molecular Therapy - Methods & Clinical Development* 3:16017. doi: 10.1038/mtm.2016.17.
- Milan, Thomas, Hera Canaj, Chloe Villeneuve, Aditi Ghosh, Frédéric Barabé, Sonia Cellot, and Brian T. Wilhelm. 2019. "Pediatric Leukemia: Moving toward More Accurate Models." *Experimental Hematology* 74:1–12. doi: 10.1016/j.exphem.2019.05.003.
- Mistry, Jaina, Sara Chuguransky, Lowri Williams, Matloob Qureshi, Gustavo A. Salazar, Erik L. L. Sonnhammer, Silvio C. E. Tosatto, Lisanna Paladin, Shriya Raj, Lorna J. Richardson, Robert D. Finn, and Alex Bateman. 2021. "Pfam: The Protein Families Database in 2021." *Nucleic Acids Research* 49(D1):D412–19. doi: 10.1093/nar/gkaa913.
- Mitelman F, Johansson B, Mertens F. 2009. "Mitelman Database of Chromosome Aberrations in Cancer." Retrieved (<http://cgap.nci.nih.gov/Chromosomes/Mitelman>)).
- Mock, Ulrike, Lauren Nickolay, Brian Philip, Gordon Weng-Kit Cheung, Hong Zhan, Ian C. D. Johnston, Andrew D. Kaiser, Karl Peggs, Martin Pule, Adrian J. Thrasher, and Waseem Qasim. 2016. "Automated Manufacturing of Chimeric Antigen Receptor T Cells for Adoptive Immunotherapy Using CliniMACS Prodigy." *Cytotherapy* 18(8):1002–11. doi: 10.1016/j.jcyt.2016.05.009.
- Montini, Eugenio, Daniela Cesana, Manfred Schmidt, Francesca Sanvito, Cynthia C. Bartholomae, Marco Ranzani, Fabrizio Benedicenti, Lucia Sergi Sergi, Alessandro Ambrosi, Maurilio Ponzoni, Claudio Doglioni, Clelia Di Serio, Christof von Kalle, and Luigi Naldini. 2009. "The Genotoxic Potential of Retroviral Vectors Is Strongly Modulated by Vector Design and Integration Site Selection in a Mouse Model of HSC Gene Therapy." *Journal of Clinical Investigation* 119(4):964–75. doi: 10.1172/JCI37630.
- Morgan, Michael A., Hildegard Büning, Martin Sauer, and Axel Schambach. 2020. "Use of Cell and Genome Modification Technologies to Generate Improved 'Off-the-Shelf' CAR T and CAR NK Cells." *Frontiers in Immunology* 11. doi: 10.3389/fimmu.2020.01965.
- Morikawa, Masato, Rik Derynck, and Kohei Miyazono. 2016. "TGF- β and the TGF- β

- Family: Context-Dependent Roles in Cell and Tissue Physiology.” *Cold Spring Harbor Perspectives in Biology* 8(5):a021873. doi: 10.1101/cshperspect.a021873.
- Moses, Blake S., William L. Slone, Patrick Thomas, Rebecca Evans, Debbie Piktel, Peggi M. Angel, Callee M. Walsh, Pamela S. Cantrell, Stephanie L. Rellick, Karen H. Martin, James W. Simpkins, and Laura F. Gibson. 2016. “Bone Marrow Microenvironment Modulation of Acute Lymphoblastic Leukemia Phenotype.” *Experimental Hematology* 44(1):50-59.e2. doi: 10.1016/j.exphem.2015.09.003.
- Mussai, Francis Jay, Christina Yap, Christopher Mitchell, and Pamela Kearns. 2015. “Challenges of Clinical Trial Design for Targeted Agents Against Pediatric Leukemias.” *Frontiers in Oncology* 4. doi: 10.3389/fonc.2014.00374.
- Paczulla, Anna M., Kathrin Rothfelder, Simon Raffel, Martina Konantz, Julia Steinbacher, Hui Wang, Claudia Tandler, Marcelle Mbarga, Thorsten Schaefer, Mattia Falcone, Eva Nievergall, Daniela Dörfel, Pauline Hanns, Jakob R. Passweg, Christoph Lutz, Juerg Schwaller, Robert Zeiser, Bruce R. Blazar, Michael A. Caligiuri, Stephan Dirnhofer, Pontus Lundberg, Lothar Kanz, Leticia Quintanilla-Martinez, Alexander Steinle, Andreas Trumpp, Helmut R. Salih, and Claudia Lengerke. 2019. “Absence of NKG2D Ligands Defines Leukaemia Stem Cells and Mediates Their Immune Evasion.” *Nature* 572(7768):254–59. doi: 10.1038/s41586-019-1410-1.
- Pende, Daniela, Paola Rivera, Stefania Marcenaro, Chien Chung Chang, Roberto Biassoni, Romana Conte, Marek Kubin, David Cosman, Soldano Ferrone, Lorenzo Moretta, and Alessandro Moretta. 2002. “Major Histocompatibility Complex Class I-Related Chain A and UL16-Binding Protein Expression on Tumor Cell Lines of Different Histotypes: Analysis of Tumor Susceptibility to NKG2D-Dependent Natural Killer Cell Cytotoxicity.” *Cancer Research* 62(21):6178–86.
- Pérez-Martínez, Antonio, Lucía Fernández, Jaime Valentín, Isabel Martínez-Romera, María Dolores Corral, Manuel Ramírez, Lorea Abad, Sandra Santamaría, Marta González-Vicent, Sara Sirvent, Julián Sevilla, José Luis Vicario, Inmaculada de Prada, and Miguel Ángel Diaz. 2015. “A Phase I/II Trial of Interleukin-15–Stimulated Natural Killer Cell Infusion after Haplo-Identical Stem Cell Transplantation for Pediatric Refractory Solid Tumors.” *Cytotherapy* 17(11):1594–1603. doi: 10.1016/j.jcyt.2015.07.011.
- Perl, Alexander E. 2019. “Availability of FLT3 Inhibitors: How Do We Use Them?” *Blood* 134(9):741–45. doi: 10.1182/blood.2019876821.
- Pieters, R., G. J. Kaspers, E. R. van Wering, D. R. Huismans, A. H. Loonen, K. Hähnen, and A. J. Veerman. 1993. “Cellular Drug Resistance Profiles That Might Explain the Prognostic Value of Immunophenotype and Age in Childhood Acute Lymphoblastic Leukemia.” *Leukemia* 7(3):392–97.
- Pieters, Rob, Paola De Lorenzo, Philip Ancliffe, Luis Alberto Aversa, Benoit Brethon, Andrea Biondi, Myriam Campbell, Gabriele Escherich, Alina Ferster, Rebecca A. Gardner, Rishi Sury Kotecha, Birgitte Lausen, Chi Kong Li, Franco Locatelli, Andishe Attarbaschi, Christina Peters, Jeffrey E. Rubnitz, Lewis B. Silverman, Jan Stary, Tomasz Szczepanski, Ajay Vora, Martin Schrappe, and Maria Grazia Valsecchi. 2019. “Outcome of Infants Younger Than 1 Year With Acute Lymphoblastic Leukemia Treated With the Interfant-06 Protocol: Results From an International Phase III Randomized Study.” *Journal of Clinical Oncology* 37(25):2246–56. doi: 10.1200/JCO.19.00261.
- Porter, David L., Bruce L. Levine, Michael Kalos, Adam Bagg, and Carl H. June. 2011. “Chimeric Antigen Receptor–Modified T Cells in Chronic Lymphoid Leukemia.”

- New England Journal of Medicine* 365(8):725–33. doi: 10.1056/NEJMoa1103849.
- Pui, Ching-Hon, Charles G. Mullighan, William E. Evans, and Mary V. Relling. 2012. “Pediatric Acute Lymphoblastic Leukemia: Where Are We Going and How Do We Get There?” *Blood* 120(6):1165–74. doi: 10.1182/blood-2012-05-378943.
- Raulet, David H. 2003. “Roles of the NKG2D Immunoreceptor and Its Ligands.” *Nature Reviews Immunology* 3(10):781–90. doi: 10.1038/nri1199.
- Raulet, David H., Stephan Gasser, Benjamin G. Gowen, Weiwen Deng, and Heiyoun Jung. 2013. “Regulation of Ligands for the NKG2D Activating Receptor.” *Annual Review of Immunology* 31(1):413–41. doi: 10.1146/annurev-immunol-032712-095951.
- Rivière, Isabelle, and Michel Sadelain. 2017. “Chimeric Antigen Receptors: A Cell and Gene Therapy Perspective.” *Molecular Therapy* 25(5):1117–24. doi: 10.1016/j.ymthe.2017.03.034.
- Robak, Tadeusz. 2003. “Purine Nucleoside Analogues in the Treatment of Myeloid Leukemias.” *Leukemia & Lymphoma* 44(3):391–409. doi: 10.1080/1042819021000035608.
- Robinson, M. D., D. J. McCarthy, and G. K. Smyth. 2010. “EdgeR: A Bioconductor Package for Differential Expression Analysis of Digital Gene Expression Data.” *Bioinformatics* 26(1):139–40. doi: 10.1093/bioinformatics/btp616.
- Robinson, Mark D., and Alicia Oshlack. 2010. “A Scaling Normalization Method for Differential Expression Analysis of RNA-Seq Data.” *Genome Biology* 11(3):R25. doi: 10.1186/gb-2010-11-3-r25.
- Rodriguez-Garcia, Alba, Asis Palazon, Estela Noguera-Ortega, Daniel J. Powell, and Sonia Guedan. 2020. “CAR-T Cells Hit the Tumor Microenvironment: Strategies to Overcome Tumor Escape.” *Frontiers in Immunology* 11. doi: 10.3389/fimmu.2020.01109.
- Rodríguez-Rodero, Sandra, Segundo González, Luis Rodrigo, Juan L. Fernández-Morera, Jesús Martínez-Borra, Antonio López-Vázquez, and Carlos López-Larrea. 2007. “Transcriptional Regulation of MICA and MICB: A Novel Polymorphism in MICB Promoter Alters Transcriptional Regulation by Sp1.” *European Journal of Immunology* 37(7):1938–53. doi: 10.1002/eji.200737031.
- Romphruk, Amornrat V., Arunrat Romphruk, Taeko K. Naruse, Sarayot Raroengjai, Chintana Puapairoj, Hidetoshi Inoko, and Chanvit Leelayuwat. 2009. “Polymorphisms of NKG2D Ligands: Diverse RAET1/ULBP Genes in Northeastern Thais.” *Immunogenetics* 61(9):611–17. doi: 10.1007/s00251-009-0394-7.
- Ruella, Marco, David M. Barrett, Saad S. Kenderian, Olga Shestova, Ted J. Hofmann, Jessica Perazzelli, Michael Klichinsky, Vania Aikawa, Farzana Nazimuddin, Mirosław Kozłowski, John Scholler, Simon F. Lacey, Jan J. Melenhorst, Jennifer J. D. Morrisette, David A. Christian, Christopher A. Hunter, Michael Kalos, David L. Porter, Carl H. June, Stephan A. Grupp, and Saar Gill. 2016. “Dual CD19 and CD123 Targeting Prevents Antigen-Loss Relapses after CD19-Directed Immunotherapies.” *Journal of Clinical Investigation* 126(10):3814–26. doi: 10.1172/JCI87366.
- Ruella, Marco, and Marcela V. Maus. 2016. “Catch Me If You Can: Leukemia Escape after CD19-Directed T Cell Immunotherapies.” *Computational and Structural Biotechnology Journal* 14:357–62. doi: 10.1016/j.csbj.2016.09.003.
- Sadelain, Michel. 2015. “CAR Therapy: The CD19 Paradigm.” *Journal of Clinical*

- Investigation* 125(9):3392–3400. doi: 10.1172/JCI80010.
- Sadelain, Michel, Renier Brentjens, and Isabelle Rivière. 2009. “The Promise and Potential Pitfalls of Chimeric Antigen Receptors.” *Current Opinion in Immunology* 21(2):215–23. doi: 10.1016/j.coi.2009.02.009.
- Sadelain, Michel, Renier Brentjens, and Isabelle Rivière. 2013. “The Basic Principles of Chimeric Antigen Receptor Design.” *Cancer Discovery* 3(4):388–98. doi: 10.1158/2159-8290.CD-12-0548.
- Sáez-Borderías, Andrea, Mónica Gumá, Ana Angulo, Beatriz Bellosillo, Daniela Pende, and Miguel López-Botet. 2006. “Expression and Function of NKG2D in CD4+ T Cells Specific for Human Cytomegalovirus.” *European Journal of Immunology* 36(12):3198–3206. doi: 10.1002/eji.200636682.
- Salih, Helmut R., Hans-Georg Rammensee, and Alexander Steinle. 2002. “Cutting Edge: Down-Regulation of MICA on Human Tumors by Proteolytic Shedding.” *The Journal of Immunology* 169(8):4098–4102. doi: 10.4049/jimmunol.169.8.4098.
- Salih, Helmut Rainer, Holger Antropius, Friederike Gieseke, Stefan Zoltan Lutz, Lothar Kanz, Hans Georg Rammensee, and Alexander Steinle. 2003. “Functional Expression and Release of Ligands for the Activating Immunoreceptor NKG2D in Leukemia.” *Blood* 102(4):1389–96. doi: 10.1182/blood-2003-01-0019.
- Sallman, David A., Elizabeth M. Sagatys, Jason Brayer, Caroline Loney, Sophie Agaugué, Eytan Breman, Bikash Verma, David E. Gilham, Frédéric F. Lehmann, and Marco L. Davila. 2018. “NKG2D-Based Chimeric Antigen Receptor Therapy Induced Remission in a Relapsed/Refractory Acute Myeloid Leukemia Patient.” *Haematologica* 103(Panel C):424–26.
- Sánchez-Martínez, Diego, Matteo L. Baroni, Francisco Gutierrez-Agüera, Heleia Roca-Ho, Oscar Blanch-Lombarte, Sara González-García, Montserrat Torrealba, Jordi Junca, Manuel Ramírez-Orellana, Talía Velasco-Hernández, Clara Bueno, José Luís Fuster, Julia G. Prado, Julien Calvo, Benjamin Uzan, Jan Cools, Mireia Camos, Françoise Pflumio, María Luisa Toribio, and Pablo Menéndez. 2019. “Fratricide-Resistant CD1a-Specific CAR T Cells for the Treatment of Cortical T-Cell Acute Lymphoblastic Leukemia.” *Blood* 133(21):2291–2304. doi: 10.1182/blood-2018-10-882944.
- Schlegel, Patrick, Kerstin Dittthard, Peter Lang, Markus Mezger, Rupert Handgretinger, and Matthias Pfeiffer. 2015. “NKG2D Signaling Leads to NK Cell Mediated Lysis of Childhood AML.” *N/A* 2015(June). doi: 10.1155/2015/473175.
- Schmittgen, Thomas D., and Kenneth J. Livak. 2008. “Analyzing Real-Time PCR Data by the Comparative CT Method.” *Nature Protocols* 3(6):1101–8. doi: 10.1038/nprot.2008.73.
- Seliger, Barbara, Ulrike Ritz, and Ferrone Soldano. 2006. “Molecular Mechanisms of HLA Class I Antigen Abnormalities Following Viral Infection and Transformation.” *International Journal of Cancer* 118(1):129–38. doi: 10.1002/ijc.21312.
- Sentman, Charles L., and Kenneth R. Meehan. 2014. “NKG2D CARs as Cell Therapy for Cancer.” *The Cancer Journal* 20(2):156–59. doi: 10.1097/PPO.0000000000000029.
- Smith, F. O., B. C. Lampkin, C. Versteeg, D. A. Flowers, P. A. Dinndorf, J. D. Buckley, W. G. Woods, G. D. Hammond, and I. D. Bernstein. 1992. “Expression of Lymphoid-Associated Cell Surface Antigens by Childhood Acute Myeloid Leukemia Cells Lacks Prognostic Significance.” *Blood* 79(9):2415–22.

- Smith, Malcolm A., Sean F. Altekruse, Peter C. Adamson, Gregory H. Reaman, and Nita L. Seibel. 2014. "Declining Childhood and Adolescent Cancer Mortality." *Cancer* 120(16):2497–2506. doi: 10.1002/cncr.28748.
- Soldin, Offie P., Hala Nsouli-Maktabi, Hala Nsouly-Maktabi, Jeanine M. Genkinger, Christopher A. Loffredo, Juan Antonio Ortega-Garcia, Drew Colantino, Dana B. Barr, Naomi L. Luban, Aziza T. Shad, and David Nelson. 2009. "Pediatric Acute Lymphoblastic Leukemia and Exposure to Pesticides." *Therapeutic Drug Monitoring* 31(4):495–501. doi: 10.1097/FTD.0b013e3181aae982.
- Sommermeier, D., M. Hudecek, P. L. Kosasih, T. Gogishvili, D. G. Maloney, C. J. Turtle, and S. R. Riddell. 2016. "Chimeric Antigen Receptor-Modified T Cells Derived from Defined CD8+ and CD4+ Subsets Confer Superior Antitumor Reactivity in Vivo." *Leukemia* 30(2):492–500. doi: 10.1038/leu.2015.247.
- Song, De-Gang, Qunrui Ye, Stephen Santoro, Chongyun Fang, Andrew Best, and Daniel J. Powell. 2013. "Chimeric NKG2D CAR-Expressing T Cell-Mediated Attack of Human Ovarian Cancer Is Enhanced by Histone Deacetylase Inhibition." *Human Gene Therapy* 24(3):295–305. doi: 10.1089/hum.2012.143.
- Sotillo, Elena, David M. Barrett, Kathryn L. Black, Asen Bagashev, Derek Oldridge, Glendon Wu, Robyn Sussman, Claudia Lanauze, Marco Ruella, Matthew R. Gazzara, Nicole M. Martinez, Colleen T. Harrington, Elaine Y. Chung, Jessica Perazzelli, Ted J. Hofmann, Shannon L. Maude, Pichai Raman, Alejandro Barrera, Saar Gill, Simon F. Lacey, Jan J. Melenhorst, David Allman, Elad Jacoby, Terry Fry, Crystal Mackall, Yoseph Barash, Kristen W. Lynch, John M. Maris, Stephan A. Grupp, and Andrei Thomas-Tikhonenko. 2015. "Convergence of Acquired Mutations and Alternative Splicing of *CD19* Enables Resistance to CART-19 Immunotherapy." *Cancer Discovery* 5(12):1282–95. doi: 10.1158/2159-8290.CD-15-1020.
- Spear, Paul, Amorette Barber, Agnieszka Rynda-Apelle, and Charles L. Sentman. 2013. "NKG2D CAR T-cell Therapy Inhibits the Growth of NKG2D Ligand Heterogeneous Tumors." *Immunology & Cell Biology* 91(6):435–40. doi: 10.1038/icb.2013.17.
- Spear, Paul, Ming-Ru Wu, Marie-Louise Sentman, and Charles L. Sentman. 2013. "NKG2D Ligands as Therapeutic Targets." *Cancer Immunity* 13:8.
- van der Stegen, Sjoukje J. C., Mohamad Hamieh, and Michel Sadelain. 2015. "The Pharmacology of Second-Generation Chimeric Antigen Receptors." *Nature Reviews Drug Discovery* 14(7):499–509. doi: 10.1038/nrd4597.
- Stephens, Henry A. F. 2001. "MICA and MICB Genes: Can the Enigma of Their Polymorphism Be Resolved?" *Trends in Immunology* 22(7):378–85. doi: 10.1016/S1471-4906(01)01960-3.
- Stern-Ginossar, Noam, Chamutal Gur, Moshe Biton, Elad Horwitz, Moran Elboim, Noa Stanietsky, Michal Mandelboim, and Ofer Mandelboim. 2008. "Human MicroRNAs Regulate Stress-Induced Immune Responses Mediated by the Receptor NKG2D." *Nature Immunology* 9(9):1065–73. doi: 10.1038/ni.1642.
- Swerdlow SH, Campo E, Harris NL, Jaffe ES, Pileri SA, Stein H, Thiele J. 2017. *WHO Classification of Tumours of Haematopoietic and Lymphoid Tissues*. 4th. Inter.
- Tamma, Syam, Xin Huang, Marianna Wong, Michael C. Milone, Linan Ma, Bruce L. Levine, Carl H. June, John E. Wagner, Bruce R. Blazar, and Xianzheng Zhou. 2010. "4-1BB and CD28 Signaling Plays a Synergistic Role in Redirecting Umbilical Cord Blood T Cells Against B-Cell Malignancies." *Human Gene Therapy*

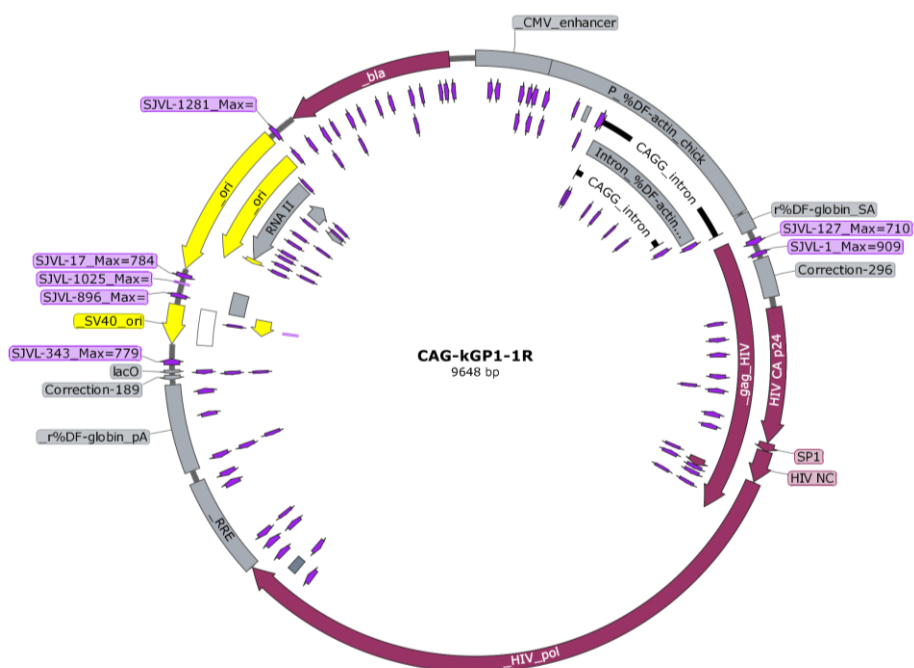
- 21(1):75–86. doi: 10.1089/hum.2009.122.
- Tarlock, Katherine, and Soheil Meshinchi. 2015. “Pediatric Acute Myeloid Leukemia.” *Pediatric Clinics of North America* 62(1):75–93. doi: 10.1016/j.pcl.2014.09.007.
- Tasian, Sarah K., and Stephen P. Hunger. 2017. “Genomic Characterization of Paediatric Acute Lymphoblastic Leukaemia: An Opportunity for Precision Medicine Therapeutics.” *British Journal of Haematology* 176(6):867–82. doi: 10.1111/bjh.14474.
- Teachey, David T., and Stephen P. Hunger. 2013. “Predicting Relapse Risk in Childhood Acute Lymphoblastic Leukaemia.” *British Journal of Haematology* 162(5):606–20. doi: 10.1111/bjh.12442.
- Teachey, David T., and Ching-Hon Pui. 2019. “Comparative Features and Outcomes between Paediatric T-Cell and B-Cell Acute Lymphoblastic Leukaemia.” *The Lancet Oncology* 20(3):e142–54. doi: 10.1016/S1470-2045(19)30031-2.
- Thomas, Dori A., and Joan Massagué. 2005. “TGF- β Directly Targets Cytotoxic T Cell Functions during Tumor Evasion of Immune Surveillance.” *Cancer Cell* 8(5):369–80. doi: 10.1016/j.ccr.2005.10.012.
- Till, Brian G., Michael C. Jensen, Jinjuan Wang, Xiaojun Qian, Ajay K. Gopal, David G. Maloney, Catherine G. Lindgren, Yukang Lin, John M. Pagel, Lihua E. Budde, Andrew Raubitschek, Stephen J. Forman, Philip D. Greenberg, Stanley R. Riddell, and Oliver W. Press. 2012. “CD20-Specific Adoptive Immunotherapy for Lymphoma Using a Chimeric Antigen Receptor with Both CD28 and 4-1BB Domains: Pilot Clinical Trial Results.” *Blood* 119(17):3940–50. doi: 10.1182/blood-2011-10-387969.
- Togashi, Yosuke, Kohei Shitara, and Hiroyoshi Nishikawa. 2019. “Regulatory T Cells in Cancer Immunosuppression — Implications for Anticancer Therapy.” *Nature Reviews Clinical Oncology* 16(6):356–71. doi: 10.1038/s41571-019-0175-7.
- Topp, Max S., Peter Kufer, Nicola Gökbuget, Mariele Goebeler, Matthias Klinger, Svenja Neumann, Heinz-A. Horst, Thorsten Raff, Andreas Viardot, Mathias Schmid, Matthias Stelljes, Markus Schaich, Evelyn Degenhard, Rudolf Köhne-Volland, Monika Brüggemann, Oliver Ottmann, Heike Pfeifer, Thomas Burmeister, Dirk Nagorsen, Margit Schmidt, Ralf Lutterbuese, Carsten Reinhardt, Patrick A. Baeuerle, Michael Kneba, Hermann Einsele, Gert Riethmüller, Dieter Hoelzer, Gerhard Zugmaier, and Ralf C. Bargou. 2011. “Targeted Therapy With the T-Cell–Engaging Antibody Blinatumomab of Chemotherapy-Refractory Minimal Residual Disease in B-Lineage Acute Lymphoblastic Leukemia Patients Results in High Response Rate and Prolonged Leukemia-Free Survival.” *Journal of Clinical Oncology* 29(18):2493–98. doi: 10.1200/JCO.2010.32.7270.
- Torelli, Giovanni F., Nadia Peragine, Sara Raponi, Daria Pagliara, Maria S. De Propriis, Antonella Vitale, Alice Bertaina, Walter Barberi, Lorenzo Moretta, Giuseppe Basso, Angela Santoni, Anna Guarini, Franco Locatelli, and Robin Foà. 2014. “Recognition of Adult and Pediatric Acute Lymphoblastic Leukemia Blasts by Natural Killer Cells.” *Haematologica* 99(7):1248–54. doi: 10.3324/haematol.2013.101931.
- Tumaini, Barbara, Daniel W. Lee, Tasha Lin, Luciano Castiello, David F. Stroncek, Crystal Mackall, Alan Wayne, and Marianna Sabatino. 2013. “Simplified Process for the Production of Anti-CD19-CAR–Engineered T Cells.” *Cytotherapy* 15(11):1406–15. doi: 10.1016/j.jcyt.2013.06.003.
- Turtle, Cameron J., Laïla-Aïcha Hanafi, Carolina Berger, Michael Hudecek, Barbara

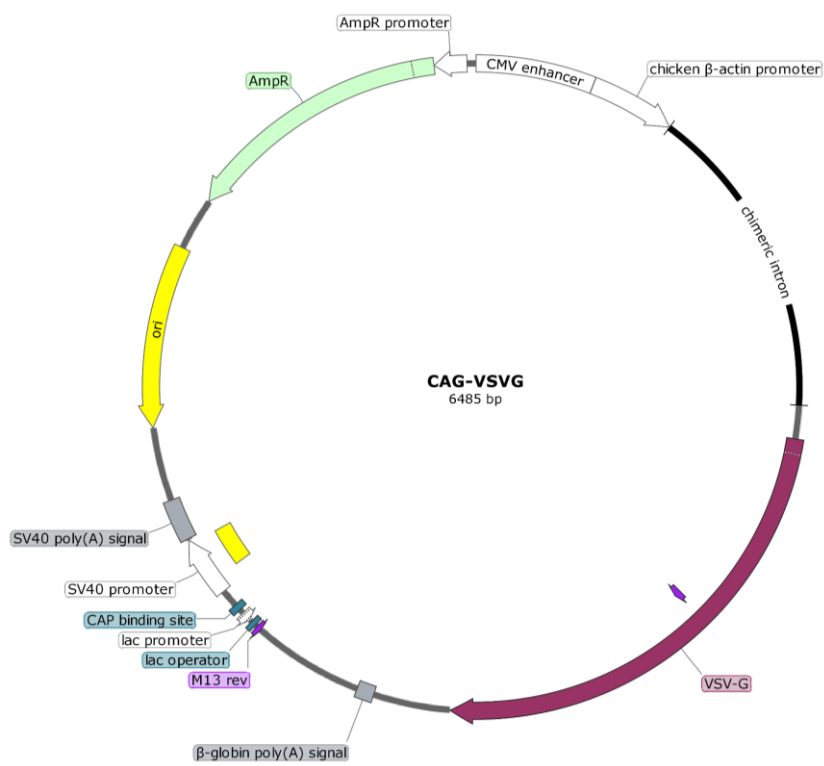
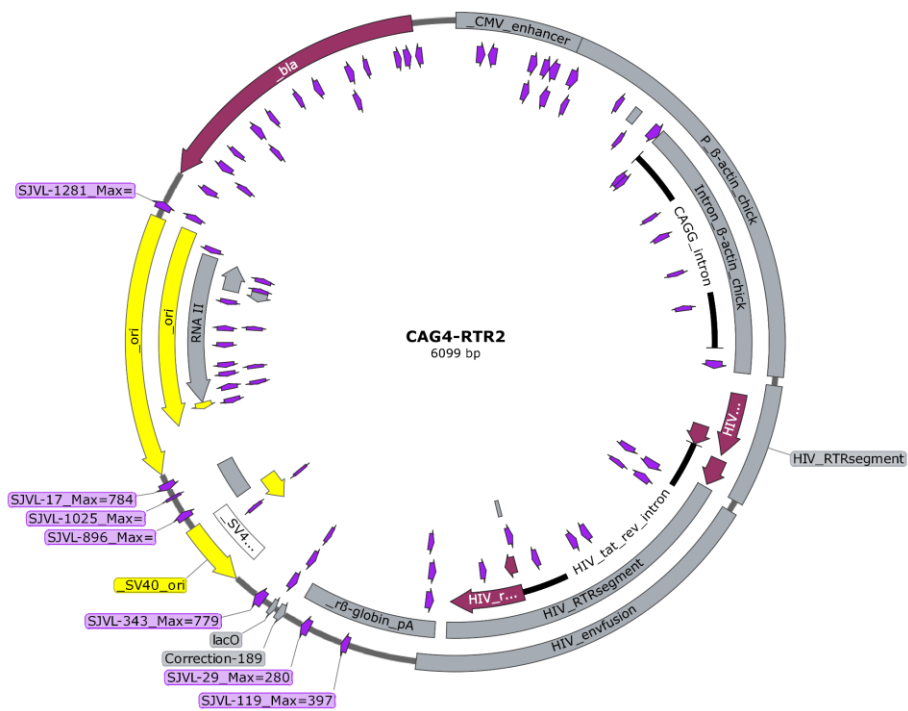
- Pender, Emily Robinson, Reed Hawkins, Colette Chaney, Sindhu Cherian, Xueyan Chen, Lorinda Soma, Brent Wood, Daniel Li, Shelly Heimfeld, Stanley R. Riddell, and David G. Maloney. 2016. "Immunotherapy of Non-Hodgkin's Lymphoma with a Defined Ratio of CD8 + and CD4 + CD19-Specific Chimeric Antigen Receptor-Modified T Cells." *Science Translational Medicine* 8(355). doi: 10.1126/scitranslmed.aaf8621.
- U.S. Food and Drug Administration. 2017a. "FDA Approval Brings First Gene Therapy to the United States." *FDA NEWS RELEASE*. Retrieved January 11, 2022 (<https://www.fda.gov/news-events/press-announcements/fda-approval-brings-first-gene-therapy-united-states>).
- U.S. Food and Drug Administration. 2017b. "FDA Approves CAR-T Cell Therapy to Treat Adults with Certain Types of Large B-Cell Lymphoma." *FDA NEWS RELEASE*. Retrieved (<https://www.fda.gov/news-events/press-announcements/fda-approves-car-t-cell-therapy-treat-adults-certain-types-large-b-cell-lymphoma>).
- U.S. Food and Drug Administration. 2021. "FDA Approves First Cell-Based Gene Therapy for Adult Patients with Multiple Myeloma." *FDA NEWS RELEASE*. Retrieved January 11, 2022 (<https://www.fda.gov/news-events/press-announcements/fda-approves-first-cell-based-gene-therapy-adult-patients-multiple-myeloma>).
- Upshaw, Jadee L., Laura N. Arneson, Renee A. Schoon, Christopher J. Dick, Daniel D. Billadeau, and Paul J. Leibson. 2006. "NKG2D-Mediated Signaling Requires a DAP10-Bound Grb2-Vav1 Intermediate and Phosphatidylinositol-3-Kinase in Human Natural Killer Cells." *Nature Immunology* 7(5):524–32. doi: 10.1038/ni1325.
- Wakeford, R. 2008. "Childhood Leukaemia Following Medical Diagnostic Exposure to Ionizing Radiation in Utero or after Birth." *Radiation Protection Dosimetry* 132(2):166–74. doi: 10.1093/rpd/ncn272.
- Wang, Jinjuan, Michael Jensen, Yukang Lin, Xingwei Sui, Eric Chen, Catherine G. Lindgren, Brian Till, Andrew Raubitschek, Stephen J. Forman, Xiaojun Qian, Scott James, Philip Greenberg, Stanley Riddell, and Oliver W. Press. 2007. "Optimizing Adoptive Polyclonal T Cell Immunotherapy of Lymphomas, Using a Chimeric T Cell Receptor Possessing CD28 and CD137 Costimulatory Domains." *Human Gene Therapy* 18(8):712–25. doi: 10.1089/hum.2007.028.
- Wayne, Alan S., Gregory H. Reaman, and Lee J. Helman. 2008. "Progress in the Curative Treatment of Childhood Hematologic Malignancies." *JNCI: Journal of the National Cancer Institute* 100(18):1271–73. doi: 10.1093/jnci/djn306.
- Weng, Andrew P., Adolfo A. Ferrando, Woojoong Lee, John P. Morris, Lewis B. Silverman, Cheryll Sanchez-Irizarry, Stephen C. Blacklow, A. Thomas Look, and Jon C. Aster. 2004. "Activating Mutations of *NOTCH1* in Human T Cell Acute Lymphoblastic Leukemia." *Science* 306(5694):269–71. doi: 10.1126/science.1102160.
- Wensveen, Felix M., Vedrana Jelenčić, and Bojan Polić. 2018. "NKG2D: A Master Regulator of Immune Cell Responsiveness." *Frontiers in Immunology* 9. doi: 10.3389/fimmu.2018.00441.
- Whitehead, Todd P., Catherine Metayer, Joseph L. Wiemels, Amanda W. Singer, and Mark D. Miller. 2016. "Childhood Leukemia and Primary Prevention." *Current Problems in Pediatric and Adolescent Health Care* 46(10):317–52. doi: 10.1016/j.cppeds.2016.08.004.

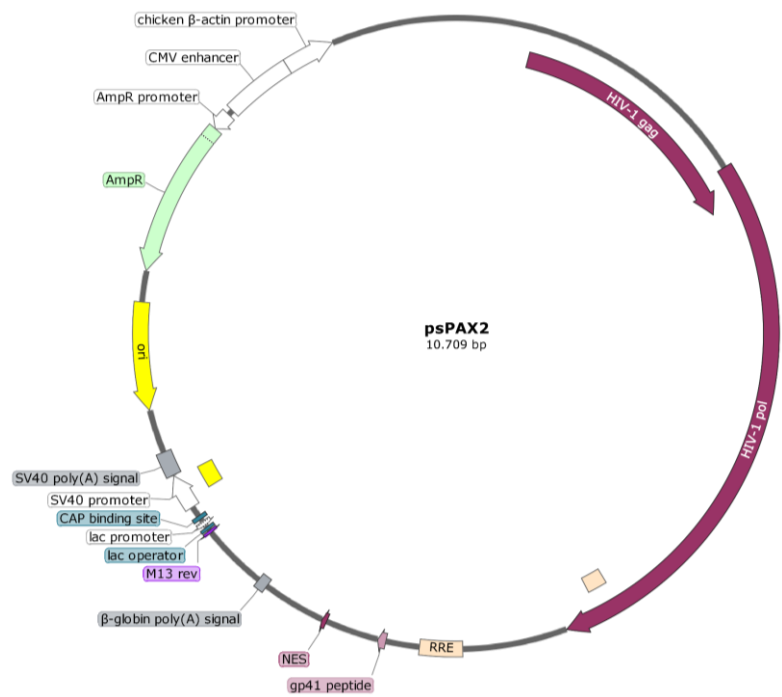
- Wu, Jun, Yaoli Song, Alexander B. H. Bakker, Stefan Bauer, Thomas Spies, Lewis L. Lanier, and Joseph H. Phillips. 1999. "An Activating Immunoreceptor Complex Formed by NKG2D and DAP10." *Science* 285(5428):730–32. doi: 10.1126/science.285.5428.730.
- Yabe, Toshio, Cynthia McSherry, Fritz H. Bach, Paul Fisch, Rebecca P. Schall, Paul M. Sondel, and Jeffrey P. Houchins. 1993. "A Multigene Family on Human Chromosome 12 Encodes Natural Killer-Cell Lectins." *Immunogenetics* 37(6). doi: 10.1007/BF00222470.
- Yang, Yinmeng, M. Eric Kohler, Christopher D. Chien, Christopher T. Sauter, Elad Jacoby, Chunhua Yan, Ying Hu, Kelsey Wanhainen, Haiying Qin, and Terry J. Fry. 2017. "TCR Engagement Negatively Affects CD8 but Not CD4 CAR T Cell Expansion and Leukemic Clearance." *Science Translational Medicine* 9(417). doi: 10.1126/scitranslmed.aag1209.
- Young, Andrew L., Grant A. Challen, Brenda M. Birman, and Todd E. Druley. 2016. "Clonal Haematopoiesis Harbours AML-Associated Mutations Is Ubiquitous in Healthy Adults." *Nature Communications* 7(1):12484. doi: 10.1038/ncomms12484.
- Zah, Eugenia, Meng-Yin Lin, Anne Silva-Benedict, Michael C. Jensen, and Yvonne Y. Chen. 2016. "T Cells Expressing CD19/CD20 Bispecific Chimeric Antigen Receptors Prevent Antigen Escape by Malignant B Cells." *Cancer Immunology Research* 4(6):498–508. doi: 10.1158/2326-6066.CIR-15-0231.
- Zanetti, Samanta Romina, Paola Alejandra Romecin, Meritxell Vinyoles, Manel Juan, José Luis Fuster, Mireia Cámos, Sergi Querol, Mario Delgado, and Pablo Menendez. 2020. "Bone Marrow MSC from Pediatric Patients with B-ALL Highly Immunosuppress T-Cell Responses but Do Not Compromise CD19-CAR T-Cell Activity." *Journal for ImmunoTherapy of Cancer* 8(2):e001419. doi: 10.1136/jitc-2020-001419.
- Zhang, Cai, Jianhua Zhang, Jiafeng Niu, Zhixia Zhou, Jian Zhang, and Zhigang Tian. 2008. "Interleukin-12 Improves Cytotoxicity of Natural Killer Cells via Upregulated Expression of NKG2D." *Human Immunology* 69(8):490–500. doi: 10.1016/j.humimm.2008.06.004.
- Zhang, Hao, Pu Zhao, and He Huang. 2020. "Engineering Better Chimeric Antigen Receptor T Cells." *Experimental Hematology & Oncology* 9(1):34. doi: 10.1186/s40164-020-00190-2.
- Zhang, Jinyu, Fahmin Basher, and Jennifer D. Wu. 2015. "NKG2D Ligands in Tumor Immunity: Two Sides of a Coin." *Frontiers in Immunology* 6. doi: 10.3389/fimmu.2015.00097.
- Zhang, Qiong-wen, Lei Liu, Chang-yang Gong, Hua-shan Shi, Yun-hui Zeng, Xiao-ze Wang, Yu-wei Zhao, and Yu-quan Wei. 2012. "Prognostic Significance of Tumor-Associated Macrophages in Solid Tumor: A Meta-Analysis of the Literature." *PLoS ONE* 7(12):e50946. doi: 10.1371/journal.pone.0050946.
- Zhang, Shuo, Xuelei Ma, Chenjing Zhu, Li Liu, Guoping Wang, and Xia Yuan. 2016. "The Role of Myeloid-Derived Suppressor Cells in Patients with Solid Tumors: A Meta-Analysis." *PLOS ONE* 11(10):e0164514. doi: 10.1371/journal.pone.0164514.
- Zhang, Tong, Amorette Barber, and Charles L. Sentman. 2006. "Generation of Antitumor Responses by Genetic Modification of Primary Human T Cells with a Chimeric NKG2D Receptor." *Cancer Research* 66(11):5927–33. doi: 10.1158/0008-5472.CAN-06-0130.

- Zhang, Tong, Bethany A. Lemoi, and Charles L. Sentman. 2005. "Chimeric NK-Receptor-Bearing T Cells Mediate Antitumor Immunotherapy." *Blood* 106(5):1544–51. doi: 10.1182/blood-2004-11-4365.
- Zhang, Tong, and Charles L. Sentman. 2013. "Mouse Tumor Vasculature Expresses NKG2D Ligands and Can Be Targeted by Chimeric NKG2D-Modified T Cells." *The Journal of Immunology* 190(5):2455–63. doi: 10.4049/jimmunol.1201314.
- Zhang, Wei, Kimberly R. Jordan, Brian Schulte, and Enkhtsetseg Purev. 2018. "Characterization of Clinical Grade CD19 Chimeric Antigen Receptor T Cells Produced Using Automated CliniMACS Prodigy System." *Drug Design, Development and Therapy* Volume 12:3343–56. doi: 10.2147/DDDT.S175113.
- Zheng, Hong, Catherine Matte-Martone, Hongmei Li, Britt E. Anderson, Srividhya Venketesan, Hung Sheng Tan, Dhanpat Jain, Jennifer McNiff, and Warren D. Shlomchik. 2008. "Effector Memory CD4+ T Cells Mediate Graft-versus-Leukemia without Inducing Graft-versus-Host Disease." *Blood* 111(4):2476–84. doi: 10.1182/blood-2007-08-109678.
- Zhong, Xiao-Song, Maiko Matsushita, Jason Plotkin, Isabelle Riviere, and Michel Sadelain. 2010. "Chimeric Antigen Receptors Combining 4-1BB and CD28 Signaling Domains Augment PI3kinase/AKT/Bcl-XL Activation and CD8+ T Cell-Mediated Tumor Eradication." *Molecular Therapy* 18(2):413–20. doi: 10.1038/mt.2009.210.
- Zhou, Sheng, John D. Schuetz, Kevin D. Bunting, Anne-Marie Colapietro, Janardhan Sampath, John J. Morris, Irina Lagutina, Gerard C. Grosveld, Mitsujiro Osawa, Hiromitsu Nakauchi, and Brian P. Sorrentino. 2001. "The ABC Transporter Bcrp1/ABCG2 Is Expressed in a Wide Variety of Stem Cells and Is a Molecular Determinant of the Side-Population Phenotype." *Nature Medicine* 7(9):1028–34. doi: 10.1038/nm0901-1028.
- Zingoni, Alessandra, Rosa Molfetta, Cinzia Fionda, Alessandra Soriani, Rossella Paolini, Marco Cippitelli, Cristina Cerboni, and Angela Santoni. 2018. "NKG2D and Its Ligands: 'One for All, All for One.'" *Frontiers in Immunology* 9. doi: 10.3389/fimmu.2018.00476.

10. ANNEXES







10.2. Table showing characteristics of B-ALL pediatric patients.

PATIENT	AGE AT Dx	STAGE	MICA	MICB	ULBP1	ULBP2	ULBP3	ULBP4	% BLASTS Dx	% BLASTS R	CYTOGENETIC Dx	CYTOGENETIC R	MRD +78	HSCT	OTHER THERAPIES	TREATMENTS COMPLICATIONS	RELAPSE	TREATMENT OF R	EXITUS CAUSE	ACTUAL STATE
#1	7	R	20.27	NA	9.91	3.05	5.81	9.33	95	Extramedullary	NA	NA	0	Yes	No	STOP induction phase due to fungal infection from day +29 for 64 days	Yes	Relapses therapeutic recommendations guide ALL-SHOP-2015	GvHD	Exitus
								4.43	NA	NA	NA	Yes	NA	NA	Yes	NA	NA			
#3	12	Dx	11.82	NA	8.02	9.13	8.72	6.51	87	-	Normal karyotype	-	16.8	Yes	Rescue cycle cladribine, VP, CF	Refractory disease	No	No	Disease progression	Exitus
		R	11.16	NA	7.30	8.06	7.54	8.42												
#4	7	Dx	10.78	NA	6.03	6.50	6.81	5.23	79	NA	NA	Transfer to another centre	Transfer to another centre	Transfer to another centre	Transfer to another centre	Transfer to another centre	Transfer to another centre	Transfer to another centre	Transfer to another centre	Transfer to another centre
#5	5	Dx	7.21	NA	3.91	3.50	5.02	3.54	65	NA	Normal karyotype	46,XY[20]	0	No	No	No	Yes	Guide SHOP-PETHMA 2015 + RT	-	Alive
#6	8	Dx	4.82	NA	3.75	3.05	3.92	2.79	97	-	NA	-	0	Yes	No	septic shock	No	No	Alive	
		F	9.53	NA	7.42	4.48	5.37	7.41												
#7	2	Dx	7.93	NA	5.89	5.22	6.20	5.55	92	-	Normal karyotype	-	0	No	NA	NA	No	NA	NA	NA
		F	7.94	NA	5.89	5.24	6.21	5.67												
#8	0	F	43.79	NA	16.08	8.78	13.99	13.32	NA	-	NA	-	NA	No	NA	NA	No	NA	NA	NA
		R	14.31	5.77	7.36	4.93	6.09	8.10												
#9	13	R	12.63	6.02	5.36	4.04	3.99	6.93	7	NA	Normal karyotype	NA	NA	No	NA	NA	Yes	CART 19	Infection	Exitus
		R	10.45	4.85	7.98	4.60	5.55	7.34												
#10	9	R	15.12	NA	6.81	6.48	10.13	6.96	57	59	NA	46,XX[6], 47,XX+5[14]	0	No	No	Blindness	Yes	ALL-SHOP 2008 + HSCT + NKALs	Septic shock	Exitus
		R	9.81	6.30	5.22	4.26	3.70	5.90												
#11	2	F	18.58	NA	8.84	6.37	5.99	7.86	85	-	Normal karyotype	-	0	No	NA	NA	No	NA	NA	NA
		F	11.15	NA	5.32	5.53	4.44	7.78												
#12	13	Dx	18.78	NA	12.80	14.19	0.00	12.09	83	-	Homozygous deletion.	-	0	No	No	Prapism hip osteonecrosis, steroid hyperglycaemia	No	No	Alive	
		Dx	5.56	NA	3.07	2.75	1.57	4.29												
#13	5	R	17.62	NA	4.73	5.11	3.73	9.31	NA	95	Abnormal clone with a 5q- , a 9p+ and a 9p-. The 5q deletion does not affect the critical region 5q31, so it is different from that specific to MDS-AVL.	46, XX	NA	No	No	No	Yes	ALL-SHOP-2008	Acute respiratory failure	Exitus
		F	16.62	NA	6.88	5.34	6.94	12.16												
#14	3	Dx	13.47	NA	5.32	3.54	3.71	3.88	90	NA	Normal karyotype	NA	0.00001	No	NA	NA	Yes	GJJA SHOP-PETHMA 2015	Infection	Exitus
#15	4	Dx	19.91	NA	9.25	6.81	6.91	8.88	64	-	59- 61,XXY,+4,+5del(6)(q?),+8,+8,+12,+14,+14,+16,+17,+21,+21,-msf[16]/46XY[4]	-	0.0001	No	No	NA	No	-	Alive	

PATIENT	AGE AT Dx	STAGE	MICA	MICB	ULBP1	ULBP2	ULBP3	ULBP4	%BLASTS Dx	% BLASTS R	CYTOGENETIC Dx	CYTOGENETIC R	MRD +78	HSCT	OTHER THERAPIES	TREATMENTS COMPLICATIONS	RELAPSE	TREATMENT OF R	EXITUS		ACTUAL STATE
																			CAUSE	DATE	
#16	4	Dx	47,11	NA	7,11	3,44	2,52	14,41	96	-	Normal karyotype	-	0,00001	No	NA	NA	No	NA	NA	NA	
#17	13	Dx	14,66	NA	12,56	3,48	6,04	5,12	55	-	46,XX,tv(3)(p21q27),der(5)t(5;5)(p15;q15)[25], E2A-PBX1 rearrangement t(1;19)	-	Protocol change AML-2015	Yes	2 treatment strategies (ALL/AML)	Progression during induction phase, secondary graft failure (HLH), 2nd graft, necrotizing fasciitis, multi-organ failure	No	No	Multigraft failure	Exitus	
#18	6	Dx	36,31	NA	12,50	4,21	7,08	16,28	87	-	Karyotype altered, t(9;11)(p21;p11), t(1;19)(p13;p11), t(1;19)(p13;p11)	46, XX, t(7)(q10),t(7;9)(p21;q21),der(19)t(1;19)(q23;p13)[19]/46,XX[2]	0	No	No	Post-HSCT relapse --> CAR-T (clinical trial) --> extramedullary relapse.	No	Yes	ALL-SEHOP-PETHEMA 2015 for relapses + HSCT	Progression	Exitus
#19	5	R	14,30	6,35	8,41	4,60	7,55	7,36	NA	93	E2A-PBX1 rearrangement, t(1;19) translocation	NA	NA	No	-	No	Yes	ALL-SEHOP-PETHEMA 2015 for relapses + HSCT	-	Exitus	
#20	3	Dx	10,74	4,84	5,19	3,63	4,93	7,52	16	-	Normal karyotype	No	0	No	No	Catheter-associated thrombosis	No	No	-	Alive	
#21	5	Dx	12,12	4,00	3,46	2,48	4,41	3,57	98	-	ETV6-RUNX1(TEL-AML1) rearrangement, t(12;21)	-	0	No	No	No	No	-	-	Alive	
#22	2	R	7,80	5,59	4,69	4,38	3,06	6,55	11	88	Normal karyotype	47,Y, add(X)(p22), +5,del(6)(q21),add(8)(q22)[6]/46,XY[10]	0	No	No	No	Yes	ALL-SEHOP-PETHEMA-2015 for relapses + HSCT	-	Alive	
#23	4	Dx	6,96	4,85	4,83	4,92	3,47	5,83	90	-	46,XX,t(9)(q10),der(19)t(1;19)(q23;p13)[15]/46,XX[5], E2A-PBX1 rearrangement t(1;19) translocation, Trisomy of chromosome 9	-	0,000,00 (bis)	No	No	No	No	No	-	Alive	
#24	7	Dx	7,13	5,42	3,04	3,19	2,65	5,18	98	2,5	Hyperdiploid karyotype 53,XY,+X,+5,+6,+17,+18,+21,+21[16/20]	-	0	No	No	No	No	No	-	Alive	
#25	9	R	13,93	6,67	8,74	5,22	4,16	8,43	NA	NA	NA	NA	NA	NA	NA	NA	Yes	NA	NA	NA	
#26	10	Dx	9,62	5,95	3,46	3,30	3,09	8,30	38	-	Normal karyotype, 9q deletion that includes ABL1.	-	0	No	No	No	No	No	-	Alive	
#27	3	Dx	8,39	4,64	4,83	3,65	3,57	9,82	39	-	46,XY,add(19)(q13)[10]/46,XY[10], TEL-AML1 rearrangement.	-	0,00	No	No	No	No	No	-	Alive	
#28	1	R	11,27	7,76	5,56	5,15	4,34	11,03	NA	NA	Normal karyotype	NA	NA	No	HSCT for relapse, CAR-T for relapse post HSCT, transplant for relapse post CAR-T CD 19	Early BM relapse --> HSCT --> post HSCT relapse --> CAR-T 19 relapse post CAR-T CD 19 relapse --> transplant	Yes	ALL-SEHOP-PETHEMA-2015 FOR RELAPSES	Disease progression	Exitus	

PATIENT	AGE AT Dx	STAGE	MICA	MICB	ULBP1	ULBP2	ULBP3	ULBP4	% BLASTS Dx	% BLASTS R	CYTOGENETIC Dx	CYTOGENETIC R	MRD +78	HSCT	OTHER THERAPIES	TREATMENTS COMPLICATIONS	RELAPSE	TREATMENT OF R	EXITUS CAUSE	ACTUAL STATE
#29	2	R	11,24	6,30	5,46	4,12	3,85	8,47	NA	33	Partial trisomy of chromosome 9 and a dicentric (9;12)(p13;p13).	46,XX,t(2;14)(p13;q32),t(9;10)(t18)/46,XX[2]	0	No	No	No	Yes	SEHOP- PETHEMA- 2015 RELAPSES	-	Alive
		F	6,56	4,41	3,53	2,89	3,91	1,01												
#30	7	Dx	4,88	3,71	2,49	2,65	1,76	3,63	75	-	Normal karyotype	-	0/0,00 (bis)	No	No	Diabetes mellitus corticoidea, infección SARS-CoV-2 con desarrollo de HLH-like	No	No	-	Alive
#31	5	Dx	10,80	7,03	4,50	4,49	4,49	11,57	50	-	RUNX1 (x4)	-	0	No	No	No	No	No	-	Alive
#32	8	Dx	3,68	3,14	2,31	2,53	2,14	1,00	91	-	Normal karyotype	-	2,65	Yes	Ruxolitinib (inicio 30/01/2019 -> 7 in 24/01/2020)	Iron overload	No	No	-	Alive
#33	14	Dx	6,45	3,61	2,57	3,18	8,20	1,00	50	-	Normal karyotype	-	<0,01	No	No	Vincristine associated osteonecrosis of the femoral condyles, Li Fraumeni (germline TP53)	No	No	-	Alive
#34	15	Dx	11,90	6,55	3,50	4,47	12,62	9,28	78	-	46,XY,del(9)(p13)t(18)/46,XY[2]	-	0,09/1,88 (bis)	Yes	Ruxolitinib (KZF1) + cladribine, cyclophosphamide, and etoposide rescue cycle.	MAT post-HSCT	No	CLOFARABINE + GMP-ETOPO SIDE later, haploidentical HSCT in second complete	Infection	Exitus
#35	0	R	6,29	NA	2,50	2,97	6,89	3,96	65	16	t(2;15), MLL	46,XX,t(2;15)(p24;q21),7q-9p-,12q-,13p-Xq-(5)	Myeloblastic	No	auto-HSCT	No	Yes	LAL/SEHOP 2008 for relapsed ALL + HSCT	-	Alive
#36	15	Dx	9,51	4,43	3,45	2,73	10,29	4,42	80	-	46,XY,t(9;14)(q35;q32),t(9;22)(q34;q11)t(17)/46,XY[3]. BCR-ABL1 rearrangement	-	0	No	IMATINIB	Avascular osteonecrosis, hyperglycemia, catheter-associated thrombosis.	No	No	-	Alive
#37	12	F	9,18	NA	5,05	3,39	7,93	5,09	NA	40	46,XX,add(12)(p11.2),add(21)(q22)[6]/46,XX[14]	NA	0	No	No	No	Yes	HSCT	-	Alive
#38	0	Dx	5,37	NA	3,65	2,59	4,52	2,26	70	-	NA	-	0	Yes	No	Myocarditis	No	N/A	Myocarditis (TRM)	Exitus
		F	5,38	NA	3,83	2,59	4,68	2,27												

10.3. Table showing characteristics of T-ALL pediatric patients.

PATIENT	AGE AT Dx	STAGE	MICA	MICB	ULBP1	ULBP2	ULBP3	ULBP4	% BLASTS Dx	% BLASTS R	CYTOGENETIC Dx	CYTOGENETIC R	MRD +78	HSCT	OTHER THERAPIES	TREATMENTS COMPLICATIONS	RELAPSE	TREATMENT OF R	EXITUS CAUSE	ACTUAL STATE
#1	13	R	10,4		7,75	5,28	9,83	3,65				46, XY, 12q+, 18p+	0	No	No	No	Yes	SHOP 2008 (refractory) ; nelarabine y HSCT	Disease progression	Exitus
		R	7,41	1,61	4,32	3,97	5,09	5,05			96	Normal karyotype								
		F	8,19	1,59	4,80	4,12	5,64	5,17	27											
		F	16,16		13,78	8,34	6,52	9,46												
		F	28,5		14,01	8,65	9,25	17,80												
#2	14	Dx	11,41	NA	7,69	5,92	7,74	4,5	91	-	Normal karyotype	-	0,47	No	No	Fasciitis	No	No	-	Alive
#3	10										Homozygous deletion of CDKN2A/B, r(9)(q13)(q10;q10)-13	NA	0,24	Yes	transfer to another centre	transfer to another centre	transfer to another centre	transfer to another centre	transfer to another centre	
		Dx	11,68	NA	6,26	4,42	4,07	6,03	78	NA						transfer to another centre				
#4	0	Dx	6,57	5,12	3,35	3,7	2,12	0,99				Homozygous deletion of CDKN2A, 46, XY, t(7;9)(p13;p13); /46,XY[t(4;6)(p13;p13); q24]t(16;46,X)(t14)	0	Yes	Rescue cycle with nelarabine, VP, CF	Bacteremia due to Klebsiella and rotavirus mucicapsula. Relapse after AP3 block, after which rescue with a cycle of nelarabine, CF and VP-w as proposed	Yes	Rescue with Nelarabine (650mg/m2, five doses), etoposide (100mg/m2, 5 doses) and cyclophosphamide	Disease progression	Exitus
		F	8,47	4,01	3,61	3,25	7,02	3,59	65	75										
		R	4,92	3,29	1,88	2,91	6,6	8,72												
		R	5,25		1,31	1,59	4,74	1,97												
#5	12	F	12,55	NA	11,1	8,7	7,38	5,81	NA	NA	46, XX t(6;11)	Altered karyotype	0	Yes	No	Arterial hypertension, reversible posterior leukoencephalopathy, diarrhea due to adenovirus, acute pancreatitis and drug-induced hepatitis.	Yes	Cell therapy	Third relapse	Exitus
#6	8	Dx	15,57	NA	7,12	5,56	13,83	6,91	NA	NA	Normal karyotype	NA	N/A	No	No	Five relapses	Yes	HSCT	Disease progression	Exitus

10.4. Table showing characteristics of AML pediatric patients.

PATIENT	AGE AT Dx	STAGE	MICA	MICB	ULBP1	ULBP2	ULBP3	ULBP4	% BLASTS Dx	% BLASTS R	PHENOTYPE Dx	PHENOTYPE R	CYTOGENETIC Dx	RESPONSE TO TREATMENT	HSCT	RELAPSE	TREATMENT	EXITUS CAUSE	ACTUAL STATE
#1	8	Dx	5.55	1.02	4.96	5.03	4.86	1.02	87	7	CD45+m, CD34+, CD117+, DR+, CD38+F, CD13+, CD33+F, CD15+m, MPO+d, CD14-, CD36-, CD64-, CD11b-, CD9-, CD35-, CD123+m, CD71+m, CD41-	CD45+m, CD34+, CD117+, DR+, CD38+F, CD13+, CD33+F, CD15+m, MPO+d, CD14-, CD36-, CD64-, CD11b-, CD9-, CD35-, CD123+m, CD71+m, CD41-	Normal karyotype, WT1 overexpression.	CR after first induction block	No	yes	Rescue chemotherapy	Multiborganic failure	exitus
		R	6.14	NA	4.77	3.46	6.92	5.17											
		S	9.53	NA	7.27	9.01	7.93	7.55											
#2	12	S	9.87	NA	8.94	5.09	7.69	4.10	NA	47	NA	CD45+m, CD34+hel, CD71+m, CD4+, CD33+F, CD71b+ qCD117-, CD56+d, CD34+d, CD13+	NA	Refractory	No	No	NA	NA	NA
#3	8	Dx	12.46	NA	6.7	7.57	8.04	6.94	13	12	NA	-	FLT-3-ITD	Refractory	No	No	Rescue chemotherapy	Disease progression	Exitus
		F	13.68	NA	11.46	11.54	8.53	5.23											
		Dx	8.11	1.03	6.67	8.54	5.1	4.41											
#4	3	Dx	10.4	NA	7.75	5.28	9.83	3.65	14	16	NA	CD45+m, CD34+, CD117+, CD13+, CD33+F, CD15+F, CD14-, CD64+, CD35-, DR+, CD71+m	NA	-	yes	yes	Palliative care	Disease progression	Exitus
#5	8	R	14.83	1.10	8.27	5.91	4.77	6.23	NA	NA	NA	NA	NA	CR after first induction block	yes	yes	Rescue chemotherapy + HSCT	Disease progression	exitus
		S	10.25	1.10	9.21	7.47	4.60	7.74											
		S	25.89	1.17	10.76	8.10	8.19	11.27											
#6	14	Dx	15.36	1.03	6.7	5.29	6.2	4.66	40	NA	CD117-, CD34-, DR+, CD45+f, CD123+, CD9+, CD33+F, CD13+F, CD11b+hel, CD15+, CD64+, CD14-, CD36-, MPO-	M.LL rearrangement t(9;11)	Refractory	yes	No	-	septic shock	exitus	







PATIENT	AGE AT Dx	STAGE	MICA	MICB	ULBP1	ULBP2	ULBP3	ULBP4	% BLASTS Dx	% BLASTS R	PHENOTYPE DX	PHENOTYPIC	CYTOGENETIC Dx	RESPONSE TO TREATMENT	HSCT	RELAPSE	TREATMENT	EXITUS CAUSE	ACTUAL STATE
#7	3	S	11.30	NA	4.47	3.71	4.93	7.62	6	2	NA	CD117+	Normal karyotype, WT1 overexpression	MDS	yes	No	-	-	Alive
#8	0	Dx	6.57	3.84	3.32	2.64	2.12	2.4	65	50	NA	CD45-m, CD34-, CD117+, DR-het-, CD38++ , CD13+, CD33+ , CD15-, MPO-, CD14+, CD38+, CD34-, CD11b+, CD9+ -d, CD35-, CD123-m, CD41-, CD56++ , CD7+	CR after first induction block	No	No	-	-	Alive	
#9	2	Dx	21.06	9.15	12.14	6.44	9.61	14.01	60	NA	CD45+ , DR+ -d, CD123+m, CD34-, CD117-, CD15+ , CD33+ , CD13+, CD11b-, CD64+ , CD4+, CD14-, CD35-, CD36-, REM-, CD9-	NA	FLT3-ITD	CR after first induction block	No	No	-	-	Alive
#10	17	Dx	10.66	7.45	5.64	5.07	4.05	10.23	45	30	NA	CD117+ , DR+ , CD38+ , CD13+ , CD33- , CD15+ , MPO- , CD14- , CD34- , REM- , CD36-	Deletion long arm chromosome 6. Partial duplication of chromosome 1 arms	-	yes	-	-	Alive	
#11	5	Dx	5.75	3.07	3.39	2.53	2.35	1.04	70	NA	CD45+ , CD34- , CD117+ , DR+/- , CD15- , CD13+ -F, CD33+ -F, CD34+ , CD9+ , CD56- , CD14-, CD36- , CD71- , CD41- , CD123+ , MPO+	Chromosome 8 trisomy, PML-RA-Ra rearrangement.	CR after first induction block	No	No	-	-	Alive	
#12	6	Dx	1.52	2.38	1.11	2.14	2.43	NA	60	NA	CD45+ , CD34- , CD117+ , DR+/- , het, CD13+ -F, CD33+ -F, CD34+ , CD9+ , CD15- , CD36- , CD16-, CD14-, CD36- , CD71- , CD41-, CD123-m, MPO+	Normal karyotype 46XX- Del(6)(p21), PML-RA-Ra rearrangement, WT1 overexpression	CR after first induction block	No	No	-	-	Alive	

Manuscripts

- **Fernández A**, Navarro-Zapata A, Escudero A, Matamala N, Ruz-Caracuel B, Mirones I, Pernas A, Cobo M, Casado G, Lanzarot D, Rodríguez-Antolín C, Vela M, Ferreras C, Mestre C, Viejo A, Leivas A, Martínez J, Fernández L, Pérez-Martínez A. "Optimizing the Procedure to Manufacture Clinical-Grade NK Cells for Adoptive Immunotherapy". *Cancers*. 2021 Feb 2;13(3):577. doi: 10.3390/cancers13030577
- Fernández L, **Fernández A**, Mirones I, Escudero A, Cardoso L, Vela M, Lanzarot D, de Paz R, Leivas A, Gallardo M, Marcos A, Romero AB, Martínez-López J, Pérez-Martínez A. "GMP-Compliant Manufacturing of NKG2D CAR Memory T Cells Using CliniMACS Prodigy". *Front Immunol*. 2019 Oct 10;10:2361. doi: 10.3389/fimmu.2019.02361

Article

Optimizing the Procedure to Manufacture Clinical-Grade NK Cells for Adoptive Immunotherapy

Adrián Fernández ¹, Alfonso Navarro-Zapata ² , Adela Escudero ^{3,4} , Nerea Matamala ⁴ , Beatriz Ruz-Caracuel ⁴, Isabel Mirones ⁵ , Alicia Pernas ⁵, Marta Cobo ⁵, Gema Casado ^{5,6}, Diego Lanzarot ⁷, Carlos Rodríguez-Antolín ⁸ , María Vela ², Cristina Ferreras ², Carmen Mestre ², Aurora Viejo ⁹, Alejandra Leivas ^{1,10}, Joaquín Martínez ^{1,10} , Lucía Fernández ^{1,†} and Antonio Pérez-Martínez ^{2,11,*,†}

- ¹ Hematological Malignancies Lab-H120 Clinical Research Unit, Spanish National Cancer Research Centre (CNIO), 28029 Madrid, Spain; afmartin@cnio.es (A.F.); aleivas@ext.cnio.es (A.L.); jmarti01@med.ucm.es (J.M.); lvfernandez@cnio.es (L.F.)
- ² Translational Research Group in Paediatric Oncology Haematopoietic Transplantation & Cell Therapy, La Paz University Hospital Institute for Health Research-IdiPAZ, 28046 Madrid, Spain; alfonso.navarro.zapata@idipaz.es (A.N.-Z.); maria.vela@idipaz.es (M.V.); cristina.ferreras@salud.madrid.org (C.F.); carmen.mestre.duran@idipaz.es (C.M.)
- ³ Institute of Medical and Molecular Genetics (INGEMM), La Paz University Hospital, 28046 Madrid, Spain; adela.escudero@idipaz.es
- ⁴ Translational Research in Pediatric Oncology, Hematopoietic Transplantation & Cell Therapy, La Paz University Hospital Institute for Health Research-Institute of Medical and Molecular Genetics (INGEMM-IdiPAZ), 28046 Madrid, Spain; nerea.matamala.zamarro@idipaz.es (N.M.); beatriz.ruz@salud.madrid.org (B.R.-C.)
- ⁵ Advanced Therapy Medicinal Products Production Unit Pediatric Hemato-Oncology Department, La Paz University Hospital, 28046 Madrid, Spain; isabel.mirones@salud.madrid.org (I.M.); alicia.pernas@salud.madrid.org (A.P.); marta.cobo@salud.madrid.org (M.C.); mgema.casado@salud.madrid.org (G.C.)
- ⁶ Advanced Therapy Medicinal Products Production Unit, Pediatric Hemato-Oncology Service and Pharmacy Service, La Paz University Hospital, 28046 Madrid, Spain
- ⁷ Applications Department Miltenyi Biotec, 28223 Madrid, Spain; diego@miltenyi.com
- ⁸ Experimental Therapies and Novel Biomarkers in Cancer, La Paz University Hospital Institute for Health Research-IdiPAZ, 28046 Madrid, Spain; crodriguez@salud.madrid.org
- ⁹ Hematology and Hemotherapy Department, La Paz University Hospital, 28046 Madrid, Spain; aurora.viejo@salud.madrid.org
- ¹⁰ Hematology Department 12 de Octubre University Hospital, 28041 Madrid, Spain
- ¹¹ Pediatric Hemato-Oncology Department, La Paz University Hospital, 28046 Madrid, Spain
- * Correspondence: aperezmartinez@salud.madrid.org; Tel.: +34-912071408 (ext. 41408)
- † These authors contributed equally to this work.



Citation: Fernández, A.; Navarro-Zapata, A.; Escudero, A.; Matamala, N.; Ruz-Caracuel, B.; Mirones, I.; Pernas, A.; Cobo, M.; Casado, G.; Lanzarot, D.; et al. Optimizing the Procedure to Manufacture Clinical-Grade NK Cells for Adoptive Immunotherapy. *Cancers* **2021**, *13*, 577. <https://doi.org/10.3390/cancers13030577>

Academic Editor: Raquel Tarazona

Received: 2 December 2020

Accepted: 26 January 2021

Published: 2 February 2021

Publisher's Note: MDPI stays neutral with regard to jurisdictional claims in published maps and institutional affiliations.



Copyright: © 2021 by the authors. Licensee MDPI, Basel, Switzerland. This article is an open access article distributed under the terms and conditions of the Creative Commons Attribution (CC BY) license (<https://creativecommons.org/licenses/by/4.0/>).

Simple Summary: Natural Killer cells have shown promise to treat different malignancies. Several methods have been described to obtain fully activated NK cells for clinical use. Here, we use different cell culture media and different artificial antigen presenting cells to optimize a GMP compliant manufacturing method to obtain activated and expanded NK cells suitable for clinical use.

Abstract: Natural killer (NK) cells represent promising tools for cancer immunotherapy. We report the optimization of an NK cell activation–expansion process and its validation on clinical-scale. Methods: RPMI-1640, stem cell growth medium (SCGM), NK MACS and TexMACS were used as culture mediums. Activated and expanded NK cells (NKAE) were obtained by coculturing total peripheral blood mononuclear cells (PBMC) or CD45RA⁺ cells with irradiated K562mbIL15-41BBL or K562mbIL21-41BBL. Fold increase, NK cell purity, activation status, cytotoxicity and transcriptome profile were analyzed. Clinical-grade NKAE cells were manufactured in CliniMACS Prodigy. Results: NK MACS and TexMACs achieved the highest NK cell purity and lowest T cell contamination. Obtaining NKAE cells from CD45RA⁺ cells was feasible although PBMC yielded higher total cell numbers and NK cell purity than CD45RA⁺ cells. The highest fold expansion and NK purity were achieved by using PBMC and K562mbIL21-41BBL cells. However, no differences in activation and cytotoxicity were found when using either NK cell source or activating cell line. Transcriptome profile

showed to be different between basal NK cells and NKAEC cells expanded with K562mbIL21-41BBL or K562mbIL15-41BBL. Clinical-grade manufactured NKAEC cells complied with the specifications from the Spanish Regulatory Agency. Conclusions: GMP-grade NK cells for clinical use can be obtained by using different starting cells and aAPC.

Keywords: NK cell immunotherapy; NK cell activation and expansion; NKAEC cells; clinical-grade manufacturing; CliniMACS Prodigy

1. Introduction

Development of new donor lymphocyte infusions products with antitumor reactivity and reduced graft-versus-host disease (GvHD) risk represents a challenging issue in cancer immunotherapy. Natural killer (NK) cells are lymphocytes from the innate immunity with the ability to recognize and target tumor cells without prior sensitization, making them ideal therapeutic agents to treat cancer [1]. In fact, NK cell infusions are well tolerated, do not cause GvHD or autoimmunity and have been associated with complete remission in poor-prognosis patients with acute myeloid leukemia (AML) [2,3]. One limitation of using NK cells as a therapeutic tool is that they have to be fully activated and have to be infused in large numbers to observe a clinical benefit. However, activation status and NK cell numbers are low in the main sources of NK cells: PBMCs or umbilical cord blood units. To overcome this limitation, different protocols have been designed to expand and activate NK cells ex vivo before transfer to the patient. They may differ in the addition of different cytokines [4–7], the source of NK cells used [8,9], or the coculture with distinct irradiated feeder or artificial antigen presenting cells (aAPC) [10–12], among others. Nevertheless, ex vivo activated and expanded NK cells (NKAEC) share some common features [13]. In general, ex vivo NKAEC cells show an increased activation status and increased cytotoxicity, even responding against tumor targets apparently resistant to NK cell lysis [10,14,15].

Several groups have developed aAPC by engineering the K562 cell line to express the membrane-bound form of interleukin (IL)-15 (mIL-15) or IL21 and CD137 ligand. The combination of activating signals provided by the K562 cell line, costimulation via 4-1BBL (CD137L) and survival signals provided by cytokines such as IL15 or IL21 can mediate NK cell proliferation and the expansion of highly cytotoxic NK cells [11,12].

Besides, the transfer of these protocols to the clinical scale in a manageable, good manufacturing practice (GMP)-compliant way is still challenging. The multitude of necessary hands-on steps complicates the routine use of these scaled-up manual approaches as standard therapy. Recently, Miltenyi Biotec has allowed the automated clinical-scale manufacturing of NK cells using centrifugation, magnetic cell separation and cell cultivation within a closed system, namely the CliniMACS Prodigy [16]. By using this device, different groups have designed and optimized successful NK cell expansion protocols [17–19].

In parallel, improvements are also in development concerning T-cell depletion of the allogeneic hematopoietic stem cell transplantation (HSCT) graft, as it may lead to increased graft failure, relapse and infections due to delayed immune recovery. The selective depletion of the CD45RA⁺ subset can reduce GvHD through removal of naïve T cells [20]. This fraction, usually discarded, contains NK cells and potentially could be used as a starting material in the ex vivo activation and expansion of NK cell products.

The objective of this study was to optimize a protocol to activate and expand NK cells by comparing different cell culture media, different aAPC and using different starting cells. The most suitable expansion protocols have been further validated within the CliniMACS Prodigy system to obtain clinical-grade NKAEC cells for cancer immunotherapy. In summary, automated manufacturing clinical grade NK cells in CliniMACS Prodigy is feasible and NK cell products met the requirements established for the clinical use of this product by the Spanish Regulatory Agency.

2. Results

2.1. Optimization of Cell Growth Culture Media

2.1.1. NK Cells Fold Expansion and Purity Using Different Culture Media

In order to compare fold increase and purity of NK cell expansion using different growth media, we performed a total of 21 expansion experiments with buffy coats from five different healthy donors. In these experiments, PBMCs were cocultured with previously irradiated K562-mb15-41BBL (from now on, K562mbIL15) cells in a 1:1.5 ratio in the following media: RPMI, Stem cell growth medium (SCGM), NK MACS, TexMACS GMP, all of them supplemented with 5% AB human serum and IL-2.

Fold increase of total cells and NK cells, after 21 days culture with the different media is shown in Figure 1. Although we did not observe statistically significant differences in the number of total cells or NK cells expanded; NK MACS yielded the highest NK cells fold increase (903 ± 576.3) and RPMI medium the lowest (388 ± 292.7) ($p = 0.45$) (Figure 1).

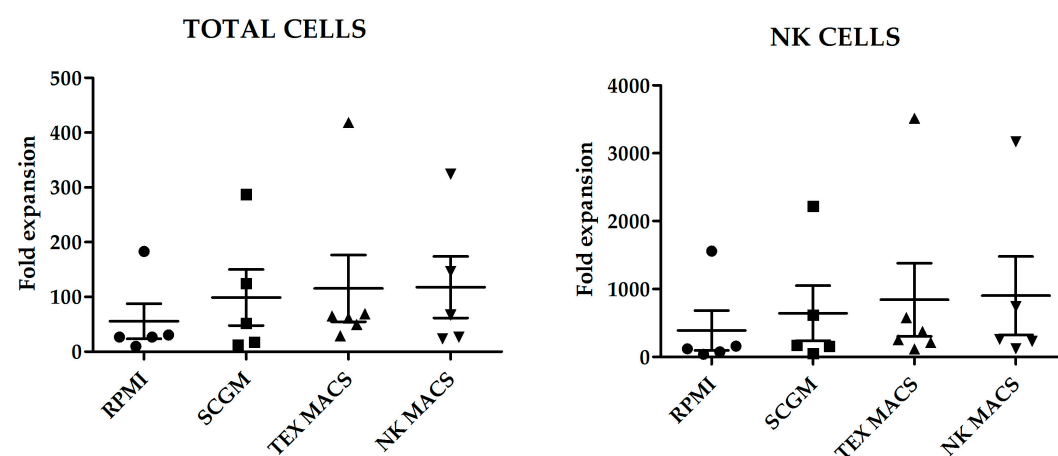


Figure 1. Fold increase of total cells and natural killer (NK) cells after the 21 days of culture with the different media. Error bars show mean \pm SEM. RPMI, SCGM and NK MACS $n = 5$. TexMACS $n = 6$. Geometrical symbols represent individual data of expanded cells from different donors by using RPMI (dots), SCGM (squares), TexMACS (triangles), NKMACS (inverted triangles).

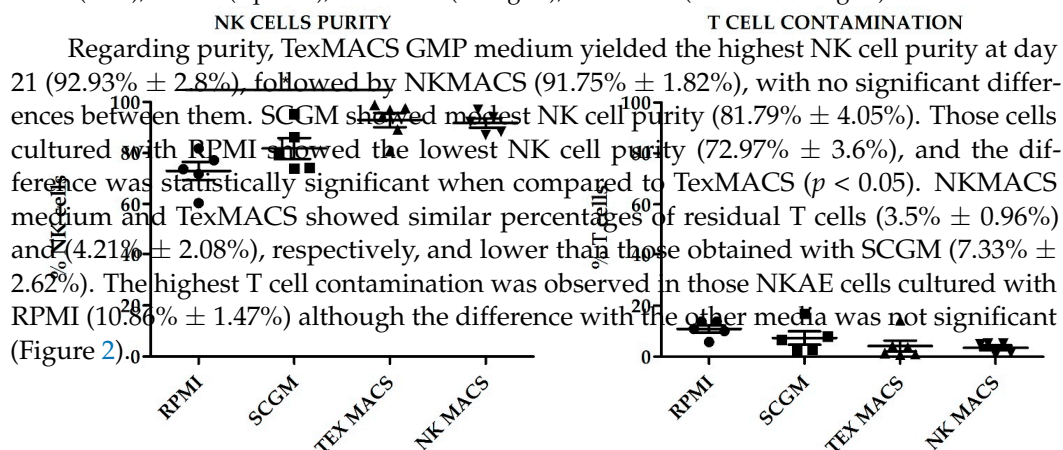


Figure 2. NK cell purity and T cell contamination on activated and expanded NK cells (NKA) expanded with different culture media. Error bars show mean \pm SEM. RPMI, SCGM and NK MACS $n = 5$. TexMACS $n = 6$. * $p < 0.05$. Geometrical symbols represent individual data of expanded cells from different donors by using RPMI (dots), SCGM (squares), TexMACS (triangles), NKMACS (inverted triangles).

2.1.2. Expression of Activating and Inhibitory Receptors on NKA Cells

The phenotype of NKA cells was evaluated by flow cytometry (FCM) at baseline and at day 21 following ex vivo expansion with K562mbIL15 cell line in RPMI, SCGM, NK MACS or TexMACS medium. We found that the surface expression of the functionally relevant receptors CD25, CD69, NK group-2 member D receptor (NKG2D), NKp30, NKp44, NKp46 and DNA accessory molecule 1 (DNAM-1) was upregulated in NKA cells cultured with all media when compared with resting NK cells. However, significant differences were only observed in NKG2A and NKp46 receptors when comparisons were

Figure 1. Fold increase of total cells and natural killer (NK) cells after the 21 days' culture with the different media. Error bars show mean \pm SEM. RPMI, SCGM and NK MACS $n = 5$. TexMACS $n = 6$. Geometrical symbols represent individual data of expanded cells from different donors by using RPMI (dots), SCGM (squares), TexMACS (triangles), NKMACS (inverted triangles).

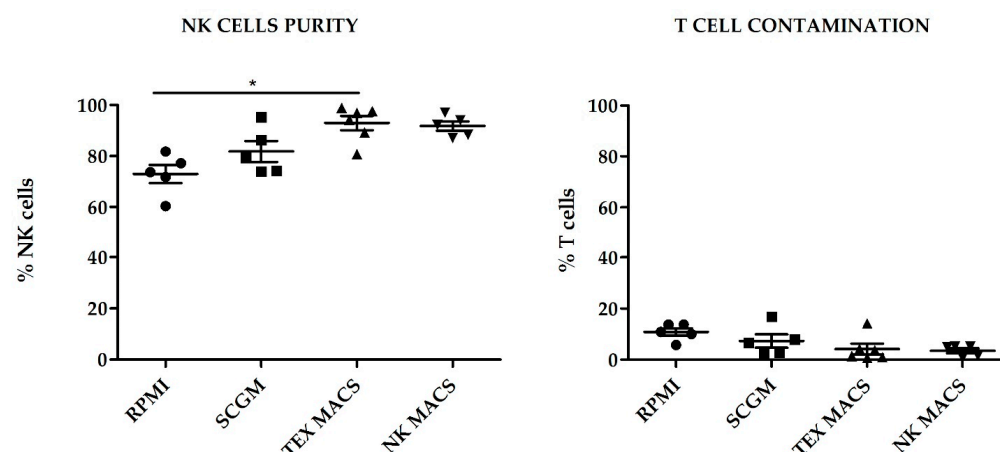


Figure 2. NK cell purity and T cell contamination on activated and expanded NK cells (NKAE) expanded with different culture media. Error bars show mean \pm SEM. RPMI, SCGM and NK MACS $n = 5$. TexMACS $n = 6$. $p < 0.05$. Geometrical symbols represent individual data of expanded cells from different donors by using RPMI (dots), SCGM (squares), TexMACS (triangles), NKMACS (inverted triangles).

2.1.2. Expression of Activating and Inhibitory Receptors on NKAE Cells

The phenotype of NKAE cells was evaluated by flow cytometry (FCM) at baseline and at day 21 following ex vivo expansion with K562mbIL15 cell line in RPMI, SCGM, NK MACS or TexMACS medium. The percentages of the different subpopulations, including NK bright and NK dim, and cell viability at different time points during the culture are indicated in Table S1. We did not observe differences in viability in the different NKAE products, NKp44, NKp46 and DNA accessory molecule 1 (DNAM-1) was upregulated in NKAE cells obtained with the different media. The percentage of bright NK cells was statistically significantly higher when RPMI was used for the expansion, compared to the other three media. Consequently, the percentage of dim NK cells was lower in those NKAE cells; however, only statistically significant differences were observed when these NKAE cells were compared to those obtained using TexMACS. No statistically significant differences were observed in the percentage of NKT or B cells expanded at day + 21.

2.1.2. Expression of Activating and Inhibitory Receptors on NKAE Cells

The phenotype of NKAE cells was evaluated by flow cytometry (FCM) at baseline and at day 21 following ex vivo expansion with K562mbIL15 cell line in RPMI, SCGM, NK MACS or TexMACS medium. We found that the surface expression of the functionally relevant receptors CD25, CD69, NK group-2 member D receptor (NKG2D), NKp30, NKp44, NKp46 and DNA accessory molecule 1 (DNAM-1) was upregulated in NKAE cells cultured with all media when compared with resting NK cells. However, significant differences were only observed in NKG2A and NKp46 receptors when comparisons were established between basal NK cells and NKAE cultured with TexMACS ($p = 0.01$) basal NK cells vs. NKAE RPMI, respectively ($p = 0.013$) (Figure 3).

established between basal NK cells and NKAE cultured with TexMACS ($p = 0.01$) basal NK cells vs. NKAE RPMI, respectively ($p = 0.013$) (Figure 3).

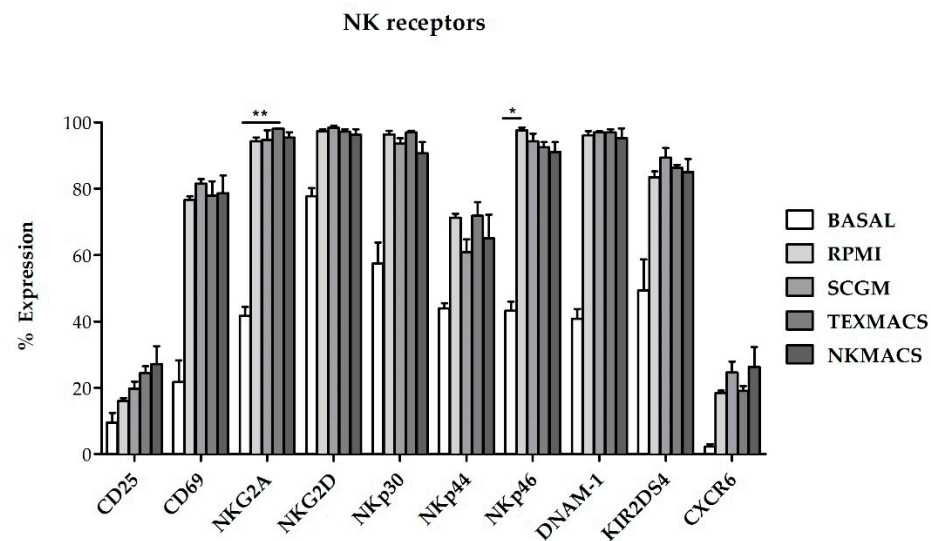


Figure 3. Expression of activating and inhibitory receptors on NKAE cells expanded with different culture media. The different receptors were upregulated on NKAE cells compared to basal NK cells. No differences in the expression of the analyzed receptors on NKAE cells were found when using different cell growth media. Error bars show mean \pm SEM. $n = 3$ for each condition; (* $p = 0.013$, ** $p = 0.01$).

2.1.3. Cytotoxicity of NKAE Cells

We next evaluated the cytolytic activity of NKAE cell products obtained using the different growth media against K562 target cells and we observed no significant differences in their lytic activity (Figure 4) (Figure 4).

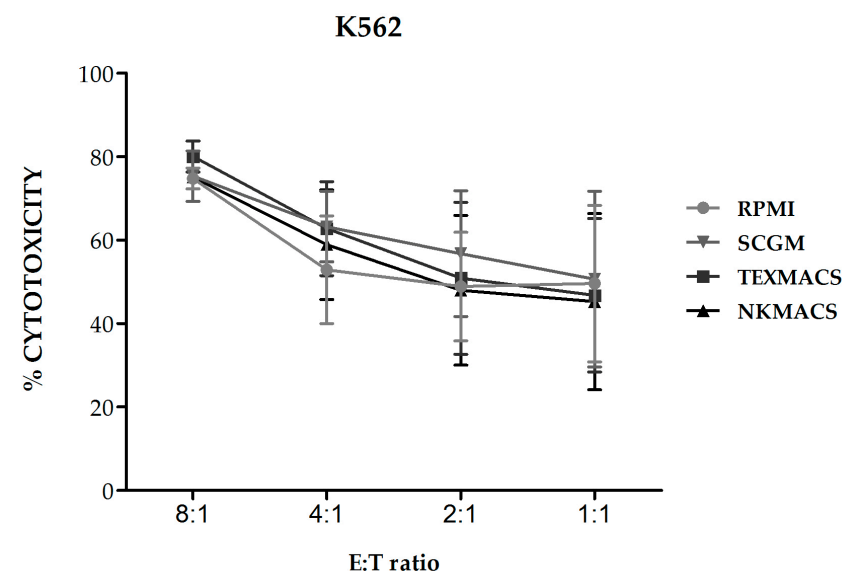


Figure 4. Cytotoxicity of NKAE cells expanded with different culture media against K562 cells. The NKAE cells expanded with the different culture media did not show differences in their cytolytic ability against K562 cells. Error bars show mean \pm SEM. $n = 3$ for each condition.

2.2. Use of CD45RA⁺ Cells as a Source of NK Cells to Obtain NKAE

CD45RA⁺ cells are enriched in naïve T cells and NK cells. This fraction is depleted and discarded in some HSCT procedures to remove alloreactive T cells and reduce the risk of GvHD. On the contrary, CD45RA⁺ memory T cells show decreased alloreactivity and lack naïve T cells, thus improving engraftment and protecting the recipient from infections.

CD45RA⁺ cells are enriched in naïve T cells and NK cells. This fraction is depleted and discarded in some HSCT procedures to remove alloreactive T cells and reduce the risk of GvHD. On the contrary, CD45RA⁺ memory T cells show decreased alloreactivity and lack naïve T cells, thus improving engraftment and protecting the recipient from infections. CD45RA⁺ cells can be infused into patients undergoing haploHSCT either as part of the graft, along with the mobilized CD34⁺ cells, or as donor lymphocyte infusions (DLI). CD45RA⁺ depleted grafts are usually obtained from peripheral infusions after pharmacologic stem mobilization or usually obtained from healthy donors after pharmacologic mobilization of hematopoietic stem cells using G-CSF [21], although some other protocols use non-mobilized apheresis [22]. CD45RA⁺ depleted fractions for DLI are obtained after non-mobilized apheresis [23]. To evaluate the feasibility of expanding NK cells using the CD45RA⁺-wasted fraction, we performed expansions from CD45RA⁺ cells obtained after mobilized and non-mobilized apheresis and compared them with expansions using PBMCs. According to the NK cell purity data previously obtained, we used TexMACS growth medium for these expansions. The basal (preculture) composition of the different starting cell products is shown in Figure 5. CD45RA⁺ cells from mobilized apheresis showed the lowest percentage of initial NK cells purity (1.7% ± 0.6%) followed by CD45RA⁺ cells from non-mobilized apheresis (7.5% ± 2.5%) and PBMCs that had the highest basal percentage of NK cells (16.9% ± 2.7%). Total cells at the beginning of the expansion are shown in Figure S1. Fold expansion of NK cells, NK1 cells, T cells and B cells after 21 days are shown in Figure 6. CD45RA⁺ mobilized fraction showed the lowest NK cells fold expansion (7.6 ± 4.2 fold); ($p = 0.011$ compared to PBMC) and the highest B cells expansion (306.3 ± 79.9 fold); ($p = 0.014$ compared to PBMCs (306.3 ± 79.9 fold); $p = 0.014$).

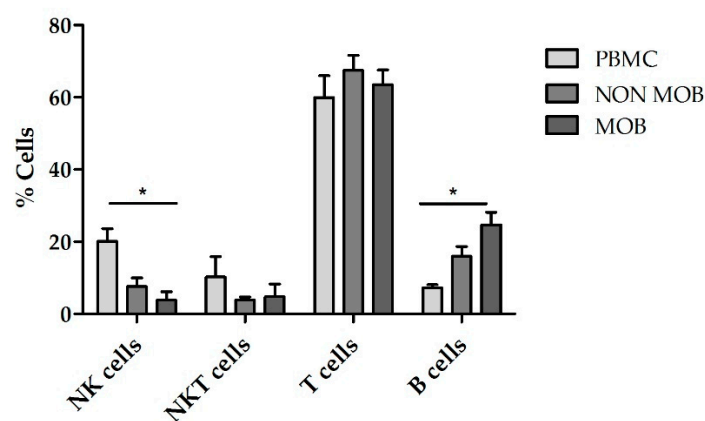


Figure 5. Cell subsets contained in PBMC, CD45RA⁺ cells from mobilized apheresis (mob) and CD45RA⁺ cells from non-mobilized apheresis (non-mob) before NK cell expansion. Mobilized CD45RA⁺ cells contain less NK and more B cells compared to PBMC ($p = 0.003$ and $p = 0.001$ respectively, PBMC ($n = 5$), non-mob ($n = 3$) and mob ($n = 3$). Error bars show mean ± SEM, $p < 0.05$.

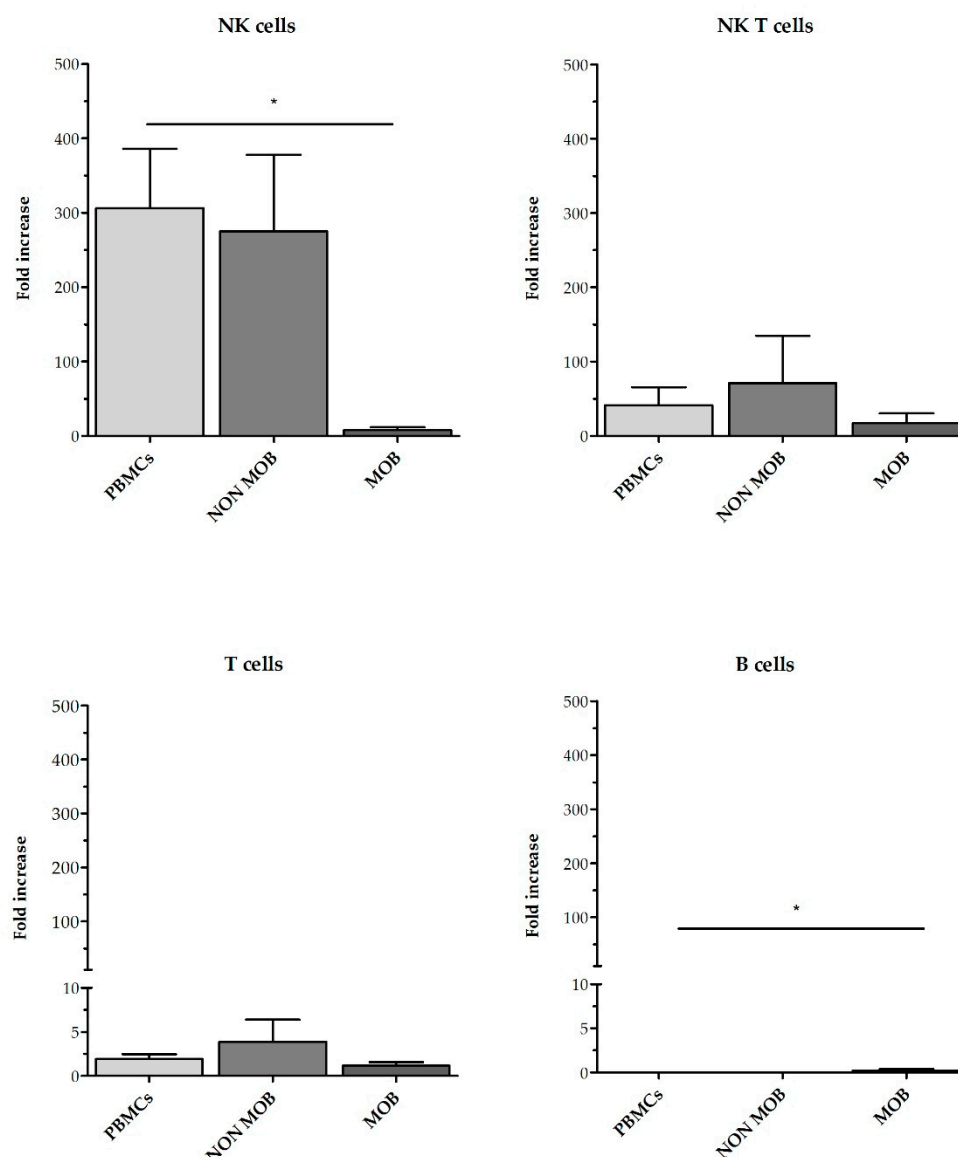


Figure 6. Fold increase of the different cell subsets in NKAE cells obtained from PBMC, CD45RA⁺ mobilized apheresis and CD45RA⁺ non-mobilized apheresis at day + 21. Those NKAE cells expanded from mobilized apheresis had less NK cells at the end of the expansion compared to NKAE cells from PBMC and non-mob apheresis. PBMC ($n = 5$), non-mob ($n = 3$) and mob ($n = 3$). Error bars show mean \pm SEM. * $p < 0.05$.

2.3. Expansion of NKAE Cells by Using Different aAPC

2.3. Expansion of NKAE Cells by Using Different aAPC

Once we had determined the best suited cell culture media and proven the feasibility of expanding NK cells from CD45RA⁺ fraction, we next wanted to explore if there were differences in those NKAE cells expanded with K562-mb11-15 or K562-mb21-41BBL (from now on K562-mb11-21) stimulatory cell lines. In these experiments, we expanded NK cells from six different donors using PBMCs or CD45RA⁺ cells as starting material and TexMACS as expansion medium. At 21 days of culture, we evaluated total cell expansion, NK cell purity (percentage), cytotoxicity against four different pediatric tumor cell lines: A673 (sarcoma), RH30 (rhabdomyosarcoma), Jurkat (T-ALL), LAN-1 (neuroblastoma) and K562 cells as control. PBMCs tended to yield higher total cell numbers and NK cell purity compared to CD45RA⁺ (2.34 $\times 10^6 \pm 5.04 \times 10^5$ vs. $1.08 \pm 4.38 \times 10^5$, $p = 0.004$) compared to CD45RA⁺ (2.34 $\pm 5.10\%$ vs. $5.04 \pm 2.68\%$, $p = 1.08 \times 10^{-5}$) respectively. When PBMCs were used as starting cells, expansion with K562-mb11-21 respectively higher total cell numbers and

using K562mbIL15 ($3.36 \times 10^8 \pm 6.63 \times 10^7$ and $1.3 \times 10^8 \pm 5.03 \times 10^7$, respectively, $p = 0.03$) and tended to achieve higher NK cell purity ($84.67\% \pm 4.82\%$ vs. $59.85\% \pm 12.42\%$, $p = 0.09$). When CD45RA⁺ cells were used, those expansions using K562mbIL21 tend to show higher total cells ($7.31 \times 10^7 \pm 2.18 \times 10^7$ vs. $1.32 \times 10^8 \pm 8.7 \times 10^7$) and NK cell purity ($73.91\% \pm 5.82\%$ vs. $56.2\% \pm 11.11\%$) than those using K562mbIL15, although these differences were not statistically significant ($p = 0.55$ and $p = 0.19$, respectively). NKAE cells obtained after coculture with K562mbIL15 tended to yield lower cell numbers ($1.02 \times 10^8 \pm 2.75 \times 10^7$ vs. $3.34 \times 10^8 \pm 1.07 \times 10^8$, $p = 0.003$) and achieved less NK cell purity ($58.03\% \pm 9.73\%$ vs. $81.95\% \pm 9.00\%$, $p = 0.02$) than those expanded with K562mbIL21, no matter the source of NK cells that were used (PBMC or CD45RA⁺) (Figure 7). Representative data of NK cell purity analyzed by FCM along the expansion procedure in the different conditions are shown in Figure S2. The flow cytometry analysis showed a comparable expression of surface markers in all NKAE cell products regardless of the NK cell source and the APC used for the expansion (Figure 8). Representative data of NK cell receptors expressed on CD45RA⁺ PBMC and CD45RA⁺ cells in NKAE conditions and in NKAE cells at day +21 of expansion are shown in Figure S3. Consistent with the expression of activating receptors, the different NKAE cells had similar cytolytic ability against the five different tumor cell lines tested (Figure 9).

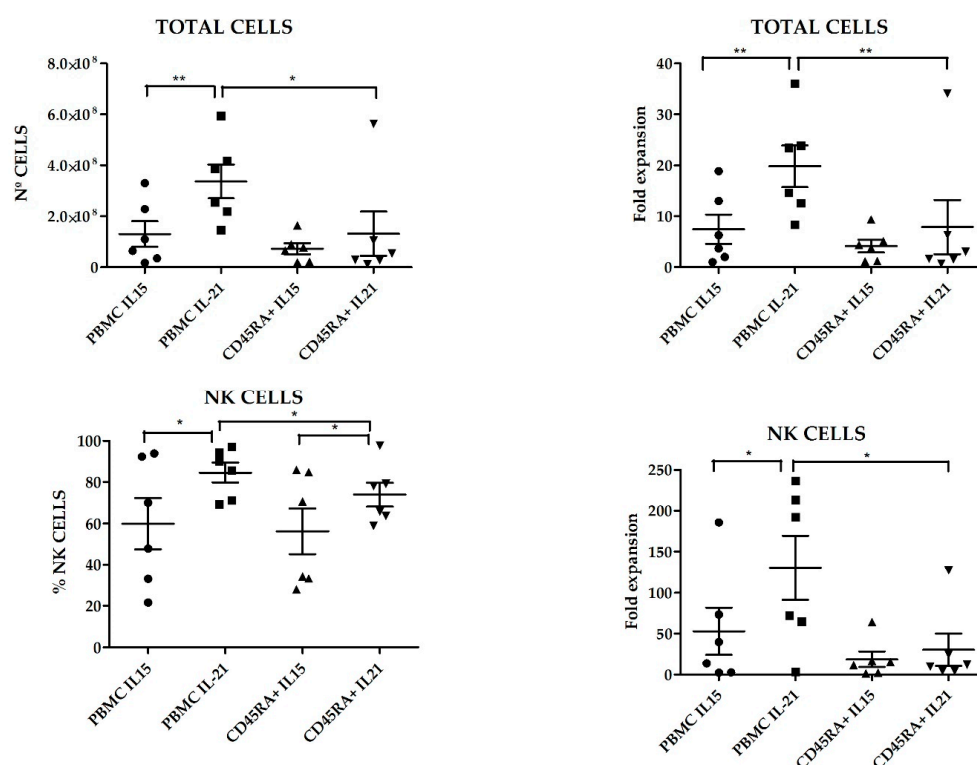


Figure 7. Total cell numbers, NK cell purity and fold expansion of total and NKAE cells using different NK cell sources and different artificial antigen presenting cells (aAPC) ($n = 6$ in each condition). Error bars show mean \pm SEM. * $p < 0.05$, ** $p < 0.01$. Geometrical symbols represent individual data of NKAE obtained from different donors in the conditions specified in the X axis: Dots: PBMC + K562mbIL15; Squares: PBMC + K562mbIL21; triangles: CD45RA⁺ + K562mbIL15; inverted triangles: CD45RA⁺ + K562mbIL21.

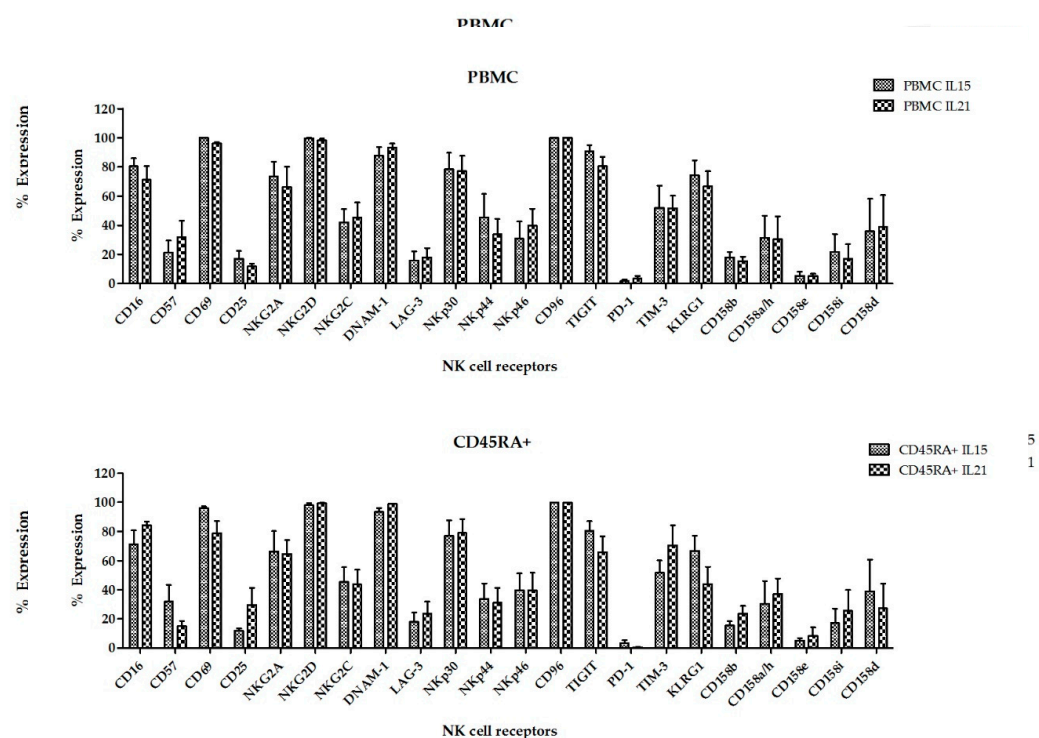


Figure 8. Expression of different NK cell receptors on NKAE cells expanded from PBMC or CD45RA+ cells using K562mbIL15 or K562mbIL21 as aPAP. **Figure 9.** Cytotoxicity of NKAE cells expanded from PBMC or CD45RA+ cells using K562mbIL15 or K562mbIL21 as aPAP. No differences in antitumor ability were observed among the different NKAE cell products. Error bars show mean \pm SEM. *T ratio was 2:1. Geometrical symbols represent individual data of NKAE obtained from different donors in the conditions specified in the X axis. Dots: PBMC; squares: CD45RA+; triangles: K562mbIL15; inverted triangles: K562mbIL21.

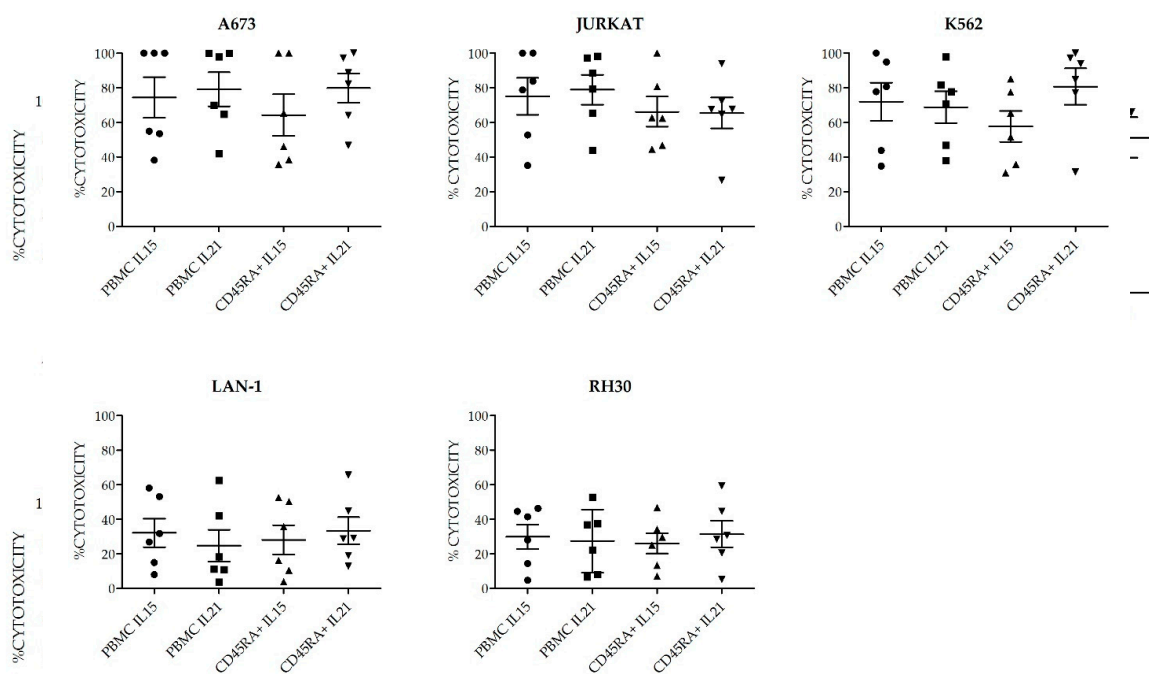


Figure 9. Cytotoxicity of NKAE cells expanded from PBMC or CD45RA+ cells using K562mbIL15 or K562mbIL21 as aPAP. No differences in antitumor ability were observed among the different NKAE cell products. Error bars show mean \pm SEM. *T ratio was 2:1. Geometrical symbols represent individual data of NKAE obtained from different donors in the conditions specified in the X axis. Dots: PBMC; squares: CD45RA+; triangles: K562mbIL15; inverted triangles: K562mbIL21.

2.4. Transcriptome Analysis of Basal NK Cells and Different NKAE Cell Products

To further explore the differences in gene expression of basal NK cells obtained from PBMC or CD45RA⁺ and their respective NKAE cell products expanded with different aAPC (K562mbIL15 or K562mbIL21), RNAseq analysis of two representative donors was performed.

Unsupervised hierarchical clustering of the 15,919 genes remaining after filtering divided the samples into two groups: basal NK cells and NKAE cell products (Figure 10A). NKAE cells were in turn separated into IL21 and IL15-stimulated cells, but no cluster of PBMC and CD45RA⁺-derived NKAE cells was observed. We found a total of 2185 differentially expressed genes (DEGs) in unstimulated and stimulated NK cells. Of the 2185 DEGs, 1178 were upregulated and 1007 were downregulated in stimulated NK cells at a false discovery rate (FDR) of 0.05 and log fold change (log FC) of 2 (Figure 10B). A comprehensive list of the top DEG is provided in Table S2. Kyoto Encyclopedia of Genes and Genomes (KEGG) pathway analysis showed that the DEGs were concentrated in 30 pathways, most of them related to cell growth, cell death and metabolism (cell cycle, hematopoietic cell lineage, p53 signaling pathway, pyrimidine metabolism, etc.) (Table 1). In addition, the DEG was grouped according to their associated gene ontology (GO) terms. While overexpressed genes clustered to biological processes such as cell division, DNA replication and cell proliferation, under expressed genes were involved in cell adhesion and cell migration.

Comparison of IL21 and IL15-stimulated NKAE cells led to the identification of 609 DEGs, 29 of them showing upregulation and 580 showing downregulation in IL21-stimulated NKAE cells (Figure 10C and Table S3). The number of DEGs between IL21 and IL15-stimulated NKAE cells was larger when the cell source was PBMC compared with CD45RA (547 vs. 381 DEGs). The 22 enriched pathways were related to the inflammatory response and the immune system (cytokine–cytokine receptor interaction, hematopoietic cell lineage, asthma, inflammatory bowel disease (IBD), primary immunodeficiency, IL-17 signaling pathway, etc.) (Table 1). GO term enrichment analysis showed cluster to biological processes such as immune response, inflammatory response, phagocytosis, complement activation, B cell receptor signaling pathway and cell adhesion.

Many cytokines and cytokine receptors involved in cell differentiation and activation were overexpressed under IL15 stimulation when compared with IL21 stimulation (CD5, CD4, CD8B, CD3G, CD19, CD22, CD24, CD20, CD23, CD35, IL4, IL5, CD116, CD123, CD33, CD126, CD13, IL1A, IL1B, CD121, IL9R, CD125, CD36 and CD41). Regarding the expression of NK activating and inhibitory receptors, we only identified one killer-cell immunoglobulin-like receptor (KIR) gene differentially expressed between IL21 and IL15-expanded NK cells, KIR2DL3, which was overexpressed in IL-21-expanded NK cells. Differences in the expression of leukocyte immunoglobulin like receptor B1 (LIR1), natural-killer group 2 member A (NKG2A), C (NKG2C) and D (NKG2D) and natural cytotoxicity receptors (NCRs) were not found. Concerning inhibitory checkpoint receptors, programmed cell death 1 (PD1) was overexpressed in IL15-expanded NK cells. We did not find significant changes in the expression of markers of apoptosis and proliferation such as caspase 3 (CASP3), caspase 8 (CASP8), BCL2 apoptosis regulator (BCL2), BCL2 associated X apoptosis regulator (BAX), BCL2-Like 14 apoptosis facilitator (BCL2L14), cyclin dependent kinase inhibitor 2A (CDKN2A), telomerase reverse transcriptase (TERT), MYB proto-oncogene like 2 (MYBL2), BUB1 mitotic checkpoint serine/threonine kinase (BUB1), polo like kinase 1 (PLK1), cyclin E1 (CCNE1), cyclin D1 (CCND1) and cyclin B1 (CCNB1).

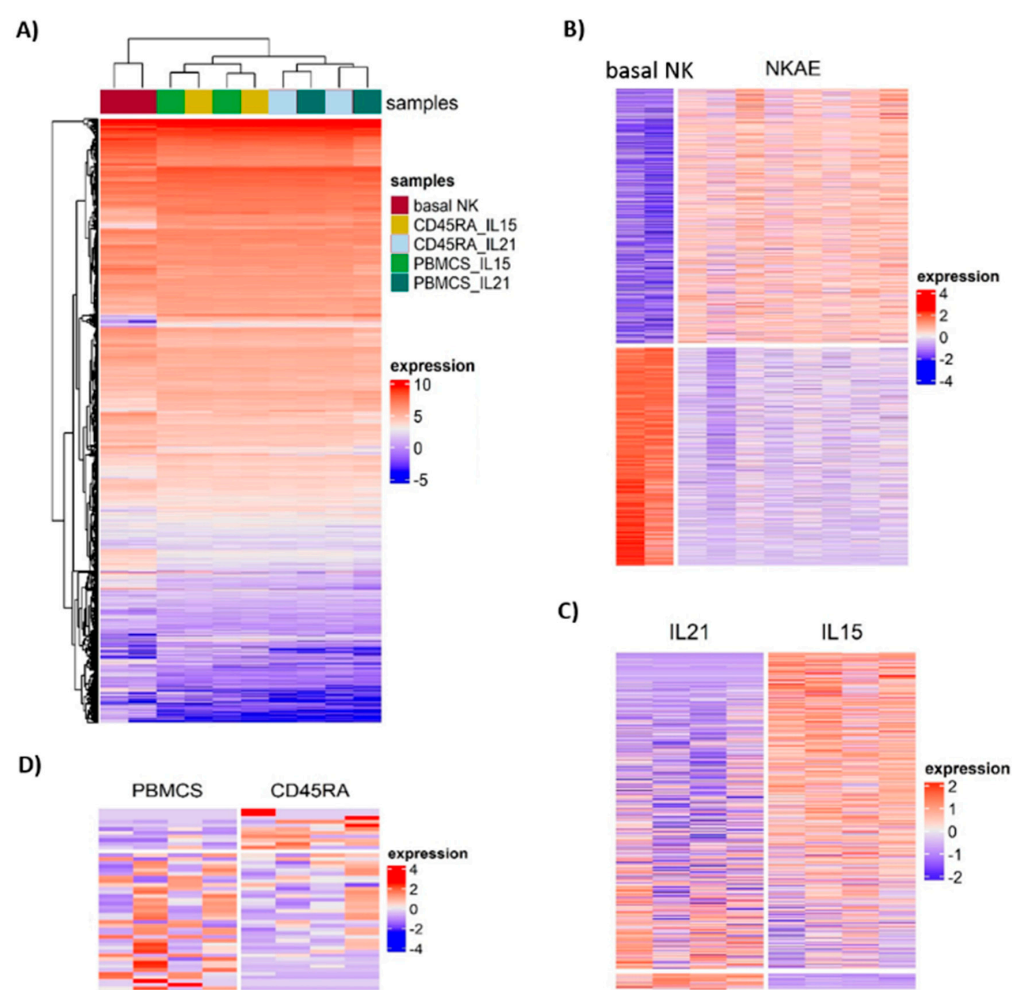


Figure 10. Gene expression profiles of basal NK cells and NKA cell products. (A) Unsupervised hierarchical clustering of NK cells using the 15,919 genes remaining after filtering of NK cells and 15,919 genes remaining after filtering of NK cells. (B) Heatmap of normalized expression values for 118 genes that are differentially expressed between basal NK cells and NKA cell products. (C) Heatmap of normalized expression values for 609 genes that are differentially expressed between IL21 and IL15-stimulated NKA cells. (D) Heatmap of normalized expression values for 48 genes that are differentially expressed between PBMCS and CD45RA⁺-derived NKA cells. Heat map colors correspond to gene expression as indicated in the color key: red (overexpressed) and blue (underexpressed). Each row in the heatmap represents a gene and each column, an individual sample. Deep red line: basal NK cells, CD45RA⁺-derived NKA cells, PBMCS-derived NKA cells, correspond to gene type CD45RA⁺ as indicated in the color key: red (overexpressed) and blue (underexpressed). Each row in the heatmap represents a gene and each column, an individual sample. Deep red line: basal NK cells, green line: IL15-stimulated PBMCS-derived NKA cells, yellow line: IL15-stimulated CD45RA⁺-derived NKA cells, light blue line: IL21-stimulated CD45RA⁺-derived NKA cells, emerald green line: IL21-stimulated PBMCS-derived NKA cells.

Finally, a small number of DEGs was observed between PBMCS and CD45RA⁺-derived NKA cells. Of the 48 DEGs, 37 showed upregulation and 11 downregulation in PBMCS-derived NKA cells (Figure 10D and Table S4). No KEGG pathways or GO terms were significantly enriched for the DEG genes. Nevertheless, among the IL21-stimulated NKA cells, two pathways were enriched when comparing PBMCS and CD45RA⁺-derived NKA cells: hematopoietic cell lineage and arachidonic acid metabolism.

Table 1. KEGG pathways enrichment analysis by differentially expressed genes (DEGs).

	N° of Differentially Expressed Genes	KEGG Significant Pathways
NKAE vs. basal NK cells	2185 DEG (1178 UP + 1107 DOWN)	Cell cycle, Cytokine-cytokine receptor interaction, Viral protein interaction with cytokine and cytokine receptor, Hematopoietic cell lineage, p53 signaling pathway, Cell adhesion molecules (CAMs), Inflammatory bowel disease (IBD), Pyrimidine metabolism, Transcriptional misregulation in cancer, Biosynthesis of amino acids, Glycine, serine and threonine metabolism, Prostate cancer, PI3K-Akt signaling pathway, Antifolate resistance, Asthma, Small cell lung cancer, MAPK signaling pathway, Oocyte meiosis, Human T-cell leukemia virus 1 infection, Chemokine signaling pathway, Leishmaniasis, Cellular senescence, Starch and sucrose metabolism, Tryptophan metabolism, One carbon pool by folate, Carbon metabolism, Glioma, JAK-STAT signaling pathway, Melanoma, HIF-1 signaling pathway
IL21 vs. IL15-stimulated NKAE cells	609 DEG (29 UP + 580 DOWN)	Cytokine-cytokine receptor interaction, Hematopoietic cell lineage, Asthma, Inflammatory bowel disease (IBD), Primary immunodeficiency, IL-17 signaling pathway, Viral protein interaction with cytokine and cytokine receptor, Leishmaniasis, Fc epsilon RI signaling pathway, Osteoclast differentiation, Transcriptional misregulation in cancer, Rheumatoid arthritis, Protein digestion and absorption, Chemokine signaling pathway, T cell receptor signaling pathway, Th17 cell differentiation, JAK-STAT signaling pathway, Arachidonic acid metabolism, Malaria, NF-kappa B signaling pathway, Cell adhesion molecules (CAMs), Ether lipid metabolism
PBMC vs. CD45RA+ derived NKAE cells	48 DEG (37 UP + 11 DOWN)	-

2.5. Production of Clinical Grade NKAE Cells in CliniMACS Prodigy

After the optimization of the conditions to better expand NK cells, we wanted to test the feasibility of manufacturing these NKAE cells for clinical use. To this aim, we performed a clinical-scale completely automated expansion procedure using the CliniMACS Prodigy® device (Miltenyi Biotec, Bergisch Gladbach, Germany). According to our previous results, we used non-mobilized apheresis as a starting material and TexMACS GMP-compliant medium (Miltenyi Biotec, Bergisch Gladbach, Germany). For the clinical manufacturing, GMP-compliant additional steps of CD3 depletion and CD56 selection were performed to abbreviate NK cell expansion times. Either irradiated K562mbIL15 or K562mbIL21 cells were used as aAPC.

A total of $2\text{--}2.5 \times 10^6$ of purified CD56⁺ cells were cocultured with 40×10^6 of irradiated K562mbIL15 or K562mbIL21 cells, at an approximate ratio of 1:20. Viability, number of total cells, percentage and number of NK cells of starting CD56⁺ cells at days +7 and +14 of coculture are shown in Table 2. FCM data showing NK cell purity along the manufacturing process are shown in Figure S4.

Table 2. Characteristics of CD56 starting cells and expanded NKAIE cells a day +7 and +14 (end of culture). (*) Viability measured in CD45⁺ cells. (**) At day 0, analysis was performed in CD56⁺ cells before coculture with K562mbIL15 cells.

K562mbIL15	% Viability (*)	% NK Cells	% T Cells	Total Cells	Total NK Cells
Day 0 (**)	96	87	22.8	2.9×10^6	2.5×10^6
Day +7	95	87.1	1	80×10^6	76×10^6
Day +14	97	97.1	1.2	654×10^6	635×10^6
K562mbIL21	% Viability (*)	% NK Cells	% T Cells	Total Cells	Total NK Cells
Day 0 (**)	96	77	14.8	3.4×10^6	2×10^6
Day +7	99.3	90.7	3.5	107.5×10^6	97.5×10^6
Day +14	97	93	1.6	1498×10^6	1393×10^6

On day 0, before the expansion, both CD56⁺ cells and aAPC met the acceptance criteria (sterility, mycoplasma negative and viability $\geq 70\%$).

At the end of coculture (Day +14), NKAIE cells expanded in CliniMACS Prodigy showed an upregulation of all the receptors analyzed (Figure 11).

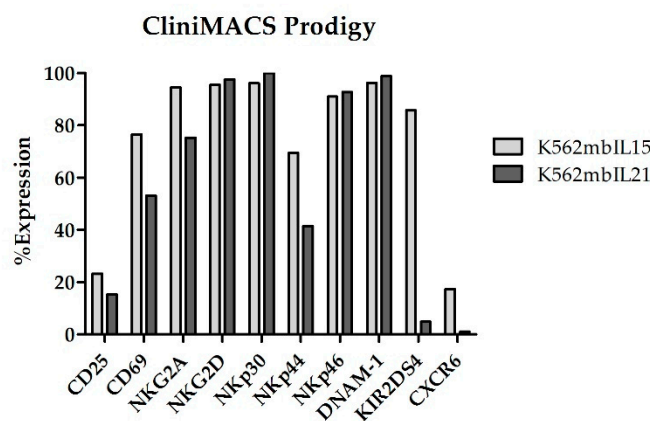


Figure 11. NK cell receptors are upregulated on NKAIE cells manufactured in CliniMACS Prodigy.

The acceptance criteria for the manufactured NKAIE cells at the end of the process included: viability $\geq 70\%$, cytotoxicity against K562 cells at an 8:1 E:T ratio $\geq 50\%$, mycoplasma negative, sterility (0 colony forming units, CFU), endotoxins ≤ 0.25 EU/mL, undetectable bcr/abl (absence of residual aAPC) and no overexpression of oncogenic genes C-MYC and TERT. As shown in Table 3, the manufactured NKAIE cell products complied with the specifications and met the release criteria and, thus, were suitable for clinical use.

The manufactured NKAIE cells met the established acceptance criteria.

Table 3	APC	Sterility	Mycoplasma	Endotoxins	c-myc/tert	Bcr/abl	Cytotoxicity
K562mbIL15	APC	0 CFU	Negative	<0.01 EU/mL	No expression	0%	100%
K562mbIL21	APC	0 CFU	Negative	<0.03 EU/mL	No expression	0%	100%
K562mbIL21	APC	0 CFU	Negative	<0.03 EU/mL	No expression	0%	100%

3. Discussion

Natural killer cells can rapidly kill tumor cells, and have been used in clinical trials

3. Discussion

Natural killer cells can rapidly kill tumor cells, and have been used in clinical trials to treat patients with different malignancies [24]. In this context, significant progress has been made in NK-cell based therapies, both in haploidentical stem cell transplantation (haploSCT) [25–27] or the non-transplant setting [28–30], since NK cells contribute to the graft versus leukemia/tumor (GvL/GvT) effect with no signs of GvHD [26,27,31].

The clinical use of NK cells as therapeutic weapons against cancer has some limitations: (1) these cells represent a small fraction of peripheral white blood cells and large numbers are needed to achieve clinical benefits and (2) NK cells need to be fully activated to induce tumor cell killing. Overcoming these limitations rely on the development of GMP-compliant manufacturing methods. Several protocols to obtain fully activated NK cells for clinical use have been developed. They may differ (among others) in the source of NK cells used: PBMC [32], umbilical cord blood [33] and NK-92 cell line [34]; the addition of different activating cytokines [7,35] or in the use or not of stimulating feeder cells [14,34–36].

The aims of this study were (1) to optimize in small scale NK cell activation and expansion protocol, (2) to test the feasibility of large-scaling this procedure to manufacture NKA cells emulating a clinical application and (3) to demonstrate that the manufactured NKA cell products met the requirements established by the Spanish Regulatory Agency for clinical use. To optimize the best cell culture growth media, we expanded NK cells by coculturing PBMC with irradiated K562mbIL15 in four different GMP-grade growth media (RPMI, SCGM, TexMACs and NK MACS). We found all the cell culture media used yielded similar numbers of total cells and NK cells. Although RPMI expanded lower numbers of cells, the differences with the rest of the media were not statistically significant. TexMACs and NK MACS showed the highest percentage of NK cells and the lowest T cell contamination, indicating they should be the preferred growth culture media to obtain the purest NKA cell products. These results are similar to those published by Klöß et al. [19], showing NK MACs as the best culture medium when compared with X-VIVO-10, SCGM and TexMACS. However, in this publication, compared to the NK cell proliferation in the NK MACS medium, cell expansion rates in the other cell cultures containing X-VIVO-10, SCGM or TexMACS media were significantly lower. These differences could be explained by the continued use of higher concentrations of IL-2 in their experiments (1000 IU/mL vs. 10–100 IU/mL), or the use of different starting cells (purified CD56+CD3+ cells instead of total PBMC), and the coculture of starting cells with irradiated aAPC in our experiments. The lowest total cell and NK cells fold expansion that we observed in those cultures containing RPMI are in line with the observations of Duck et al. who described a better activation and expansion of NK cells when using SCGM compared to RPMI-1640 [37].

Once we had optimized the cell culture medium, we tested the feasibility of obtaining NKA cells from CD45RA⁺ fraction. CD45RA⁺ cells were enriched in the central memory and effector memory T cells and had the ability to target previous pathogens or vaccines. Additionally, CD45RA⁺ cells decreased alloreactivity and lacked naïve T cells, responsible for GVH reactions. One way to protect the host from infections after HSCT is to infuse CD45RA⁺ cells as DLI [38]. CD45RA⁺ cells are obtained upon depletion of CD45RA⁺ cells. This fraction is enriched in naïve T cells and NK cells, and thus, could be a potential source of NK cells to obtain NKA cells. When CD45RA⁺ cells from G-CSF mobilized apheresis were used to obtain NKA cells, no expansion of either total or NK cells was observed. However, those CD45RA⁺ cells from non-mobilized apheresis yielded similar numbers of total and NK cells to those obtained from total PBMC, proving the feasibility of using this cell fraction as a source of NK cells to obtain NKA. The inability to expand NK cells from G-CSF mobilized apheresis that we observed could be somehow expected, as the negative impact of G-CSF on NK cells mobilization and cytotoxicity has been previously reported [39,40]. In the future, if mobilization of progenitor hematopoietic cells is needed, we could consider the use of plerixafor, as it has been proved to effectively mobilize NK cells to the peripheral blood [41].

After we proved the feasibility of expanding NK cells from CD45RA⁺ fraction, we analyzed potential differences in NKA cells obtained from total PBMC or CD45RA⁺ cells after coculture with irradiated K562mbIL15 or K562mbIL21 cells. Taking into account only the source of NK cells used, we observed a higher fold increase of total and NK cells when PBMC were used compared to CD45RA⁺ cells. Additionally, when K562mbIL21 cells were used as aAPC larger numbers of total cells and higher NK cell purity were achieved, regardless of the NK cell source used. All these data taken together suggest that coculture of PBMC with K562mbIL21 cells should be the method of choice to achieve large numbers of purified NKA cells. The enhanced proliferation ability of K562mbIL21 expanded NK cells was demonstrated before [42]. In this report, Denman C J et al. observed that those NK cells that expanded with K562mbIL21 presented less senescence and longer telomeres than those expanded with K562mbIL15, suggesting this could be a possible mechanism to explain their sustained proliferation. Nevertheless, the NKA cells obtained by using different NK cell sources or aAPC, showed a similar expression of NK cell receptors and comparable antitumor cytotoxicity in vitro against different tumor cell lines.

When transcriptome was analyzed, marked differences were observed in the gene expression profile of stimulated and unstimulated NK cells, with DEGs mostly related to cell growth and metabolism. These changes in gene expression reflect the activation and expansion taking place during NK stimulation. Some of these DEGs have been previously identified with high fold change when comparing expanded and unstimulated NK cells [11,43] such as ubiquitin conjugating enzyme E2 C (UBE2C), thymidine kinase 1 (TK1), aurora kinase B (AURKB), ribonucleotide reductase regulatory subunit M2 (RRM2) and ficolin 1 (FCN1), and many of them are involved in cell cycle progression.

A high number of DEG was identified between IL21 and IL15-stimulated NKA cells, especially when the cell source was PBMC. These results indicate that IL21 and IL15 had different effects on NK cell expansion, producing changes in the expression of different cytokines and cytokine receptors. Most of the DEG were downregulated in IL21-stimulated NKA cells when compared with IL15-stimulated NKA cells. Since these genes were involved in pathways such as hematopoietic cell lineage, chemokine signaling pathway, JAK-STAT signaling pathway and PI3K-Akt signaling pathway, the differential expression of these genes could promote a more undifferentiated phenotype of NK cells under IL21 stimulation, while a more activating phenotype could be associated to IL15 stimulation.

When comparing IL21 and IL15-expanded NK cells, Denman et al. [42] found similar expression profiles, with CD160 as the only differentially expressed gene. Nevertheless, only 96 genes were assessed by these authors in contrast to the 15,919 genes analyzed in this work, which explains the lack of overlap between both studies. In addition, these authors observed an increase in the proliferation of IL21-expanded NK cells, which was associated with an increased in telomere length. In the present study, although we observed a more proliferative phenotype of IL21-expanded NK cells, we did not find an increase in the expression of telomerase reverse transcriptase (TERT) and other genes involved in telomere length regulation. However, the decrease in cytokines and cytokine receptors related to cell differentiation could explain a more proliferative phenotype. The similar expression of cytotoxicity receptors observed in the transcriptome analysis between IL21 and IL15-expanded NK cells is in accordance with the comparable surface expression of NK cell receptors observed in FCM, and the functional experiments, where no significant differences in cytotoxicity were observed.

In sum, we observed a similar gene expression profile between PBMC and CD45RA⁺-derived NKA cells, which suggests that stimulation of both cell sources give rise to NK cells with similar phenotypes, and this hypothesis was confirmed at least in part through the analysis of the surface expression of NK cell receptors by FCM. Nevertheless, when IL21-stimulated, PBMC-derived NKA cells showed downregulation of the hematopoietic cell lineage pathway, suggesting a more proliferative phenotype than CD45RA⁺-derived NKA cells. These results were in accordance with the cell culture experiments, where PBMC-derived NKA cells expanded more than CD45RA⁺-derived NKA cells.

Once we had optimized the cell culture growth medium and the preferred NK cells source, we moved a step further to translate these protocols to the clinical and we manufactured clinical-grade NKA cells in GMP-compliant conditions. We ran two manufacturing processes in CliniMACS Prodigy coculturing CD56⁺ cells with irradiated K562mbIL15 or its counterpart aAPC with IL21. In the clinical setting is critical to consider two important issues (1) the need to infuse the patients as early as possible and (2) to avoid undesirable GvH reactions caused by residual T cells. Thus, in an attempt to shorten the NK cell expansion times and minimize the risk of T cell contamination in the final NKA cell products, we used already purified CD56⁺ cells instead of total PBMC as starting cells. Both protocols using either K562mbIL15 or K562mbIL21 achieved large numbers of fully activated and highly cytotoxic NKA cells, and these manufactured NK cell products met the release criteria and complied with the specifications from the Spanish Regulatory Agency for manufacturing under aseptic conditions. However, co-culture of CD56⁺ cells with K562mbIL21 cells yielded an NK cell fold increase 2.7 times higher, and the NKA cells showed a more potent cytolytic capacity against K562 cells than those expanded with K562mbIL15 cells. Indicating that, as we had observed in the small-scale research-grade experiments, the use of K562mbIL21 cells as aAPC could be advantageous. Nevertheless, it is important to note that only one GMP-grade large-scale manufacturing process with each cell line and using two different healthy donors was performed, for this reason, the differences that we observed could also be explained, at least in part, by the interdonor variability. In previous clinical trials carried out in our group, clinical-grade NKA cells were obtained by manual coculture of PBMC and irradiated K562mbIL15 in IL-2+AB serum-supplemented RPMI [32]. By these means, the total cells, total NK cells and the NK cell purity ($639.78 \times 10^6 \pm 435.81$, $515.23 \times 10^6 \pm 345.03$ and $79.93\% \pm 17.43\%$, respectively) were lower than those we obtained in the present study. Thus, the results reported in this manuscript could demonstrate that the use of CD56⁺ cells as the starting cells, K562mbIL21 as aAPC, TexMACS as the cell culture growth medium and the CliniMACS Prodigy device constitute a much more advantageous strategy to obtain clinical-grade NKA cells.

In summary, we optimized a protocol to expand large numbers of fully functional NK cells from different sources, culture media and aAPC, and we demonstrated the feasibility of clinical-scale this procedure by using the CliniMACs Prodigy device, a semiautomated closed system. The NKA cells manufactured by these means are suitable for direct infusion to the patient or cryopreservation and could also serve as a platform for more advanced NK cell therapies such as a combination with BiKs or genetic modification to express chimeric antigen receptors (CARs).

4. Materials and Methods

4.1. Source of NK Cells and aAPC

Peripheral blood mononuclear cells (PBMCs) were isolated from buffy coats from healthy volunteers by using Ficoll–Paque gradient centrifugation. CD45RA⁺ fractions were obtained after magnetic enrichment using CD45RA microbeads and running “Pessel” program in the AutoMACS device (both from Miltenyi Biotec) following manufacturer instructions. As the CD45RA⁺ fraction is a commonly discarded material from haploidentical transplantation procedures, in some cases, CD45RA⁺ cells were obtained from the Hematology Service at Hospital La Paz after written informed consent, in accordance with the Declaration of Helsinki and La Paz University Hospital Ethics Committee (ethical code 4917), and this study is part of an approved clinical trial with EudraCT: 2016-003578-42. Buffy coats were obtained from the Transfusions Centre of the Comunidad de Madrid upon institutional review board approval. All donors complied with the requirements regarding quality and safety for the donation, obtaining, storage, distribution and preservation of human cells and tissues under the Spanish specific regulation.

K562mbIL15 and K562mbIL21 cells were kindly provided by Prof. Campana (National University Hospital, Singapore) and Prof. Lee (Nationwide Children’s Hospital, Ohio, EEUU), respectively and irradiated with 100 Gy before coculture.

4.2. Expansion Procedure

For the culture medium optimization, PBMCs were cocultured with irradiated K562mbIL15 cells in a 1:1.5 ratio in the indicated growth medium: RPMI-1640 (RPMI, Lonza, Basel, Belgium), stem cell growth medium (SCGM, Cellgenix, Freiburg, Germany), NK MACS (Miltenyi Biotec, Bergisch Gladbach, Germany) or TexMACS GMP medium (TexMACS, Miltenyi Biotec, Bergisch Gladbach, Germany). All media were supplemented with 10% human AB serum (Sigma, St. Louis, MO, USA) and IL-2 (Miltenyi Biotec, Bergisch Gladbach, Germany) at 10 IU/mL for the first week and 100 IU/mL thereafter. Fresh medium was added every 2 days to a final concentration of $1\text{--}2 \times 10^6$ cell/mL.

To explore the feasibility of expanding NK cells from the CD45RA⁺ fraction, PBMCs or CD45RA⁺ cells from mobilized or non-mobilized apheresis were cocultured with irradiated K562mbIL15 in a 1:1.5 ratio, using complete TexMACs.

To determine the best NK cell source and aAPC, either PBMC or CD45RA⁺ cells were cocultured with irradiated K562mbIL15 or K562mbIL21 in a 1:1.5 ratio, using complete TexMACs.

Total cell expansion, percentage of NK cells and other lymphocyte subpopulations and viability of the cultures were monitored every week by flow cytometry. Cytotoxicity of expanded NK cells was tested against different tumor target cells between days 14 and 21 of NK cell expansion.

4.3. Antibodies and Flow Cytometry

Lymphocyte subpopulations were determined in a Navios flow cytometer (Beckman Coulter, Brea, CA, USA) using the conjugated antibodies listed in Table S5. T lymphocytes were defined as CD45⁺CD3⁺CD56[−], B lymphocytes as CD45⁺CD19⁺CD20⁺, NKT as CD45⁺CD3⁺CD56⁺ and NK cells as CD45⁺CD56⁺CD3[−] and further subdivided in dim (CD56^{dim}CD16⁺) and bright (CD56^{bright}CD16[−]) subsets.

Expression of functionally relevant receptors was evaluated within the NK population. FlowJo v10.0.7 software (BD, San Jose, CA, USA) was used for data analysis.

4.4. In Vitro Cytotoxicity Assays

Cytotoxicity of NKAIE cells was assayed between days 13 and 20 of expansion by performing conventional 4 h Europium-TDA assays. K562, Jurkat, A673, RH30 and LAN-1 cell lines were used as targets. K562, Jurkat, A673 and LAN-1 cells were purchased from American Type Culture Collection (ATCC). RH30 was kindly provided by Dr. Roma (Vall D'Hebron Institute of Research, VHIR). All cell lines were cultured following ATCC's recommendations and routinely tested for mycoplasma. Conventional 4-h europium-TDA release assays (Perkin Elmer, Waltham, MA, USA) at different effector:target ratios (starting at 8:1) were performed as previously described [44].

The following formulas were used to calculate spontaneous and specific cytotoxicity: % specific release = (experimental release – spontaneous release)/(maximum release – spontaneous release) × 100%, spontaneous release = (spontaneous release-background)/(maximum release-background) × 100.

4.5. Gene Expression Profiling

4.5.1. Library Preparation and Sequencing

NK cells from two representative donors (1 and 2) were obtained pre and post-expansion. Total RNA was isolated using the RNeasy Mini kit (QIAGEN, Hilden, Germany) according to the manufacturer's instructions. To remove residual genomic DNA, the RNA samples were digested with DNase I. The RNA concentration was assessed by fluorescence quantitation using Qubit 2.0 and the HS RNA assay kit (Thermo Fisher Scientific Inc., Waltham, MA, USA), the RNA purity by spectrophotometry using Nanodrop 2000 (Thermo Fisher Scientific Inc., Waltham, MA, USA) and the RNA integrity by electrophoresis using TapeStation 4200 RNA ScreenTape (Agilent Technologies, Santa Clara, CA, USA). Library preparation and RNA sequencing were performed at Nimgenetics Com-

pany (Madrid, Spain). Library samples were prepared with the TruSeq Stranded mRNA Library Prep kit (Illumina, San Diego, CA, USA) as recommended by the manufacturer. Paired-end sequencing (2×100 pb) was performed with NovaSeq 6000 system (Illumina, San Diego, CA, USA), with a minimum of 25 million reads per sample and read quality of $90\% > Q30$.

4.5.2. RNA Sequencing Analysis of NK Cells

The resulting reads were aligned using HISAT2 and hg19 as a reference. Transcript assembly and quantification were achieved with StringTie and the differential gene expression analysis between the different conditions was performed with edgeR [45] using log fold change ($\log FC \geq 2$) and false discovery rate ($FDR < 0.05$) as the threshold. Clustered heatmaps were done with genes that have at least one count per million reads in more than one sample. The functional analysis was performed with clusterProfiler [46] using the enrichKEGG function.

4.6. Manufacturing of Clinical-Grade NKAE Cells

In an attempt to shorten the times to obtain clinical-grade NKAE cell products with highest NK cell purity and less T cell contamination, ready to infuse into the patients with no further processing, we purified the $CD56^+$ fraction before the expansion. The ex vivo immunomagnetic purification procedure comprised $CD3$ depletion followed by $CD56$ cell selection as previously described [47]. Automated activation and expansion process were performed in CliniMACS Prodigy instrument using the CliniMACS T520 tubing set and T cell transduction (TCT) protocol. In detail, at day 0, the coculture was initiated by using 2×10^6 – 2.5×10^6 NK cells and 4×10^7 K562mbIL15 or K562mbIL21 cells previously irradiated with 100 Gy. Cells were cultured in 70 mL of GMP-grade TexMACs medium supplemented with 5% human AB serum (Sigma) and 100 IU/mL of IL-2 (Miltenyi Biotec). NK cells were incubated in the culture chamber (37°C and 5% CO_2) in a static culture for the first week. At day +7, agitation was started and 70 mL of fresh complete medium were added to the culture. Cells were expanded for 14 days before being harvested. Sampling was performed at day +7 for process controls, including cell counts, viability, analysis of $CD56^+ / CD3^-$ cell content by FCM, mycoplasma and sterility. At the end of the expansion, cells were automatically collected in 0.9% sodium chloride solution supplemented with 0.5% human serum albumin (Albutein 20%, Grifols, Barcelona, Spain), in a sterile bag. Release quality controls: total cell counts, viability, analysis of $CD56^+ / CD3^-$, $CD3^+ / CD56^-$ and $CD56^+ / CD3^+$ cell content by FCM, cytotoxicity against K562 cells, Gram staining, endotoxins, cell impurities (K562mbIL15 or K562 mbIL21) by qPCR, mycoplasma and sterility were performed at the end of the process.

4.6.1. Analysis of Cell Count, Viability and NK Cell Purity

NKAE cells were counted in a CELL-DYN Emerald hematology analyzer (Abbott) and analyzed for their viability, immunophenotype and activation status by FCM as previously described.

4.6.2. Cytotoxicity

Potency of manufactured NKAE cells was tested by performing Europium-TDA conventional assays against K562 cells at 8:1, 4:1, 2:1 and 1:1 E:T ratios.

4.6.3. Microbiological Tests

The expansion cell products were tested for sterility, according to Eu Ph 2.6.21. The microbiological tests were developed by the Clinical Microbiology and Parasitology Service of HULP by conventional microbiology techniques. In summary, sample tests were inoculated into separate culture media and the growth of viable microorganisms was tested after several days.

4.6.4. Analyses of Non-Cellular Impurities

The detection of non-cellular impurities was carried out in accordance with the methodology recommendations of Chapter 2.6.21 and 2.6.7 of the European Pharmacopeia (EuPh) for mycoplasma and Chapter 2.6.14 for endotoxins. A DNA-binding dye-based qPCR system was employed for the detection of mycoplasma DNA in cell cultures. In the final products, the levels of endotoxins were quantified by the endotoxin test Endosafe-PTS (Charles River). Both assays were developed by the Clinical Microbiology and Parasitology Service of HULP.

4.6.5. Analysis of Cellular Impurities

Given that the aAPC used for NK cell activation and expansion is a tumor cell line is necessary to ensure the absence of residual K562mbIL15 or K562mbIL21 cells in the final NKA-E cells products. Both aAPC contain the fusion gene BCR/ABL, so the presence of residual cells was analyzed by performing a real-time PCR (RT-PCR) for the Mbcr transcript as previously described [48].

4.6.6. Genetic Tests

Genetic tests were carried out at the end of the manufacturing process.

The expression of oncogenes c-Myc and telomerase reverse transcriptase (TERT) by RT-PCR. Briefly, the total RNA was isolated using the RNeasy kit (Sigma), and reverse transcription was performed with SuperScript IV (Invitrogen, ThermoFisher Scientific Inc., Waltham, MA, USA). The qRT-PCR was performed on the ABI Prism 7900HT sequence detection system (Applied Biosystems, ThermoFisher Scientific Inc., Waltham, MA, USA), using the TaqMan universal PCR master mix and TaqMan gene expression assay probes (Applied Biosystems), according to the manufacturer's specifications. The assay identification numbers were as follows: c-Myc, Hs00153408_m1; TERT, Hs00972656_m1 and GUS β , Hs00939627_m1. The thermal cycler conditions were: 10 min at 95 °C and 40 cycles of 95 °C for 15 s followed by 60 °C for 1 min. All the reactions were performed in triplicate. The amplification data were analyzed with ABI Prism sequence detection software 2.1 (Applied Biosystems) and the relative c-MYC and TERT expression was calculated by normalization against human GUS β expression.

To rule out chromosomal aberrations, comparative genomic hybridization (CGH) was performed in NKA-E cells. DNA from the NKA-E cell products was isolated using the AllPrep DNA/RNA Micro Kit (Qiagen, Hilden, Germany) and hybridized with male reference DNA (Promega Biotech, Alcobendas, Madrid, Spain) on a 60,000 oligonucleotide CGH-SNP platform (Agilent, Santa Clara, CA, USA). The data were analyzed with Agilent CGH analytics 3.4 software (Santa Clara, CA, USA), using the statistical algorithm ADAM-2 according to a sensitivity threshold of 6.0 and an average window of 0.5 Mb. Alterations in the DNA copy number were considered when at least 5 consecutive probes were altered. Probes were annotated against the human assembly GRCh37 (also known as hg19).

4.7. Statistical Analysis

Statistical analysis was performed using GraphPad Prism software. Results are shown as mean \pm standard error of the mean (SEM). Data sets were analyzed for Gaussian distribution by using Kolmogorov–Smirnov, D-Agostino and Pearson and Shapiro–Wilk tests. Those data without normal distribution were compared with non-parametric tests. Two-tailed Student's paired *t* test was used when cells from the same donor in different conditions were compared. For comparisons between three or more groups, a one-way ANOVA test was used to determine statistical significance. Dunn's multiple comparisons post hoc tests were run in conjunction with one-way ANOVAs and all groups were compared with one another. When two or more variables were compared, two-way ANOVA tests followed by Bonferroni post hoc tests to compare replicates were run. In all cases, a *p* value of <0.05 was deemed to be statistically significant.

5. Conclusions

In this report, we optimized a protocol to obtain NKAE cells by using four different culture growth media (RPMI, SCGM, TexMACs and NKMACs), two different NK cell sources: PBMC or CD45RA⁺ cells and two distinct irradiated aAPC (K562mbIL15 or K562mbIL21). We determined that TexMACs was the most suitable cell culture medium to expand NK cells. NK cells could be activated and expanded from those CD45RA⁺ cells obtained from non-mobilized apheresis, although the use of PBMC as the NK cell source yielded the highest numbers of purified NKAE cells. When K562mbIL21 was chosen as aAPC, the highest numbers of NKAE cells with less contamination of T cells were achieved regardless of the NK cell source used. All NKAE cells obtained from either PBMC or CD45RA⁺ expanded with K562mbIL15 or K562mbIL21 showed comparable antitumor ability against sarcoma, T-ALL, CML, neuroblastoma and rhabdomyosarcoma cells. Finally, we fulfilled clinical manufacturing of NKAE cells in an automated closed system CliniMACS Prodigy by using CD56⁺ cells and either irradiated K562mbIL15 or K562mbIL21. In both processes, sufficient numbers of NKAE cells with high purity and low T cell contamination were manufactured after 14 days of culture. The different release tests performed showed that manufactured NKAE cells met the requirements and specifications from the regulatory agency, and thus were suitable for clinical use.

Supplementary Materials: The following are available online at <https://www.mdpi.com/2072-6694/13/3/577/s1>, Figure S1: Total cell numbers contained in PBMC, CD45RA⁺ cells from mobilized and no-mobilized apheresis. Figure S2: Representative FCM data of NK cell purity observed along the expansion in the different conditions. Figure S3: Representative data of the expression of NK cell receptors expressed in PBMC, CD45RA⁺ cells and in NKAEs at day +21. Figure S4: NK cell purity along the manufacturing protocol in CliniMACS Prodigy. Table S1: Total cell number, viability and percentages of lymphocyte subsets found in NKAEs at different time points cultured in RPMI, SCGM, TexMACs or NK MACS. Table S2: Top 100 overexpressed and 100 underexpressed genes in stimulated NK cells when compared with unstimulated NK cells, ranked by fold change. Table S3: Top 25 overexpressed and 25 underexpressed genes in IL21-stimulated NK cells when compared with IL15-stimulated NK cells, ranked by fold change, Table S4: DEG between PBMC- and CD45RA⁺-derived NK cells ranked by fold change.

Author Contributions: Conceptualization, L.F. and A.P.-M.; Data curation, A.E., N.M., I.M. and L.F.; Formal analysis, A.F., A.N.-Z., A.E., N.M., I.M., C.M. and L.F.; Funding acquisition, J.M. and A.P.-M.; Investigation, A.F., A.N.-Z., A.E., N.M., I.M., M.C., G.C., D.L., C.R.-A., M.V., C.M., A.V., A.L., L.F. and A.P.-M.; Methodology, A.F., A.N.-Z., A.E., N.M., B.R.-C., I.M., A.P., M.C., G.C., D.L., C.R.-A., M.V., C.M., A.L. and L.F.; Project administration, C.F. and A.P.-M.; Resources, A.V., J.M. and A.P.-M.; Software, B.R.-C. and C.R.-A.; Supervision, A.E., I.M. and L.F.; Validation, A.E., N.M., B.R.-C., I.M., A.L., J.M., L.F. and A.P.-M.; Visualization, A.E., I.M., J.M., L.F. and A.P.-M.; Writing—original draft, M.V. and L.F.; Writing—review and editing, A.E., N.M., I.M., D.L., C.F., L.F. and A.P.-M. All authors have read and agreed to the published version of the manuscript.

Funding: This work was supported by the National Health Service of Spain, Instituto de Salud Carlos III (ISCIII), FONDOS FEDER grant (FIS) PI18/01301 to Pérez-Martínez A, CRIS Foundation to Beat Cancer to Escudero A, Fernández A; Navarro A, Mirones I, and Fundación Mari Paz Jiménez Casado and La Sonrisa de Álex to Vela M.

Institutional Review Board Statement: The study was conducted according to the guidelines of the Declaration of Helsinki and approved by the Ethics Committee of La Paz University Hospital (ethical code 4917, approved in Madrid on the 26th of December 2017). This study is part of an approved clinical trial with EudraCT: 2016-003578-42.

Informed Consent Statement: Informed consent was obtained from all subjects involved in the study.

Data Availability Statement: The RNAseq data discussed in this publication have been deposited in NCBI's Gene Expression Omnibus (Edgar et al., 2002, doi:10.1093/nar/30.1.207) and are accessible through GEO Series accession number GSE165849 (<https://www.ncbi.nlm.nih.gov/geo/query/acc.cgi?acc=GSE165849>).

Conflicts of Interest: D.L. works for Miltenyi Biotec. The rest of authors declare no conflict of interest.

References

- Shimasaki, N.; Jain, A.; Campana, D. NK cells for cancer immunotherapy. *Nat. Rev. Drug Discov.* **2020**, *19*, 200–218. [\[CrossRef\]](#) [\[PubMed\]](#)
- Miller, J.S.; Soignier, Y.; Panoskaltsis-Mortari, A.; McNearney, S.A.; Yun, G.H.; Fautsch, S.K.; McKenna, D.; Le, C.; Defor, T.E.; Burns, L.J.; et al. Successful adoptive transfer and in vivo expansion of human haploidentical NK cells in patients with cancer. *Blood* **2005**, *105*, 3051–3057. [\[CrossRef\]](#) [\[PubMed\]](#)
- Terme, M.; Ullrich, E.; Delahaye, N.F.; Chaput, N.; Zitvogel, L. Natural killer cell-directed therapies: Moving from unexpected results to successful strategies. *Nat. Immunol.* **2008**, *9*, 486–494. [\[CrossRef\]](#) [\[PubMed\]](#)
- Cella, M.; Otero, K.; Colonna, M. Expansion of human NK-22 cells with IL-7, IL-2, and IL-1beta reveals intrinsic functional plasticity. *Proc. Natl. Acad. Sci. USA* **2010**, *107*, 10961–10966. [\[CrossRef\]](#) [\[PubMed\]](#)
- Koehl, U.; Sorensen, J.; Esser, R.; Zimmermann, S.; Gruttner, H.P.; Tonn, T.; Seidl, C.; Seifried, E.; Klingebiel, T.; Schwabe, D. IL-2 activated NK cell immunotherapy of three children after haploidentical stem cell transplantation. *Blood Cells Mol. Dis.* **2004**, *33*, 261–266. [\[PubMed\]](#)
- Son, Y.I.; Dallal, R.M.; Mailliard, R.B.; Egawa, S.; Jonak, Z.L.; Lotze, M.T. Interleukin-18 (IL-18) synergizes with IL-2 to enhance cytotoxicity, interferon- γ production, and expansion of natural killer cells. *Cancer Res.* **2001**, *61*, 884–888.
- Pérez-Martínez, A.; Fernández, L.; Valentín, J.; Martínez-Romera, I.; Corral, M.D.; Ramírez, M.; Abad, L.; Santamaría, S.; González-Vicent, M.; Sirvent, S.; et al. A phase I/II trial of interleukin-15-stimulated natural killer cell infusion after haplo-identical stem cell transplantation for pediatric refractory solid tumors. *Cytotherapy* **2008**, *17*, 1594–1603. [\[CrossRef\]](#)
- Hosseini, E.; Ghasemzadeh, M.; Kamalizad, M.; Schwarzer, A.P. Ex vivo expansion of CD3depleted cord blood-MNCs in the presence of bone marrow stromal cells; an appropriate strategy to provide functional NK cells applicable for cellular therapy. *Stem Cell Res.* **2017**, *19*, 148–155. [\[CrossRef\]](#)
- Masuyama, J.; Murakami, T.; Iwamoto, S.; Fujita, S. Ex vivo expansion of natural killer cells from human peripheral blood mononuclear cells co-stimulated with anti-CD3 and anti-CD52 monoclonal antibodies. *Cytotherapy* **2016**, *18*, 80–90. [\[CrossRef\]](#)
- Lee, H.R.; Son, C.H.; Koh, E.K.; Bae, J.H.; Kang, C.D.; Yang, K.; Park, Y.S. Expansion of cytotoxic natural killer cells using irradiated autologous peripheral blood mononuclear cells and anti-CD16 antibody. *Sci. Rep.* **2017**, *7*, 1–13. [\[CrossRef\]](#)
- Fujisaki, H.; Kakuda, H.; Shimasaki, N.; Imai, C.; Ma, J.; Lockey, T.; Eldridge, P.; Leung, W.H.; Campana, D. Expansion of highly cytotoxic human natural killer cells for cancer cell therapy. *Cancer Res.* **2009**, *69*, 4010–4017. [\[CrossRef\]](#) [\[PubMed\]](#)
- Wang, X.; Lee, D.A.; Wang, Y.; Wang, L.; Yao, Y.; Lin, Z.; Cheng, J.; Zhu, S. Membrane-bound interleukin-21 and CD137 ligand induce functional human natural killer cells from peripheral blood mononuclear cells through STAT-3 activation. *Clin. Exp. Immunol.* **2013**, *172*, 104–112. [\[CrossRef\]](#) [\[PubMed\]](#)
- Granzin, M.; Wagner, J.; Köhl, U.; Cerwenka, A.; Huppert, V.; Ullrich, E. Shaping of natural killer cell antitumor activity by ex vivo cultivation. *Front. Immunol.* **2017**, *8*. [\[CrossRef\]](#) [\[PubMed\]](#)
- Cho, D.; Shook, D.R.; Shimasaki, N.; Chang, Y.-H.; Fujisaki, H.; Campana, D. Cytotoxicity of Activated Natural Killer Cells against Pediatric Solid Tumors. *Clin. Cancer Res.* **2010**, *16*, 3901–3909. [\[CrossRef\]](#) [\[PubMed\]](#)
- Gong, W.; Xiao, W.; Hu, M.; Weng, X.; Qian, L.; Pan, X.; Ji, M. Ex vivo expansion of natural killer cells with high cytotoxicity by K562 cells modified to co-express major histocompatibility complex class I chain-related protein A, 4-1BB ligand, and interleukin-15. *Tissue Antigens* **2010**, *76*, 467–475. [\[CrossRef\]](#) [\[PubMed\]](#)
- Apel, M.; Brüning, M.; Granzin, M.; Essl, M.; Stuth, J.; Blaschke, J.; Spiegel, I.; Müller, S.; Kabaha, E.; Fahrendorff, E.; et al. Integrated clinical scale manufacturing system for cellular products derived by magnetic cell separation, centrifugation and cell culture. *Chemie-Ingenieur-Technik* **2013**, *85*, 103–110. [\[CrossRef\]](#)
- Oberschmidt, O.; Morgan, M.; Huppert, V.; Kessler, J.; Gardlowski, T.; Matthies, N.; Aleksandrova, K.; Arseniev, L.; Schambach, A.; Koehl, U.; et al. Development of Automated Separation, Expansion, and Quality Control Protocols for Clinical-Scale Manufacturing of Primary Human NK Cells and Alpharetroviral Chimeric Antigen Receptor Engineering. *Hum. Gene Ther. Methods* **2019**. [\[CrossRef\]](#)
- Granzin, M.; Soltenborn, S.; Müller, S.; Kollet, J.; Berg, M.; Cerwenka, A.; Childs, R.W.; Huppert, V. Fully automated expansion and activation of clinical-grade natural killer cells for adoptive immunotherapy. *Cytotherapy* **2015**, *17*, 621–632. [\[CrossRef\]](#)
- Klöß, S.; Oberschmidt, O.; Morgan, M.; Dahlke, J.; Arseniev, L.; Huppert, V.; Granzin, M.; Gardlowski, T.; Matthies, N.; Soltenborn, S.; et al. Optimization of Human NK Cell Manufacturing: Fully Automated Separation, Improved Ex Vivo Expansion Using IL-21 with Autologous Feeder Cells, and Generation of Anti-CD123-CAR-Expressing Effector Cells. *Hum. Gene Ther.* **2017**, *28*, 897–913. [\[CrossRef\]](#)
- Triplett, B.M.; Shook, D.R.; Eldridge, P.; Li, Y.; Kang, G.; Dallas, M.; Hartford, C.; Srinivasan, A.; Chan, W.K.; Suwannasae, D.; et al. Rapid memory T-cell reconstitution recapitulating CD45RA-depleted haploidentical transplant graft content in patients with hematologic malignancies. *Bone Marrow Transplant.* **2015**, *50*, 968–977. [\[CrossRef\]](#)
- Sisinni, L.; Gasior, M.; de Paz, R.; Querol, S.; Bueno, D.; Fernández, L.; Marsal, J.; Sastre, A.; Gimeno, R.; Alonso, L.; et al. Unexpected High Incidence of Human Herpesvirus-6 Encephalitis after Naive T Cell-Depleted Graft of Haploidentical Stem Cell Transplantation in Pediatric Patients. *Biol. Blood Marrow Transplant.* **2018**, *24*, 2316–2323. [\[CrossRef\]](#) [\[PubMed\]](#)

22. Mamcarz, E.; Madden, R.; Qudeimat, A.; Srinivasan, A.; Talleur, A.; Sharma, A.; Suliman, A.; Maron, G.; Sunkara, A.; Kang, G.; et al. Improved survival rate in T-cell depleted haploidentical hematopoietic cell transplantation over the last 15 years at a single institution. *Bone Marrow Transplant.* **2020**, *55*, 929–938. [[CrossRef](#)] [[PubMed](#)]
23. Maschan, M.; Blagov, S.; Shelikhova, L.; Shekhovtsova, Z.; Balashov, D.; Starichkova, J.; Al, E. Low-dose donor memory T-cell infusion after TCR alpha/beta depleted unrelated and haploidentical transplantation: Results of a pilot trial. *Bone Marrow Transplant.* **2018**, *53*, 264–273. [[CrossRef](#)] [[PubMed](#)]
24. Geller, M.A.; Miller, J.S. Use of allogeneic NK cells for cancer immunotherapy. *Immunotherapy* **2011**, *3*, 1445–1459. [[CrossRef](#)] [[PubMed](#)]
25. Stern, M.; Passweg, J.R.; Meyer-Monard, S.; Esser, R.; Tonn, T.; Soerensen, J.; Paulussen, M.; Gratwohl, A.; Klingebiel, T.; Bader, P.; et al. Pre-emptive immunotherapy with purified natural killer cells after haploidentical SCT: A prospective phase II study in two centers. *Bone Marrow Transplant.* **2013**, *48*, 433–438. [[CrossRef](#)] [[PubMed](#)]
26. Barkholt, L.; Alici, E.; Conrad, R.; Sutlu, T.; Gilljam, M.; Stellan, B.; Christensson, B.; Guven, H.; Björkström, N.K.; Söderdahl, G.; et al. Safety analysis of ex vivo-expanded NK and NK-like T cells administered to cancer patients: A Phase I clinical study. *Immunotherapy* **2009**. [[CrossRef](#)] [[PubMed](#)]
27. Vela, M.; Corral, D.; Carrasco, P.; Fernández, L.; Valentín, J.; González, B.; Escudero, A.; Balas, A.; de Paz, R.; Torres, J.; et al. Haploidentical IL-15/41BBL activated and expanded natural killer cell infusion therapy after salvage chemotherapy in children with relapsed and refractory leukemia. *Cancer Lett.* **2018**, *422*, 107–117. [[CrossRef](#)] [[PubMed](#)]
28. Bachanova, V.; Burns, L.J.; McKenna, D.H.; Curtsinger, J.; Panoskaltis-Mortari, A.; Lindgren, B.R.; Cooley, S.; Weisdorf, D.; Miller, J. Allogeneic Natural Killer Cells for Refractory Lymphoma. *Cancer Immunol. Immunother.* **2010**, *59*, 1739–1744. [[CrossRef](#)]
29. Curti, A.; Ruggeri, L.; D’Addio, A.; Bontadini, A.; Dan, E.; Motta, M.R.; Trabanelli, S.; Giudice, V.; Urbani, E.; Martinelli, G.; et al. Successful transfer of alloreactive haploidentical KIR ligand-mismatched natural killer cells after infusion in elderly high risk acute myeloid leukemia patients. *Blood* **2011**, *118*, 3273–3279. [[CrossRef](#)]
30. Iliopoulou, E.G.; Kountourakis, P.; Karamouzis, M.V.; Doufexis, D.; Ardavanis, A.; Baxevanis, C.N.; Rigatos, G.; Papamichail, M.; Perez, S.A. A phase I trial of adoptive transfer of allogeneic natural killer cells in patients with advanced non-small cell lung cancer. *Cancer Immunol. Immunother.* **2010**, *59*, 1781–1789. [[CrossRef](#)]
31. Szmania, S.; Lapteva, N.; Garg, T.; Greenway, A.; Lingo, J.; Nair, B.; Stone, K.; Woods, E.; Khan, J.; Stivers, J.; et al. Ex vivo-expanded natural killer cells demonstrate robust proliferation in vivo in high-risk relapsed multiple myeloma patients. *J. Immunother.* **2015**, *38*, 24–36. [[CrossRef](#)] [[PubMed](#)]
32. Fernández, L.; Leivas, A.; Valentín, J.; Escudero, A.; Corral, D.; de Paz, R.; Vela, M.; Bueno, D.; Rodríguez, R.; Torres, J.M.; et al. How do we manufacture clinical-grade interleukin-15-stimulated natural killer cell products for cancer treatment? *Transfusion* **2018**, *58*, 1340–1347. [[CrossRef](#)] [[PubMed](#)]
33. Vasu, R.S.; Berg, M.; Davidson-Moncada, J.; Tian, X.; Cullis, H.; Childs, R.W. A Novel Method to Expand Large Numbers of CD56+ Natural Killer Cells from a Minute Fraction of Selectively Accessed Cryopreserved Cord Blood for Immunotherapy Post-transplantation. *Cytotherapy* **2015**, *11*, 1582–1593. [[CrossRef](#)] [[PubMed](#)]
34. Kloess, S.; Kretschmer, A.; Stahl, L.; Fricke, S.; Koehl, U. CAR-Expressing Natural Killer Cells for Cancer Retargeting. *Transfus. Med. Hemotherapy* **2019**, *46*, 4–13. [[CrossRef](#)]
35. Wagner, J.; Pfannenstiel, V.; Waldmann, A.; Bergs, J.W.J.; Brill, B.; Huenecke, S.; Klingebiel, T.; Rödel, F.; Buchholz, C.J.; Wels, W.S.; et al. A two-phase expansion protocol combining interleukin (IL)-15 and IL-21 improves natural killer cell proliferation and cytotoxicity against rhabdomyosarcoma. *Front. Immunol.* **2017**, *8*. [[CrossRef](#)]
36. Kweon, S.; Phan, M.T.T.; Chun, S.; Yu, H.B.; Kim, J.; Kim, S.; Lee, J.; Ali, A.K.; Lee, S.H.; Kim, S.K.; et al. Expansion of human NK cells using K562 cells expressing OX40 ligand and short exposure to IL-21. *Front. Immunol.* **2019**, *10*. [[CrossRef](#)]
37. Cho, D.; Campana, D. Expansion and activation of natural killer cells for cancer immunotherapy. *Korean J. Lab. Med.* **2009**, *29*, 89–96. [[CrossRef](#)]
38. Talleur, A.; Ying, L.; Salem, A.; Aksay, S.; Qudeimat, A.; Srinivasan, A.; Mamcarz, E.; Madden, R.; Gottschalk, S.; Triplett, B.M. Haploidentical CD45RA-Negative Donor Lymphocyte Infusions Are Feasible, Safe and Associated with Clinical Benefit. *Biol. Blood Marrow Transplant.* **2020**, *26*, S268. [[CrossRef](#)]
39. Saraceni, F.; Shem-Tov, N.; Olivieri, A.; Nagler, A. Mobilized peripheral blood grafts include more than hematopoietic stem cells: The immunological perspective. *Bone Marrow Transplant.* **2015**, *50*, 886–891. [[CrossRef](#)]
40. Su, Y.C.; Li, S.C.; Hsu, C.K.; Yu, C.C.; Lin, T.J.; Lee, C.Y.; Liao, H.F. G-CSF downregulates natural killer cell-mediated cytotoxicity in donors for hematopoietic SCT. *Bone Marrow Transplant.* **2012**, *47*, 73–81. [[CrossRef](#)]
41. Wong, P.P.C.; Kariminia, A.; Jones, D.; Eaves, C.J.; Foley, R.; Ivison, S.; Couban, S.; Schultz, K.R. Plerixafor effectively mobilizes CD56bright NK cells in blood, providing an allograft predicted to protect against GVHD. *Blood* **2018**, *131*, 2859–2863. [[CrossRef](#)] [[PubMed](#)]
42. Denman, C.J.; Senyukov, V.V.; Somanchi, S.S.; Phatarpekar, P.V.; Kopp, L.M.; Johnson, J.L.; Singh, H.; Hurton, L.; Maiti, S.N.; Huls, M.H.; et al. Membrane-bound IL-21 promotes sustained Ex Vivo proliferation of human natural killer cells. *PLoS ONE* **2012**, *7*. [[CrossRef](#)] [[PubMed](#)]
43. Un, P.K.; Ping, J.; Sabatino, M.; Feng, J.; Civini, S.; Khuu, H.; Berg, M.; Childs, R.; Stroncek, D. Gene expression analysis of ex-vivo expanded and freshly isolated NK cells from cancer patients. *J. Immunother.* **2010**, *33*, 945–955. [[CrossRef](#)]

-
44. Fernández, L.; Metais, J.Y.; Escudero, A.; Vela, M.; Valentín, J.; Vallcorba, I.; Leivas, A.; Torres, J.; Valeri, A.; Patiño-García, A.; et al. Memory T cells expressing an NKG2D-CAR efficiently target osteosarcoma cells. *Clin. Cancer Res.* **2017**, *23*, 5824–5835. [[CrossRef](#)] [[PubMed](#)]
 45. Robinson, M.D.; McCarthy, D.J.; Smyth, G.K. edgeR: A Bioconductor package for differential expression analysis of digital gene expression data. *Bioinformatics* **2009**, *26*, 139–140. [[CrossRef](#)]
 46. Yu, G.; Wang, L.G.; Han, Y.; He, Q.Y. ClusterProfiler: An R package for comparing biological themes among gene clusters. *OMICS* **2012**, *16*, 284–287. [[CrossRef](#)]
 47. Koehl, U.; Brehm, C.; Huenecke, S.; Zimmermann, S.Y.; Kloess, S.; Bremm, M.; Ullrich, E.; Soerensen, J.; Quaiser, A.; Erben, S.; et al. Clinical grade purification and expansion of NK cell products for an optimized manufacturing protocol. *Front. Oncol.* **2013**, *3*, 118. [[CrossRef](#)]
 48. Leivas, A.; Perez-Martinez, A.; Blanchard, M.J.; Martín-Clavero, E.; Fernández, L.; Lahuerta, J.J.; Martinez-Lopez, J. Novel treatment strategy with autologous activated and expanded natural killer cells plus anti-myeloma drugs for multiple myeloma. *Oncoimmunology* **2016**, *5*. [[CrossRef](#)]



GMP-Compliant Manufacturing of NKG2D CAR Memory T Cells Using CliniMACS Prodigy

Lucía Fernández^{1*}, Adrián Fernández¹, Isabel Mirones², Adela Escudero³, Leila Cardoso³, María Vela², Diego Lanzarot⁴, Raquel de Paz⁵, Alejandra Leivas^{1,6}, Miguel Gallardo^{1,6}, Antonio Marcos⁵, Ana Belén Romero⁵, Joaquín Martínez-López^{1,6} and Antonio Pérez-Martínez^{2,7*}

¹ Hematological Malignancies H12O, Clinical Research Unit, Spanish National Cancer Research Centre (CNIO), Madrid, Spain, ² Translational Research in Pediatric Oncology, Hematopoietic Transplantation and Cell Therapy, IdiPAZ, Hospital Universitario La Paz, Madrid, Spain, ³ Pediatric Molecular Hemato-Oncology Department, Instituto de Genética Médica y Molecular (INGEMM), Hospital Universitario La Paz, Madrid, Spain, ⁴ Applications Department, Miltenyi Biotec S.L., Madrid, Spain, ⁵ Hematology Department, Hospital Universitario La Paz, Madrid, Spain, ⁶ Hematology Department, Hospital Universitario 12 de Octubre, Madrid, Spain, ⁷ Pediatric Hemato-Oncology Department, Hospital Universitario La Paz, Madrid, Spain

OPEN ACCESS

Edited by:

Alberto Anel,
University of Zaragoza, Spain

Reviewed by:

Jan Joseph Melenhorst,
University of Pennsylvania,
United States
Pappanaicken R. Kumaresan,
University of Texas MD Anderson
Cancer Center, United States

*Correspondence:

Lucía Fernández
lvfernandez@cnio.es
Antonio Pérez-Martínez
aperezmartinez@salud.madrid.org

Specialty section:

This article was submitted to
Cancer Immunity and Immunotherapy,
a section of the journal
Frontiers in Immunology

Received: 13 June 2019

Accepted: 19 September 2019

Published: 10 October 2019

Citation:

Fernández L, Fernández A, Mirones I, Escudero A, Cardoso L, Vela M, Lanzarot D, de Paz R, Leivas A, Gallardo M, Marcos A, Romero AB, Martínez-López J and Pérez-Martínez A (2019) GMP-Compliant Manufacturing of NKG2D CAR Memory T Cells Using CliniMACS Prodigy. *Front. Immunol.* 10:2361. doi: 10.3389/fimmu.2019.02361

Natural killer group 2D (NKG2D) is a natural killer (NK) cell-activating receptor that recognizes different stress-induced ligands that are overexpressed in a variety of childhood and adult tumors. NKG2D chimeric antigen receptor (CAR) T cells have shown potent anticancer effects against different cancer types. A second-generation NKG2D CAR was generated by fusing full-length human NKG2D to 4-1BB costimulatory molecule and CD3 ζ signaling domain. Patient-derived CAR T cells show limitations including inability to manufacture CAR T cells from the patients' own T cells, disease progression, and death prior to return of engineered cells. The use of allogeneic T cells for CAR therapy could be an attractive alternative, although undesirable graft vs. host reactions may occur. To avoid such adverse effects, we used CD45RA⁺ memory T cells, a T-cell subset with less alloreactivity, as effector cells to express NKG2D CAR. In this study, we developed a protocol to obtain large-scale NKG2D CAR memory T cells for clinical use by using CliniMACS Prodigy, an automated closed system compliant with Good Manufacturing Practice (GMP) guidelines. CD45RA⁺ fraction was depleted from healthy donors' non-mobilized apheresis using CliniMACS CD45RA Reagent and CliniMACS Plus device. A total of 10⁸ CD45RA⁺ cells were cultured in TexMACS media supplemented with 100 IU/mL IL-2 and activated at day 0 with T Cell TransAct. Then, we used NKG2D-CD8TM-4-1BB-CD3 ζ lentiviral vector for cell transduction (MOI = 2). NKG2D CAR T cells expanded between 10 and 13 days. Final cell products were analyzed to comply with the specifications derived from the quality and complementary controls carried out in accordance with the instructions of the Spanish Regulatory Agency of Medicines and Medical Devices (AEMPS) for the manufacture of investigational advanced therapy medicinal products (ATMPs). We performed four validations. The manufacturing protocol here described achieved large numbers of viable NKG2D CAR memory T cells with elevated levels of NKG2D CAR expression and highly cytotoxic against Jurkat and 531MII tumor target cells. CAR T cell final products met release

criteria, except for one showing *myc* overexpression and another with viral copy number higher than five. Manufacturing of clinical-grade NKG2D CAR memory T cells using CliniMACS Prodigy is feasible and reproducible, widening clinical application of CAR T cell therapies.

Keywords: NKG2D CAR, memory T cells, automated production, large-scale, clinical-grade, CliniMACS prodigy

INTRODUCTION

Redirected chimeric antigen receptor (CAR) T cells (CART) have shown effective potency against hematologic tumors (1, 2). Second-generation CARs are hybrid receptors comprising a recognition domain, normally derived from a single-chain antibody fragment (scFv), fused to costimulatory, and cytotoxic signaling domains that enhance T cell function (3, 4). This restricts CAR T cells to recognize a single tumor antigen in a defined set of tumors, such as CD19 in B-cell malignancies. CD19-specific CAR T cell therapy for the treatment of CD19-positive B cell malignancies such as B-cell acute lymphoblastic leukemia (B-ALL), B-cell non-Hodgkin lymphoma (NHL), or chronic lymphocytic leukemia (CLL) has had remarkable success (5–8), resulting in their recent US Food and Drug Administration (FDA) approval. However, relapse of leukemia through CD19 loss variants in leukemia/lymphoma patients and immunosuppressive microenvironment or lack of tumor-associated antigens (TAAs) in solid tumors (9–11) represents major challenges for CAR T cell therapies. These inconveniences along with antigen-loss escape make it necessary to focus in other possible TAAs (9).

Natural killer group 2D (NKG2D) is an activating receptor expressed on different immune effector cells [natural killer (NK), CD8, and $\gamma\delta$ T cells], although is in the NK cells where it has a main role in tumor surveillance. Ligands for NKG2D receptor, namely, MIC-A, MIC-B, and the UL-16 binding proteins, are expressed in 70% of human cancers including leukemia, osteosarcoma, or Ewing sarcoma (11–13), whereas their expression in healthy tissues is rare. We have produced a second-generation NKG2D CAR by fusing the full-length extracellular domain of human NKG2D to 4-1BB, which provides a costimulatory signal, and CD3 ζ signaling domain. Thus, through the expression of this CAR, T cells acquire NK cell anti-tumor specificity while maintaining T-cell ability to expand and persist *in vivo*. The main advantages of this CAR are (1) the recognition of different ligands, widening clinical application, and potentially avoiding tumor immune escape by single antigen loss, and (2) it is a fully human CAR, causing less immunogenicity.

Most clinical trials use autologous T cells to express CARs; however, owing to low T-cell numbers, poor quality, or rapid disease progression, manufacturing of patient-derived CAR T cells is not always possible. To overcome these limitations, we propose here the use of allogeneic CAR T cells. Allogeneic cells expressing CARs have been infused into patients after a hematopoietic stem cell transplantation (HSCT) from the same healthy donor (14, 15). Nevertheless, the universal availability of large numbers of healthy donor T cells to express CARs

and their infusion into patients without the requirement of a prior HSCT would be major challenges of CAR T cell immunotherapy. One potential risk of the use of allogeneic T cell-based therapies is the T-cell response against normal tissue: graft-vs.-host disease (GvHD). To avoid undesirable GvH reactions, T-cell products lacking an alloreactive T-cell receptor (TCR) are needed. Several methods have attempted to intensify graft-vs.-tumor (GvT) effects while minimizing GvH responses to lower toxicity and improve the outcome of treatment (14, 16, 17). One approach to enrich non-allogeneic T cells is by using antigen-experienced memory T cells for CAR transduction (16, 18). Predictably, the vast majority of T cells with a memory phenotype are likely to have encountered antigens other than the allogeneic type. Thus, selection for memory phenotype cells should enrich for a non-alloreactive repertoire. Indeed, memory T cells showed less potential to generate GvHD in murine models (19, 20), in part owing to non-alloreactive TCR enrichment along with the evidence that memory T cells are less likely to traffic to GvHD organs such as the gastrointestinal tract. Different extracellular markers can be used to differentiate naïve from memory T cells. Commonly, naïve T cells are CD45RA⁺CD45RO[−]CCR7⁺CD62L⁺, central memory T cells (T_{CM}) are CD45RA[−]CD45RO⁺CCR7⁺CD62L⁺, effector memory T cells (T_{EM}) are CD45RA[−]CD45RO⁺CCR7[−]CD62L[−], and effector cells are CD45RA⁺CD45RO[−]CCR7[−]CD62L[−] (21). Thus, one marker to roughly distinguish naïve from memory T cells is CD45RA (22). CD45RA is expressed on naïve T cells and a minor population of T memory stem cells (T_{SCM}) (21), whereas CD45RO is expressed on memory T cells (22). CD45RA⁺ naïve T cells have high potential for alloreactivity against recipient-specific antigens upon adoptive transfer, causing clinical GvHD (23, 24). In contrast, CD45RA[−]CD45RO⁺ T cells exert a memory response to prior pathogens or vaccines and can mediate GvT effects without inducing GvHD (19, 25).

In the present study, we describe the manufacturing process to produce large-scale NKG2D CAR memory T cells from healthy donors for clinical use. In CAR T cell therapies, besides the designing of genetic constructs, the choice of effector cells to transduce, and the clinical trial design, the methods used to produce CAR T cells are key for clinical success. Thus, detailed description of each step along the manufacturing process and the full analysis of CAR T cell products composition at every step are essential. In fact, and according to the Good Manufacturing Practice (GMP) manufacturing standard, during the manufacturing procedure, in-process controls are carried out at different times. Optimization of manufacturing protocols to improve reproducibility, cost-effectiveness, and scalability will enable a broad application of CAR T cell therapies.

The NKG2D CAR memory T cells showed in this study were manufactured after 10–13 days of *ex vivo* processing, described in detail below, including activation with TransAct and IL-2, transduction with an NKG2D-CD8TM-4-1BB-CD3 ζ lentiviral vector at multiplicity of infection (MOI) = 2, and expansion in CliniMACS Prodigy device. The NKG2D CAR memory T cells collected after this process fulfilled the release criteria with respect to safety, purity, and potency established in the protocols adhered to the guidelines of the current GMP (26–28). The manufacturing process developed in this study allows the automated GMP-compliant production of large doses of clinical-grade NKG2D CAR T cells in a short time and provides a robust and flexible base for further optimization of NKG2D CAR T cells manufacturing for their clinical application in different tumor types.

MATERIALS AND METHODS

Starting Material

Non-mobilized apheresis was obtained from healthy donors at the Bone Marrow Transplant and Cell Therapy Unit (BMTCT) of Hospital Universitario La Paz (HULP) by using CliniMACS Plus device (Miltenyi Biotec). All donors gave their written informed consent in accordance with the Declaration of Helsinki protocol, and the study was performed according to the guidelines of the local ethics committee. All donors comply with the requirements regarding quality and safety for donation, obtaining, storage, distribution, and preservation of human cells and tissues under the Spanish specific regulation. CD45RA⁺ cells were depleted by immunomagnetic separation using CliniMACS CD45RA Reagent (701-46) and CliniMACS Plus system, both from Miltenyi Biotec, following manufacturer instructions. CD45RA⁺ cells were either processed immediately or stored at 2–8°C for subsequent processing no later than 24 h after depletion. The viability and purity of CD45RA⁺ fraction were analyzed by flow cytometry (FCM) before activation, transduction, and expansion.

Construction and Production of Lentiviral Vector

The HL20i4r-MNDantiCD19bbz lentiviral vectors were derived from the clinical vector CL20i4r-EF1a-hgcOPT27 but expressed an NKG2D CAR. The anti-CD19-4-1BB-CD3 ζ CAR designed by Imai et al. (29) was used as backbone to build the NKG2D CAR construct. It contained the extracellular domain of NKG2D (designed by Wai-Hang Leung and Wing Leung), the hinge region of CD8a, and the signaling domains of 4-1BB and CD3 ζ . The cassette was driven by a prMND. The viral supernatant was produced according to GMP guidelines by transient transfection of HEK293T cells with the vector genome plasmid and lentiviral packaging helper plasmids pCAGG-HIVgpc, pCAGG-VSVG, and pCAG4-RTR2. Lentiviral plasmids were kindly provided by Dr. Byoung (St. Jude Children's Research Hospital). The virus supernatants were harvested and filtered through 0.22 μ m filters. Virus supernatant was concentrated by ultracentrifugation and titrated on HeLa cells by serial dilution followed by a quantitative polymerase chain reaction (qPCR) to determine vector genome copy number.

Manufacturing of Clinical-Grade NKG2D CAR T Cells

Activation, transduction, and expansion of CD45RA⁺ cells were performed on the CliniMACS Prodigy using Tubing set TS520 (170-076-600) and T-cell transduction (TCT) process. In detail, at day 0, cultivation was initiated with 10⁸ CD45RA⁺ cells in a total volume of 70 mL of TexMACs GMP medium (170-076-306) + 100 IU/mL of MACS GMP human recombinant IL-2 (170-076-147). MACS GMP TransAct CD3/CD28 Kit (170-076-156) was used for a 24-h activation at a final dilution of 1:17.5, as recommended by the manufacturer. At the following day, cells were transduced with NKG2D-4-1BB-CD3 ζ lentiviral particles at MOI = 2. The vector was diluted in 10 mL of medium in a 150-mL transfer bag, which was attached to the CliniMACS Prodigy by sterile welding. The vector was automatically transferred in the culture chamber, and the vector bag was further rinsed with 20 mL of medium to bring the total culture volume to 100 mL. Residual TransAct was removed by an automated culture wash on day 4. Cells were then expanded for 10–13 days before being harvested. Sampling was performed at days +6 and +8 for in-process controls including cell counts, cytotoxicity, and FCM. At the end of the expansion, cells were automatically collected in 0.9% sodium chloride solution supplemented with 0.5% human serum albumin (Albutein 20%, Grifols) and transferred into a sterile bag. Release quality controls were performed at the end of the process.

Analysis of Viability and Surface Immunophenotype by FCM

At day +6 and between days +8 and +10, as in-process controls, and at harvest, as release controls, NKG2D CAR memory T cell products were counted in a CELL-DYN Emerald hematology analyzer (Abbott) and analyzed for their viability, immunophenotype, NKG2D CAR expression, and activation status by FCM. The following anti-human fluorochrome-labeled monoclonal antibodies (mAb) were purchased from BioLegend: CD45RA-APC (Clone H100, 304111), CD3-PE/Cy7 (Clone HIT3a, 300316), CD4-APC/Cy7 (Clone OKT4, 317417), CD8 FITC (Clone KK1, 344703), NKG2D-PE (Clone 1D11, 320806), CD4 PerCP (Clone OKT4, 31743125), PD-1 APC (Clone EH12.2H7, 329907), Tim-3 APC Cy7 (Clone F38-2E2, 345025), CD25 APC (Clone BC96, 302610), and CD127 PE/Cy7 (Clone A019D5, 351320). Anti-human CD45RO-APC-Vio770 (Clone REA611, 130-114-083) was purchased from Miltenyi Biotec. Anti-human CCR7 PE (Clone 3D12, 552176) was purchased from BD Biosciences. The viability was tested by using DAPI or 7AAD as dead cell exclusion markers. Cells were analyzed using FACS CANTO II (BD Biosciences) and FlowJo v10.5.3 software (TreeStar). To ensure the expression of NKG2D CAR in the manufactured NKG2D CAR T cell products, we performed western blot with an antibody detecting CD3 ζ . Total peripheral blood mononuclear cells (PBMC), activated and expanded NK cells (NKAE), untransduced CD45RA⁺, and NKG2D CAR T cells were pelleted and frozen at –80°C. Cell lysates were obtained by incubating cell pellets with RIPA (Millipore, 20188) supplemented with phosphatase inhibitor (PhosSTOP,

04906845001) and a cocktail of protease inhibitors (cOmplete Mini, 11836153001), both from Roche. Proteins were quantified using Bradford reagent (Bio-Rad Laboratories, 500-0205) and measuring absorbance at 595 nm in a Victor Plate Reader. Cell lysates were then mixed with the Laemmli sample buffer (Bio-Rad Laboratories, 161-0747), and equal amounts of protein (20 µg) were loaded on 4–15% Mini-PROTEAN TGX Gels (Bio-Rad Laboratories, 456-1086). Gels were transferred to polyvinylidene difluoride (PVDF) membranes. Blots were incubated with the mouse anti-human CD3ζ (BD Biosciences, 551033) or rabbit anti-human β-actin (Cell Signaling Technology, 4967S) primary antibodies at 4°C overnight. Horseradish peroxidase (HRP)-conjugated anti-mouse (Agilent, P0447) and anti-rabbit (Agilent, P0448) were used as secondary antibodies. The membranes were developed by enhanced chemiluminescence and exposed on Clarity Western ECL substrate (Bio-Rad Laboratories, 170-5060). The immunoblotting images were analyzed using the Image Lab software.

Effector Function

The mechanism of action of CAR cells is complex, and there are no standardized methods to determine the degree of action. Although methods are available to determine potency, comparison of results is not easy owing to the absence of standardization (26). In our study, to test the cytotoxicity of manufactured NKG2D CAR T cells, conventional 4-h europium-TDA assays (PerkinElmer, AD0116) were performed as previously described (30) using a 20:1 effector to target ratio. The NKG2DL-expressing cell lines Jurkat and 531MII were used as targets. Cytotoxicity assays were performed on days +6 and +8 and at the end of the process. The 531MII primary osteosarcoma cell line was kindly provided by Dr. Patiño-García (Centro de Investigación Médica Aplicada (CIMA), Universidad de Navarra, Spain) and was cultured in minimum essential medium (MEM; GIBCO, 22571-020) supplemented with 10% heat-inactivated fetal bovine serum (FBS; GIBCO, 10270-098) and penicillin-streptomycin (P/S; GIBCO, 15140-122). The T-ALL Jurkat cell line was acquired from American Type Culture Collection (ATCC) and kept in culture in Roswell Park Memorial Institute (GIBCO, 61870-010) and 10% FBS and P/S. Both cell lines were routinely tested for mycoplasma.

Analyses of Non-cellular Impurities

The detection of non-cellular impurities was carried out in accordance with the methodology recommendations of Chapter 2.6.21 and 2.6.7 of the European Pharmacopeia (Eu Ph) for mycoplasma and Chapter 2.6.14 for endotoxins. A DNA-binding dye-based qPCR system was employed for the detection of mycoplasma DNA in cell cultures. The assay was developed by the Genomics Unit in collaboration with the Monoclonal Antibodies Unit, both from CNIO, to detect 16s rRNA gene sequences from up to 70 *Mollicutes* species. Both specificity and sensitivity were extensively tested through benchmarking with established commercial systems (MTC-NI System, Millipore/GEN-PROBE Cat. No. 4573 and MycoAlert™ PLUS Mycoplasma Detection Kit, Lonza Cat. No. LT07-705). The Clinical Microbiology and Parasitology Service of HULP carried

out the endotoxin test Endosafe-PTS (Charles River) to quantify endotoxin levels at day +8 and in final products.

Microbiological Tests

At days +6 and between days +8 and +10 as in-process controls and at the end of manufacturing protocol, NKG2D CAR memory T cell products were tested for sterility according to Eu Ph 2.6.1. The microbiological tests were developed by the Clinical Microbiology and Parasitology Service of HULP by conventional microbiology techniques. In summary, sample tests were inoculated into separate culture media, and the growth of viable microorganisms was tested after several days. When a rapid result was required, Gram staining was used as a non-culture method, although it is a less sensitive technique than techniques based on culture (26).

Genetic Tests, Genome Integrated Vector Copy Number, and Determination of Replication Competent Lentivirus in the Supernatant

Genetic tests and determination of vector copy number (VCN) and replication competent lentivirus (RCL) in the supernatant were carried out at days +6 and between days +8 and +10 as quality controls during process validation and at the end of the manufacturing process between days 10 and 13. To rule out chromosomal aberrations caused by lentiviral transduction, comparative genome hybridization (CGH) analysis was performed as previously described (30). Genome integrated lentiviral copy number and viral particles in supernatant were measured by qPCR according to Christodoulou et al. (31) using TaqMan Universal PCR Master Mix (Thermo Fisher; 4304437) and LightCycler 480 (Roche) after viral RNA extraction with RNeasy (Qiagen, 74104) and cDNA retrotranscription with Superscript II (Thermo Fisher, 18064014). The lack of oncogenic effects of the NKG2D CAR T cell products was verified using reverse transcriptase (RT)-PCR to detect c-MYC and telomerase (*TERT*) expression. Total RNA was isolated from the PBMCs using the RNeasy kit from Qiagen (PN 74104), followed by reverse transcription using SuperScript™ IV First-Strand Synthesis System from Thermo Fisher (PN 18091050). The resulting cDNA was amplified with the following specific TaqMan probes: Hs00972650_m1 (*TERT*), Hs00153408_m1 (*MYC*), and Hs02800695_m1 (*HPRT1*, housekeeping) from Life Technologies and the LightCycler 480 System from Roche. Finally, the data were analyzed by the comparative Ct methods as previously described (32). The genetic tests were performed at the Institute of Medical and Molecular Genetics of HULP (INGEMM).

Effects of Cryopreservation on NKG2D CAR T Cells

As infusion of freshly manufactured CAR T cells is not always possible, we wanted to determine if cryopreservation could have a negative impact on viability, NKG2D CAR expression, and cytotoxicity of NKG2D CAR T cells. To this aim, spare CAR T cells were frozen at a concentration of $2.5\text{--}3 \times 10^5$ cells/µL

either by using HypoThermosol, M199 media supplemented with 10% human serum albumin and 5% dimethyl sulfoxide (DMSO), or in autologous plasma supplemented with 5% DMSO. One year after cryopreservation, NKG2D CAR T cells were thawed and evaluated for viability, NKG2D expression, and CD45RA[−] purity by FCM and for cytotoxicity by europium-TDA as described above.

Statistics Analyses

All statistical analyses in this study were performed using GraphPad Prism. Except indicated in another way, results are shown as median and interquartile range.

RESULTS

Manufacturing Process: Activation, Transduction, and Expansion

CD45RA[−] cells from four different donors were activated, transduced, and expanded in CliniMACS Prodigy in four different experiments. In-process tests were carried out at days +6 and +8. At the end of culture (between days +10 and +13), cells were harvested, and quality/release assays performed. A schema of the different steps for NKG2D CAR T cells manufacturing and the quality tests conducted along the process is shown in Figure 1.

Purity of CD45RA[−] Starting Cells

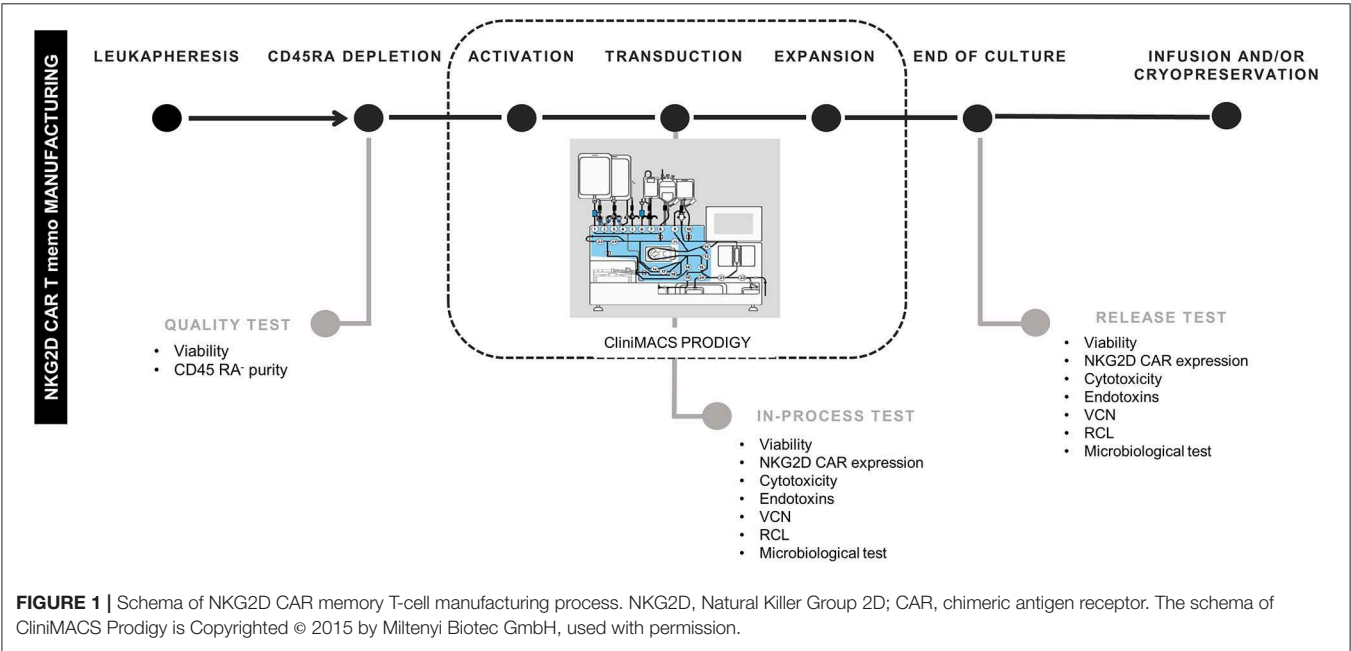
Non-mobilized apheresis from four different healthy donors were obtained and depleted for CD45RA⁺ cells at CliniMACS Plus. After depletion of CD45RA⁺ cells, median of purity of CD45RA[−] population was 99.8 (range 99.7–99.9), and median of viability was 97.9 (range 97.7–99.9). Data of CD45RA[−] purity and viability from each experiment are shown in Table 1.

Transduction Efficiency

We transduced CD45RA[−] cells 1 day after cell activation. A lentiviral construct encoding for NKG2D CAR was used at MOI = 2. As CD45RA[−] cells only have basal levels of NKG2D receptor expression, we considered that the expression of NKG2D observed by FCM in NKG2D CAR T cell products corresponds to NKG2D CAR. Our target goal was to achieve ≥50% transduction of total cells. This goal was achieved for all four final products. Data from NKG2D CAR expression along the process are shown in Table 2. Representative dot plots of NKG2D staining at the different times are shown in Figure 2A. The anti-NKG2D antibody that we use for FCM does not discriminate between the NKG2D endogenous receptor and the NKG2D CAR. In order to analyze the expression of NKG2D CAR in the transduced cells, we performed a western blot using an anti-CD3ζ antibody to detect the CAR protein. NKG2D CAR protein is 40 kDa, whereas endogenous CD3ζ is 16 kDa. As shown in Figure 2B, bands corresponding to the NKG2D CAR were only observed in those cell lysates from transduced CD45RA[−] cells, whereas they were absent in the different negative controls (activated and expanded NK cells, PBMC, and CD45RA[−] untransduced cells). Additionally, PCR analysis using specific primers for endogenous NKG2D and NKG2D CAR genes further confirmed these results (Supplementary Figure 1).

TABLE 1 | Purity and viability of CD45RA[−] starting cells.

Validation	% Viability	% of CD45RA [−]
#1	98.1	99.8
#2	99.9	99.9
#3	97.7	99.9
#4	97.7	99.7



Expansion

After CD45RA⁺ depletion, 10⁸ of CD45RA[−] cells were transferred into a sterile bag and connected to CliniMACS Prodigy for further processing. The number of cells recovered after CD45RA depletion exceeded this limit for all experiments. For the final products, the fold expansion ranged from 13.4 to 38.6; thus, in all cases, the total number of cells obtained was enough to perform a clinical treatment in a multiple-dose regimen. Data of cell expansion from each experiment are shown in **Figure 3**.

TABLE 2 | Data from transduction efficiency and viability.

Validation	% NKG2D CAR expression			Viability		
	Day +6	Day +8	Final	Day +6	Day +8	Final
#1	73	60.5	60.6	85	82.5	86.3
#2	41	43	55	73	77	65
#3	24	82	87.4	70	83	81.4
#4	62	75	91	80	84	82

NKG2D, natural killer group 2D; CAR, chimeric antigen receptor.

Immunophenotype

Starting and final CAR T cell products were analyzed for viability and CD3, CD4, and CD8 contents. Naïve and memory populations were also identified by using CD45RA and CCR7 markers. The activation/exhaustion status of starting and final cells was analyzed by CD25, PD-1, and TIM-3 markers. The presence of CD4⁺CD25⁺CD127^{low/neg} (Tregs) was also analyzed in the starting and final products. Both starting

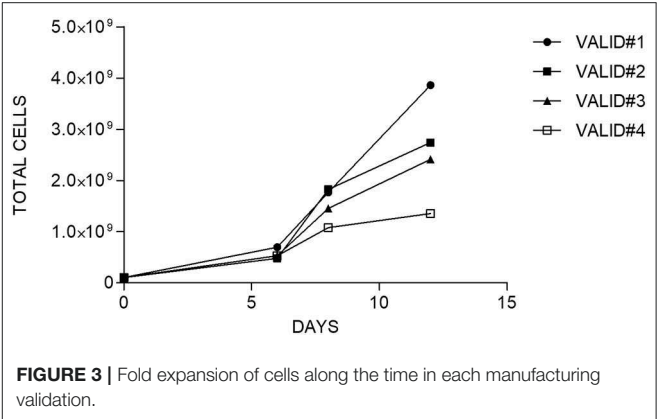


FIGURE 3 | Fold expansion of cells along the time in each manufacturing validation.

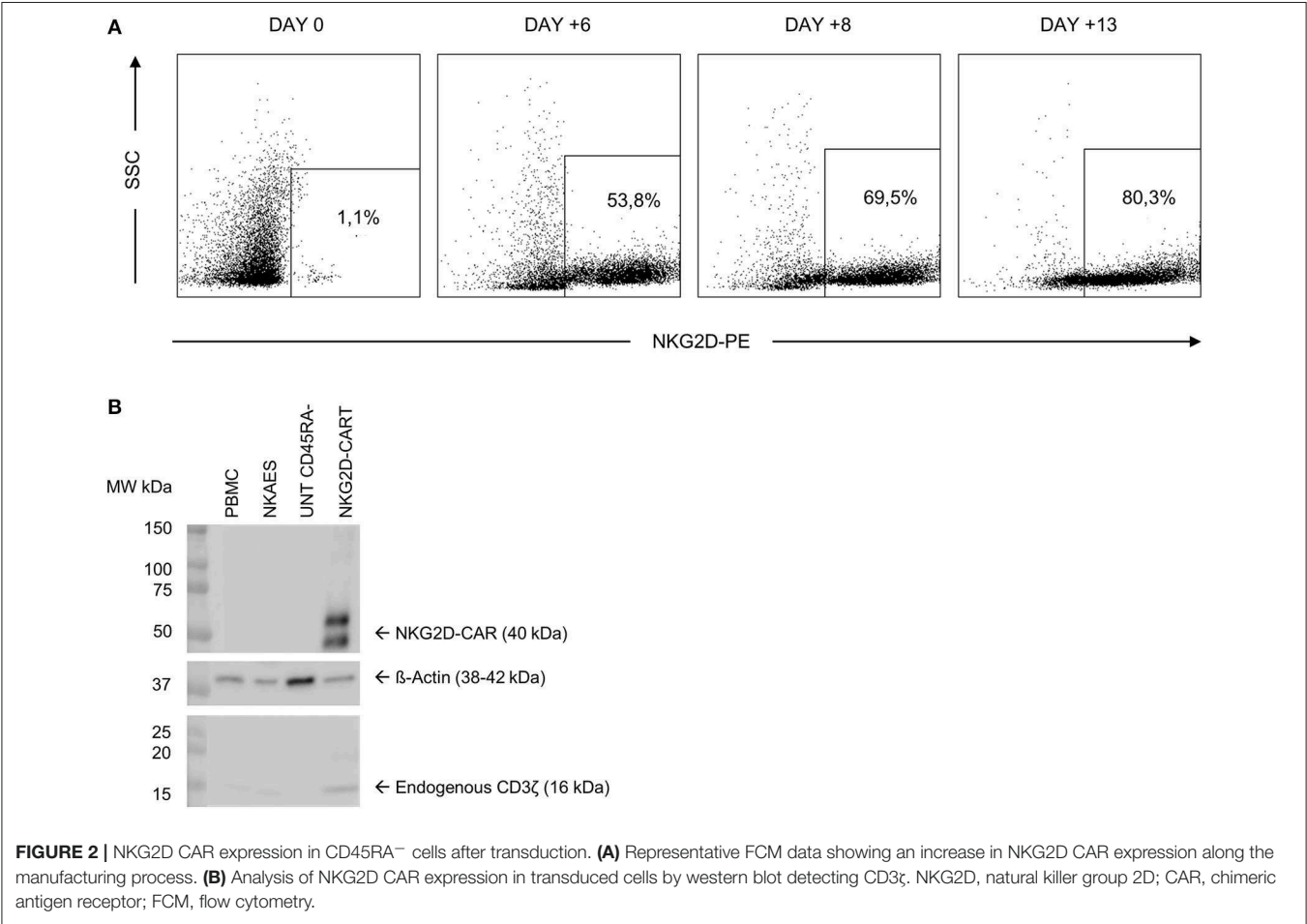


FIGURE 2 | NKG2D CAR expression in CD45RA[−] cells after transduction. (A) Representative FCM data showing an increase in NKG2D CAR expression along the manufacturing process. (B) Analysis of NKG2D CAR expression in transduced cells by western blot detecting CD3ζ. NKG2D, natural killer group 2D; CAR, chimeric antigen receptor; FCM, flow cytometry.

CD45RA[−] cells and final NKG2D CAR memory T cell products were CD3⁺ and showed an enrichment in CD4⁺ vs. CD8⁺ T cells. Before and after manufacturing process, T cells were negative for CD45RA and CCR7, indicating an effector memory (T_{EM}) phenotype. Tim-3 and CD25 activation/exhaustion markers were upregulated in final NKG2D CAR memory T cell products compared to starting CD45RA[−] cells; however, PD-1 expression was downregulated at the end of the process (Figure 4). Additionally, only a low proportion of T_{regs} (CD4⁺CD25⁺CD127^{low/neg}) was found on starting CD45RA[−] cells and final NKG2D CAR T cells compared with total PBMC (Supplementary Figure 2).

Effector Function

Lysis ability of NKG2D CAR T cells was tested against the NKG2DL-expressing cell lines Jurkat (T-ALL) and 531MII (metastatic osteosarcoma) by performing conventional 4-h europium-TDA assays. Although donor variability was observed, all final NKG2D CAR T cell products analyzed could target Jurkat and 531MII cells with a percentage of cytotoxicity ≥20%, thus meeting the established requirements. For validation #1, owing to technical issues, cytotoxicity against Jurkat cells was only tested using cryopreserved NKG2D CAR T cells. Cytotoxicity

of final NKG2D CAR T cells against Jurkat was higher (median 80%, range 28.2–100%) than against 531MII cells (median 42.3%, range 20–74.6%) for all analyzed products, although this difference was not statistically significant. Data of cytotoxicity levels from each experiment are shown in Table 3. Additionally, the cytotoxicity of manufactured NKG2D CAR T cells against Jurkat cells is shown in Supplementary Video 1.

Safety and Purity Tests

To meet regulatory specifications (acceptable thresholds in parentheses), samples were taken at days +6 and between days

TABLE 3 | Cytotoxicity of NKG2D CAR memory T cells against Jurkat and 531MII target cells.

Validation	% Cytotoxicity vs. Jurkat	% Cytotoxicity vs. 531MII
#1	NR	74.6
#2	100	19.5
#3	79.8	42.3
#4	28.2	NR

NKG2D, natural killer group 2D; CAR, chimeric antigen receptor; NR, non-reproducible experiment.

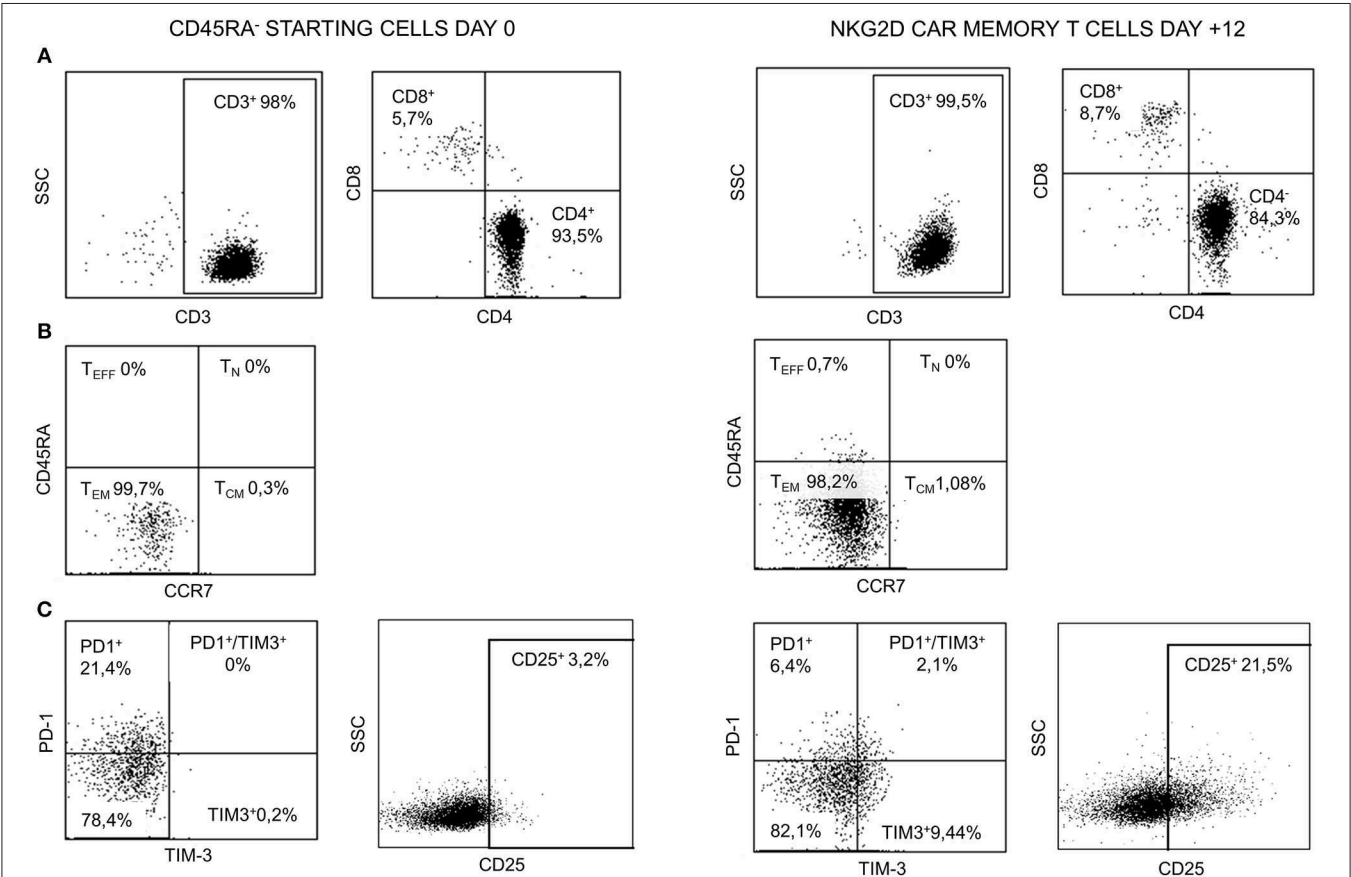


FIGURE 4 | Representative FCM data of starting CD45RA[−] cells (day 0) and NKG2D CAR memory T cell products at the end of manufacture process (day +12). (A) CD3, CD4, and CD8 contents. (B) Naïve/memory phenotype. (C) Expression of activation/exhaustion markers. FCM, flow cytometry; NKG2D, natural killer group 2D; CAR, chimeric antigen receptor.

+8 and +10 as in-process controls and at the end of process as release controls and were evaluated for VCN (≤ 5 copies/cell), free lentiviral particles in the supernatant (LVPS) ($\leq 0.05\%$), oncogenic gene expression (no overexpression), and genetic stability (normal CGH). A Gram stain (no organisms seen) as a quick method and microbiological tests [0 colony-forming unit (CFU)] ensured no bacterial contamination. Other release controls performed included those relating to the purity of the final product: measurement of endotoxin levels, whose limits for administration depend on the product and the parenteral administration route, where the pyrogenic threshold dose of endotoxin per kilogram of body mass in a single hour in the case of transduced cells is 5 IU/kg/h. All final products analyzed fulfilled the specifications except for validation #3, which showed VCN of 12 instead of ≤ 5 copies/cell, and for validation #4, which showed overexpression of myc. Complete data regarding genetic tests are shown in **Table 4**. All samples showed no microbiological contamination. Endotoxin levels were below 5 IU/kg/h, and the presence of mycoplasma was undetectable (**Table 5**).

Stability of Cryopreserved NKG2D CAR T Cells

CliniMACS Prodigy allows the production of sufficient number of CAR T cells to be administered in multiple doses. Although the first dose could be administered right after harvesting, spare cells need to be cryopreserved for future infusions. To explore if cryopreservation could have a negative impact on manufactured CAR T cells, we tested three different freezing media and evaluated cell counts, viability CD45RA⁺ purity, NKG2D expression, and cytotoxicity of cryopreserved NKG2D CAR T cells 1 year after freezing. We observed that those NKG2D CAR T cells cryopreserved in autologous plasma +5% DMSO showed the highest viability and cytotoxicity indicating that, whenever possible, this should be the freezing media

of preference, followed by M199 + 10% albumin and 5% DMSO (**Table 6**).

DISCUSSION

In the last decades, CAR T cell-based immunotherapies have demonstrated to be an effective and safe approach for cancer treatment. The clinical success of two CART19 cell products (KymriahTM and YescartaTM) for the treatment of B cell malignancies has led to their recent FDA and European Medicines Agency (EMA) approval, emphasizing the great potential of this technology. Targeting myeloid and non-B lymphoid cell hematological malignancies such as T-ALL, biphenotypic, and infant leukemia or solid tumors has been much harder, owing to the lack of specific antigens and the immunosuppressive tumor microenvironment (33–36). We present data on NKG2D CAR, which has the ability to recognize multiple ligands that are overexpressed in different tumor types including AML, T-ALL, and sarcomas (12, 13, 37–39). In fact, D. Sallman et al. have recently reported a case of remission in a patient suffering from relapsed/refractory AML after multiple infusions of autologous T cells redirected with a first-generation CAR recognizing NKG2DL (40). Aside from CAR specificity, choice of signaling domains and selection of effector cell subset to transduce, manufacturing process, and full characterization of final CAR T cell products are essential for clinical success. In the present study, we validate and provide detailed description of our manufacturing protocol and the characteristics of NKG2D CAR T cells. We show the feasibility of producing large numbers of allogeneic NKG2D CAR memory T cells using a 10–13 days' protocol, which includes activation with TransAct reagent, transduction with an NKG2D-4-1BB-CD3 ζ lentiviral vector and expansion with rhIL-2 in CliniMACS Prodigy, an automated closed system compliant with GMP guidelines.

The main objectives of this study were (1) to show the feasibility and reproducibility of automated manufacturing of GMP-grade NKG2D CAR T cells in an academic institution and (2) to demonstrate that manufactured NKG2D CAR T cells meet the requirements established by the Spanish Regulatory Agency for clinical use. A total of four manufacturing processes were completed, and the CAR T cell products obtained were analyzed

TABLE 4 | Results from genetic tests.

Validation	VCN	LVPS	CGH	tert expression	myc expression
#1	NA	Undetectable	Normal	No overexpression	No overexpression
#2	3.6	Undetectable	Normal	No overexpression	No overexpression
#3	12.3	Undetectable	Normal	No overexpression	No overexpression
#4	2.4	Undetectable	Normal	No overexpression	myc overexpression

VCN, vector copy number; LVPS, free lentiviral particles in the supernatant; CGH, comparative genome hybridization.

TABLE 5 | Results from sterility tests.

Validation	Gram staining	Mycoplasma	Endotoxins EU/mL
#1	Negative	Negative	NA
#2	Negative	Negative	0.019
#3	Negative	Negative	0.0035
#4	Negative	Negative	0.01

TABLE 6 | Stability of manufactured NKG2D CAR memory T cells after cryopreservation.

Freezing medium	% Viability	% NKG2D	% CD45RA ⁺	% Cytotox vs. Jurkat	% Cytotox vs. 531MII
M199 + ALB + DMSO V4	47.9	61.5	99.2	55.2	17.3
Hypothermosol v4	14.1	61.5	99.2	NA	NA
Auto plasma + DMSO V5	74.6	69.9	97.1	78.6	60.3

NKG2D, natural killer group 2D; ALB, albumin; DMSO, dimethyl sulfoxide.

at three different time points: day +6 and between days +8 and +10, as in-process controls, and at the end of culture, between days 10 and 13, when quality tests were performed to analyze if NKG2D CAR memory T cell products met release criteria.

We used CD45RA⁺ cells from healthy donors to produce our NKG2D CAR T cells in order to develop a safe allogeneic therapy. The lack of alloreactivity of CD45RA⁺ cells has been explored before in preclinical studies from our group and others (18, 30). Furthermore, Maschan et al. have described the safety of low-dose infusions of CD45RA⁺ lymphocytes in mismatched-related HSCT (41). Recently, our group has reported the safety of high-dose infusions of donor-derived CD45RA⁺CD45RO⁺ T cells after haploidentical transplantation (42).

The manufacturing process starts with a non-mobilized apheresis from a healthy donor followed by depletion of CD45RA⁺ cells in CliniMACS Plus device. Although CD45RA⁺ cells can be currently depleted at CliniMACS Prodigy, at the moment when these experiments were carried out, the software to do so was unavailable. After depletion, CD45RA⁺ cells were tested for viability and purity. All CD45RA⁺ cell products showed viability >95%. Purity of CD45RA⁺ cells after depletion of CD45RA⁺ subset was at least 99.7%, indicating that carryover of naïve T cells was minimal and meets the established criteria for further processing to obtain NKG2D CAR T cells. Activation, transduction, and expansion were conducted in CliniMACS Prodigy. Median of fold expansion was 24.4 (range 13.5–38.6), and the mean of total cells obtained was 2.44×10^9 (range 1.35×10^9 – 3.86×10^9). These expansion data are in line with other manufacturing protocols using CliniMACS Prodigy (43, 44). Additionally, according to the number of CAR T cells that have been infused in other clinical trials (45, 46), the number of NKG2D CAR T cells we achieved would have been enough to treat patients in a multiple-dose base. Over the manufacturing procedure, viability of the harvested cells has shown to be robust and above 80% except for validation 2, which showed a viability of 65%. During the process, a decrease in viability was observed on day +6 compared with that observed in starting cells, and this temporary drop on viability after transduction has been already reported by other groups (44, 47, 48). Some authors have reported that NKG2D CAR T cells may induce fratricide, hindering the expansion and the viability of cultured cells (49, 50). Additionally, a CD4/CD8 ratio bias and enhanced effector memory differentiation have been described when using PBMCs as starting cells to express NKG2D CAR. The fold NKG2D CAR T cell expansion observed in this study, along with the viability of the final cell products, suggests that no NKG2D CAR T cell-mediated fratricide is occurring during the manufacturing protocol. This observation could be related to the T-cell subset used as starting cells, as CD45RA⁺ compartment is already enriched in CD4⁺ T cells with an effector memory and central memory phenotypes. However, more experiments need to be performed to explore the susceptibility of different T-cell subsets to NKG2D CAR T cell-mediated fratricide to confirm this hypothesis. To further explore if fratricide could be taking place in our experiments, the expression of NKG2DL

on NKG2D CAR T cells expanded at small scale was analyzed by FCM. No upregulation of NKG2DL was observed in these cells (data not shown). Nevertheless, we only analyzed the expression of NKG2DL at day +8 post-activation, and it has been described that activated T cells upregulate NKG2DL in a temporary manner, specially between days 2 and 5 upon activation (49, 50). Thus, with our data, we cannot totally rule out an upregulation of NKG2DL and, consequently, a fratricide phenomenon in other moments of the culture. A more detailed study of NKG2DL expression kinetics on NKG2D CAR T cells along the manufacturing procedure would shed light on this question.

Activated CD45RA⁺ cells were lentivirally transduced with MOI = 2 because small-scale preclinical data using the same vector achieved transduction efficiencies higher than 95% (30). This MOI of 2 is low compared with that of other works where MOIs of 5–10 are reported (43, 48). We used a fluorochrome-labeled anti-NKG2D mAb for CAR detection by FCM, as untransduced CD45RA⁺ cells only have basal expression of the NKG2D receptor, and then we can consider that the NKG2D expression observed in manufactured cells comes from the CAR (30). The expression of NKG2D CAR in transduced CD45RA⁺ cells was further confirmed by western blot and PCR analysis. As previously observed in small-scale experiments, the expression of NKG2D increased during the expansion of cells. In two out of four batches, NKG2D CAR expression was over 80%, whereas the other two achieved an expression of 55 and 60.6%. These expression values (55–60.6%) are comparable with those reported in other publications (43, 51) and were enough to efficiently eliminate Jurkat and primary osteosarcoma cells (531MII) at a 20:1 effector to target ratio. Owing to technical issues, some cytotoxicity assays were non-reproducible, and thus, potency of NKG2D CAR T cells could not be evaluated at some time points either during manufacturing procedure or at the end of culture. Nevertheless, those cytotoxicity assays that were reproducible also fulfilled the specification for potency, indicating manufactured NKG2D CAR T cells are cytotoxic against the target cells.

At the end of the activation–transduction–expansion protocol, different quality tests need to be performed to ensure safety and purity of manufactured CAR T cells before they are administered in patients. Sterility tests were negative, and no mycoplasma was detected. The concentration of bacterial endotoxins was within the limits set by Eu Ph for intravenous injectable products in all validations. Genetic stability of NKG2D CAR T was confirmed by normal CGH, indicating no chromosomal aberrations are caused by lentiviral transduction. Three out of four validations showed <5 genome integrated vector copies, fulfilling the specifications required. However, in validation #3, up to 12.3 genome integrated vector copies were detected. These data are striking, as a MOI of 2 was used in all experiments and does not match the hypothesis that one viral particle is able to infect one cell. Despite that higher-than-expected VCN was found in these cells, the percentage of NKG2D CAR positive cells in this validation was 87%,

indicating transduction efficiency was not above the usual levels. Additionally, CGH and expression of *myc* and *tert* oncogenes were normal in this batch, suggesting that even though more than five copies were integrated, they caused no genetic alterations. To rule out a potential oncogenic effect of NKG2D CAR T cells, the expression of *myc* and *tert* oncogenes was analyzed. All validations showed no overexpression of these genes except for validation #4, which presented overexpression of *myc*, and consequently did not fulfill the specifications required. Although *myc* overexpression in NK cell products has been previously demonstrated to be safe and to induce no complications nor secondary neoplasia in patients (52), it would be important to be aware and increase monitoring of these cell products to ensure safety before being administered to patients. The specification of the percentage of RCL in the supernatants is established at a maximum of 0.05%. All NKG2D CAR T cell products remained under that limit, indicating that there is no potential risk of virus infection after infusion.

In summary, the data here reported demonstrate the feasibility and reproducibility of a manufacturing protocol to obtain clinical-grade large-scale NKG2D CAR CD45RA⁺ T cells in CliniMACS Prodigy system. NKG2D CAR T cells met the release criteria for expansion, NKG2D CAR expression, cytotoxicity, and sterility, although grade of expansion and product characteristics showed variability. Most importantly, the manufacturing process described here shows flexibility and admits further improvements for future NKG2D CAR T cell trials.

DATA AVAILABILITY STATEMENT

All datasets generated for this study are included in the manuscript/Supplementary Files.

ETHICS STATEMENT

The studies involving human participants were reviewed and approved by The Ethics Committee from Hospital La Paz. Non-mobilized apheresis was obtained from healthy donors at the Bone Marrow Transplant and Cell Therapy Unit (BMTCT) of Hospital Universitario La Paz (HULP) by using CliniMACS Plus device (Miltenyi Biotec). All donors gave their written informed consent in accordance with the Helsinki protocol, and the study was performed according to the guidelines of the Ethics Committee from Hospital La Paz. The patients/participants provided their written informed consent to participate in this study.

REFERENCES

1. Lee YH, Kim CH. Evolution of chimeric antigen receptor (CAR) T cell therapy: current status and future perspectives. *Arch Pharm Res.* (2019) 42:607–16. doi: 10.1007/s12272-019-01136-x
2. Maus MV, June CH. Making better chimeric antigen receptors for adoptive T-cell therapy. *Clin Cancer Res.* (2016) 22:1875–84. doi: 10.1158/1078-0432.CCR-15-1433

AUTHOR CONTRIBUTIONS

LF, IM, and AP-M: conception and design. LF, AF, IM, DL, AM, and AR: development of methodology. LF, AE, MV, LC, AF, AL, MG, IM, RP, and AP-M: acquisition of data (acquired and managed patients, provided facilities, etc.). LF, AF, IM, AE, JM-L, and AP-M: analysis and interpretation of data (e.g., statistical analysis, biostatistics, computational analysis). LF, AF, IM, and AP-M: writing, review, and/or revision of the manuscript. LF, AF, IM, and AE: administrative, technical, or material support (i.e., reporting or organizing data, constructing databases). LF and AP-M: study supervision.

FUNDING

This study was funded in part by the National Health Service of Spain, Instituto de Salud Carlos III (ISCIII), FONDOS FEDER grant (FIS) PI18/01301, by the Unoentrecienmil Foundation and by CRIS Cancer Foundation to beat Cancer (<http://criscancer.org>). LF, AF, IM, and AE are granted by CRIS Cancer Foundation to beat cancer.

ACKNOWLEDGMENTS

We thank St. Jude Children's Research Hospital, especially Dr. Byoung and Dr. Robert Throm, for the vector core, for the design, and for transfer of lentiviral plasmids. We also thank the Monoclonal Antibodies, Genomics and Flow Cytometry Units at the CNIO, and Microbiology Department from HULP for technical support. We are especially grateful to the family of 531MII, MEZ, whose generosity and capacity to see beyond have allowed so many scientific achievements.

SUPPLEMENTARY MATERIAL

The Supplementary Material for this article can be found online at: <https://www.frontiersin.org/articles/10.3389/fimmu.2019.02361/full#supplementary-material>

Supplementary Figure 1 | PCR showing expression of endogenous NKG2D receptor and NKG2D CAR in transduced cells. NKG2D CAR expression is absent in CD45RA⁺ cells and PBMC negative controls.

Supplementary Figure 2 | Representative FCM data of CD4⁺CD25⁺CD127^{low/-} (Treg) content in total PBMC from a healthy donor (first row), starting CD45RA⁺ cells from validation 2 (second row), and NKG2D CAR T cells from validation 4 at the end of manufacturing process (third row).

Supplementary Video 1 | 3.35 h Time-lapse showing how NKG2D CAR memory T cells (labeled in orange with CMTMR) recognize, bind, and eliminate Jurkat cells (labeled in green with CFSE).

3. Barrett DM, Singh N, Porter DL, Grupp SA, June CH. Chimeric antigen receptor therapy for cancer. *Annu Rev Med.* (2014) 65:333–47. doi: 10.1146/annurev-med-060512-150254
4. June CH, O'Connor RS, Kawalekar OU, Ghassemi S, Milone MC. CAR T cell immunotherapy for human cancer. *Science.* (2018) 359:1361–5. doi: 10.1126/science.aar6711
5. Davila ML, Riviere I, Wang X, Bartido S, Park J, Curran K, et al. Efficacy and toxicity management of 19-28z CAR T cell therapy in

- B cell acute lymphoblastic leukemia. *Sci Transl Med.* (2014) 6:224ra25. doi: 10.1126/scitranslmed.3008226
6. Maude SL, Frey N, Shaw PA, Aplenc R, Barrett DM, Bunin NJ, et al. Chimeric antigen receptor T cells for sustained remissions in leukemia. *N Engl J Med.* (2014) 371:1507–17. doi: 10.1056/NEJMoa1407222
 7. Kochenderfer JN, Dudley ME, Kassim SH, Somerville RPT, Carpenter RO, Stetler-Stevenson M, et al. Chemotherapy-refractory diffuse large B-cell lymphoma and indolent B-cell malignancies can be effectively treated with autologous T cells expressing an anti-CD19 chimeric antigen receptor. *J Clin Oncol.* (2015) 33:540–9. doi: 10.1200/JCO.2014.56.2025
 8. Turtle JC, Hanafi LA, Beger C, Hudecek M, Pender B, Robinson E, et al. Immunotherapy of non-Hodgkin's lymphoma with a defined ratio of CD8+ and CD4+CD19-specific chimeric antigen receptor-modified T cells. *Sci Transl Med.* (2016) 8:355ra116. doi: 10.1126/scitranslmed.aaf8621
 9. Ruella M, Maus MV. Catch me if you can: leukemia escape after CD19-directed T cell immunotherapies. *Comput Struct Biotechnol J.* (2016) 14:357–62. doi: 10.1016/j.csbj.2016.09.003
 10. Sotillo E, Barret DM, Black KL, Bagashev A, Oldridge D, Wu G, et al. Convergence of acquired mutations and alternative splicing of CD19 enables resistance to CART-19 immunotherapy. *Cancer Discov.* (2015) 5:1282–95. doi: 10.1158/2159-8290.CD-15-1020
 11. Hilpert J, Grosse-Hovest L, Grünebach F, Buechele C, Nuebling T, Raum T, et al. Comprehensive analysis of NKG2D ligand expression and release in leukemia: implications for NKG2D-mediated NK cell responses. *J Immunol.* (2012) 189:1360–71. doi: 10.4049/jimmunol.1200796
 12. Fernández L, Valentín J, Zalacain M, Leung W, Patiño-García A, Pérez-Martínez A. Activated and expanded natural killer cells target osteosarcoma tumor initiating cells in an NKG2D–NKG2DL dependent manner. *Cancer Lett.* (2015) 368:54–63. doi: 10.1016/j.canlet.2015.07.042
 13. Lehner M, Götz G, Proff J, Schaft N, Dorrie J, Full F, et al. Redirecting T cells to Ewing's sarcoma family of tumors by a chimeric NKG2D receptor expressed by lentiviral transduction or mRNA transfection. *PLoS ONE.* (2012) 7:e31210. doi: 10.1371/journal.pone.0031210
 14. Cruz CRY, Micklethwaite KP, Savoldo B, Ramos CA, Lam S, Ku S, et al. Infusion of donor-derived CD19-redirection virus-specific T cells for B-cell malignancies relapsed after allogeneic stem cell transplant: a phase 1 study. *Blood.* (2013) 122:2965–74. doi: 10.1182/blood-2013-06-506741
 15. Brudno JN, Somerville RPT, Shi V, Rose JJ, Halverson DC, Fowler DH, et al. Allogeneic T cells that express an anti-CD19 chimeric antigen receptor induce remissions of B-cell malignancies that progress after allogeneic hematopoietic stem-cell transplantation without causing graft-versus-host disease. *J Clin Oncol.* (2016) 34:1112–21. doi: 10.1200/JCO.2015.64.5929
 16. Terakura S, Yamamoto TN, Gardner RA, Turtle CJ, Jensen MC, Ridell SR. Generation of CD19-chimeric antigen receptor modified CD8+ T cells derived from virus-specific central memory T cells. *Blood.* (2012) 119:72–82. doi: 10.1182/blood-2011-07-366419
 17. Pule MA, Savoldo B, Myers GD, Rossig C, Russell HV, Dotti G, et al. Virus-specific T cells engineered to coexpress tumor-specific receptors: persistence and antitumor activity in individuals with neuroblastoma. *J Exp Med.* (2009) 14:1264–70. doi: 10.1038/nm.1882
 18. Chan WK, Suwannasena D, Throm RE, Li Y, Elridge PW, Houston J, et al. Chimeric antigen receptor-redirection CD45RA-negative T cells have potent antileukemia and pathogen memory response without graft-versus-host activity. *Leukemia.* (2014) 29:1–9. doi: 10.1038/leu.2014.174
 19. Anderson BE, McNiff J, Yan J, Doyle H, Mamula M, Shlomchik MJ, et al. Memory CD4+ T cells do not induce graft-versus-host disease. *J Clin Invest.* (2003) 112:101–8. doi: 10.1172/JCI200317601
 20. Foster AE, Marangolo M, Sartor MM, Alexander SI, Hu M, Kenneth FB, et al. Human CD62L– memory T cells are less responsive to alloantigen stimulation than CD62L+ naive T cells: potential for adoptive immunotherapy and allodepletion. *Cell.* (2008) 104:2403–9. doi: 10.1182/blood-2003-12-4431
 21. Golubovskaya V, Wu L. Different subsets of T cells, memory, effector functions, and CAR-T immunotherapy. *Cancers.* (2016) 8:36. doi: 10.3390/cancers8030036
 22. Mahnke YD, Brodie TM, Sallusto F, Roederer M, Lugli E. The who's who of T-cell differentiation: human memory T-cell subsets. *Eur J Immunol.* (2013) 43:2797–809. doi: 10.1002/eji.201343751
 23. Chen BJ, Deoliveira D, Cui X, Le NT, Son J, Whitesides JF, et al. Inability of memory T cells to induce graft-versus-host disease is a result of an abortive alloresponse. *Blood.* (2007) 109:3115–23. doi: 10.1182/blood-2006-04-016410
 24. Chérel M, Choufi B, Trauet J, Cracco P, Dessaint JP, Yakoub-Agha I, et al. Naïve subset develops the most important alloreactive response among human CD4+ T lymphocytes in human leukocyte antigen-identical related setting. *Eur J Haematol.* (2014) 92:491–6. doi: 10.1111/ejh.12283
 25. Zheng H, Matte-Martone C, Li H, Anderson BE, Venketesan S, Tan HS, et al. Effector memory CD4+ T cells mediate graft-versus-leukemia without inducing graft-versus-host disease. *Blood.* (2008) 111:2476–84. doi: 10.1182/blood-2007-08-109678
 26. Hollyman D, Stefanski J, Przybylowski M, Bartido S, Borquez-Ojeda O, Taylor C, et al. Manufacturing validation of biologically functional T cells targeted to CD19 antigen for autologous adoptive cell therapy. *J Immunother.* (2009) 32:169–80. doi: 10.1097/CJI.0b013e318194a6e8
 27. Singh H, Figliola MJ, Dawson MJ, Olivares S, Zhang L, Yang G, et al. Manufacture of clinical-grade CD19-specific T cells stably expressing chimeric antigen receptor using Sleeping Beauty system and artificial antigen presenting cells. *PLoS ONE.* (2013) 8:1–11. doi: 10.1371/journal.pone.0064138
 28. Gee AP. Manufacturing genetically modified T cells for clinical trials. *Cancer Gene Ther.* (2015) 22:67–71. doi: 10.1038/cgt.2014.71
 29. Imai C, Mihara K, Andreansky M, Nicholson IC, Pui CH, Geiger TL, et al. Chimeric receptors with 4-1BB signaling capacity provoke potent cytotoxicity against acute lymphoblastic leukemia. *Leukemia.* (2004) 18:676–84. doi: 10.1038/sj.leu.2403302
 30. Fernández L, Metais JY, Escudero A, Vela M, Valentín J, Vallcorba I, et al. Memory T cells expressing an NKG2D-CAR efficiently target osteosarcoma cells. *Clin Cancer Res.* (2017) 23:5824–35. doi: 10.1158/1078-0432.CCR-17-0075
 31. Christodoulou I, Patsali P, Stephanou C, Antoniou M, Kleanthous M, Lederer CW. Measurement of lentiviral vector titre and copy number by cross-species duplex quantitative PCR. *Gene Ther.* (2016) 23:113–8. doi: 10.1038/gt.2015.60
 32. Schmittgen TD, Livak KJ. Analyzing real-time PCR data by the comparative C(T) method. *Nat Protoc.* (2008) 3:1101–8. doi: 10.1038/nprot.2008.73
 33. Fan M, Li M, Gao L, Geng S, Wang J, Wang Y, et al. Chimeric antigen receptors for adoptive T cell therapy in acute myeloid leukemia. *J Hematol Oncol.* (2017) 10:1–14. doi: 10.1186/s13045-017-0519-7
 34. Scherer LD, Brenner MK, Mamontkin M. Chimeric antigen receptors for T-cell malignancies. *Front Oncol.* (2019) 9:126. doi: 10.3389/fonc.2019.00126
 35. Knochelmann HM, Smith AS, Dwyer CJ, Wyatt MM, Mehrotra S, Paulos CM. CAR T cells in solid tumors: blueprints for building effective therapies. *Front Immunol.* (2018) 9:1–20. doi: 10.3389/fimmu.2018.01740
 36. Martinez M, Moon EK. CAR T cells for solid tumors: new strategies for finding, infiltrating, and surviving in the tumor microenvironment. *Front Immunol.* (2019) 10:1–21. doi: 10.3389/fimmu.2019.00128
 37. Spear P, Wu MR, Sentman ML, Sentman CL. NKG2D ligands as therapeutic targets. *Cancer Immunity.* (2013) 13:8.
 38. Schlegel P, Dittthard K, Lang P, Mezger M, Michaelis S, Handgretinger R, et al. NKG2D signaling leads to NK cell mediated lysis of childhood AML. *J Immunol Res.* (2015) 2015:473175. doi: 10.1155/2015/473175
 39. Torelli GF, Peragine N, Raponi S, Pagilara D, De Propis MS, Vitale A, et al. Recognition of adult and pediatric acute lymphoblastic leukemia blasts by natural killer cells. *Haematologica.* (2014) 99:1248–54. doi: 10.3324/haematol.2013.101931
 40. Sallman DA, Brayer J, Sagatys EM, Loney C, Breman E, Agaogué S, et al. NKG2D-based chimeric antigen receptor therapy induced remission in a relapsed/refractory acute myeloid leukemia patient. *Haematologica.* (2018) 103:424–6. doi: 10.3324/haematol.2017.186742
 41. Maschan M, Blagov S, Shelikhova L, Shekhovtsova Z, Balashov, D'Starichkova J, et al. Low-dose donor memory T-cell infusion after TCR alpha/beta depleted unrelated and haploidentical transplantation: results of a pilot trial. *Bone Marrow Transplant.* (2018) 53:264–73. doi: 10.1038/s41409-017-0035-y
 42. Gasior M, Bueno D, De Paz R, Mozo Y, Rosich B, Sisinni L, et al. Safety and outcome of high-dose donor CD45RO+ memory T-cells infusion after allogeneic transplantation. *Bone Marrow Transplant.* (2019) 54.

43. Zhang W, Jordan KR, Schulte B, Purev E. Characterization of clinical grade CD19 chimeric antigen receptor T cells produced using automated CliniMACS Prodigy system. *Drug Des Dev Ther.* (2018) 2018:3343–56. doi: 10.2147/DDDT.S175113
44. Mock U, Nickolay L, Philip B, Cheung WKG, Zhang H, Johnston ICD, et al. Automated manufacturing of chimeric antigen receptor T cells for adoptive immunotherapy using CliniMACS prodigy. *Cytotherapy.* (2016) 18:1002–11. doi: 10.1016/j.jcyt.2016.05.009
45. Geyer MB, Brentjens RJ. Review: current clinical applications of chimeric antigen receptor (CAR) modified T cells. *Cytotherapy.* (2016) 18:1393–409. doi: 10.1016/j.jcyt.2016.07.003
46. Baumeister SH, Murad J, Werner L, Daley H, Trebeden-Negre H, Gicobi JK, et al. Phase I trial of autologous CAR T cells targeting NKG2D ligands in patients with AML/MDS and multiple myeloma. *Cancer Immunol Res.* (2018) 7:100–12. doi: 10.1158/2326-6066.CIR-18-0307
47. Tumaini B, Lee DW, Lin T, Castiello L, Stroncek DF, Mackall C, et al. Simplified process for the production of anti-CD19-CAR-engineered T cells. *Cytotherapy.* (2013) 15:1406–15. doi: 10.1016/j.jcyt.2013.06.003
48. Dominick L, Mockel-Tenbrinck N, Drechsel K, Barth C, Mauer D, Schaser T, et al. Automated manufacturing of potent CD20-directed chimeric antigen receptor T cells for clinical use. *Hum Gene Ther.* (2017) 28:914–25. doi: 10.1089/hum.2017.111
49. Breman E, Demoulin B, Agaagué S, Mauën S, Michaux A, Springuel L, et al. Overcoming target driven fratricide for T cell therapy. *Front Immunol.* (2018) 9:2940. doi: 10.3389/fimmu.2018.02940
50. Song DG, Ye Q, Santoro S, Fang C, Best A, Powell DJ Jr. Chimeric NKG2D CAR-expressing T cell-mediated attack of human ovarian cancer is enhanced by histone deacetylase inhibition. *Hum Gene Ther.* (2013) 24:295–305. doi: 10.1089/hum.2012.143
51. Zhu F, Shah N, Xu H, Schneider D, Orentas R, Dropulic B, et al. Closed-system manufacturing of CD19 and dual-targeted CD20/19 chimeric antigen receptor T cells using the CliniMACS Prodigy device at an academic medical center. *Cytotherapy.* (2018) 20:394–406. doi: 10.1016/j.jcyt.2017.09.005
52. Leivas A, Perez-Martinez A, Blanchard MJ, Martín-Clavero E, Fernández L, Lahuerta JJ, et al. Novel treatment strategy with autologous activated and expanded natural killer cells plus anti-myeloma drugs for multiple myeloma. *Oncoimmunology.* (2016) 5:e1250051. doi: 10.1080/2162402X.2016.1250051

Conflict of Interest: DL works for Miltenyi Biotec S.L.

The remaining authors declare that the research was conducted in the absence of any commercial or financial relationships that could be construed as a potential conflict of interest.

Copyright © 2019 Fernández, Fernández, Mirones, Escudero, Cardoso, Vela, Lanzarot, de Paz, Leivas, Gallardo, Marcos, Romero, Martínez-López and Pérez-Martínez. This is an open-access article distributed under the terms of the Creative Commons Attribution License (CC BY). The use, distribution or reproduction in other forums is permitted, provided the original author(s) and the copyright owner(s) are credited and that the original publication in this journal is cited, in accordance with accepted academic practice. No use, distribution or reproduction is permitted which does not comply with these terms.